REDUCING BIO-OIL OXYGEN CONTENT VIA *IN-SITU* DEOXYGENATION AND HYDROGEN PRODUCTION

by

Kyle A. Rogers

BScE. In Chemical Engineering, University of New Brunswick, 2014

A Dissertation Submitted in Partial Fulfillment
of the Requirements for the Degree of

Doctor of Philosophy (PhD)

in the Graduate Academic Unit of Chemical Engineering

Supervisor: Ying Zheng, PhD, Chemical Engineering

Examining Board: William Cook, PhD, Chemical Engineering
Laura Romero-Zeron, PhD, Chemical Engineering
Kripa Singh, PhD, Civil Engineering

External Examiner: Kevin Smith, PhD, Chemical and Biological Engineering,
University of British Columbia

This dissertation is accepted by the
Dean of Graduate Studies

THE UNIVERSITY OF NEW BRUNSWICK

January 2020

ABSTRACT

Crude bio-oil produced through biomass thermal decomposition processes such as pyrolysis needs to be upgraded via hydroprocessing to remove oxygen. This requires hydrogen gas which is problematic as it represents an additional cost and sustainability issues as most hydrogen is produced from non-renewable sources. Therefore, hydrogen requirements need to be reduced. The options for reducing hydrogen requirements that have been explored include increasing hydrogen efficiency via selective deoxygenation, using water-gas-shift reaction (WGSR) to regenerate hydrogen, and reducing oxygen content during the biomass decomposition.

To initially demonstrate biomass thermal decomposition with *in-situ* deoxygenation, glucose was decomposed in the presence of monometallic and bimetallic catalysts on SiO_2 with small amounts of hydrogen gas at 350°C for 1-hour. As glucose decomposed, intermediates/products underwent deoxygenation. The catalysts that were dominant in furanic compound deoxygenation selectivity were 4%Co/SiO_2, 0.5%Ni4%Fe/SiO_2, and 0.5%Co4%Fe/SiO_2. Catalysts were shown to influence glucose decomposition. Catalysts with exposed Ni helped reduce solid residue.

NiFe catalysts supported on ceria-zirconia were developed for the purpose of performing both WGSR and deoxygenation. These catalysts were used to deoxygenate guaiacol in the presence of CO and H_2O instead of H_2 at 350°C. Nano-casting ceria-zirconia on MCM-41 produced an active support good for oxygen storage with comparatively high surface area

(to other ceria-zirconia catalysts), CZ-41. Sequentially prepared 2%Ni4%Fe/CZ-41 was capable of producing H_2 internally and using it to convert guaiacol to products such as phenol. Adding 0.5 wt% Co to the Fe phase improved hydrogen production.

The aforementioned CZ-41 catalysts were used for the decomposition of glucose with internal hydrogen production and deoxygenation without the addition of H_2. The trimetallic NiCoFe/CZ-41 catalyst provided superior yields of liquid product. The addition of Co to Fe as an alloy improves reducibility of Fe and improves metal-support interactions. Future work should focus on reactor design without the use of a solvent and mild reforming to improve H_2 generation all along with continued catalyst development.

ACKNOWLEDGEMENTS

I am grateful to NBIF, NSERC, CRC (Canada Research Chairs) and CFI (Canadian Foundation for Innovation) programs for scholarships, project, and lab funding.

Thank you to my advisor, Dr. Ying Zheng for graciously providing me with guidance, helping me with my vision for this PhD project, and encouraging me to publish peer-review papers and attend conferences. Thank you also to Dr. Mladen Eic for supervising my lab space. Thank you, Dr. William Cook, Dr. Laura Romero-Zeron, and Dr. Kripa Singh for taking part in the examining committee. Thank you, Dr. Kevin Smith of the University of British Columbia for giving a thorough review of my dissertation.

I would also like to thank all of the UNB staff that helped me conduct my experiments and perform analyses. Thank you Adon Briggs of the UNB Chemical Engineering Machine Shop for helping me with the design and construction of my batch reactor. Thank you to Sandra Riley for helping me maintain the labs. Thank you to Steven R. Cogswell of the UNB Microscopy and Microanalysis center for helping me with electron microscopy analyses and teaching me how to do image processing using ImageJ and FIJI. Thank you Ven Reddy of the UNB Earth Sciences department for assisting me with XRD analyses.

A special thanks also goes to my family and Jirapinya (Mint) Kongtuk for supporting me and providing me with encouragement and a positive attitude. Also thank you to Andrew Mergl and Seyyedmajid Sharifvaghefi for listening to my bad jokes daily.

Table of Contents

List of Tables

List of Figures

List of Abbreviations

2MF – 2-methylfuran

CZ – Ceria-zirconia mixed oxide

CZ-15 – Ceria-zirconia mixed oxide prepared via nano-casting on SBA-15

CZ-41 – Ceria-zirconia mixed oxide prepared via nano-casting on SBA-15

DCO – Decarbonylation

DCO_2 – Decarboxylation

DDO – Direct deoxygenation reaction route (pertaining to phenolic compounds)

DFT – Density functional theory

DME – Demethylation (ie. DME of guaiacol, producing catechol and methane)

DMF – 2,5-dimethylfuran

DMO – Demethoxylaton (ie. DMO of guaiacol, producing phenol and methanol)

DTA – Differential thermal analysis (negative derivative of TGA weight loss profile)

EDS – Energy-dispersive X-ray spectroscopy

FID – Flame Ionization Detector

GC – Gas Chromatograph

HAADF-STEM – High angle annular darkfield scanning transmission electron microscopy

HDO – Hydrodeoxygenation

HMF – 5-hydroxymethylfurfural

HRTEM – High resolution transmission electron microscopy

HYD – Hydrogenation-deoxygenation reaction route (pertaining to phenolic compounds)

kPaA – Pressure unit of measurement kilopascals (kPa); absolute pressure

kPaG – Pressure unit of measurement kilopascals (kPa); gauge pressure

MS – Mass Spectrometry

MSR – Methane steaming reforming: $CH_4 + H_2O \rightarrow CO + 3H_2$

nmL/min – mL/min at NTP conditions

SDO – Selective deoxygenation

SHH – Selective hydrogenation/ hydrogenolysis reaction route (pertaining to furanics)

STEM – Scanning transmission electron microscopy

TGA – Thermogravimetric Analysis

TPR – Temperature programmed reduction

WGSR – Water-gas-shift reaction: $CO + H_2O \leftrightarrow CO_2 + H_2$

XRD – X-ray diffraction

Chapter 1: Introduction

1.1 Background and Problem Statement

Increasing interest in sustainable and renewable energy has made the prospect of producing biofuels more attractive. The desire for carbon neutral transportation fuels has led to the development and introduction of first-generation biofuels such as bioethanol and FAME biodiesel in society. Due to concerns regarding fuel compatibility and consumption of food resources for fuel, there is a motive for developing second generation biofuels that have reduced oxygen content and are from non-edible feedstocks [1-3].

A common way to produce second generation biofuels is to use a thermal process such as pyrolysis to first produce a crude bio-oil. In these thermal processes, biomass – often lignocellulosic material such as wood or switchgrass – is decomposed at high temperatures in the absence of oxygen. Condensing the volatile compounds results in a bio-oil product along with solid residue (often consisting of char) and gaseous components including H_2, CO, CO_2, and CH_4 [4-9]. The bio-oil however, tends to have a high oxygen content making it not very useful as a direct fuel as it has a low energy density and poor stability [2, 10-12]. Therefore, an upgrading process is required.

Much like petroleum products, useful biofuels can be produced from crude bio-oil via hydrotreating. To remove sulfur and nitrogen, oil usually goes through hydrodesulfurization (HDS) and hydrodenitrogenation (HDN) where sulfur and nitrogen containing compounds react with H_2 over a catalyst to remove S and N as H_2S and NH_3.

Similarly, to remove oxygen, bio-oil goes through hydrodeoxygenation where H_2 is used to remove O as H_2O, CO, and CO_2. The problem then is the requirement of expensive H_2 in high volumes [3, 13-15]. On top of issues regarding costs and availability, there is also the question of whether the product can be considered sustainable/renewable as most of the world's supply of H_2 comes from non-renewable resources such as methane steam reforming. In any case, a lower H_2 requirement is most appealing.

The challenge is then to determine how H_2 requirements can be successfully reduced or satisfied in a sustainable/renewable fashion. The options are then as follows:

1. Stop using H_2 altogether – This is somewhat possible for converting vegetable oils however, it is not possible to do so with crude bio-oil from thermal processes due the presence of aromatic compounds such as phenol.
2. Develop catalysts that utilize H_2 very efficiently, reducing overall H_2 requirement – Here the aim would be to perform "selective deoxygenation" where H_2 is primarily used to remove oxygen and not necessarily used to saturate carbon-double-bonds [16, 17]. Although this may not be the perfect solution, decreasing H_2 requirements and making processes more efficient is desirable.
3. Change the source of H_2 – For example: produce H_2 from different processes other than methane steam reforming such as water electrolysis or biomass gasification. Although this would potentially make the process entirely renewable, there would be extensive costs associated with the change.
4. Reduce the oxygen in the bio-oil during the thermal processing stage – Eliminating the amount of oxygen retained in the liquid product early on in the process would

ultimately mean less hydrogen needs to be removed downstream. Up until this point, this has not been explored in great detail.

1.2 Scope and Objectives

This thesis explores all four options for reducing H_2 requirements with a focus on the fourth option. During biomass decomposition, it was noted that useful gases/vapours are produced such as H_2, CO, H_2O, and CH_4. These gases may be useful for removing oxygen *in-situ* and producing additional H_2 during thermal processing with the addition of an appropriate catalyst. Therefore, the aim of this PhD project was to research the different alternatives for reducing hydrogen requirements and demonstrate *in-situ* deoxygenation during biomass decomposition along with the development of appropriate heterogeneous catalysts. Later, catalysts were developed for the purpose of producing internal H_2 as well as deoxygenation. The use of hydrogen donor solvents and aqueous-phase reforming techniques are discussed briefly however, they were not within the main scope of this project.

On top of deoxygenation and hydrogen production, this project also focused on how the addition of heterogeneous catalysts impacts the biomass decomposition. Glucose was used as the primary biomass material as a model compound for cellulose. Glucose is considered an intermediate of cellulose decomposition and offers a less convoluted reaction network allowing easier analysis [8, 9, 18]. Inevitably, the three reaction systems – glucose decomposition (thermolysis), hydrogen production, and deoxygenation (upgrading) – are all expected to have an influence on each other (see Figure 1-1).

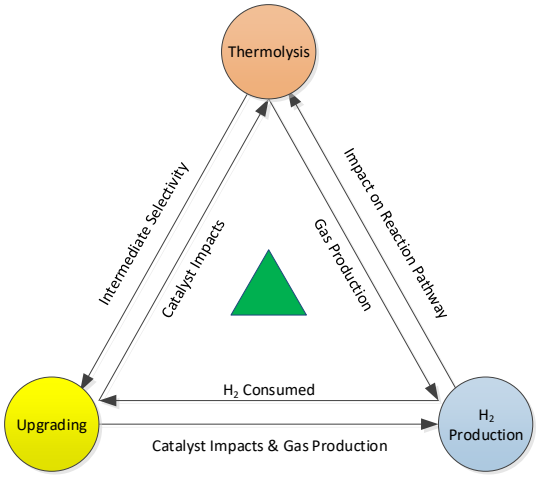

Figure 1-1: Impact triangle – the interactions between the three reaction networks – thermolysis, hydrogen production, and upgrading.

The work presented in this dissertation is a new concept as biomass thermolysis with *in-situ* deoxygenation and hydrogen production has not previously been studied in literature. In addition, the catalysts developed in this work may also have other applications regarding deoxygenation and water-gas-shift reactions. Overall, the implications of this work is to develop catalysts and a strategy for reducing hydrogen requirements in bio-refineries.

1.3 Outline

This dissertation consists of eight chapters including a literature review (Chapter 2), a chapter illustrating the experimental set-up and preliminary tests (Chapter 3), four chapters detailing the experimental phases and results (Chapters 4-7), and a summary of conclusions and recommendations. In total, five journal papers have been derived from this work, including a review paper. Each paper listed here was primarily written by the candidate with advice/revisions from co-authors including Supervisor, Dr. Ying Zheng.

The literature review in Chapter 2 is split into two parts. The first part of the literature review highlights biomass decomposition, hydrogen production from thermal processing, and water-gas-shift reaction. The second part discusses the deoxygenation of bio-oils including vegetable oils. The topic of "selective deoxygenation" is discussed thoroughly along with the potential of using no hydrogen or different sources of hydrogen. Part two (Section 2.2 of Chapter 2) of the literature review is a published journal article titled "Selective Deoxygenation of Biomass-derived Bio-oils within Hydrogen-Modest environments: A Review with New Insights". This paper was published in July 2016 by the *ChemSusChem* journal (Volume 9, Issue 14, pages 1750-1772). This paper reviewed catalysts and the various reactions mechanisms for selectively deoxygenating vegetable oils, phenolic compounds, and furanic. Insights were also provided on how to develop systems that are more hydrogen-efficient using specific catalysts or sources of hydrogen including the use of the water-gas-shift reaction. For this paper, the candidate was the primary writer with advice/revisions given by Dr. Ying Zheng.

Chapter 3 describes the main experimental set-up and the results from preliminary tests. Specific procedures for each section of the project are further covered in each individual chapter (Chapters 4-7). Preliminary tests validated the idea that additives can be added to the biomass (cellulose) decomposition process for the purpose of producing hydrogen.

The first experimental demonstration of *in-situ* deoxygenation during glucose decomposition using monometallic catalysts in an environment with a very limited amount of hydrogen was performed in Chapter 4. From this work, a journal paper titled

"Decomposition of Glucose with *in situ* Deoxygenation in a Low H_2 Pressure Environment – Part I: Monometallic Catalysts" was derived. This paper was published by the *Applied Catalysis A: General* in January 2019 (volume 569, pages 75-85). This paper studied the addition of monometallic catalysts such as 4%Ni/SiO_2 and 4%Co/SiO_2 to a horizontally stirred batch reactor during the decomposition of glucose. Various monometallic catalysts were studied for their ability to perform *in-situ* deoxygenation of glucose decomposition products using a small portion of H_2 gas. The study also determined the impact that the catalysts have on glucose decomposition. It was concluded that 4%Co/SiO_2 was ideal for the in-situ deoxygenation of furanic compounds while Ni catalysts were the best at reducing solid residue. Experimental work was performed by the candidate, who was also primary author of the paper. Advice and revisions were provided by Dr. Ying Zheng.

Chapter 5 focuses on the development of bimetallic catalysts for *in-situ* deoxygenation during glucose decomposition. This work contributes to the development of both a system for biomass decomposition with *in-situ* deoxygenation and bimetallic catalysts for selective deoxygenation. This work was used in the development of a paper titled "Decomposition of Glucose with *in situ* Deoxygenation in a Low H_2 Pressure Environment – Part II: Bimetallic Catalysts", which is a follow-up to the paper presented in Chapter 4. This paper was published by the *Applied Catalysis A: General* journal in May 2019 (volume 578, pages 10-19). This paper studied the use bimetallic catalysts for *in-situ* deoxygenation during glucose decomposition including 0.5%Ni4%Fe/SiO_2 and 0.5%Pd4%Fe/SiO_2 catalysts. Like in Chapter 4, the catalysts were studied for their impact on glucose decomposition. This work also studied the effect of preparation techniques for bimetallic

catalysts: co-impregnation vs. sequential impregnation. A 0.5%Ni4%Fe/SiO_2 catalyst that was sequentially prepared was found to be ideal for both *in-situ* deoxygenation furanic compounds and reducing solid residue. Experimental and written work for this paper was performed by the candidate with revisions from Dr. Ying Zheng.

Chapter 6 focuses on developing multifunctional catalysts that can perform deoxygenation using only hydrogen that is produced via water-gas-shift reaction. This was done using guaiacol as a model compound in an atmosphere containing H_2O and CO rather than H_2. This work was formatted as journal article titled "Guaiacol Deoxygenation using Ceria-Zirconia Based Catalysts with Hydrogen Produced Internally via Water-Gas-Shift Reaction" which will be submitted to the *Applied Catalysis A: General* journal in the near future. This paper focuses on the development of multifunctional ceria-zirconia catalysts such as 2%Ni4%Fe/CeO_2-ZrO_2 for deoxygenating guaiacol without the addition of H_2. From this work it was determined that a Ni-Fe catalysts supported on ceria-zirconia nano-casted from MCM-41 is ideal for deoxygenation with hydrogen that is produced internally via the water-gas-shift reaction. Experimental work was performed by the candidate who was also the primary author of this paper. Dr. Ying Zheng provided advice and revisions for this paper. The published paper will also include contributions from Jile Fu of Western University.

The last experimental phase is discussed in Chapter 7, which refocuses on glucose decomposition with *in-situ* deoxygenation without supplying external H_2. Multifunctional catalysts (which were developed in Chapter 6) were used to perform *in-situ* deoxygenation

using only H_2 that was produced internally. The effect of the catalysts on glucose decomposition and product yield is discussed. This work will be published as a journal paper entitled "Glucose Decomposition with Internal Hydrogen Production and Deoxygenation via Nano-Casted Ceria-Zirconia Catalysts", which will be submitted to *Applied Catalysis A: General*. The publication of this paper is dependent on the paper presented in Chapter 6. All experimental work and preparation of the draft for this paper was conducted by the PhD candidate. Dr. Ying Zheng has provided revisions for this work.

Chapter 2: Literature Review

2.1 Biomass Decomposition, Hydrogen Production, and Water-Gas-Shift

In order to develop a system in which biomass material is converted to a more useful, liquid fuel, one must consider the process and mechanisms by which it occurs. As discussed in Chapter 1, this project focuses on biomass conversion – cellulose (and glucose as its model compound) which constitutes as much as 40-50% of wood. For the process of decomposing cellulose and performing *in-situ* deoxygenation with internal hydrogen production, it is important to understand the following:

- How cellulose (or biomass in general) decomposes?
- What methods are available for enhancing hydrogen production?
- What catalysts can be used to promote hydrogen production and what are their reaction mechanisms?
- What effects do catalysts have on cellulose/glucose decomposition?

2.1.1 Cellulose Decomposition

A very common way for producing bio-oil via biomass decomposition is through a thermal process such as pyrolysis. During pyrolysis, biomass is heated to temperatures greater than 500°C (up to 800°C) in the absence of oxygen leading to depolymerization, chemical degradation, and fragmentation via the breaking of covalent bonds [4, 19]. Depolymerization and other primary pyrolysis reactions typically occur within the temperature range of 250-500°C [4].

The pyrolysis of cellulose has received much research regarding the production of liquid fuel, gases, and solid char. However, the chemical mechanisms for cellulose decomposition has been studied to a lesser extent. Shen & Gu, [8] investigated the mechanisms for the pyrolysis of cellulose using a lab scale pyrolysis unit within the temperature range of 430 to 730^{o}C to examine both the primary and secondary pyrolytic reactions. In their work, they found that the most predominate product at all temperatures was levoglucosan along with small amounts of furanic compounds (such as 5-hydroxymethylfurfural) and smaller compounds (such as hydroxyacetaldehyde). It was also found that increasing the temperatures increased the production of the furanic compounds, short oxygenated hydrocarbons, water, and non-condensable gases while the production of levoglucosan decreased.

The most interesting and desirable products were the furanic compounds derived from 5-hydroxymethylfurfural (HMF). Shen & Gu, [8] argued that these compounds could be produced from two separate reaction pathways – both requiring dehydration reactions. The first pathway is a direct decomposition pathway from cellulose requiring first ring-opening, dehydration, followed by cyclization into a furan ring. The second pathway proposed was a secondary pyrolysis reaction from levoglucosan at elevated temperatures. Shen & Gu, [8] did not confirm this second pathway. The presence of furanic compounds in the liquid products is very interesting as these compounds are easy to identify in the products (due to their furan rings) and are considered difficult to undergo deoxygenation (see section 2.2.3).

Wang, et al.,[20] on the other hand looked at the mechanism for the pyrolysis of hemicellulose and monosaccharides. Hemicellulose, like cellulose, is an organic polymer consisting of sugar molecules but instead of repeating glucose structures, hemicellulose consists of various hexoses (such as glucose at galactose) and pentoses (such as xylose). In such a way, the pyrolysis of hemicellulose may be comparable to that of cellulose. In their work, Wang, et al.,[20] confirmed that HMF is produced from hexoses via ring-opening, dehydration, and cyclization. In their work though, furan compounds were most prevalent amongst other primary products such as 1-hydroxy-2-propanone and 4-hydroxydihydrofuran-2(3H)-one. Of these products, they determined that the furanic compounds were thermodynamically more favorable. It is unclear though why dehydration reactions were so prevalent in their system compared to the work of Shen & Gu, [8]. It may be deduced that the pyrolysis of cellulose and hemicellulose structures are non-comparable, and that the pyrolysis of the monosaccharides provides a different product selection. Thus, if furanic compounds are desired, it may be required to hydrolyze cellulose into glucose before pyrolysis.

The first major reactions to occur on cellulose during pyrolysis are depolymerization reactions including depropagation and thermal hydrolysis, producing levoglucosan and glucose [9, 21]. Evans & Milne, [21] suggested that depolymerization can be followed by ring-opening – in which glucose is the intermediate – producing a radical compound (on the pyranose oxygen) that undergoes cyclization with C2 producing a furanose structure. This furanose structure can then undergo two dehydration reactions to produce HMF.

More recently, Vinu & Broadbelt, [9] developed a mechanistic model for cellulose decomposition during fast pyrolysis based on the reaction kinetics. It was reported that cellulose could undergo a variety of depolymerization reactions in series and parallel including initiation, depropagation, end-chain initiation, and thermohydrolysis. The main products being levoglucosan and glucose. Vinu & Broadbelt, [9] described a model for glucose decomposition (see Figure 2-1). Reportedly, glucose can decompose to produce a variety of intermediates and products including, acetol, levoglucosan, HMF, and furfural. As demonstrated in Figure 2-1, glucose can readily undergo a series of dehydration, ring-opening, and recyclization reactions to produce HMF. In their model, Vinu & Broadbelt [9] also considered the formation of char which is derived from a variety of intermediates along with CO_2, H_2O, and H_2. Although they did not describe in full the mechanism by which char is formed, based on the dehydrated intermediates, it is suspected that char is formed first by the production of heavy, tar compounds via a series of dehydration and aromatization reactions. Brewer et al., [22] suggested that the formation of biochar involves aromatic structures consisting of at least seven rings. Mayes et al., [23] confirmed the reaction pathways for producing HMF from glucose using a theoretical model and proposed that catalysts could be used to improve its selectivity.

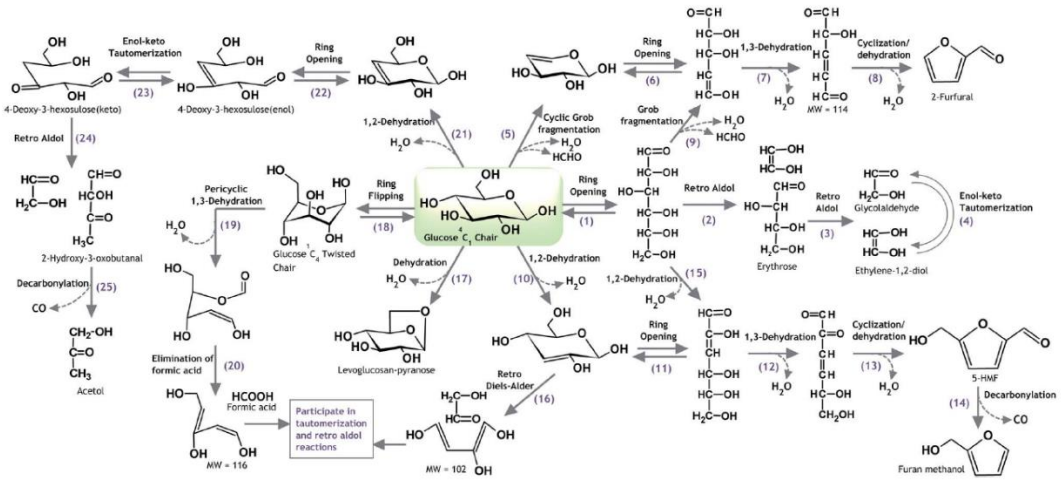

Figure 2-1: Glucose decomposition model developed by Vinu & Broadbelt, [9]

2.1.2 Hydrogen Production During Biomass Decomposition

In recent years the Harris group from the University of Sydney, Australia has researched biomass pyrolysis focusing on hydrogen production through tar cracking, reforming, and water-gas-shift reactions [24-31].

Tar cracking and reforming reactions during pyrolysis have a similar approach to gasification processes where the water produced during biomass decomposition is used to perform reforming of light compounds [24-26, 32]. Heterogenous catalysts typically consisting of supported Ni, are used to produce excess H_2 below 700°C [25, 26, 31-33]. Steam formation and build-up was reported to occur within the temperature range 300°C to 425°C. As such, elevated H_2 production via reforming was witnessed within the temperature range of 350-400°C [25, 27]. Reportedly, the catalysts, such as Co/SBA-15, promote tar cracking producing additional light compounds (see Table 2-1). Volatile

organic compounds may then undergo a variety of cracking and reforming reactions [26, 27].

Table 2-1: Biomass decomposition, cracking, reforming, and gasification reactions [26, 27]

Definition	Reaction/Equation	$\Delta H°_{298.15}$ (kJ/mol)
Thermal decomposition	Biomass → H_2O + CO + CO_2 +organic volatiles + volatile tars + char	
Tar cracking (catalytic)	Tars → H_2O + H_2 + CO + CO_2 +CH_4 +C_xH_y +CH_3OH + CH_2O + CH_3CHO	
Catalytic cracking	$CH_3OH \rightarrow CH_2O + H_2$	+85.0, endothermic
Catalytic cracking	$CH_2O \rightarrow CO + H_2$	+5.4, endothermic
Catalytic cracking	$CH_3CHO \rightarrow CH_4 + CO$	−19.6, exothermic
Catalytic cracking/coking	$CH_4 \rightarrow C + 2H_2$	+75, endothermic
Water-gas shift	$CO + H_2O \rightarrow CO_2 + H_2$	−41.1, exothermic
Steam reforming	$CH_4 + H_2O \rightarrow CO + 3H_2$	+206.2, endothermic
Steam reforming	$C_xH_y + {}_xH_2O \rightarrow {}_xCO + (n+0.5m)H_2$	Endothermic
Dry reforming	$CH_4 + CO_2 \rightarrow 2CO + H_2$	+247.3, endothermic
Char gasification	$C + CO_2 \rightarrow 2CO$	+172.3, endothermic
Char gasification	$C + 2H_2O \rightarrow CO_2 + 2H_2$	+72.3, endothermic

Zhao et al., [31] later used a bimetallic 10wt% $NiCo_2$/SBA-15 catalyst for tar cracking and reforming and demonstrated increasingly higher yields of H_2 (as high as 295 cm^3/g cellulose) due to improved reducibility and dispersion of NiCo alloy sites. Another bimetallic catalyst, Pt doped Ni/MCF (mesocellular-foam silica) was used by Widyaningram et al.,[24] who showed that the addition of 0.7wt% Pt increased H_2 production from cellulose by 15% at 85 cm^3/g cellulose. Ruppert et al., [32] on the other hand demonstrated a synergistic effect between Ni and supporting material, ZrO_2 for the conversion of cellulose to H_2. Increasing gas yields via tar cracking, reforming, and

gasification may have a drawback as the reforming of lighter compounds may reduce desirable liquid product yield. As such, using lower temperatures to prevent steam accumulation and using an alternative method to produce H_2 may be more appropriate.

Indeed, another method that has been approached for producing hydrogen is by promoting the water-gas-shift reaction (WGSR). Florin & Harris, [28] first demonstrated enhanced water-gas-shift during biomass steam gasification using CaO to capture CO_2, thermodynamically forcing WGSR to produce more H_2. This was later adopted by Widyawati et al.,[29] who used CaO for CO_2 capture during biomass pyrolysis. From their TGA-MS results, they found that the addition of CaO to cellulose (molar ratio of n_{Ca}/n_C = 0.5) increased the relative concentration of H_2 produced during their experiments. They concluded that below a temperature of 450^{o}C, this increase in hydrogen production was due to the promotion of the water-gas-shift reaction. Cellulose was shown to have a peak rate of weight loss at 362°C which was also associated with the temperature at which the maximum H_2 production rate occurred.

Widyawati, et al.,[29] also highlighted that if water reacts with CaO to produce $Ca(OH)_2$, $Ca(OH)_2$ can also react with CO_2 to produce water and $CaCO_3$. Due to uncertainties within their results for cellulose without CaO addition, Widyawati, et al.,[29] were unable to determine a statistically significant difference in the results. In addition, as their experiments were optimized to test for gas evolution, they were unable to determine the effects that CaO has on the liquid fuel product distribution. One issue that was highlighted was the stability of the CaO sorbent which was later addressed by Amos, et al., [30] who

developed CaO sorbents supported on ceramic materials. Since CO and H_2O are not useful for increasing liquid product yield, using these components to produce additional H_2 appears to be a viable solution. Mild/selective reforming of light hydrocarbons with very low carbon count (such as CH_4) may also be useful as reforming these compounds would not affect the liquid product yield.

2.1.3 Water-Gas-Shift Reaction

In search of producing hydrogen via the water-gas-shift reaction during biomass decomposition, attention should be paid towards catalysts that promote WGSR. Water-gas-shift is a common reaction process that is used in industry in conjunction with natural gas steam reforming to boost hydrogen production. This process has had an important role for the production of hydrogen at petroleum refineries for upgrading processes, the production of ammonia, and the production of hydrocarbons via the Fischer-Tropsch process [34]. Ratnasamy & Wagner, [34] performed an extensive review of water-gas-shift catalysts and mechanisms including catalysts that are commonly used in industrial processes. In industry, WGSR is performed at high temperature (350-450°C) using iron oxide based catalysts and low temperature (190-250°C) using copper-zinc oxide catalysts.

The iron oxide catalysts – which are stabilized by chromium oxide – use a redox couple mechanism for producing H_2 (see Equations 2-1 and 2-2) [34]. Low temperature WGSR catalysts follow a surface redox model, like that of the iron oxide catalysts, at low pressures (~1 bar) [35, 36]. At higher pressures (20 bar), it was suggested that a formate intermediate is formed on the catalyst surface which, although not deemed part of the cycle for CO

conversion to CO_2 could produce methanol upon hydrogenation [35]. Overall, excessively high temperatures will decrease WGSR conversion as the overall reaction is exothermic. As such, developing a catalyst that offers superior kinetics at reduced temperatures is favourable. On top of that, a major concern with WGSR catalysts currently used in industry is that upon activation, they can become very pyrophoric which creates safety concerns [34]. As a result, researchers have begun to investigate possible alternatives such as precious metals (Pt, Au, Ru, etc.) supported on partially reducible oxide catalysts (ZrO_2, TiO_2, CeO_2, etc.).

$$2Fe_3O_4 + H_2O \rightleftharpoons 3Fe_2O_3 + H_2 \quad \textbf{2-1}$$

H_2 production through Fe oxidation [34]

$$3Fe_2O_3 + CO \rightleftharpoons 2Fe_3O_4 + CO_2 \quad \textbf{2-2}$$

CO_2 production through Fe reduction [34]

The use of monometallic and bimetallic catalysts – including nonprecious metals such as Ni and Fe over oxide supports has since gained a lot of attention. Wang & Gorte, [37] studied the use of Pd/CeO_2 for low temperature water-gas-shift (200°C) using various oxide monolayers (Fe, Sn, Cr, Mo, Pb…) as promoters. For Pd/CeO_2 the proposed mechanism is as shown in Equations 2-3 to 2-5.

$$CO + Pd^* \rightarrow Pd \cdot CO \quad \textbf{2-3}$$

Adsorption of CO on active Pd site (Pd^*) [37]

$$H_2O + Ce_2O_3 \rightarrow 2CeO_2 + H_2 \quad \textbf{2-4}$$

Oxidation of ceria oxygen vacancy site with water [37]

$$Pd \cdot CO + 2CeO_2 \rightarrow CO_2 + Ce_2O_3 + Pd^* \quad \textbf{2-5}$$

Reduction of ceria via CO adsorbed on Pd [37]

Of all the catalysts that were tested, the Fe monolayered catalyst, Pd/Fe-CeO_2 proved to be the most attractive. Interestingly, the addition of Fe_2O_3 to the bulk CeO_2 did not provide similar benefits suggesting that the results witnessed for the Pd/Fe-CeO_2 catalyst were related to surface chemistry alone where iron oxides are more active for WGSR [37]. The use of ceria is beneficial because of it has well established oxygen storage capabilities, suffers little damage from oxidation, and is not as pyrophoric as traditional WGSR catalysts.

Boaro et al., [38] observed that Pt and Au based catalysts supported on ZrO_2 and CeO_2-ZrO_2 mixed oxides were effective for WGSR achieving up to ~80% CO conversion at 300°C. Conversion of CO increased passed equilibrium due to small methanation activity at temperatures above 300°C. The supported gold catalysts outperformed the platinum catalysts at low temperature due to a consistently small Au particle size (1.2-2.0 nm) and high dispersion, which was independent of the supporting material. Boaro et al., [38] concluded that the most important feature of the supporting material is the metal-support interface, which leads to a synergism between the metal and the support. Ultimately, the redox properties of the support have a secondary role compared to the active metals (Pt and Au) in terms of WGSR activity.

The use of catalysts consisting of low cost metals such as Cu and Ni supported by ZrO_2 and CeO_2-ZrO_2 were studied by Chamnankid et al., [39]. At high temperatures (>350°C), the Ni catalysts provided the highest conversion of CO; however, CO_2 yield was greatest over the CeO_2ZrO_2 supported catalyst. Nevertheless, at lower temperatures the Cu/CeO_2-ZrO_2 was superior with higher conversions and better stability. At temperatures <200°C, the Ni catalysts experienced irreversible adsorption of CO and promoted methanation. In general, Chamnankid et al., [39] concluded that the ceria-zirconia catalysts performed the best over a wider temperature range due to CeO_2's oxygen storage capabilities and the stabilization/promotion effects from ZrO_2. In regards to the reaction mechanism, Chamnankid et al., [39] noted the formation of a formate intermediate on the catalyst surface. It was suggested that CO_2 is produced from the decomposition of this intermediate which is the rate limiting step particularly at low temperatures.

In order to improve catalysts activity and WGSR selectivity, bimetallic PtNi catalysts supported on various oxide supports were developed by Wang et al., [40]. Acknowledging the two separate mechanisms that have been proposed for WGSR over supported metal catalysts – the redox mechanisms and the formate decomposition mechanism – Wang et al., [40] noted that in both mechanisms, the role of the metal is to adsorb CO. Therefore, reducing CO binding energy to an appropriate amount would be beneficial. Indeed, they did demonstrate that the addition of Ni Pt effectively reduced the Co binding energy possibly leading to an increase in WGSR activity. It was also concluded that reducible supports allow for higher WGSR activity in general with the following trend: CeO_2> ZrO_2 (high surface area) > TiO_2 ≈ γ-Al_2O_3 > SiO_2 > ZrO_2 (low surface area).

Watanabe et al., [41] took a different approach to bimetallic catalysts and used Ni with an oxophilic metal, Fe, with a mesoporous ceria-zirconia support. Their NiFe/CeO_2-ZrO_2 catalyst, in which ceria-zirconia was prepared using nano-casting on KIT-6 as a hard template, provided superior results (~75% CO conversion at ~350°C) compared to catalysts prepared using CeO_2 and co-precipitated ceria-zirconia. A greater surface area was achieved when using the nano-casting preparation technique. The addition of zirconia provided structural stabilization and enhanced the mobility of lattice oxygen in the mixed oxide. It was reported that alloying Ni and Fe also enhanced oxygen mobility while suppressing CO methanation. Watanabe et al., [41] described the mechanism by which their catalyst promoted WGSR as a redox model – see Equations 2-6 to 2-10.

$$(CeZr)O_x + NiFe^* \rightarrow (CeZr)O_{x-\delta} + NiFe \cdot O \quad \textbf{2-6}$$

Oxygen transferred from mixed oxide support to Fe catalyst sites [41]

$$^*NiFe + CO \rightarrow CO \cdot NiFe \quad \textbf{2-7}$$

Weak adsorption of CO at Ni sites [41]

$$NiFe \cdot O + CO \cdot NiFe \rightarrow CO_2 + {}^*NiFe + NiFe^* \quad \textbf{2-8}$$

Bi-functional CO oxidation at neighboring NiFe sites [41]

$$NiFe^* + H_2O \rightarrow H_2 + NiFe \cdot O \quad \textbf{2-9}$$

H_2 formation via preferential oxidation of metallic Fe sites by H_2O [41]

$$(CeZr)O_{x-\delta} + NiFe \cdot O \rightarrow (CeZr)O_x + NiFe^* \quad \textbf{2-10}$$

Oxygen back transferred to the mixed oxide support from Fe [41]

In their review, Ratnasamy & Wagner [34] noted that for low temperature WGSR, catalysts typically consist of copper in industry; however, copper has also been studied for high temperature reactions. Cu and Re monometallic and bimetallic catalysts on ceria and Gd-doped ceria based supports were studied by Tepamatr et al., [42]. The catalysts were shown to be very suitable as WGSR catalysts at high temperatures (80% CO conversion at 400°C) due to their stability and resistance to deactivation in CO_2-rich gas (as opposed to traditional iron oxide catalysts). The addition of Re to Cu apparently increased activity significantly to a conversion of 93% at 400°C as the Re helped reduce the ceria support producing additional oxygen vacancies. It is noted though that a conversion of 93% at 400°C likely exceeds equilibrium conversion suggesting that either methanation prevails significantly, or either H_2 or CO_2 is being consumed by another reaction.

2.1.4 Impact of Catalysts on Biomass Decomposition

With the prospect of introducing additives or heterogenous catalysts to the thermal decomposition of biomass processes, it is necessary to understand how these additives will impact the decomposition reactions. In Section 2.1.2 catalysts and additives were highlighted for producing internal hydrogen via reforming and WGSR. Although liquid product yield and catalytic impact on biomass decomposition was not significantly important to the studies performed by the Harris group, the impact on decomposition can be gleaned from their thermogravimetric analysis (TGA) and corresponding derivative weight loss (DTA) results [25-27, 31]. A decrease in biomass decomposition temperature indicates the effect of the catalysts during the early stages of decomposition such as dehydration or fragmentation.

TGA/DTA results from Zhao, et al., [26] demonstrated that 5wt%Ni/MCM-41 and 15wt%Ni/γ-Al_2O_3 reduced the temperature at which major cellulose decomposition occurred. The same authors later demonstrated similar results with a Co/γ-Al_2O_3 catalyst [27]. Co supported on silica however did not appear to reduce the decomposition temperature but instead reduced the rate of weight loss. Bimetallic Ni-Co catalysts supported on SBA-15 on the other hand were shown to reduce the decomposition temperature [31]. This demonstrates that both supporting material and active promoter metals of heterogeneous catalysts have an impact on cellulose decomposition. In addition, Widyaningrum et al., [25] tested a 5wt%Ni/γ-Al_2O_3 (as opposed to 15wt% from earlier) that significantly altered the derivative weight loss profile with two major periods of decomposition, the first occurring much earlier than the single period without catalyst. This suggests that loading, particle size, and/or dispersion may have a role. When using CaO to promote WGSR by capturing CO_2, Widyawati et al., [29] did not note a change in temperature in which the maximum weight loss rate occurred. Instead, the addition of CaO dampened the rate of weight loss likely due to the capturing of an otherwise volatilized species (ie. CO_2 or even H_2O).

The impacts of salts and impregnated metals on the decomposition of biomass has also received attention as biomass material may naturally contain these minerals or these minerals could be added to assist in pyrolysis [43-48]. Patwardhan, et al.,[43] looked at the effects that inorganic salts containing alkaline or alkaline-earth metals such as $CaCl_2$, $Ca(OH)_2$, and $CaCO_3$ have on the product distribution of the primary pyrolysis reaction of

cellulose. They found that the inclusion of the salts significantly reduced the yield of levoglucosan in favor of other compounds such as glycolaldehyde and, in the case of alkali-earth metals, furanic compounds highlighting that such minerals promote dehydration. Patwardhan, et al.,[43] also found that there is a dependence on the anion as well.

In general, chloride salts have been shown to significantly impact biomass decomposition. Carvalho et al., [44] reported that the temperature of the maximum decomposition rate of sweet sorghum bagasse biomass decreased by ~44°C when the catalyst was impregnated with 5% $ZnCl_2$. It was suggested that the Lewis acidity of $ZnCl_2$ promoted heavy dehydration and char formation due to C-C and C-O bond cleavage. This was also demonstrated by Lu et al., [47] who reported that not only did $ZnCl_2$ significantly promote dehydration, it also promoted the production of furfural and acetic acid. Liu et al., [46] tested the impact of loading salts, NaCl, KCl, $MgCl_2$, and $CaCl_2$, onto cellulose had on decomposition and reported that although the salts had significant impact on dehydration reactions due to their Lewis acidity, they did not have a large influence on depolymerization reactions.

Collard et al., [45] alternatively studied the influence of transition-metals on decomposition reactions by impregnating biomass with nickel nitrate and iron nitrate. Both metals were found to promote char formation and reduction in tar formation. The addition of Ni however helped depolymerize xylan and increased hydrogen production – in agreement with topics discussed in Section 2.1.2.

Although scarce, some traditional heterogenous catalysts have been studied for their direct impact on biomass decomposition. Zabeti, et al.,[49] found that alkali-modified amorphous silica alumina was capable of promoting dehydration reactions leading to the production of alkylated furanic compounds. It was concluded that a material with milder acidity (inferring fewer Brønsted-Lowry acid sites) is beneficial for the production of furanic compounds. Jeon et al., [50] reported that mildly acidic AlSBA-15 promoted the dehydration and cracking of pyrolysis vapours. However, in their experiments, biomass was separated from the catalyst thereby inhibiting direct interactions.

More recently, a catalyst that more closely resembles those discussed in Section 2.1.3 for WGSR (and deoxygenation), NiCu/γ-Al_2O_3 was tested by Kan et al., [51] for the catalytic pyrolysis of coffee grounds. The addition of the catalyst led to a change in decomposition rates within the temperature range of 360-513°C and produced more CO and CO_2. Increasing Cu content lead to a further increase in CO and CO_2. As a result, the addition of the catalyst led to decreased liquid product yields.

2.1.5 Summary

Cellulose decomposition has been shown to produce glucose as an intermediate which then produces furanic compounds. During decomposition, several strategies can be adopted to enhance hydrogen production – performing tar cracking and consume light components in reforming reactions or use the already available CO and H_2O to produce H_2 by promoting WGSR. Although high yields of H_2 can be achieved by using the reforming route, it may potentially reduce liquid product yield. Therefore, promoting WGSR is most ideal.

Traditional WGSR catalysts tend to be pyrophoric and can suffer from oxidation related damages. As such, new bimetallic catalysts supported on mixed oxides are worth exploring. Overall, the catalyst used in the proposed system for biomass decomposition with *in-situ* hydrogen production and deoxygenation have the potential for directly impacting biomass decomposition. This is most apparent with catalyst that have Lewis acid sites.

2.2 Selective Deoxygenation of Biomass-derived Bio-oils Within Hydrogen Modest Environments

Within recent years, there has been an increasing interest in the development of biofuels because of the threat of global climate change and a shortage of oil reserves [3, 14, 17, 52]. It is in current society's best interest that engineers and scientists endeavour to develop new and sustainable energy resources whilst reducing greenhouse-gas emissions. Within the transportation industry, biofuels are the only carbon neutral alternatives that are becoming increasingly important as they possess the potential to be incorporated into existing infrastructure [53].

Some biofuels have already begun to merge into the transportation industry including bioethanol and biodiesel composed of fatty acid methyl esters (FAME). There are however concerns about these first-generation biofuels. First of all, they cannot totally replace fossil fuels – gasoline and diesel – due to differences in properties such as reduced energy densities and viscosities at low temperatures [1-3]. Secondly, especially for the first-generation bioethanol, biofuels ideally should not be produced from food sources. Second generation biofuels aim to resolve the issues with the first-generation fuels by producing

fully compatible fuels from sources that cannot be used for food such as non-edible vegetable oils, lignocellulosic material, and wastes.

The second part of this literature review concerns second generation biofuels produced via thermal processes such as pyrolysis and liquefaction. Compared to typical hydrocarbon fuels, both vegetable oil and bio-oil are poor selections as direct fuels due to their high oxygen content, which leads to high viscosities, low volatility, corrosiveness, poor solubility in other hydrocarbons, and low energy content [2, 10-12]. These oils tend to be hydrophilic, which can lead to high water contents and/or polymerization. Bio-oil typically has oxygen content within the range of 10-40 wt% or even as high as 50 wt% and a water content of 15-30% [54, 55]. One solution to the oxygen-related problems is to perform deoxygenation via a heterogeneous catalyst similar to how petroleum oil undergoes desulfurization and denitrification via a hydrotreatment process. The main objective is to effectively remove oxygen in the form of CO_2, CO, or H_2O.

Therein lies an issue – the use of hydrogen. Hydrogen has been a major requirement for performing deoxygenation of vegetable oils and bio-oils [13, 14, 55]. However, there is a desire to reduce hydrogen consumption and use systems that are either hydrogen-modest (low hydrogen pressures/flow rates) or use an inert atmosphere (no hydrogen) [3, 13, 14]. This is due to the costs associated with the use of hydrogen and the fact that the majority of the world's hydrogen production comes from fossil fuel reforming. Ideally, biofuels, which are supposed to be considered sustainable and renewable, should not be heavily dependent on non-renewable sources.

Gosselink *et al*., [3] reviewed the deoxygenation of vegetable oils, fatty acid esters, and free fatty acids with a major focus on reaction pathways – especially in the presence of H_2. Santillan-Jimenez & Crocker, [14] focused primarily on reaction pathways for the deoxygenation of fatty acids in inert atmospheres. De *et al*., [17] provided an overview of recent work in the hydrodeoxygenation of bio-oil compounds derived from thermal processes. Mortensen *et al*., [55] briefly covered hydrodeoxygenation processes of bio-oil. Reviews have also been conducted for the individual constituents that comprise bio-oil such as Nakagawa *et al*., [56] whom reviewed the upgrading of holocellulose-derived furanic compounds with a focus on general reaction pathways while Bu *et al*., [16] discussed lignin-derived phenolic compounds.

Despite the plethora of research carried out within the past decade, there appears to be a lack of acknowledgement towards the development of catalysts for selectively deoxygenating bio-oils in hydrogen modest environments. Therefore, the purpose of this review is to summarize work conducted in the development of the deoxygenation of vegetable oils and major bio-oil compounds (phenolic and furanic compounds) within H_2-modest environments.

Herein, hydrogen-modest environments are defined as having a severely reduced external supply of H_2 gas with pressures near atmospheric pressures, well below typical minimum pressures required for HDO processes. Emphasis and insights are provided for the development of catalysts that promote major reaction pathways that require low amounts

of H_2. It has been shown that traditional catalysts such as sulfide catalysts provide unfavorable results within these H_2-modest systems. On the other hand, bimetallic catalysts containing an oxophilic metal and an active metal are shown to promote selective deoxygenation reactions that would prove beneficial in H_2-modest systems. Finally, the potential for research on catalytic deoxygenation that makes use of internal hydrogen resources is also highlighted.

Through thermodynamic calculations for deoxygenation reactions, several authors have demonstrated that equilibrium does not constrain these reactions and thus reaction kinetics are deemed the constraining factor for product selectivity [14, 55, 57]. The foremost decision in promoting selectivity is catalyst selection followed by the optimization of the reaction conditions. Therefore, the study herein focuses primarily on the selection of an appropriate catalyst with recognition towards the effects of reaction conditions.

2.2.1 Vegetable Oils/Triglycerides/Fatty Acids

The general deoxygenation of fatty acids and triglycerides from both edible and non-edible vegetable oils is widely discussed in literature [3, 13, 14, 58-81]. Reaction conditions that have typically been applied are temperatures ranging from 230°C to 375°C and H_2 pressures ranging from 10 bar to 110 bar; however, some researchers have begun to study the application of atmospheric pressures or even inert atmospheres. Researchers have evaluated the processes by looking at various compounds and model oils such as the vegetable oils themselves, methyl and ethyl esters, and fatty acids. Vegetable oils are comprised mostly of triglycerides and some free fatty acids. The structure of triglycerides

contains three fatty acids bound to a single propane unit via ester bonds (see Figure 2-2). It is worth noting that all fatty acids have even-numbered carbon chains. When performing catalytic deoxygenation of vegetable oils, the main objective is typically to produce paraffins or olefins that may later undergo further processing into useful fuels.

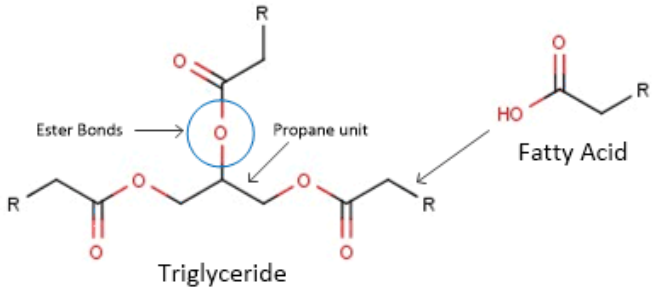

Figure 2-2: Structures of triglycerides and fatty acids

2.2.1.1 Reaction Mechanisms

2.2.1.1.1 Breakdown of Triglycerides

Compared to deoxygenation reaction pathways for fatty acids, the reaction mechanisms by which the initial breakdown of triglycerides may occur have received far less attention and require additional research before they can be completely understood. Nonetheless, with vegetable oils as a feedstock, it is important to note how these reactions are dependent on reaction conditions especially H_2 pressure.

It is often reported that during catalytic deoxygenation processes, the breakdown of triglycerides leads to the production of fatty acids and propane. Within the reaction conditions stated earlier for vegetable oils; the mechanism that is widely reported/accepted for the initial breakdown of triglycerides is termed as β-elimination [3, 14, 70, 77]. The β-elimination mechanism starts off with the removal of one fatty acid unit, leaving a glycol

difatty ester unit (see Figure 2-3) [14, 70]. In order to subsequently remove the other fatty acids, the carbon double bond must be hydrogenated [70]. Therefore, within an inert atmosphere, triglycerides may produce fatty acid intermediates; however, conversion via β-elimination is limited to how much hydrogen is available either on the catalyst surface or produced via side reactions (for example, dehydrogenation of fatty acid chains). Although many authors have accepted β-elimination as the primary reaction mechanism for the breakdown of triglycerides, there is still a need for additional proof.

Researchers have also proposed other reaction mechanisms that may lead to the breakdown of triglycerides including direct deoxygenation, γ-hydrogen transfer, and hydrolysis [3, 13, 70, 75-77]. Figure 2-3 depicts all four major reaction mechanisms that have been proposed for the breakdown of triglycerides. There are limited research studies in the area of γ-hydrogen transfer and direct deoxygenation reaction mechanisms within the typical deoxygenation reaction conditions. Direct deoxygenation is characterized by a reaction in which the intermediates that are produced from the breakdown of the triglyceride remain adsorbed onto the catalyst surface without a fatty acid intermediate. This mechanism has yet to receive any quantifiable evidence required to deem it a major pathway [75, 76]. For producing hydrocarbons at a low H_2 consumption, the γ-hydrogen transfer mechanism does look promising, however it is expected to be a more prevalent reaction mechanism for hydrocracking processes rather than for deoxygenation reaction processes. This mechanism produces C_{n-2} hydrocarbons from the original fatty acid carbon chains at temperatures around 450°C as opposed to the typical deoxygenation reaction temperature

range of 230-375°C [3, 70]. At such temperatures, cracking of the hydrocarbon chains should be anticipated [82-85].

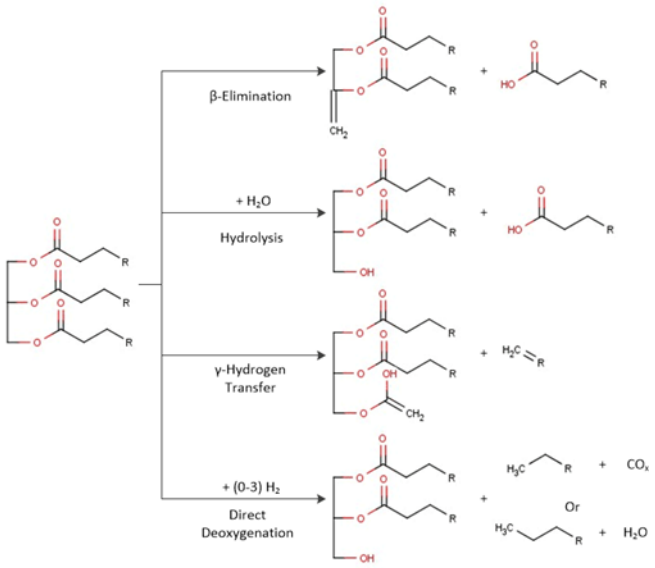

Figure 2-3: Initial break down of triglycerides [3, 13, 70, 75-77]

The hydrolysis reaction route successfully produces fatty acids while producing 1 mole of glycerol rather than propane [13, 86, 87]. It has been reported as a potential reaction step in the deoxygenation reaction process. For example, Senol *et al*., [88] suggested that during the deoxygenation of methyl hexanoate within a temperature range of 250-300°C at 1.5 MPa, the methyl ester may undergo de-esterification via a hydrolysis reaction over sulfided catalysts supported on γ-Al_2O_3. Gosselink, *et al*., [3] suggested that this may also be applicable to triglycerides. Hollak *et al*., [87] further demonstrated the hydrothermal deoxygenation of triglycerides that involved the hydrolysis of triglycerides and deoxygenation of subsequent fatty acids at 250°C without H_2 over a Pd/C catalyst, however they were unable to attain high yields of deoxygenated hydrocarbons.

For a typical deoxygenation process; β-elimination still remains the most predominant reaction mechanism reported throughout literature for the breakdown of triglycerides during catalytic deoxygenation [3, 14, 77]. The reliance on β-elimination is an issue when it comes to catalytic deoxygenation without hydrogen since it is required (at least to some extent) to successfully remove all three fatty acids. It is possible to remove oxygen from fatty acids without hydrogen present – as will be discussed later. As a result, it has been claimed that, in a hydrogen modest system, the rate-determining step for the deoxygenation of vegetable oils are the β-elimination reactions [63]. Therefore, in order to develop viable processes for deoxygenating vegetable oils in low H_2 atmospheres or even inert atmospheres, the challenge is either to promote one of the other reaction mechanisms – such as hydrolysis – or change the source of hydrogen.

2.2.1.1.2 Deoxygenation of Fatty Acids

Oxygen can be removed from fatty acids producing alkanes/alkenes via three main reaction pathways, hydrodeoxygenation (HDO), decarbonylation (DCO), and decarboxylation (DCO_2). These reaction pathways are summarized in Figure 2-4. The HDO pathway, which consumes the highest amount of hydrogen, is an overall exothermic reaction process that removes oxygen as water through a series of hydrogenation and hydrogenolysis reactions. DCO removes oxygen as both water and CO producing alkanes/alkenes with one less carbon than the precursor fatty acid with the consumption of 0-1 mole of hydrogen per mole of fatty acid depending on the reaction mechanism that will be discussed later in greater detail. DCO_2 releases oxygen as CO_2 while producing alkanes with one less carbon unit. DCO_2 effectively consumes no hydrogen and has actually been shown to be inhibited

by too high H_2 pressures [62, 74]. Unlike the HDO reaction pathway, the DCO_x reaction pathways are overall endothermic reactions and generally favour increasing reaction temperatures, whereas HDO reactions may experience a decline in selectivity [57, 89].

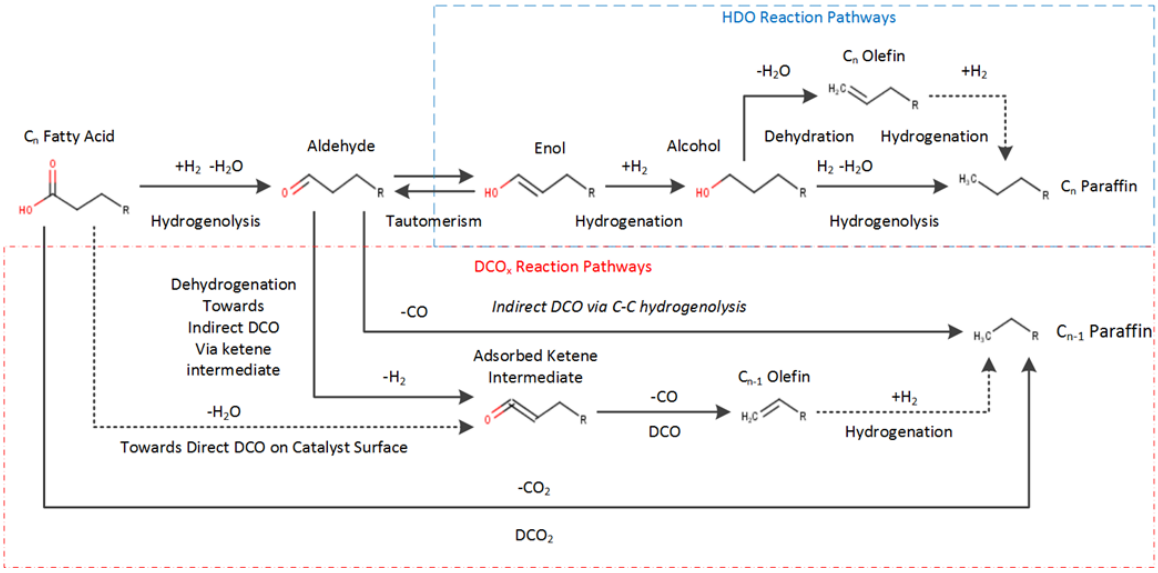

Figure 2-4: Deoxygenation pathways of fatty acids

2.2.1.1.2.1 Primary Deoxygenation Reactions

As seen in Figure 2-4, fatty acids have three initial reaction pathways that can lead to the removal of oxygen. One pathway is the removal of the hydroxyl group as H_2O via a hydrogenolysis reaction mechanism involving dehydration and hydrogenation reactions. The removal of the hydroxyl group via the first pathway is reported to lead to an adsorbed aldehyde intermediate [66-68]. However, the organic species may stay bound to the catalyst and directly undergo subsequent reactions rather than being desorbed as an aldehyde compound. This can potentially result in the "Direct DCO" reaction pathway if the adsorbed intermediate undergoes C-C scission. The third possible reaction pathway for initial deoxygenation is DCO_2.

The actual mechanisms for DCO_2 and direct DCO are not completely understood and additional research is required to verify the mechanisms that have been proposed. Currently, there are three major reaction mechanisms to consider. The first mechanism involves first dehydrogenation of the fatty acid leading to a strongly bound organic compound which, after C-C scission, would have to undergo hydrogenation in order for it to be desorbed [62]. This mechanism has been explored in great detail by Lu *et al*., [62] who researched the DCO_x reaction mechanisms of carboxylic acids (propionic acid) on a Pd(111) model surface at various hydrogen partial pressures: 0.01 bar, 1 bar, and 30 bar.

At all pressures, the DCO_2 reaction pathway was shown to begin with the partial dehydrogenation of the α-carbon followed by the dehydrogenation of the hydroxyl group, and then total dehydrogenation of the α-carbon leading to a strongly adsorbed organic compound. C-C scission releases CO_2. Before the product may be released, it must undergo hydrogenation and hydrogen-transfer to produce either an alkene or an alkane [62]. The direct DCO reaction mechanism begins with the partial dehydrogenation of the α-carbon. In a very low hydrogen environment (0.01 bar), this step is followed by dehydrogenation of the β-carbon then removal of –OH group. At the higher H_2 partial pressures, the previous two steps are in reverse order. Prior to C-C scission releasing CO, the β-carbon is once again dehydrogenated. A final alkene or alkane product is released upon hydrogenation of the carbon pool [62]. Overall, the direct DCO route was found to be more kinetically favourable, however it was found that both reaction pathways suffered as hydrogen pressure was increased. It is also important to note that the re-hydrogenation of the carbon

pool was deemed as one of the rate-limiting steps in the mechanism. This suggests that it is important that the catalyst maintain surface hydrogen in the proximity of the adsorbed carbon pool, otherwise, these reaction mechanisms pose a risk of catalyst coking.

The other possible mechanisms for direct-DCO_x include the production of formic acid as an intermediate and ketonization [73, 78-80]. It has also been proposed that DCO_2 occurs via the formation of formic acid which readily decomposes to CO_2 and H_2 [73, 78, 79]. The hydrogen that is produced would then be consumed for hydrogenating the resulting C=C bond. Alternatively, formic acid may decompose into CO and H_2O which would be favoured in hydrogen-containing environments [80]. Although there is a lack of quantifiable evidence to support this mechanism due to formic acid's rapid decomposition, this mechanism cannot be ruled out and should receive be considered [67]. Another reaction mechanism that has been postulated for the removal of oxygen from fatty acids is ketonization with subsequent deoxygenation [58, 66, 70]. This reaction mechanism, however, has not been widely discussed and is not as widely accepted as the C-C scission and formic acid mechanisms.

2.2.1.1.2.2 Secondary Deoxygenation Reactions

If hydrogenolysis occurs as the primary deoxygenation reaction, producing an aldehyde intermediate, then secondary deoxygenation reactions are required in order to remove the remaining oxygen atom. The aldehyde intermediate may undergo indirect-DCO or subsequent HDO reactions (see Figure 2-4).

For indirect-DCO, two mechanisms have been proposed, both starting with an adsorbed alkanoyl structure. One of such reaction mechanisms resembles the direct-DCO mechanism described by Lu *et al*., [62] where the aldehyde forms a ketene intermediate on the catalyst surface [68]. Ruinart de Brimont *et al*., [68] suggested that this mechanism is favourable when the alkonyl species is in close proximity to another organic species that requires hydrogen for its reaction – such as the hydrogenolysis of an adjacent fatty acid. The presence of a ketene structure on catalyst surfaces was confirmed by Peng *et al*., [66] however they proposed that it was part of a ketonization reaction pathway that led to DCO_2. This mechanism could produce an alkene at an overall consumption of no H_2 from fatty acid to alkene.

The second reaction mechanism that has been proposed for indirect-DCO involves a hydrogenolysis reaction [58, 66]. This reaction route uses surface hydrogen to break the C-CO bond producing an alkane and CO [66, 68]. Starting from a fatty acid to the production of the alkane unit, this reaction pathway consumes 1 mole of H_2. Since the alkene and alkane produced from either indirect-DCO reaction pathway may be produced from each other via hydrogenation/dehydrogenation and the fact that hydrogen is involved in both reaction pathways, it is difficult to distinguish between the two without performing an in-depth mechanistic study on a per catalyst basis.

Alternatively, the adsorbed aldehyde species may not undergo DCO and may instead follow the HDO route where it is hydrogenated to an alcohol which may then undergo dehydration/hydrogenolysis. This route is undesired as it would require two additional

moles of hydrogen to produce an alkane or one additional mole if dehydration of the alcohol is favored to produce an alkene. It has been proposed that the aldehyde and alcohol products are in hydrogenation/ dehydrogenation equilibrium due to keto-enol tautomerism [66]. The removal of the hydroxyl group is considered the final step of the HDO reaction pathway and is considered rate determining [66, 67]. In a hydrogen modest system, this reaction is not expected to significantly occur due to the fact that 3 moles of H_2 are required to produce an alkane from a fatty acid. In this regard, the indirect DCO reaction route is more desirable as it requires less hydrogen and since H_2O and CO are both produced from this pathway, there is a possibility of reproducing any H_2 that is consumed (see Section 2.2.4.3).

2.2.1.1.2.3 Side Reactions and Pathway Selection

Throughout the reaction pathways that have been mentioned, other reactions, such as hydrogenation or the reverse, dehydrogenation, are possible – depending on reaction conditions such as H_2 pressure and temperature. When little-to-no hydrogen is available, it is expected that dehydrogenation reactions will occur. Excessive dehydrogenation can lead to the formation of aromatic structures [57]. Other side reactions that must be considered are cracking reactions that can produce shorter hydrocarbon chains (such as C_4-C_{10}) from long paraffinic products such as hexadecane or even fatty acids at elevated temperatures ≥300°C [57, 59, 60, 81, 90].

DCO_2 and DCO reaction routes have been claimed as more appealing reaction routes as they require less hydrogen [14]. As DCO_x reactions are related to cracking reactions; they

have been shown to be most prevalent at elevated temperatures (typically >300°C) due to their endothermicity [13, 57, 61, 72, 90, 91].

2.2.1.2 Catalyst Selection

Although many studies have been performed for the general deoxygenation of vegetable oils and fatty acids, these studies appear to be mostly limited to the application of certain catalysts. These would include conventional sulfide catalysts that are used for desulfurization/denitrification in the petroleum industry – supported CoMoS and NiMoS catalysts – and monometallic metal catalysts – specifically Ni, Pt, and Pd. Compared to studies performed with phenolic and furanic compounds, the development of bimetallic catalysts has received very little attention for deoxygenating vegetable oils. The potential for using bimetallic catalysts with vegetable oils is discussed in Section 2.2.4.2.

2.2.1.2.1 Active Material

2.2.1.2.1.1 Sulfide Catalysts

In general, sulfided NiMo and CoMo catalysts are regarded as not being active within a hydrogen free environment [3]. Although the selectivity of sulfide catalysts may be promoted toward DCOx reactions by a second metal such as Ni or simply elevating temperature (>350°C), these catalysts are overall reported as being most active towards the HDO reaction route and rely heavily on hydrogen [61, 72, 73, 89]. Reports have stated that decreasing hydrogen pressure over a sulfide catalyst increases the selectivity towards DCO_x reactions often, at the cost fatty acid conversion and overall yield of desirable products [61, 72, 73, 90, 92]. Therefore; it can be theorized that the selectivity toward

DCO_x reactions increases because the reaction rate of the HDO route drops allowing the DCO_x to be more competitive.

Sulfide catalysts are an inappropriate choice for deoxygenating fatty acids in a hydrogen-modest system because they lack activity towards DCO_x reactions and suffer from major deactivation issues. During the hydrotreatment of vegetable oils/fatty acids, sulfide catalysts have been shown to deactivate due to the removal of sulfur from the surface as a result of oxidation and coking [72, 93, 94]. Therefore, to maintain catalyst activity, a sulfur source such as H_2S is required to be fed into the system to replenish sulfur sites on the catalyst. This has been reported as being a drawback for these catalysts with respect to environmental issues [3, 14]. In addition, maintaining activity has been shown to be difficult as some degradation of sulfur sites is irreversible [93].

2.2.1.2.1.2 Monometallic Catalysts

Monometallic transition metal catalysts are becoming very common for the deoxygenation of fatty acid/triglycerides. The most commonly researched catalysts are Ni and noble metals, Pt and Pd. In general, these catalysts have been shown to be selective towards DCO_x reactions [13, 57, 60, 64, 66, 71, 95]. Snåre *et al*., [57] screened various catalysts for their activity towards DCO_x reactions at 300°C with a He pressure of 6 bar. They determined that the reactivity of the catalysts proceed in the follow order: Pd>Pt>Ni>Rh>Ir>Ru>Os [57].

Monometallic catalysts have been tested in both hydrogen-rich and inert/low-hydrogen environments. Rozmyslowicz *et al*., [67] demonstrated that in both a hydrogen-rich and a

hydrogen-free environment, Pd is selective towards DCO_x. In comparison, reactions within the inert atmosphere were far less active as the yield of hydrocarbons was 36% less than that of the hydrogen-rich environment. Later, Hengst *et al*., [60] reported that when treating oleic acid in a hydrogen environment, adding 0.5 wt% Pd to a γ-Al_2O_3 support increased conversion and C_{17}-selectivity from 50% at 0% selectivity (without the addition of Pd) to 90% at 30% selectivity. Further increasing Pd content to 2 wt% increased conversion to 99% and C_{17}-selectivity to 47 wt% selectivity [60]. In conjunction, Alotaibi, *et al*., [58] reported that DCO_x only occurred on Pt and Pd catalysts when in the presence of a hydrogen atmosphere. The higher dependence on H_2 that was reported by Alotaibi *et al*., [58] may be due to the use of an acidic salt, $Cs_{2.5}H_{0.5}PW_{12}O_{40}$, as a support.

Peng *et al*., [66] reported that their Ni/ZrO_2 catalyst favoured palmitic acid DCO_x at 12 bar H_2 (temperature of 260°C) with a selectivity towards pentadecane of 90% and overall conversion of 100%. However, upon changing to an inert N_2 atmosphere, selectivity and conversion decreased to 16% and 3.5% respectively. It is therefore concluded that even though monometallic catalysts favour DCO_x reactions, a source for disassociated hydrogen protons on the catalyst surface is still required in order to provide adequate results. The optimum amount of hydrogen required is yet to be determined.

In Section 2.2.1.1, it was suggested that direct-DCO_x reactions diminish with increasing H_2 pressures, as was demonstrated by Lu *et al*., [62]'s microkinetic model on a Pd(111) surface. Since Pd and Pt catalysts have been shown to persevere in hydrogen environments, it is likely that, as Peng *et al*., [66] suggested for their Ni catalyst, the Pd and Pt catalysts

follow an indirect-DCO route which is faster than direct-DCO_x reaction in the presence of H_2 [58, 66, 67].

One, well known issue with monometallic transition metals used for the deoxygenation of fatty acids is severe catalyst deactivation, which has been reported for catalysts in inert atmospheres [57, 59, 96]. For example, Bernas *et al*., [59] observed that within 28 hours of treating dodecanoic acid in Ar at 300°C their 1% Pt/Sibunit catalyst activity decreased as conversion dropped from 85% to 3%. It was determined that catalyst deactivation was due to coking [59]. This may be explained by the reaction mechanisms that were described by Lu *et al*., [62] who concluded that one of the rate limiting steps in DCO_2 and direct-DCO is the hydrogenation of the hydrocarbon pool. A catalyst's inability to hydrogenate the hydrocarbon pool would effectively lead to carbon deposition.

Based on the literature, it is concluded that transition metal catalysts are an appropriate selection for the deoxygenation of fatty acid containing oils within a hydrogen modest system – especially when compared to sulfide catalysts. Two issues that are worth considering though are costs and deactivation. Due to the high costs associated with the noble metal catalysts, it is recommended that work be done to develop catalysts that are equally active yet more cost effective. It has been claimed that Ni catalysts with an increased metal content can achieve comparable results as the noble catalysts [77]. In order to further promote selective deoxygenation with minimal hydrogenation activity, researchers are advised to study the deoxygenation of triglycerides with catalysts that have been developed for phenolic and furanic compounds such as bimetallic catalysts. Processes

that are completely hydrogen free do not appear to be viable due to reduced activity, increased deactivation, and the fact that complete conversion of triglycerides is difficult due to limitations with regards to β-elimination reactions. Therefore, a low-hydrogen containing environment should be used with a catalyst that is able to maintain high activity.

2.2.1.2.2 Catalyst Support

Catalyst supports that have been widely used by researchers include carbonaceous (for noble metal catalysts in particular) and SiO_2 supports as these materials are generally inert towards the deoxygenation. Many studies have also applied alumina and zeolite as supporting materials as they are conventional supports use in the hydroprocessing of petroleum fuels. An ideal support should be one that works in tandem/synergistically with the active material.

The acidity of catalysts can impact their activity by providing additional reaction sites, which may be used for hydrogen disassociation or adsorption of the oxygenated compounds. Some supporting materials such as zeolites and alumina are regarded as acidic supports and, especially for the case of zeolites, contain an abundance of Brønsted acid sites (alumina supports tend to consist of more Lewis acid sites) [3, 66]. Brønsted acid sites promote sequential hydrogenation-dehydration-hydrogenation reaction routes – such that would favour HDO reaction pathways [66, 97]. However, the presence of strong acid sites, such as those found on zeolites, have been shown to be prone to rapid deactivation due to coke deposition [60].

Lewis acid sites, on the other hand, were observed to promote indirect-DCO reactions [66, 69, 98]. Addition of appropriate Lewis acidity to catalyst may be considered for enhancing selective deoxygenation. Peng *et al*., [66] demonstrated with the deoxygenation of palmitic acid at 260°C with 12 bar H_2, switching from Pt and Pd supported on C to ZrO_2 increased conversion from 20-30% to >98%. Although the DCO_x selectivity on the Pt catalyst decreased from 98% to 61%; the selectivity towards DCO_x on the Pd catalyst was maintained at 98%. In addition, Ni/ZrO_2 favoured DCO_x with a selectivity of 90% at a conversion of ~100%. It was concluded that the ZrO_2 support had shifted the reaction pathway from direct-DCO to indirect-DCO [66].

Reducible oxide supports containing Lewis acid sites such as ZrO_2, TiO_2, CeO_2, and Cr_2O_3 are able to selectively reduce carboxylic acids to aldehydes [66]. These supports adsorb the oxygenated compounds via oxygen vacancies. It was proposed that this occurs via the abstraction of the hydrogen from the –OH group and an α-hydrogen producing water and a ketene intermediate [66]. This intermediate is hydrogenated to produce an aldehyde by Ni, which eventually undergoes decarbonylation [66]. As a result, the active metal behaves synergistically with the supporting material (see Figure 2-5). Therefore, the presence of a reducing agent such as H_2 remains important for reducible oxide supports as without such, these supports cannot maintain activity.

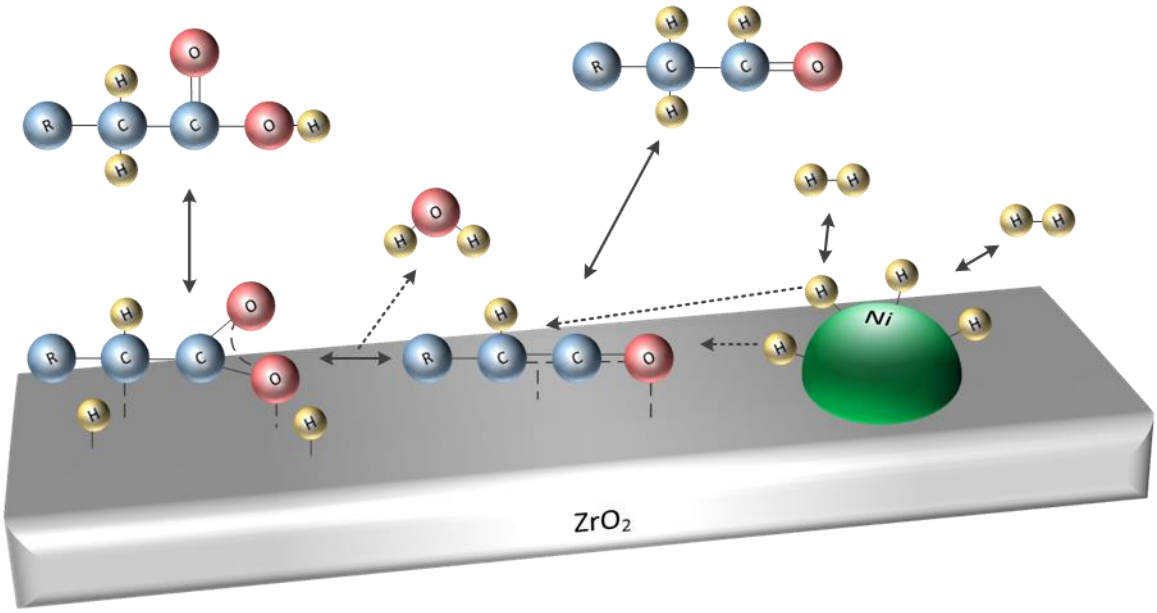

Figure 2-5: Synergism of Ni and ZrO_2 [66]

A novel approach to the development of reducible oxide supports was demonstrated by Shim *et al*., [69] who studied a combination of CeO_2 and ZrO_2 (produced via the co-precipitation of zirconyl nitrate and cerium nitrate) for the deoxygenation of oleic acid. The premise of this was to exploit the nature of these materials to store oxygen, especially CeO_2, and develop a catalytic support material that has improved redox properties and thermal resistance. Reaction studies showed that $Ce_{0.6}Zr_{0.4}O_2$ alone had an oxygen removal efficiency of 32.2% and was selective towards DCO_x reactions when treating oleic acid with 1 atm mixture of 20% H_2 in N_2 [69]. The reactivity of the material was attributed to the cubic phase of the material as it has a higher capability of producing a redox couple between Ce^{4+} and Ce^{3+}. The $Ce_{0.6}Zr_{0.4}O_2$ material was also noted to promote cracking reactions so it was concluded that contact time should be minimized [69].

If a hydrogen-free system is applied in order to deoxygenate fatty acid containing oils, it is advised that the selected catalyst support be inert by nature – such as carbon or SiO_2. Reducible oxide catalyst supports have been deemed unsuitable for a hydrogen-free environment as they require hydrogen for activation. If however, a low-hydrogen-containing environment is desired – such as described in the previous section, the selection of a reducible oxide material as a support may be suitable as they have been shown to have synergistic effects with relevant catalysts such as Ni that improve the overall activity and selectivity towards desirable DCO reactions.

2.2.2 Phenolic Compounds

As research into the possible applications of bio-oil developed via thermal processing of lignocellulosic material is becoming more extensive; work has been conducted to understand and develop processes for the catalytic deoxygenation. Bio-oil is a very complex mixture of various oxygenated compounds due to the various breakdown reactions of cellulose, hemicellulose, and especially lignin; which are dependent on processing conditions and the original feed. In excess of 300 different compounds have been identified in bio-oil [99]. Of these compounds, phenolic compounds, derived from lignin, are prevalent. Most phenolic compounds that are present are either alkyl-substituted phenols such as cresol, or methoxyl-substituted phenols such as guaiacol (see Figure 2-6 for examples of phenolic compounds) [16].

In comparison to fatty acids, phenolic compounds are considered more difficult to deoxygenate due to the aromatic structure. The major challenge for developing

deoxygenation processes for phenolic compounds is the development of catalysts that can perform deoxygenation without saturating the aromatic rings so as to minimize the consumption of hydrogen [16, 17].

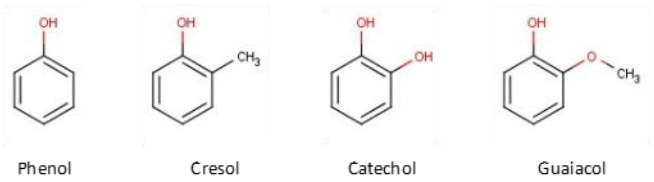

Figure 2-6: Structure of example phenolic compounds

2.2.2.1 Reaction Mechanisms

The actual reaction mechanisms for compounds such as phenol, cresol, and guaiacol (see Figure 2-6) have receive little attention. However, based on the structures of these compounds; it is clear that hydrogen is required to remove oxygen as water. Unlike fatty acids, oxygen cannot be removed in the form of CO or CO_2 therefore, deoxygenation will not occur without a source of hydrogen. Fortunately, work has been conducted to develop catalysts that minimize hydrogen consumption by selectively using hydrogen to remove oxygen and not to saturate the aromatic ring [100-104].

2.2.2.1.1 General Deoxygenation Reaction Pathways

There are two overall reaction pathways that may be followed for deoxygenation of phenolic compounds. The first reaction route involves the complete saturation of the aromatic ring followed by cleavage of the C-O bond likely via dehydration generating a C=C bond to be hydrogenated again [16, 17]. This exothermic reaction pathway is often referred to as the “hydrogenation route” (HYD). The second reaction route is known as the direct deoxygenation route (DDO) and involves a hydrogenolysis reaction to selectively

break the C-O bond while keeping the aromatic structure (see Figure 2-7) [16, 100]. The actual catalytic mechanism for this hydrogenolysis reaction is not fully understood and requires additional research. Although both reaction pathways are exothermic, Mortensen, et al., [55] reported that thermodynamic equilibrium will not have a major hindrance on the reactions at temperatures below 600°C.

The selectivity of DDO reactions over HYD appears to be very dependent on the properties of the catalysts. DDO appears to be dependent on the catalysts ability to adsorb oxygen using oxygen vacancy sites or the use of an oxophilic metal. The phenolic compounds adsorb primarily via the hydroxyl groups with weak interactions with the aromatic ring [100, 105, 106]. In contrast, catalysts that favour HYD reactions do not possess any Lewis acid sites and adsorption occurs via the aromatic ring [54, 106, 107]. These catalysts suffer the inability to surpass the reaction energy barrier required to directly remove oxygen from the ring-structure and must saturate the ring first in order to lower the energy barrier.

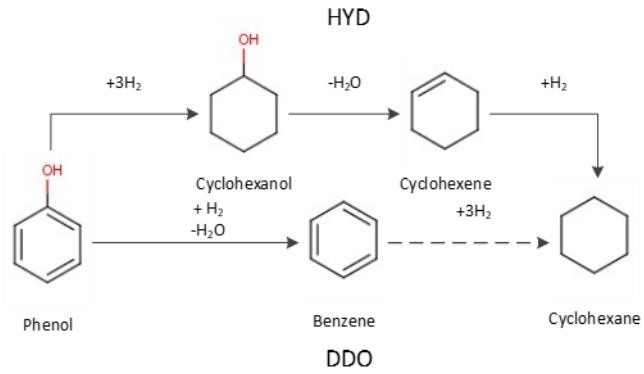

Figure 2-7: DDO and HYD reaction pathways for the conversion of phenol [16, 100]

2.2.2.1.2 Deoxygenation of Substituted Phenolic Compounds

Ortho-substituted phenolic compounds have been deemed as difficult to deoxygenate due to steric hindrance [55, 108]. Guaiacol is a typical example due to the ortho-substituted methoxyl group that requires deoxygenation as well. The catalytic reaction mechanisms for removing the methoxyl group of guaiacol and similar compounds has not been widely discussed. A hydrogenolysis reaction could either break the C-O at the site of the aromatic ring producing methanol (demethoxylation – DMO) or at the methyl group producing methane (demethylation –DME) whilst leaving a hydroxyl group which may undergo subsequent removal from the aromatic ring [101, 102, 109]. For example, Bui *et al*., [102] found both catechol and phenol were the major products from the catalytic deoxygenation of guaiacol. The production of catechol in significant amounts from guaiacol has also been witnessed by Zhao *et al*., [104].

On the contrary, Prasomsri *et al*., [100] witnessed trans-alkylation reactions of methoxyl groups during the deoxygenation of anisole [100]. This therefore demonstrates that in addition to the DMO and DME reaction routes, methyoxyl groups may also undergo trans-alkylation reactions. This was also demonstrated by Runnebaum *et al*., [110] who suggested that it was due to acidic sites on the catalyst support. Figure 2-8 depicts the general reactions related to the deoxygenation of phenolic compounds containing methoxyl groups such as guaiacol.

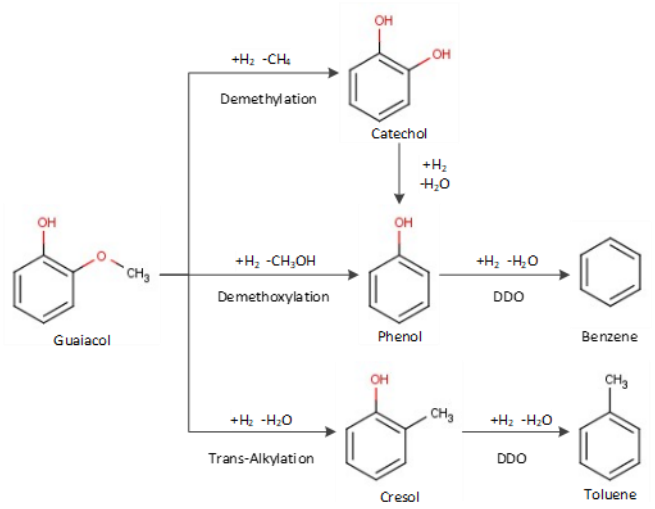

Figure 2-8: Summary of reaction pathways for the selective deoxygenation of guaiacol

One major consideration that must be made when deoxygenating phenolic compounds is that due to fuel regulations, producing benzene is not favourable if the product is to be potentially used in the fuel market. Therefore, focus should be applied to maintaining or possibly adding methyl groups to the aromatic structure. One example would be to attempt to develop a catalyst that is both selective towards the DDO of hydroxyl groups while being selective towards the trans-alkylation of methoxyl groups.

2.2.2.2 Catalyst Selection

Although studies regarding the reaction mechanisms of phenolic compounds is lacking, there appears to be extensive research in the development of catalysts – especially ones that promote high levels of deoxygenation while minimizing hydrogen consumption via ring-saturation and ring-opening reactions. In comparison to work being done with triglycerides/fatty acids; a larger variety of catalysts have been developed for the deoxygenation of phenolic compounds. Catalysts that have received attention include

conventional metal-sulfides, metal-oxides, transition metals, transition metal phosphides, metal carbides, and bimetallic catalysts.

2.2.2.2.1 Active Material

2.2.2.2.1.1 Sulfide Catalysts

Compared to fatty acids, the use of metal-sulfide catalysts has received far less attention. Although promoted MoS_2 is found to be more active than non-promoted MoS_2; sulfide catalysts in general have been found to support the HYD reaction route [101, 111]. In comparison to noble metal catalysts, sulfide catalysts have been shown to produce more DDO reaction pathway products [112]. On the other hand, deactivation of sulfide catalysts during deoxygenation of bio-oils is a widely studied topic. Like for vegetable oil, a sulfur source must be added to the bio-oil in order to maintain activity which likewise has been deemed unfavourable [55, 113-115]. The major issue is with regards to the high water content in bio-oil; which has been observed to rapidly oxidize and deactivate sulfide catalysts by replacing sulfur and/or producing a sulfate phase that blocks active sites [114, 116, 117]. At elevated reaction temperatures, sulfide catalysts have also been shown to deactivate due to coking [113, 114]. It is noteworthy that in comparison to other catalysts, sulfide catalysts have received more attention in the literature with regards to deactivation and are therefore considered more mature.

2.2.2.2.1.2 Metal-Oxide Catalysts

Metal-oxide catalysts have received much attention. It has been proposed that due to oxygen vacancies, which act as acid sites, some metal oxide catalysts may be selective towards DDO [55, 100, 118]. This was demonstrated by Prasomsri *et al*., [100] who used

a MoO_3 catalyst to deoxygenate various model compounds for biomass-derived oxygenates. Aromatic oxygenates were successfully converted to oxygen free aromatics confirming that the catalyst promoted the DDO reaction pathway. As for deactivation; the catalyst may be regenerated by a simple calcination procedure. It was suggested that hydrogen pressure should be increased in order to prevent water from blocking active sites, however, this would not be viable in systems where the attempt is actually to minimize hydrogen consumption [100]. See Figure 2-9 for the general deoxygenation mechanism of MoO_3. Based on results obtained by Whiffen & Smith, [119] who found that MoO_3 is less active than MoS_2; Mortensen *et al*., [55] suggested that WO_3 may be a more suitable catalyst than MoO_3.

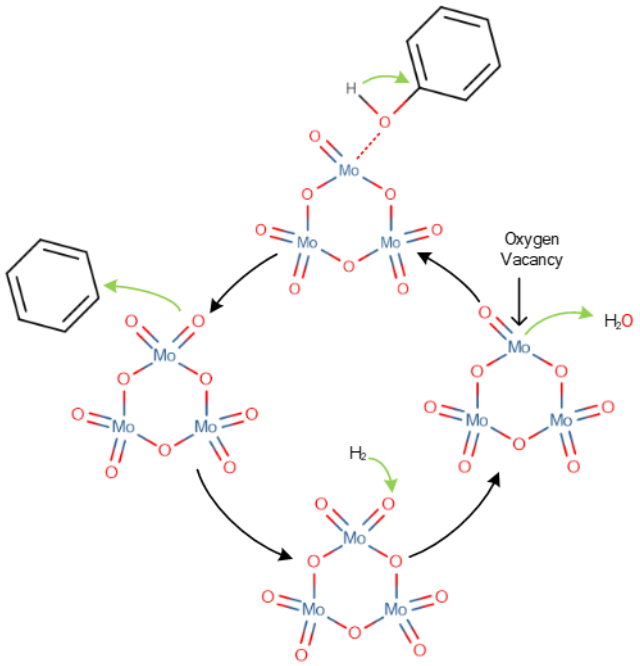

Figure 2-9: General deoxygenation mechanism of MoO_3 [100]

2.2.2.2.1.3 Metal-Phosphide Catalysts

A new type of catalyst that has been proposed for catalytic deoxygenation of bio-oil compounds is the transition metal phosphide. Zhao *et al*., [104] proposed the use of transition metal phosphide catalysts for the catalytic deoxygenation of guaiacol.

After testing a variety of transition-metal phosphide catalysts supported on SiO_2; Ni_2P was found to be the most active and stable. At 300°C and atmospheric pressure, the Ni_2P catalyst was shown to be selective towards the production of benzene with a ~60% selectivity at a conversion of 80% [104]. In later work, the same research group proposed that transition metal phosphide catalysts, such as Ni_2P, are comparable to noble metal catalysts based on acidic supports because they are bi-functional and display both acidic and metallic properties [120]. In addition, it was determined that these catalysts (Ni_2P in particular) are resistant to deactivation. It was suggested that, Ni_2P for example, has excess phosphorus in the form of phosphate species on the surface which interacts with water, effectively preventing the oxidation of Ni_2P particles [120].

2.2.2.2.1.4 Metal-Carbide Catalysts

In contrast to sulfide, oxide, and phosphide catalysts, attention has also been given towards metal carbide catalysts - most specifically tungsten and molybdenum carbides. The purpose for their development was to potentially produce cost-effective catalysts that behaved like noble metals [121]. These catalysts are typically supported on carbon supports to eliminate the need for methane for carburization [121, 122]. Boullosa-Eiras *et al*., [123] compared Mo_2C to oxide, phosphide, and nitride catalysts for the deoxygenation of phenol. The trend in activity (based on conversion) that they established was $Mo_2C > MoO_3 > Mo_2N > MoP$.

All catalysts were shown to be most selective towards DDO reactions, however the phosphide catalyst experienced more hydrogenation reactions [123].

Jongerius *et al*., [122] studied the use of W_2C and Mo_2C catalysts at 55 bar H_2 within a temperature range of 300-375°C for the deoxygenation of guaiacol. They reported that the catalysts were mostly selective towards the production of phenol via demethoxylation with very few ring-saturation reactions. This was also demonstrated by Ma *et al*., [124] and Santillan-Jimenez, *et al*., [121]. Overall, Jongerius *et al*., [122] demonstrated that Mo_2C is more active and stable than W_2C, which deactivated quickly due to oxidation and the increase in particle size [122]. Both catalysts experienced difficulties in regaining activity with reactivation (via recarburization), the Mo_2C catalyst for example experienced a decrease from 68% conversion to 51% when the catalyst was recycled and recarburized between two consecutive runs [122]. This was attributed to possibly the encapsulation of the carbide particles within the support or irreversible coke formation – as was confirmed by Santillan-Jimenez, *et al*., [121].

Although carbide catalysts appear to favour reaction routes that do not involve ring-saturation thereby reducing H_2 consumption; they may be considered unsuitable for extended usage. This is because the carburization process requires extremely high temperatures (1000°C) and once deactivated, the catalysts cannot be successfully regenerated.

2.2.2.2.1.5 Monometallic Catalysts

Transition metals (noble metals in particular) have attained some interest in the deoxygenation of phenolic compounds because they are able to activate hydrogen. Noble metals have been shown to achieve higher degrees of deoxygenation than commercial sulfide catalysts [107]. However, these catalysts have been shown to require high hydrogen pressures. As was demonstrated by French *et al*., [54] who tested noble metals catalysts (Pt, Pd, and Ru) and compared them to a conventional sulfide NiMo catalyst while using hydrogen pressures of 70-170 bar. Even at such high hydrogen pressures; oxygenated aromatic compounds were found in the products. Increasing temperature from 340-400°C was found to increase conversion of phenolic compounds to aromatics and cycloalkanes. Although the Pt catalyst was shown to be the only one to decrease coking with increase in temperature, the yield of deoxygenated liquid products was found to be lower than with the conventional NiMoS catalyst [54]. The Pd catalyst on the other hand, favours ring saturation over deoxygenation reactions demonstrating high hydrogen consumption. Nie & Resasco, [125] also demonstrated that Pt favours ring-saturation reactions, however they proposed that the catalyst offered a variation of the HYD reaction mechanism in which a cyclic ketone is formed (via keto-enol tautomerism) and then hydrogenated.

In summary, monometallic catalysts such as Ni, Co, Pt, and Pd are not ideal catalysts due to their high H_2 requirements and the fact that they generally favour ring saturation reactions over DDO [106, 107, 125, 126].

2.2.2.2.1.6 Bimetallic Catalysts

The use of bimetallic catalysts for the deoxygenation of both phenolic and furanic compounds has received much attention in recent years. Their purpose is to improve the activity of monometallic catalysts towards DDO reaction pathways over HYD and ring-opening reactions, and to increase catalyst stability [106, 127]. Alonso *et al*., [127] reviewed a variety of bimetallic catalysts that have been developed for various intentions and discussed how the addition of a second metal may affect the catalyst overall. Within the past three years, many researchers have been focusing on the combination of active metals such as Pt, Pd, and Ni with other metals that are typically less active for deoxygenation such as Co, Cu, Fe, and Sn [105, 106, 128-134]. The consensus has been that the addition of the secondary metals alters the catalyst selectivity, promoting the DDO reaction route.

One bimetallic catalyst that has received attention is the addition of Cu to Ni for a NiCu bimetallic catalyst. Zhang, *et al.*, [134] worked on the addition of 5 wt% and 15 wt% Cu to a 10 wt% Ni catalyst for the deoxygenation of guaiacol. The addition of 5wt% Cu to a Ni catalyst decreased selectivity towards cyclohexane from 97.0% to 80.8%. These decreases were balanced by increases in selectivity towards benzene and toluene demonstrating that the addition of Cu promoted trans-alkylation reactions. Further increasing Cu content to 15 wt% decreased cyclohexane selectivity to 60.1% however conversion was found to also decrease [134].

Huynh *et al*., [132] further studied the substitution of Ni with Cu on a 19 wt% Ni/HZSM-5 catalyst in order to improve the reducibility of Ni. It was found that rather than alloying with Ni, Cu formed as a separate phase with large particle sizes. The substitution of 2 wt% Ni with Cu decreased conversion of phenol from 98% to 50% [132]. Khromova *et al*., [133] also tested the effect of Ni content on $NiCu/SiO_2$ catalysts using anisole as a model compound. In all cases, the catalysts appeared to be most selective toward ring-saturation. Increasing Ni content was found to increase coke formation likely as a result of interactions with aromatic rings. Copper-rich (15 wt% Ni and 85 wt% Cu - based on active phase alone) catalysts were found to be more selective towards hydrogenolysis reactions than nickel-rich (85 wt% Ni), however conversions were capped at 80% compared to the 100% for the nickel-rich catalyst [133]. Evidently, the use/development of NiCu catalysts appears to be conflicted and further research is warranted.

Compared to the addition of Cu to active metals, the addition of Fe is also appealing, and it is gaining popularity. Nie *et al*., [105] reported the use of NiFe with m-cresol. They observed that at 300°C and atmospheric H_2 pressure; adding 5 wt% Fe to 5 wt% Ni decreased conversion from 16.2% to 13.7%. However, the selectivity towards toluene increased from 14.2 wt% to 52.6 wt% while the selectivity towards saturated-ring products decreased to 0%. It is also noteworthy that trans-alkylation reactions were also observed on the NiFe catalyst. The authors proposed that, in comparison to the Ni catalyst which adsorbs the phenolic compound via the ring; the addition of Fe caused the compound to adsorb vertically via the oxygen upon tautomerism of the hydroxyl group into a carbonyl group, promoting the DDO reaction route [105]. Nevertheless, they suggested that alloying

active metals with oxophilic metals reduces ring-interactions and increases interactions with oxygen-containing groups.

Similar to NiFe, the combination of Fe and Pd has also undergone extensive investigations [106, 130, 131]. Sun *et al*., [106] studied the deoxygenation of vapour-phase guaiacol over a PdFe/C catalyst. In their work, Pd was selected over Pt and Ru because it was less active in ring-opening reactions. A catalyst containing 2 wt% Pd and 10 wt% Fe attained a yield of oxygen-free compounds of 25.9% compared to a 10 wt% Fe catalyst that achieved a yield of 6.3% and a 5 wt% Pd catalyst that achieved a yield of 2.7% [106]. The overall conversion of guaiacol with the PdFe catalyst was found to be comparable to the 5 wt% Pd catalyst. Unlike precious metal catalysts, the PdFe catalyst was shown to favour DDO reactions and experienced no ring-opening/ring-saturation reactions [106]. Through DFT calculations, the combination of Pd and Fe was shown to weaken the bond between the aromatic ring and the catalyst compared to both monometallic catalysts [106]. It was proposed that the function of the catalyst is such that Fe facilitates the adsorption of the oxygenated compound while Pd facilitates H_2 disassociation and the reduction of the iron oxide that is developed during DDO [106]. This synergistic behavior between PdFe was further studied by Hong *et al*., [131] who demonstrated a hydrogen spill-over from Pd to Fe which could also be applied to other noble metals with results expected to follow the order of H_2 sticking probability.

Hensley *et al*., [130] further proposed a catalytic mechanism for the DDO on PdFe. Through DFT calculations, it was determined that the most likely catalytic mechanism is

dehydroxylation. In contrast to Nie *et al*., [105] who proposed adsorption occurs on the Fe atom vertically, Hensley *et al*., [130] suggested that phenolic compounds are more stably adsorbed onto the surface in a more horizontal fashion with weak bonds with the aromatic ring. With phenol as a model compound; the tilted/horizontal adsorption mechanism facilitates the direct removal of the hydroxyl group producing an adsorbed phenyl group [130]. Benzene and water are then produced upon subsequent hydrogenation and desorption – see Figure 2-10.

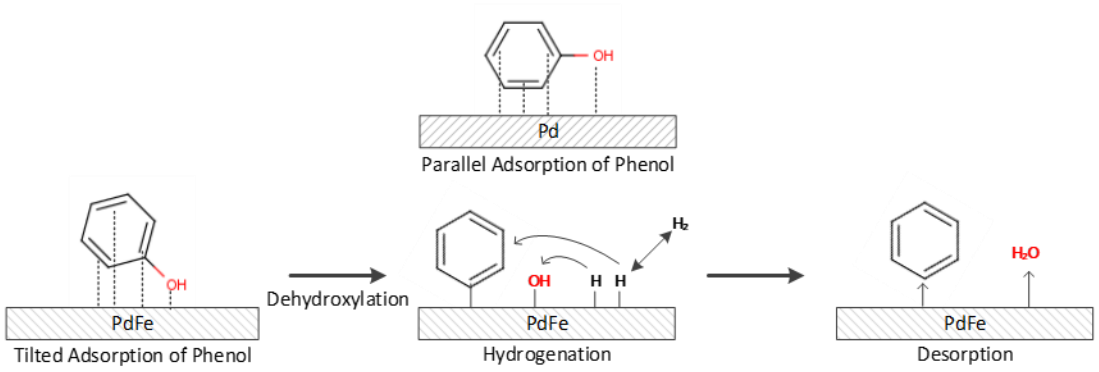

Figure 2-10: Adsorption of phenol on Pd compared to adsorption and dehydroxylation of phenol on PdFe [130]

Other bimetallic catalysts that have received attention include PtSn, PtNi, PtCo, PtRe and NiCo [128, 129, 132, 135]. The addition of oxophilic Sn to Pt is expected to behave in a similar nature to the addition of Fe to activate metals. González-Borja & Resasco, [129] reported that a PtSn catalyst possessed higher initial activity than a Pt catalyst. The addition of either Ni or Co to Pt was found to increase the catalysts' overall activity; however, these catalysts promoted the production of saturated-ring products [128]. Ohta *et al*., [135] studied the deoxygenation of 4-propylphenol at 280°C in an aqueous environment and reported that at these conditions, the addition of Re stabilized Pt and provided higher

conversions than the addition of other oxophilic metals such as Sn and Fe. Huynh *et al*., [132] also demonstrated that the addition of Co to Ni did not effectively promote DDO as both Ni and NiCo catalysts were both shown to promote ring-saturation reactions. However, it was noted that the addition of Co to Ni decreased the Ni particle size, thus increasing conversion and preventing catalyst deactivation via coke deposition.

2.2.2.2.2 Catalyst Support

Overall, there appears to be a lack of comprehensive studies that investigate the effect that the support has on the deoxygenation of phenolic compounds. As a result, additional research is required in order to clarify the role of catalyst supports. The most common supports that have been considered for the deoxygenation of phenolic compounds include acidic supports such as the reducible oxide supports first introduced in Section 2.2.1.2 and activated carbon. Of these supports, acidic supports such as Al_2O_3 and ZrO_2 have retained a lot of attention.

A variety of authors have indicated that the combination of a noble metal catalyst and acidic support can be very beneficial for the deoxygenation of phenolic compounds [17, 110, 136, 137]. Contrary to the high interest in acidic supports, Al_2O_3 has recently been ruled out as a viable support [54, 55]. As mentioned earlier, bio-oil tends to contain a significant amount of water and the catalytic deoxygenation of phenols produces a significant amount of water as well. In the presence of such high amount of water, Al_2O_3 has been shown to convert to boehmite ($Al_2O(OH)$) which reduces the activity of the active material via oxidation [55, 117].

On the other hand, ZrO_2 as a weaker acidic support has been deemed more suitable. De Souza, *et al*., [138] reported that the use of ZrO_2 as a support for Pd behaves similarly to the addition of an oxophilic metal to an active metal as Pd/ZrO_2 was found to favour the production of toluene from *m*-cresol at 300°C and atmospheric H_2 pressure [138]. Ohta *et al*., [135] compared various supports (ZrO_2, Al_2O_3, TiO_2, CeO_2, and SiO_2) for their PtRe catalyst in an aqueous environment at 280°C and demonstrated that the ZrO_2 supported catalyst offered higher conversions (67%) while SiO_2 was the least active catalyst (8.1% conversion) [135]. However, they reported an environment with such a high water concentration, that the catalyst deactivated dramatically due to structural change in the ZrO_2 and subsequent wrapping of the Pt particles. No such deactivation was reported when water was not used as the solvent.

Work performed by Mortensen, et al., [139] contradicts the notion that the addition of an active metal to a reducible support promotes the DDO reaction pathway. They reported that at a temperature of 275°C and H_2 pressure of 100 bar, their Ni catalysts on supports such as ZrO_2 and CeO_2 promoted the HYD reaction pathway. ZrO_2 was shown to convert phenol to cyclohexane while supports containing CeO_2 mainly produced cyclohexanol. The massive differences observed in reaction pathway selectivity may be attributed to the highly reductive environment that was employed by Mortensen, et al., [139] in comparison the work performed by De Souza, et al., [138]. Obviously, a higher H_2 pressure may favour the kinetics of the HYD pathway over DDO. A higher H_2 pressure may also lead to the production of more oxygen vacancies on the support thus increasing its acidity.

Currently, based on the limited literature available, it can be claimed that catalysts supported on mildly acidic materials are expected to provide the most desired results. However, in comparison to acidic supports, carbon supports may be more stable [54]. The use of activated carbon has been demonstrated for other deoxygenation processes (to be discussed in Section 2.2.3) and has been found to promote reactions that require minimum amounts of hydrogen [17]. This warrants future studies on the impact of carbon as a support with a comparison to acidic supports such as ZrO_2.

2.2.3 Furanic Compounds

Furanic compounds such as furfural and 5-hydroxymethylfurfural (HMF) are produced from cellulose and hemicellulose through dehydration reactions which may occur during thermal processing. These compounds are characterized as having a carbonyl group, and in the case of HMF, a hydroxymethyl group attached to a furanic ring. The conversion of these compounds to 2-methylfuran (2-MF) and 2,5-dimethylfuran (2,5-DMF) is becoming increasingly popular amongst researchers [17, 56]. This is because these compounds are potentially viable subjects for blending with gasoline due to comparable properties and higher energy densities than ethanol (~40% greater for 2,5-DMF) [140-143]. In addition, 2,5-DMF has also received attention in the chemical industry as a potential precursor for *p*-xylene [56]. Figure 2-11 lists various important furanic compounds.

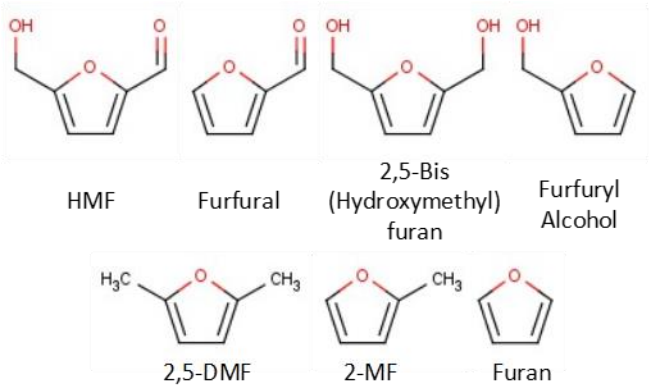

Figure 2-11: Structures of important furanic compounds involved in selective deoxygenation process

The challenge of producing 2,5-DMF and 2-MF from HMF and furfural is in line with topics discussed in this paper – selective deoxygenation while minimizing hydrogen consumption by restricting ring saturation [17]. Comparatively; completely saturated C_4-C_6 hydrocarbons ring-opening products are viewed as byproducts having lower value as they are not suitable for use as transportation fuels [56].

2.2.3.1 Reaction Mechanisms

During the selective deoxygenation of furfural and HMF, whereby the aromatic structures are retained, the three main reactions that may occur are hydrogenation of the C=O bonds, decarbonylation (DCO), and hydrogenolysis of C-O bonds. Selective hydrogenation/ hydrogenolysis (SHH) reactions utilize surface hydrogen to effectively convert carbonyl groups to hydroxymethyl groups and eventually to methyl groups (see Figure 2-12) [141, 142, 144-148]. Similar to fatty acids, increasing temperature may have an impact on the selectivity towards DCO and SHH reaction pathways as the former is endothermic while the latter is exothermic.

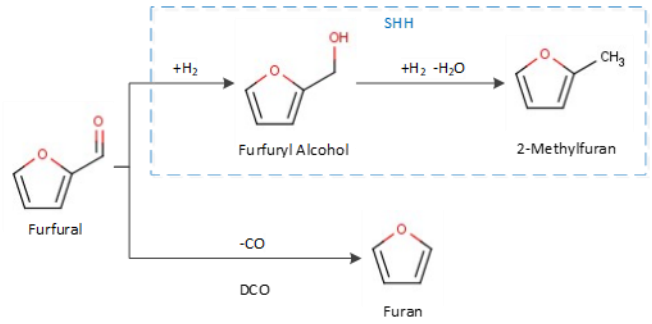

Figure 2-12: DCO vs. SHH of furfural [141, 142, 144-148]

2.2.3.1.1 Deoxygenation of Carbonyl Groups

Decarbonylation, which stoichiometrically does not require hydrogen, has been found to occur when it is adsorbed onto a catalyst via the furan ring which subsequently leads to the adsorption of the carbonyl group [144]. Pang & Medlin, [144] reported that hydrogen on the carbonyl group is first abstracted by the catalyst followed by C-C scission producing CO and a strongly adsorbed furyl ring which must be hydrogenated before desorption.

It has been proposed that C=O hydrogenation may also occur from the same initial adsorbed intermediate [146, 149]. Hydrogenation of the C=O produces 2,5-bis(hydroxymethyl)furan (2,5-BHMF) from HMF or furfuryl alcohol from furfural. Regardless, the hydrogenation of the C=O bond to a C-OH bond must begin with its adsorption on the catalyst surface. However, this has been most predominant when the compound adsorbed onto the catalyst surface most strongly by the carbonyl group as strong interactions with the aromatic ring tends to lead to DCO or possibly ring-saturation and/or ring-opening reactions [142, 146].

2.2.3.1.2 Deoxygenation of Hydroxymethyl Groups

Hydroxymethyl groups attached to furan rings may not undergo deoxygenation via simple dehydration reactions due to the lack of an α-hydrogen. Instead, to produce methyl groups, the hydroxymethyl groups must be reduced via a hydrogenolysis reaction pathway [141, 145, 150]. Sitthisa *et al*., [146] described the hydrogenolysis reaction as occurring when the alcoholic compound is adsorbed at the oxygen of the hydroxymethyl group. For this mechanism to work, 2-MF or 2,5-DMF would be produced after the saturation of an adsorbed intermediate that is bound with the furanic oxygen [151]. Consequently, it may be possible that when starting from a carbonyl group; the intermediate hydroxymethyl group may remain adsorbed and directly undergo subsequent hydrogenolysis. Jenness & Vlachos, [151] also proposed another possible mechanism in which the furan ring is first activated via partial hydrogenation on the α-hydrogen essentially enabling a dehydration reaction to occur; however, they were not able to successfully demonstrate it on a Lewis acid site of a RuO_x due to the formation of the conjugate base. Due to limited literature, the catalytic mechanism for the hydrogenolysis of hydroxymethyl groups on furan rings requires additional clarifications.

Alternatively, existing hydroxymethyl groups may undergo DCO. Pang & Medlin, [144] also proposed that upon dehydrogenation, an adsorbed hydroxymethyl group may be converted into an adsorbed carbonyl group and undergo DCO while producing hydrogen. Such was also described by Zheng *et al*., [148] and Sitthisa *et al*., [146] who attributed this effect to a strong interaction between the catalyst and furan ring.

2.2.3.1.3 Summary of Reaction Pathways

Figure 2-13 summarizes all the reaction routes of HMF and furfural that have been discussed for the deoxygenation of carbonyl and hydroxymethyl groups. As suggested earlier there are two overall routes for furfural: SHH which leads to 2-MF and DCO which leads to furan. HMF on the other hand has three overall reaction routes: SHH of both functional groups produces 2,5-DMF, DCO of both functional groups produces furan, or a combination of the SHH of the hydroxymethyl group and DCO of the carbonyl group produces 2-MF.

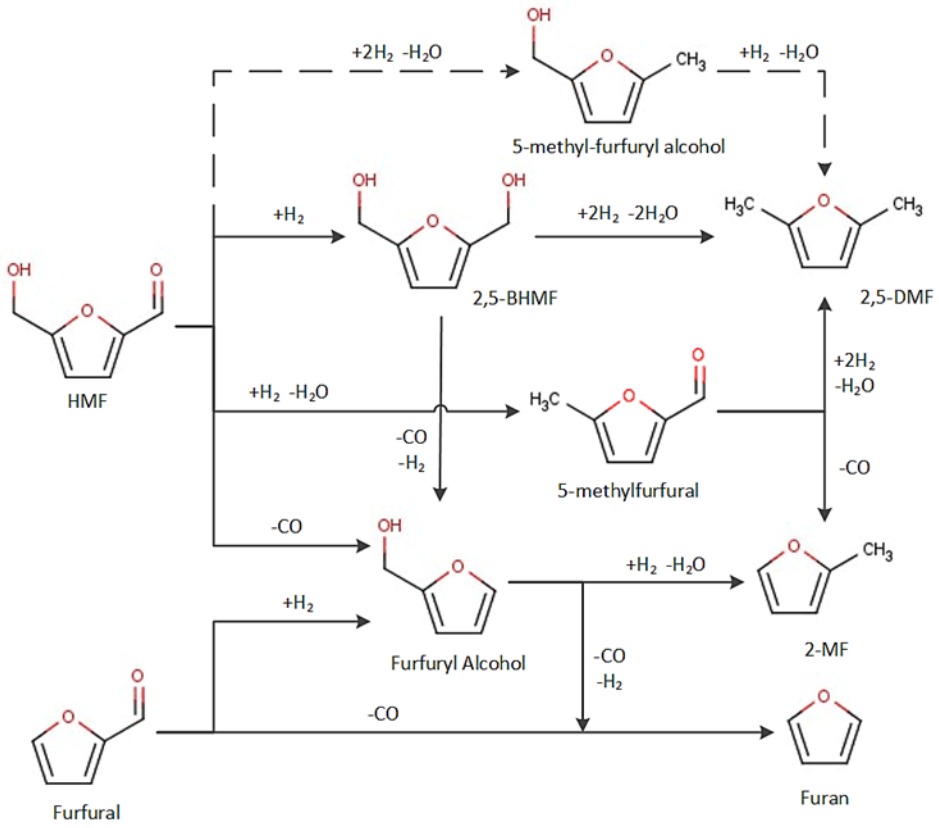

Figure 2-13: Summary of selective deoxygenation reaction pathways for HMF and furfural

2.2.3.2 Catalyst Selection

In comparison to fatty acid and phenolic compounds; the use of conventional sulfide catalysts has received far less attention for the deoxygenation of furanic compounds likely due to the required of co-fed sulfur to maintain activity. Instead, much work has been done to develop new novel catalysts that are selective to reducing substituted hydroxymethyl and carbonyl groups without performing ring-opening reactions. Studies in the development of catalyst for the reduction of HMF, furfural, or subsequent products such as furfuryl alcohol have been performed at temperatures ranging from 180-260°C and even as high as 350°C and typical hydrogen pressures of 10-40 bar [17, 56]. Typical catalysts that have been studied include monometallic catalysts and a variety of bimetallic catalysts.

2.2.3.2.1 Active Material

2.2.3.2.1.1 Monometallic Catalysts

Monometallic Ni catalysts have been ruled out for the possible selective deoxygenation of furfural and HMF while retaining the furan ring. Ni reportedly interacts too strongly with the furan ring promoting decarbonylation and hydrogenolysis that leads to the opening of the ring structure [142, 146, 152]. Since Ni is also very predominant at activating hydrogen on its surface; Ni is also known to promote the saturation of C=C bonds from the furan ring thus decreasing selectivity and increasing hydrogen consumption [152]. Overall, at lower temperatures (210°C) Ni catalysts are shown to favour hydrogenation reactions of the furan ring or even just the reduction of the oxygenated substituent to a methyl group (at low conversions however). At higher temperatures (250°C) Ni becomes selective towards DCO and ring-opening [142].

Like Ni, noble metals such as Pt and Pd have also been shown to interact with the furan ring [142, 144, 153]. This means that these catalysts favour DCO reaction routes.[144] This was described on a Pd catalyst in detail by Pang & Medlin, [144] who reported that both hydroxymethyl and carbonyl groups were reduced via DCO as a result of strong interactions with the furan ring. It was also suggested that ring-opening reactions may also occur as a result of such interaction. Wang *et al*., [154] supports the notion that a Pd catalyst can promote ring-opening reactions as they described ring-opening occurring due to ring activation as a result of partial hydrogenation.

Unlike Ni and noble metals, HMF and furfural adsorb onto Cu via the carbonyl group only – there is no interact with the furan ring [142]. This successfully leads to the hydrogenation of the C=O bond to C-OH and potentially hydrogenolysis to a methyl group. Sitthisa & Resasco, [142] reported a Cu catalyst was able to achieve moderate conversion (~50-75%) of furfural within a temperature range of 230-290°C (depending on the ratio of feed to catalyst). However, they reported that the Cu catalyst was mostly selective towards initial hydrogenation to furfuryl alcohol (as high as 71% yield) rather than 2-MF (as high as 8.2% yield) [142]. Incorporating Ru or CrO_4 with Cu; however, has been shown to be selective towards the production of 2,5-DMF from HMF with selectivities of 79% and 61%.[141]

2.2.3.2.1.2 Bimetallic Catalysts

The development of bimetallic catalysts – such as PtSn and NiFe– is becoming popular for the production of selective deoxygenation catalysts for deoxygenating furanic compounds. Like the use of bimetallic catalysts for phenolic compounds; most bimetallic catalysts are

appealing because of their ability to selectively deoxygenate oxygen-containing functional groups attached to an aromatic ring whilst hindering major interactions with the aromatic ring. On top of that; various studies have suggested that the addition of an oxophillic metal with an active metal can help to improve selective deoxygenation [142, 146, 147]. Oxophilic metals promote the adsorption of carbonyl groups – minimizing catalyst-ring interactions. Hydrogen that is transferred from the active metal effectively reduces the C=O bond, possibly producing a methyl group.

The combination of Fe and Ni to form a bimetallic NiFe catalyst, which was first described in Section 2.2.2., has received much attention for the selective deoxygenation of furfural and HMF. It has been widely demonstrated that the addition of Fe successfully reduces interactions between Ni and the furan ring while promoting SHH reactions [146, 147, 155, 156]. Sitthisa *et al*., [146] reported that at 250°C, 1 bar (H_2/feed ratio = 25), the addition of 2wt% Fe to 5 wt% Ni on SiO_2 increased the yield of 2-MF produced from furfural from <10% to as high as 39.1% [146]. Yu *et al*., [155] tested NiFe for the selective deoxygenation of HMF with various ratios of Ni:Fe. All NiFe and Ni catalysts had conversions as high as 100%. The highest selectivity (91.3%) towards DMF was achieved with a Ni:Fe ratio of 2 at a temperature of 200°C. No ring-opening was observed over the NiFe catalyst. Comparatively, Ni catalysts were only able to achieve a DMF selectivity as high as 8.1% with the balance attributed to oxygenated furanic compounds and saturated-ring products [155]. The NiFe (2:1 ratio) catalyst was also noted as being relatively stable and could be reactivated via a calcination process. Deactivation was suggested to have

occurred as a result of the slow formation of polymeric humins which would cover the catalyst surface [155].

Yu *et al*., [156] proposed that furfuryl alcohol is produced as an intermediate of furfural when using NiFe. They demonstrated that upon addition of Fe, there is a strong interaction between the C=O bond and the catalyst surface; however, there are also interactions with the furan ring. It was determined that on Ni, the furan ring of furfural is adsorbed more parallel to the Ni (111) surface whereas on the FeNi (111) surface, the furan ring is more tilted (see Figure 2-14) [156]. This in combination with the strong interaction with the oxygen containing constituents on the furan ring favours conversion to 2-MF. In a later study, Yu & Chen, [147] also suggested that the aromatic ring of furfural may still adsorb onto to the catalyst surface along with the carbonyl group which could result in some DCO reactions. This would likely be dependent on Fe content.

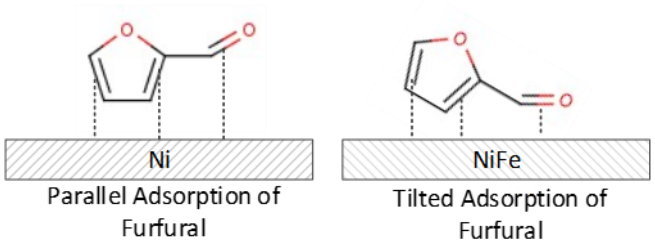

Figure 2-14: Adsorption of furfural on NiFe compared to Ni [156]

Other bimetallic catalysts that have been investigated include the addition of various metals (such as Co, Re, Sn, and Zn) with Pt, NiPd, PdCu, and Rh/Ir catalysts modified with RuO_x. Chen *et al*., [157] studied the use of NiPd, PtRe, PtSn, and PtIn catalysts for the selective reduction of furfural to furfuryl alcohol. NiPd was found to favour ring saturation

producing tetrahydrofurfuryl alcohol with yields as high as 93.4%. PtRe (2 wt% Pt and 1 wt% Re) was shown to be the most selective towards the reduction of furfural to furfuryl alcohol at a selectivity of 95.7% at a conversion of 100%. Comparatively, PtSn achieved a furfuryl alcohol selectivity of 47.8/5 at 98.3% conversion while PtIn achieved a selectivity of 74.9% at a conversion of 73.3% [157]. Based on these results; with further optimizations, PtRe may be a viable catalyst to produce 2-MF from furfural.

Much like the addition of Re to Pt; Lesiak *et al*., [158] demonstrated that the addition of Cu to Pd also hinders ring-saturation reactions. Eventually, PtSn may also become a competitive option as this catalyst has received conflicting results. For example, Merlo *et al*., [159] used PtSn to produce furfuryl alcohol from furfural at high selectivities (96-98%).

Surprisingly, another catalyst to consider is the addition of Co to Pt [154, 160]. Although Co is not known as an oxophilic metal, Wang *et al*., [154] reported a 100% conversion of HMF with a DMF yield of 98% with their PtCo catalyst. The reason for the decrease in catalyst-ring-interactions compared to Pt catalysts is currently not well understood.

Although there has yet to be any significant experimental work done with the use of PtZn as a catalyst for the reduction of furanic compounds; it is likely that such a catalyst will receive much attention in future work. Shi & Vohs, [161] presented insights for the reaction mechanism by which furfural would be reduced on a PtZn catalyst. They stated that, similar to other combinations of active and oxophilic metals, furfural primarily bonds via the carbonyl group of furfural. In contrast; they proposed that rather than producing furfuryl

alcohol as an intermediate as suggested by Yu *et al*., [156] for a NiFe catalyst, furfural undergoes a direct oxygen removal reaction [161]. The resulting product is adsorbed onto the catalyst via a di-unsaturated methyl group attached to the furan ring. Subsequent hydrogenation and desorption produces 2-MF and water.

The mechanism described by Shi & Vohs, [161] closely resembles the catalytic mechanism for phenol on a bimetallic catalyst containing and active metal phase and an oxophilic metal described by Hensley *et al*., [130]. On monometallic catalysts, both furanic and phenolic catalysts reportedly favour adsorption and interaction with the aromatic rings leading to saturation and possibly ring-opening. For both types of compounds, adding a second, oxophilic metal changes the adsorption behavior, favouring the adsorption of the compounds primarily via the oxygen containing constituents causing the aromatic rings to tilt away from the surface. Unlike furfural, 5-HMF has both a carbonyl group and hydroxymethyl group which may present a competitive adsorption mechanism. This competitive nature is yet to be studied thoroughly. It is believed that 5-HMF favours adsorption via the carbonyl group which upon subsequent direct deoxygenation (like that described in Figure 2-15) produces 5-methyl-furfuryl alcohol (see Figure 3-12).

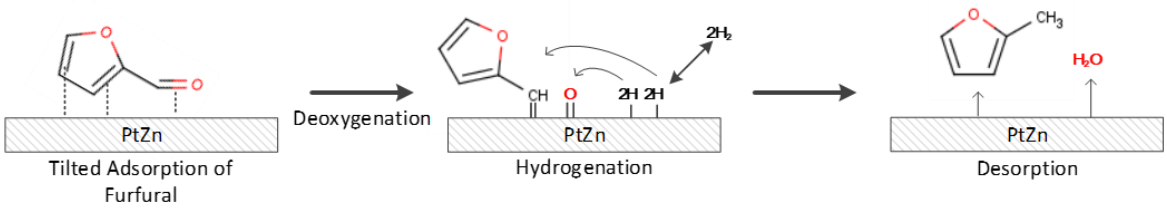

Figure 2-15: Deoxygenation of furfural on PtZn [161]

The development of bimetallic catalysts with a metal oxide catalyst such as RuO_x is currently conflicted. Tamura *et al*., [162] developed an Ir-RuO_x catalyst that was shown to be active towards hydrogenolysis and selective hydrogen due to the formation of a hydride species. However, Rh-RuO_x and Ir-RuO_x catalysts have also been shown to promote ring-opening reactions of tetrahydrofurfuryl alcohol due to a hydrogen transfer reaction from the hydroxymethyl group [163, 164].

In a hydrogen-free environment, deoxygenation of HMF or furfural does appear possible over catalysts such as Ni and noble metals due to their strong interactions with the furan ring. This would produce furan, CO, and in the case of HMF, H_2. However, furan may not be as desirable as 2-MF and 2,5-DMF and in addition, ring-opening reactions and catalyst deactivation are also likely scenarios. Although selective deoxygenation reduces hydrogen consumption, 1 mole of HMF still requires 3 moles of H_2 to be converted to 2,5-DMF. Therefore, in order to minimize H_2, it may be most favourable to proceed with a balance between DCO and selective hydrogenolysis reactions to produce from HMF and furfural 2,5-DMF, 2-MF, and furan (to be discussed more in Section 2.2.4). A NiFe bimetallic catalyst may be a potential candidate for such an application as it was found to promote selective hydrogen and hydrogenolysis while having some activity towards DCO reactions.

2.2.3.2.2 Catalyst Support

The effect of using various catalyst supports for the selective deoxygenation of furanic compounds has received very little attention. Most research studies have developed catalysts based on neutral SiO_2 or carbon supports. For the most part, acidic catalyst

supports should be avoided – especially when not saturating the furan ring. This is because acidic catalysts promote rearrangement and polymerization reactions which can quickly lead to catalyst deactivation [56]. Polymerization of HMF, furfural, and their derivatives reportedly occurs on acidic catalysts when hydrogenation is slow or does not occur [56, 165, 166]. Thus limiting contact time and inadvertently, reducing conversion, is required in such case.

Catalyst supports such as TiO_2 and Fe_2O_3 however, have received some attention due to their interactions with active metals [56, 145, 167]. As elucidated in section 2.2.1., catalysts that demonstrate strong metal-support interactions promote selective hydrogenation/ hydrogenolysis reactions in a similar fashion as oxophilic metals added onto active metal catalysts [167]. Scholz *et al*., [145] reported that Pd and Ni supported on an oxophilic Fe_2O_3 support altered the reaction pathway of the Pd catalyst from favouring strong interactions with the furan ring as opposed to SHH reactions of the carbonyl and hydroxymethyl groups on HMF. They also observed saturated-ring products which may be due to extended catalyst contact times. It is noteworthy that these reactions involved catalytic hydrogen transfer rather than hydrogen. Due to the decent performance of NiFe bimetallic catalysts observed in the previous section, it would be interesting to see how well a Ni/Fe_2O_3 catalyst would perform the selective deoxygenation of furfural/HMF with a limited amount of atmospheric hydrogen. Active metals supported on ZrO_2 may also be a viable option as such was shown to be successful for similar use with phenolic compounds. However, care would have to be taken with regards to acidity.

2.2.4 Discussion – Future Work and New Implications

2.2.4.1 Hydrogen-Free vs. Hydrogen-Modest Environments

It has been shown that a plethora of studies have been conducted to minimize the consumption of hydrogen when performing catalytic deoxygenation of vegetable oils, phenolic compounds, and furanic compounds. The consensus is that, depending on the compounds, it is theoretically possible to perform deoxygenation without hydrogen present. However, hydrogen is typically involved in the reactions in some way and thus without hydrogen, low conversion, high catalyst deactivation, and undesired products are expected.

The deoxygenation of vegetable oils has a problem at the very first step – the β-elimination reactions require hydrogen for complete conversion. One alternative could possibly be to promote hydrolysis reactions for the breakdown of triglycerides. Due to a lack of research in the use of hydrolysis, it is not clear how viable such an alternative would be. One would have to consider the impact of glycerol as by-product as it is unusable as a direct fuel and how elevated concentrations of water would affect subsequent deoxygenation reactions. To address these issues, it may be appropriate to conceive a two-step process in which triglycerides are broken down into fatty acid in one reaction step followed by fatty acid deoxygenation in a second reaction step. Such a process would likely require separation stages between the two reaction steps. Such a two-step process would closely resemble a process used to produce FAME biodiesel such as the process described by Kusdianna & Saka, [168]. It is noteworthy though that some researchers have begun to develop

hydrothermal processes for the deoxygenation of fatty acids as well as possibly a one-step hydrolysis-deoxygenation process [13, 86, 87, 169].

In any case, the deoxygenation of fatty acids presents a challenge of its own. Although the deoxygenation of fatty acids without hydrogen is possible through DCO_x, deactivation is an issue. Hydrogen is therefore required to fully break down triglycerides in vegetable oils and maintain activity. In addition, indirect-DCO reactions appear to be must faster than direct-DCO reactions. Having some hydrogen available would promote indirect-DCO likely improving conversion.

Similarly, the deoxygenation of furanic compounds can be done without hydrogen; however, hydrogen is still required in order to maintain catalytic activity. In addition, furan produced via deoxygenation of HMF or furfural without hydrogen may not be as desirable as products such as 2,5-DMF and 2-MF, which can be produced via selective deoxygenation in the presence of a minimal amount of hydrogen. Undesired ring-opening products are also a possibility.

Phenolic compounds on the other hand, need a source of hydrogen to remove oxygen. Since there is no reaction pathway that removes oxygen as CO or CO_2, hydrogen is required to selectively remove oxygen as water. In addition, an onslaught of catalyst deactivation is brought upon the catalyst's inability to hydrogenate oxygen and carbon structures that are strongly adsorbed on the catalyst surface. Oxygen that is not hydrogenated to water effectively oxidizes the catalyst while carbon pools that are not saturated lead to coking.

To achieve desirable products via catalytic deoxygenation, a limited amount of hydrogen should be available. Thus, hydrogen-modest systems should be applied rather than hydrogen-free systems. The amount of hydrogen that is used should be less than conventional, non-selective deoxygenation processes, ideally at near stoichiometric amounts or enough to maintain catalyst activity.

2.2.4.2 Insights on Future Catalyst Developments

Throughout this review, various catalysts have been identified as being appropriate (or inappropriate) for hydrogen-modest processes. However, it has been observed that catalyst selection tends to differ between researchers depending on which resource they are focusing on. For example, researchers in the field of vegetable oils have focused on the use of metal-sulfide, noble metals, and common transition metal catalysts such as nickel. On the other hand, phenolic compounds have seen the development of metal-oxide and transition-metal-phosphide catalysts, while bimetallic catalysts have been development for both furanic and phenolic compounds. Overall, it appears as though all three resources benefit from the use of catalysts containing bifunctionality – the ability to adsorb the compounds via the oxygen-containing functional groups and the ability to activate hydrogen.

In Section 2.2.1, it was discussed that in order to minimize hydrogen consumption, one should consider the promotion of DCO_x reaction pathways. Of all DCO_x reaction pathways, indirect-DCO, which requires the presence of hydrogen, appeared to be the fastest reaction.

Direct-DCO or DCO_2 reactions are hindered in the presence of hydrogen and they present a mechanism by which catalyst deactivation may occur quickly. In order to perform indirect-DCO, the first step is a hydrogenolysis reaction into an aldehyde intermediate followed by DCO. One catalyst that appeared to benefit this reaction route was Ni/ZrO_2 because of the synergistic effect/bifunctionality of the catalyst, which supported the hydrogenolysis step.

The use of an active metal such as Ni on a reducible support such as ZrO_2 was also discussed in Sections 2.2.2.2 and 2.2.3.2. In these sections, it was elucidated that these catalysts were very comparable in function to bimetallic catalysts containing an active metal and an oxophilic metal such as NiFe. It is therefore suggested that future work be done to explore the use of bimetallic catalysts for the deoxygenation of fatty acids. It is predicted that a catalyst such as NiFe or PdFe will promote the adsorption of fatty acids via oxygen atoms leading into a direct removal of oxygen. In order to enable the subsequent DCO reaction though, the catalyst will likely need to maintain some monometallic properties and it is there suggested that for application with fatty acids, the content of oxophilic metal (Fe) should be lower than those used for phenolic and furanic compounds.

Another type of catalyst that may present the necessary bifunctionality properties for the deoxygenation of fatty acids would be a transition-metal phosphide catalyst. It is expected that a phosphide catalyst such Ni_2P would also be comparable to a catalyst like Ni/ZrO_2. As Cecilia *et al*., [120] has concluded, Ni_2P functions similarly to active metals on acidic supports exhibiting both metallic and acidic properties which would be necessary for

indirect-DCO. Indeed some work has already been performed demonstrating that Ni_2P promotes DCO_x reactions [170]. Additional research would be beneficial to understand how this catalyst compares to other catalysts that have been studied for vegetable oils deoxygenation.

In Sections 2.2.2 and 2.2.3, several comparisons were made with regards to the development of catalyst for the deoxygenation of furanic and phenolic compounds – especially for bimetallic catalysts. In order to minimize hydrogen consumption, both types of compounds appear to require the same treatment – selective deoxygenation of oxygen-containing constituents while minimizing ring-saturation and ring-opening reactions. Bimetallic catalysts such as NiFe and PdFe appear to be suitable selections for achieving these goals. In addition, it was determined that there are not enough investigations towards the use of different catalyst supports. Therefore, it is recommended that future studies should explore the further use of active metals supported on reducible oxides. The use of various combinations of reducible oxides such as CeO_2 and ZrO_2 are also very interesting. A support with an enhanced oxygen storage capacity, as reported for a CeO_2 and ZrO_2, with a highly dispersed active metal phase would likely be beneficial for the selective deoxygenation of furanic and phenolic compounds. As stated in Section 2.2.3.2., care should be taken with regards to catalyst acidity when deoxygenating furanic compounds as it may lead to rapid catalyst deactivation due to polymerization reactions.

In the development of catalysts for phenolic or furanic model compounds, it is important that researchers consider whether the catalyst would also be appropriate for the other. This

is because phenolic and furanic compounds, as well as various other compounds, exist together in bio-oil and are treated together rather than separately. Thus, a catalyst that is selected for deoxygenating HMF should also be stable for the deoxygenation of guaiacol.

2.2.4.3 Additional Strategies for Reducing Fossil-Fuel-Derived H_2 Dependence

Throughout this review, the major strategy for reducing the requirement of H_2 gas has been to perform selective deoxygenation in order to reduce H_2 consumption. Other strategies that are currently undergoing research include the production of H_2 from renewable sources and the use of internal hydrogen – otherwise known as *in-situ* hydrogen.

2.2.4.3.1 External Sources of Hydrogen

The production of hydrogen through processes such as gasification of biomass has received some attention as a potential candidate for a supply of hydrogen for deoxygenation processes. However, there are concerns regarding the costs associated with the actual process of gasifying the biomass then purifying the hydrogen for use in a hydrotreater. As an alternative, Tanneru & Steele, [15] proposed the use of syngas directly for the purpose of deoxygenation. The use of syngas was found to be successful for performing the initial steps of the catalytic deoxygenation of bio-oil with results that were comparable to the use of pure hydrogen. The success of this was partly attributed to water-gas-shift reactions, which will be discussed in greater detail later [15]. With further optimizations with regards to catalysts and conditions, it is possible that the use of syngas directly may become a viable option for industrial application.

2.2.4.3.2 Internal Sources of Hydrogen

Internally sourced hydrogen, or *in-situ* hydrogen, is hydrogen that is produced and used for reaction in the same reactor. There is no external supply of H_2 gas. An example of a system that uses *in-situ* hydrogen is the use of a hydrogen donor solvent. Another example that is presented here for the first time as a potential source of *in-situ* hydrogen and major contributor to reducing hydrogen consumption is the promotion of water-gas-shift and steam reforming reactions.

2.2.4.3.2.1 Hydrogen Donor Solvents

The use of proton donor solvents such as biomass derived acids and alcohols is becoming popular as they reduce the reliance on H_2 gas from fossil fuels and are, for the most part, easier and safer to store at isolated locations than H_2 gas [145]. The most common donors that have been considered are formic acid and light alcohols such as *iso*-propanol [145, 171-175]. The basic idea behind proton donor solvents is that they disassociate hydrogen onto the catalyst surface. For formic acid, this occurs via decomposition into hydrogen and CO_2.

Alcohols donate hydrogen via the disassociation of hydrogen from the hydroxyl group producing its conjugate ketone, such as acetone for *iso*-propanol. Results for the use of isopropanol with furfural from Scholz, et al., [145] were moderate. In some cases, high conversions of furfural and HMF were observed; however, reactions were mostly selective towards the production of hydroxymethyl groups [145]. With future reaction and catalyst optimizations, it may be possible to increase selectivity towards the production of methyl groups. On the other hand, Reddy, et al., [175] reported decent conversions of furfural and

p-cresol over Ni-Cu catalysts using *iso*-propanol as a hydrogen donor. Deoxygenation was not significant however when tests were performed with real bio-oil. In this case, *iso*-propanol was found to undergo esterification with short acids such as acetic acid which they concluded would help stabilize the bio-oil for further processing.

There are some concerns that need to be addressed with regards to catalytic hydrogen transfer processes. The major concern is cost. If formic acid is selected, there is the cost associated with the procurement of the formic acid and due to the corrosiveness of the formic acid, there will be additional capital and maintenance costs associated with its use as well. For alcohols, there is the concern about solvent consumption and recovery. Recovering the solvent will require subsequent separation process to retrieve the ketone followed by a reaction process to convert the ketone back into an alcohol. If on the other hand, the alcohol is not recovered, there will be additional procurement costs. Another concern is with regards to the origin of the solvents. Since one of the objectives to using hydrogen donor solvents is to eliminate the reliance on the fossil-fuel industry for producing hydrogen gas, one should ensure that the solvents that are used are derived from biomass. The aforementioned concerns aside, these processes can be deemed much safer than typical hydrotreating processes because they do not involve the storage and handling of high-pressure hydrogen.

2.2.4.3.2.2 Water-Gas-Shift and Reforming Reactions

One topic that appears to have been overlooked in the minimization of hydrogen consumption is the consideration of water-gas-shift reaction (WGSR) (Equation 2-11) and methane steam reforming (MSR) (Equation 2-12) reactions.

$$CO + H_2O \rightleftharpoons CO_2 + H_2 \quad \textbf{2-11}$$

Water-gas-shift reaction

$$H_2O + CH_4 \rightleftharpoons 3H_2 + CO \quad \textbf{2-12}$$

Methane steam reforming

More focus needs to be made on promoting WGSR at reaction conditions in order to regenerate H_2 gas. Removing oxygen as both CO and H_2O is lost potential as they can be used to produce H_2, which can be used again to remove oxygen. In Section 2.2.3.2. it was suggested that there should be a balance between removing oxygen selectively as H_2O and CO. Looking at Equations 2-13 to 2-15 which represent the overall SHH and DCO reaction pathways presented in Figure 2-12; it can be theoretically derived that equimolar amounts of CO and H_2O can be produced if 3 moles of HMF are split equally amongst the three reactions.

$$HMF + 3H_2 \rightarrow DMF + 2H_2O \quad \textbf{2-13}$$

Conversion of HMF to DMF

$$HMF \rightarrow Furan + H_2 + 2CO \quad \textbf{2-14}$$

Conversion of HMF to Furan

$$HMF + H_2 \rightarrow 2MF + H_2O + CO \quad \textbf{2-15}$$

Conversion of HMF to 2MF

Assuming 100% conversions, balancing these reactions with the WGS reaction (Equation 2-11) results in no net consumption of H_2 – see Equation 2-16. Simply put, all hydrogen that would be consumed would be regenerated.

$$3(HMF) \rightarrow DMF + 2MF + Furan + 3CO_2$$ **2-16**

Idealistic conversion of HMF to equal molar DMF, 2MF, and furan with no net H_2 consumption

Alternatively, one could also theoretically optimize Equations 2-11 and 2-14 to produce just 2-MF from HMF while effectively consuming no hydrogen (see Figure 2-16).

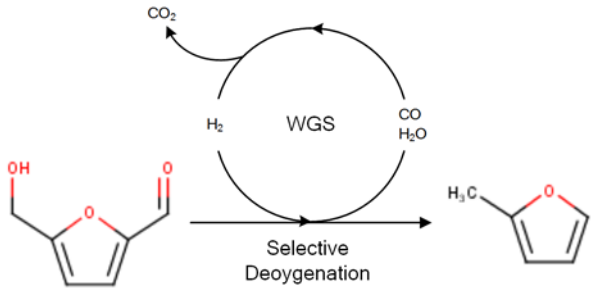

Figure 2-16: Selective deoxygenation of 5-HMF with WGSR

Theoretically, a very similar optimization could be conceived for fatty acids. Starting from a C_n fatty acid and proceeding through the indirect-DCO reaction route to the production of a C_{n-1} paraffin consumes 1 mole of H_2 and produces 1 mole of H_2O and 1 mole of CO. Balancing this with WGSR results in no net consumption of H_2 and the release of CO_2 that would resemble the DCO_2 reaction.

As for phenolic compounds, since oxygen cannot be removed as CO from phenolic compounds; the WGSR is not directly available to regenerate H_2. Instead; the deoxygenation of phenolic compounds that have a methoxyl group, such as guaiacol, can produce benzene, methane, and water – see Equation 2-17.

$$Guaiacol + 3H_2 \rightarrow Benzene + 2H_2O + CH_4 \quad \textbf{2-17}$$

Conversion of guaiacol to benzene

The presence of both methane and water would enable MSR reactions which as seen in Equation 2-12 would produce 3 moles of H_2. Therefore, assuming 100% conversion, one could theorize the production of benzene, CO, and water from guaiacol with no net consumption of H_2. Beyond that, since CO has been formed; further balancing these reactions with WGSR would lead to a net production of 1 mole of H_2 along with benzene and CO_2 – such is shown in Equation 2-18.

$$Guaiacol \rightarrow Benzene + H_2 + CO_2 \quad \textbf{2-18}$$

Guaiacol conversion combined with WGSR and MSR

It is important to note that these reactions of guaiacol are only supported by the reaction routes that produce benzene which, as mentioned in Section 2.2.2, is not particularly ideal. Alternatively, one could aim to produce toluene from guaiacol that would prevent the possibility of regenerating H_2.

Above all, the balances and ideas that have been presented here demonstrate the importance of WGSR and possibly MSR reactions. Although these propositions are far-fetched (such as assuming 100% conversion of even WGSR and MSR reactions) they do demonstrate that more can be done to reduce hydrogen consumption by producing *in-situ* hydrogen. It is therefore proposed that future work not only look at developing catalysts and additives that promote selective deoxygenation reactions in hydrogen-modest environments but also catalysts/additives that promote WGSR and MSR (or possibly other steam-reforming

reactions such as propane from vegetable oils) reactions. Bifunctional catalysts that promote both deoxygenation and WGSR/MSR may be ideal for such a proposal.

An appropriate initial step towards developing bifunctional catalysts would be to look at deoxygenation catalysts that contain materials known to promote WGS and MSR reactions (and *vice versa*) and monitor their performances at desired reaction conditions. Ratnasamy & Wagnar, [34] extensively reviewed the catalysts that are used for WGSR. In industry, catalysts that are currently used include iron oxides that are stabilized by chromium oxide (Fe_2O_3-Cr_2O_3) for high temperature WGSR (350-450°C) and Cu-ZnO-Al_2O_3 catalysts for low temperature WGSR (190-250°C) [34]. The addition of a promoter metal such as Ni, Pt, Pd, and Rh to iron-oxide based catalysts has been shown to improve the reaction kinetics of high temperature WGSR [176-178]. Ni and Pd supported on Fe_2O_3 has been shown to promote the deoxygenation of SHH and DCO of furfural by Scholz, et al., [145] at 180°C with isopropanol as a H-donor. Therefore, promoted iron oxide catalysts may be a potential candidate; however, one must consider the temperature difference (180°C vs 350°C).

Although thermodynamic equilibrium is generally not a concern for the deoxygenation of HMF, it is however a concern for WGSR, which is an exothermic reaction (ΔH = -41.1 kJ/mol). In industry, WGSR first occurs first via a high temperature step (K_P = 20.5 at 350°C) followed by a low temperature step (K_P > 100) to help shift the equilibrium to complete conversion of CO [34]. Although the hydrogen consumption via deoxygenation may shift the equilibrium even more towards the products; operating at temperatures as high as 350°C may not be suitable for phenolic and furanic compounds due the elevated

possibility of coking. Therefore, using a low temperature WGSR catalyst may be more suitable. Unfortunately, Cu-ZnO-Al_2O_3 has not received any attention for deoxygenation.

One may also look towards catalysts used for the aqueous phase reforming (APR) of glycerol to produce *in-situ* hydrogen. APR of glycerol – which is derived from triglycerides - has been shown to produce hydrogen, which is then used for the deoxygenation of fatty acids [179-181]. In general, this is an important process to consider for the deoxygenation of vegetable oils within a hydrothermal environment where glycerol need not be introduced to the system as it is produced via hydrolysis. A particular catalyst that has been shown to provide high conversions is Pt-Re/C [180, 181]. As WGSR is an important reaction within an APR process, the fact that Pt-Re/C has been established as being able to perform WGSR and deoxygenation makes it a potential candidate for other processes involving WGSR. Using glycerol APR to produce *in-situ* hydrogen for the deoxygenation of phenolic or furanic compounds may not be suitable because glycerol would need to be supplied from an external source. However, the APR of bio-oil which contains furanics, phenolics, and smaller compounds such as glycoaldehyde, which may undergo APR, may be another possible route of exploration.

The movement towards promoting both WGSR and deoxygenation within the same catalytic process will inadvertently develop processes that are not only hydrogen-modest but to some extent, hydrogen-self-sufficient. The result is a highly sustainable catalytic process that will produce desired fuels with a minimal dependence on the fossil fuel industry.

2.2.5 Conclusions

The increasing demand to produce biofuels via deoxygenation processes has been met with the challenge of decreasing H_2 gas consumption. There is a plethora of research work being poured into the development of catalysts that promote the selective deoxygenation reactions of vegetable oils, phenolic, and furanic compounds while consuming less hydrogen. Various information gaps have been determined. Research is needed to develop clear understandings of catalytic reaction mechanisms thereby allowing researchers to develop more selective catalysts.

Based on what is currently understood about reaction pathways and catalyst deactivation, it has been concluded that hydrogen-modest systems are more desirable than hydrogen-free systems. Hydrogen is required because of its role in reactions and to maintain catalyst activity. The successful conversion of biomass-derived bio-oils to desired products simply cannot proceed without hydrogen present. Hydrogen requirements can still be reduced by promoting reactions that lead to desired products via reaction pathways that require less hydrogen.

Based on current knowledge, the catalysts that look promising for selective deoxygenation are those that exhibit a combination of oxophilicity and the ability to activate hydrogen. Such has been found to reduce interactions between the catalyst surface and the carbon structure of oxygenated compounds while promoting the interaction with oxygen, thereby allowing for selective deoxygenation. Examples that have been explored include active

metals supported on reducible oxides such as Ni/ZrO_2 and supported bimetallic catalysts that combine active metal with oxophilic metals such as NiFe.

It has been proposed that researchers should continue to collaborate more in the development of catalysts for phenolic and furanic compounds. As phenolic and furanic compounds are to be processed together in bio-oil, it is essential that a catalyst that is proven to be viable for phenolic compounds be stable and active for furanic compounds, and *vice versa*.

In order to further minimize the requirement of external sources of H_2; it has been proposed that catalysts should not be developed based on just their ability to promote selective deoxygenation. They must be developed to also promote the production of *in-situ* hydrogen through water-gas-shift and steam reforming reactions. The presence of CO, H_2O, and CH_4 in the outlet gas represents a missed opportunity for regenerating hydrogen. Ideally, oxygen should leave a reactor as CO_2.

For vegetable oils/fatty acids, the reaction pathway that has been suggested as ideal for use in a hydrogen modest/hydrogen self-sufficient environment is the indirect-DCO reaction pathway. For furanic and phenolic compounds, the desired reaction routes should be based on desired products. For example, toluene, rather, than benzene may be the more the desired product from guaiacol as benzene is not desired for use as a fuel. However, it was noted that the production of toluene limits the possibility of re-generating hydrogen and

thus consumption of hydrogen is expected to be higher than that for the production of benzene.

Above all, researchers should focus on the development of catalysts that require the use of less hydrogen and where possible, promote the regeneration of hydrogen through water-gas-shift and steam-reforming reactions.

Chapter 3: Experimental Set-up and Preliminary Results

3.1 Experimental Set-up for Catalyst Activity Tests

Each experiment that was performed in Chapters 4-7 consisted of activity tests – reactions with and without catalysts followed by product analysis. Catalyst activity tests were primarily performed using a 55 mL stainless steel reactor that was horizontally stirred (200 rpm) inside a furnace for a desired reaction time and temperature (see Appendix A for details on reactor design). As this set-up involved the rotation of the whole reactor body, stir rates were maintained at 200 rpm to ensure safe operation. Most of the tests utilized a solvent, 1-methylnaphthalene (selected based on preliminary results) to help with heat transfer. The intent was to prevent biomass material from sintering to hot reactor wall. The horizontally stirred reactor orientation was selected to allow for adequate mixing of the solid (catalyst) phase with the gaseous phase allowing for gas phase reactions to occur. This was limited in a traditional, vertically stirred reactor as the gas phase could not make appropriate contact with the solid phase. WGS reactions were performed inside the reactor to demonstrate that appropriate mass transfer can occur in this reaction set-up with a solvent involved (see sections 3.3.1 and 6.3.1).

The reactor was loaded first with solid (biomass and catalysts) and liquid (solvent) components and then sealed. In the cases where catalysts consisted of reduced metal phases; reduction of these catalysts was performed in a separate unit with pure hydrogen gas. Catalysts were kept within this environment until transferred to the reactor or sample storage and immediately shielded with the solvent (in the reactor) or inert atmosphere

(storage). After purging the reactor to remove all O_2, the reactor was filled with the desired gas and attached to a stir motor, inside a furnace for the reaction. Details about the reactor and furnace set-up/assembly can be found in Appendix A. For activity tests, the reactor was heated to the desired reaction temperature (primarily 350°C – requiring 42 minutes of heat-up time) then held at this temperature for the desired reaction time (ie. 1-hour).

After reaction completion, the reactor was cooled to room temperature. A sampling apparatus consisting of a pressure gauge and septum was attached to the reactor allowing for measurement of final gas pressure and composition, which was determined using an SRS RGA200 mass spectrometer. A pressure gauge was not attached to the reactor during the activity test to reduce weight as the reactor is being spun horizontally. After testing, the remaining gas was vented, and the reactor was opened to remove the liquid and solid content that were separated using either a centrifuge or vacuum filtration. The solids were washed using acetone and dried overnight at 80°C to ensure that no liquid product remained. If solid biomass material was used, the percent solids conversion (%OSC) – that is the conversion of solid biomass material to liquid/gas products – was calculated according to Equation 3-1. Here, $m_{s,i}$ is the total mass of solid material loaded into the reactor (including catalysts), $m_{s,o}$ is the total mass of dried solids taken from the reactor, and $m_{b,i}$ is the mass of solid biomass (glucose) that was originally loaded into the reactor.

$$\%OSC = \frac{m_{s,i} - m_{s,o}}{m_{b,i}} * 100\% \qquad \textbf{3-1}$$

Analyses of the liquid products were conducted using GC-MS (Shimadzu GCMS QP5000) for qualification and GC-FID (Varian GC540) for quantification.

More specific test methods for each part of the project as well as catalyst preparation and characterization techniques are described throughout Chapters 4-7.

3.2 Assumptions and Experimental Control

The assumptions and strategies that were used to control the experiments throughout Chapters 4-7 consisted of the following:

- Gases followed the ideal gas law and as such were of uniform composition. Neither the loading gas nor product gas (at room temperature) exceeded a total pressure of 700 kPa.
- No gases were lost due to leaks or permeation. Reactors were leak tested using H_2 or He prior to purging. Gases were tested within 24 hours at room temperature.
- Liquid products were expected to be of uniform composition. Samples were shaken/stirred prior to analysis.
- It is expected that there were no changes in liquid products between reaction completion (reactor cooled to room temperature) and analysis time. Samples were stored in amber bottles within a dark, cool location. Samples were tested within a week.
- Solid material was assumed to be uniform when testing solid composition (ie. Elemental analysis). To ensure this, solid samples underwent grinding and mixing to ensure a uniform mixture.
- It was assumed that no catalyst material was lost during reactions due to mechanisms such as leaching.

3.3 Preliminary Tests

Preliminary tests were performed to demonstrate both the capability of performing the following reactions in the proposed reactor system: water-gas-shift reaction (WGSR) and enhanced H_2 production. Initially, two separate solvents, 1-methylnaphthalene (1MN) and hexadecane (C16) were used to determine the appropriate solvent for further use.

3.3.1 WGSR Tests

WGSR tests were performed to demonstrate that WGS reactions can occur within the reactor regardless of the fact that a solvent was present. These tests were performed using the reactor system described in Appendix A. The reactor was loaded with 16 g of solvent and an initial carbon monoxide pressure of 140 kPaG with an equimolar amount of water. For tests involving additives; CaO and Fe_3O_4 were each added at an additive-to-solvent mass ratio of 1:100. The purpose of these additives was to promote WGSR where Fe_3O_4 may act as a catalyst and CaO will capture CO_2, to promote further WGSR. Reactions were carried out at 350°C for 1 hour as this temperature corresponds to a typical operating temperature of iron oxide WGSR catalysts in industry [34].

With 1-methylnaphthalene (1MN) as the solvent, the concentration of H_2 in the product gas phase increased from 0.9% to 37.7% when Fe_3O_4 was added. With hexadecane (C16) as a solvent, the concentration increased from 2.2% to 43.8%. CO_2 was either in very low concentration (maximum 2.3% after adding Fe_3O_4 and CaO with C16 as the solvent) or remained below detectable limit. The significant increase in H_2 production demonstrates that WGS reactions may occur in the batch reactor in the presence of the solvent. These

results demonstrated that the reactor being stirred horizontally effectively facilitates mixing of all three phases allowing the gas phase to thoroughly contact the solid phase which would otherwise be constrained by contact with the liquid phase within a vertically stirred reactor.

3.3.2 Hydrogen Production from Cellulose

Dr. Andrew Harris' research group from The University of Sydney, Australia, previously demonstrated the possibility of producing hydrogen from cellulose and biomass in general by promoting WGSR [28-30]. Preliminary tests were performed to further demonstrate/confirm that H_2 could be produced from cellulose thermal decomposition in the proposed reactor system but at reduced temperatures (300-400°C) compared to typical pyrolysis processes. Comparisons were made between the two solvents, 1MN and C16 as well as reaction temperatures to determine the most suitable solvent and reaction temperature.

For these tests, the reactor was loaded with 16 g of solvent and 0.8 g of cellulose. Additives were added at similar ratios as mentioned for the WGSR preliminary tests. After purging, the reactor was filled with He at 310 kPaA (kPa absolute). Reactions were conducted at 300°C, 350°C, and 400°C for 1 hour.

With and without the additives (CaO and Fe_3O_4 together), the main gases constituting the product gas were H_2, CO_2, and CO. As seen in Table 3-1, increasing the temperature generally increased the output of all three gases as cellulose undergoes decomposition. This

was not a surprise as cellulose tends to decompose mostly within the range of 300-400°C, sometimes peaking around 350°C (depending on heating rate) [4, 8, 28, 29]. With the additives, H_2 production was improved. Overall, runs that were performed using C16 produced more H_2 and total gas. With the additives and the C16 solvent, 400°C appears to be more advantageous for H_2 production; however, when the 1MN solvent was used, increasing the temperature from 350°C does not appear to provide additional H_2.

Table 3-1: Thermolysis of cellulose: effects of temperature on product gas composition

Solvent	Additives	Temperature (°C)	Product Gas Partial Pressure (kPaA)		
			H_2	CO_2	CO
C16	None	300	11	102	47
		350	9	132	83
		400	17	157	151
	$CaO + Fe_3O_4$	300	13	5	25
		350	35	106	81
		400	42	106	155
1MN	None	300	4	33	26
		350	5	85	82
		400	10	134	168
	$CaO + Fe_3O_4$	300	5	0	14
		350	25	90	83
		400	23	78	136

Further testing at 350°C was also performed to determine the effect that each individual additive has on H_2 production. As seen in Table 3-2, CaO on its own has a major impact on H_2 production along with a dip in CO_2 and CO production. The dip in CO_2 is due to

carbon capture producing $CaCO_3$ while CO is consumed via WGSR. Fe_3O_4 on the other hand did not appear to produce additional amounts of H_2 on its own. However, this additive appeared to increase the production of CO_2 and CO.

Table 3-2: Thermolysis: effects of additives on product gas composition and H_2 production at 350°C

Solvent	Additives	Product Gas Partial Pressures (kPaA)		
		H_2	CO_2	CO
C16	None	9	132	83
	CaO	35	75	73
	Fe_3O_4	10	166	107
	CaO + Fe_3O_4	35	106	81
1MN	None	5	85	82
	CaO	23	78	71
	Fe_3O_4	8	105	81
	CaO + Fe_3O_4	25	90	83

A possible scenario that would explain the results for the Fe_3O_4 addition is that Fe_3O_4 catalyzed WGSR, producing H_2 and CO_2. H_2 was then consumed for hydrogenation or deoxygenation via hydrogenolysis in parallel to decarbonylation reactions producing more CO. This is supported in part by GC-MS results which detected furanic compounds including deoxygenation products and intermediates such as 2MF, DMF, furfural, and 5-methylfurfural, which are not as significantly prevalent in the results from other tests (see Figure 3-1). This was the first indication of the possibility of performing *in-situ* deoxygenation.

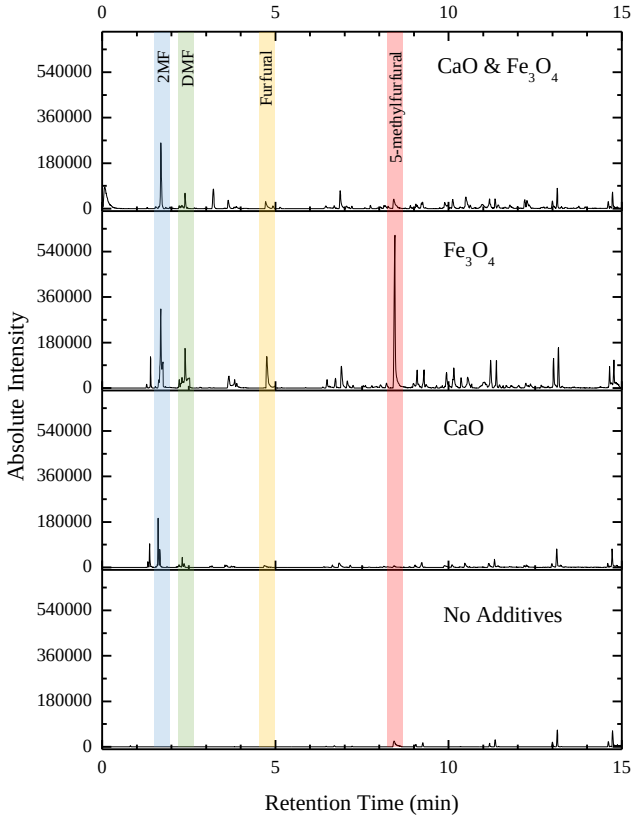

Figure 3-1: GC-MS chromatogram for cellulose decomposition experiments at 350°C with different additives and hexadecane as solvent

Throughout these tests, the solvents 1MN and C16 have been compared to one another. Tests using the C16 solvent consistently resulted in higher production of H_2 than the tests using 1MN solvent. To help explain this, GC-MS analyses were conducted on the liquid products. The chromatograms for tests using the C16 solvent at 400°C and 350°C (particularly with additives involved) revealed that the C16 solvent was susceptible to cracking which could aid the production of additional H_2. Cracking, demethylation, and trans-alkylation products were also witnessed for 1MN but only at 400°C. As a result, the most suitable solvent for further testing was deemed to be 1MN with an operating temperature of 350°C as is necessary to void the thermal cracking of the solvent. The

results from tables 3-1 and 3-2 suggest that C16 could be a possible alternative source for H_2. Co-processing hexadecane with biomass could yield promising results however this was deemed out of scope for this project.

Chapter 4: Decomposition of Glucose with *in-situ* Deoxygenation in a Low H_2 Pressure Environment – Part I: Monometallic Catalysts

4.1 Introduction

Recent advances in the past decade have seen the development of thermochemical processes and catalysts to produce biofuel from lignocellulosic material. The general process scheme has been to perform pyrolysis or liquefaction on lignocellulosic material to produce a crude bio-oil and then refine it using hydroprocessing technologies to perform deoxygenation, thereby producing fuels compatible with petroleum-based fuels [4, 17, 19, 55, 115, 182]. The challenge therein has been the reduction in hydrogen consumption. The requirement for hydrogen represents a sustainability issue as most of the world's hydrogen production (>95% in 2005) is from non-renewable sources such as methane reforming processes [183].

During the decomposition of lignocellulosic material CO_2, CO, H_2, H_2O, and light hydrocarbons are readily formed [4]. Given the presence of H_2, there is potential to use the product gas (upon separation if necessary) for deoxygenation. In addition, the presence of CO, H_2O, and light hydrocarbons represents a potential to improve H_2 concentrations by promoting the water-gas-shift reaction (WGSR) and reforming reactions. However, the infrastructure required to perform WGSR – on top of already needing additional infrastructure for deoxygenation – represents an additional challenge in terms of costs. In Chapter 2 it was discussed that future work regarding deoxygenation focus on reducing H_2 consumption by focusing on catalysts that promote both WGSR and deoxygenation. Ideally

then, it would be beneficial to perform all three reaction processes (decomposition, WGSR, and deoxygenation) in one stage – a one pot reaction stage. Therein, lignocellulosic material would be decomposed producing oxygenated compounds ready for deoxygenation. WGSR of the gas products (from biomass decomposition) would produce *in-situ* H_2, which would then be used by a catalyst to perform selective deoxygenation.

Kan et al., [51] studied the pyrolysis of coffee grounds using a NiCu catalyst and suggested that the presence of Cu promoted WGSR during pyrolysis along with reforming reactions. Supported metallic catalysts such as Ni and Pd catalysts have been investigated for tar-cracking/reforming activity during pyrolysis thus producing H_2 [24-27, 32]. A 5%Ni/MCM-41 catalyst for example was shown to increase the vol% of H_2 in the outlet gas from 1.2% (without catalyst) to 16.5% due to its activity towards tar-cracking [26].

In-situ deoxygenation of lignocellulosic decomposition products is rarely studied. However, deoxygenation reaction pathways of *in-situ* deoxygenation are expected to be consistent with the typical deoxygenation reactions that are reported for bio-oil model compounds. These model compounds have consisted of both phenolic (guaiacol) and furanic (furfural) compounds. Due to limits in hydrogen, selective/direct deoxygenation reaction pathways would be ideal for which various catalysts have been studied (see Chapter 2). Mochizuki et al., [184] reported that Co/SiO_2 favours the direct deoxygenation of guaiacol thus producing aromatic compounds, limiting hydrogen consumption. Sitthisa & Resasco [142] reported that Cu/SiO_2 was selective towards producing furyl alcohol and small amounts of 2-methylfuran (2-MF) from furfural at 1 atm H_2 while Pd/SiO_2 and

Ni/SiO_2 promoted decarbonylation (DCO) however Ni/SiO_2 also favoured ring-opening reactions. However, Ni catalysts are popular among researchers studying hydrodeoxygenation [65, 139, 185-188]. Jahromi & Agblevor [187] studied the Ni catalysts supported on red-mud, which demonstrated moderate selectivity towards non-saturated products, toluene and benzene, from guaiacol even at high H_2 pressures. In general, Ni, Cu, Pt, and Pd catalysts are popular choices for catalysis with regards to the deoxygenation/hydrogenation of furanic and phenolic compounds [54, 56, 106, 134, 139, 142, 144, 189].

Herein, a study was performed to determine possible catalyst candidates for the *in-situ* deoxygenation of products formed via the thermolysis of glucose. Glucose was used as a model compound for cellulose to limit decomposition pathways and products; therefore, products such as furfural and HMF (5-hydroxymethylfurfural), which can be easily analyzed, could be produced through predictable pathways. Being some of the most difficult oxygenated compounds to perform deoxygenation on; furanic compounds are very uniquely structured products with predictable deoxygenation pathways making them the ideal candidates for indicators of *in-situ* deoxygenation. Moderate temperature (350^oC) is used to allow for the decomposition of glucose and prevent secondary decomposition of the products into excessive carbonaceous material. The reaction system utilized 1-methylnaphthalene (1MN) as a solvent to aid with heat and mass transfer. The reactor was initially charged He and H_2 at 310 kPaA (filled at room temperature) to prevent evaporation of 1MN, which has a high boiling point and relative inactivity in the reaction system with a catalyst (such as 4wt%Ni/SiO_2). Given that *in-situ* production of H_2 via WGSR was not

yet the primary focus for the catalysts, a small source of H_2 was provided (37.6 kPaA) in order to maintain the activity of the deoxygenation catalysts.

The monometallic catalysts that were selected for this study were Ni, Cu, Fe, Co, Pt, Pd, and Re. These catalysts were mounted on a silica support at concentrations of 4% and 0.5% (by weight) for the first four non-noble metals and 0.5wt% for the noble metals. 4% and 0.5% were selected to demonstrate the impact of metallic site dispersion and amount of active metal. The noble metal catalysts were employed only at 0.5% concentrations due to solubility limits. The aforementioned metals were selected due their popularity and potential activity towards selective deoxygenation. Unlike the other metals, Co and Re are far less popular, however Co has been proven to promote selective deoxygenation pathways of various bio-oil compounds [65, 184, 188, 190] and Re-based catalysts have provided interesting results in recent studies [157, 191, 192]. Fe was selected because it has the potential to promote selective deoxygenation due to its oxophilic nature. It was understood though that on its own, Fe is not a very active and it is instead often incorporated into bimetallic catalysts [106, 146]. An inactive support, silica, was used in order to focus on the active roles of the metals.

4.2 Experimental

4.2.1 Catalyst Preparation

Ni, Co, Cu, Fe, Re, Pt, and Pd catalysts supported by silica (Aerosil 200) were prepared via incipient wetness impregnation using the following salts from Sigma Aldrich: nickel (II) nitrate hexahydrate, cobalt (II) nitrate hexahydrate, copper (II) nitrate

hemi(pentahydrate), iron (III) nitrate nonahydrate, ammonium perrhenate, tetraamineplatinum (II) nitrate, and palladium (II) nitrate dihydrate. Prior to impregnation, the silica support was dried at 120°C for 6 hours and calcined at 550°C for 4 hours. Upon impregnation, catalysts were dried at 120°C for 6 hours and calcined in air at 550°C for 6 hours with heating rates of 5°C/min. For performance testing, catalysts were pelletized and crush to a size range of 40-60 mesh. Catalyst were reduced in flowing H_2 at 50 nmL/min at desired reduction temperatures with a heating rate of 10°C/min. The specific reduction temperatures that were used were as follows: 450°C for Ni [142], 550°C for Co [139], 400°C for Cu [39], 550°C for Fe [139], 400°C for Re [192], 500°C for Pt [159], and 250°C for Pd [142]. Non-noble catalysts were prepared in concentrations of 4% (weight percent) and 0.5% (ie. 4%Ni/SiO_2 and 0.5%Ni/SiO_2) while noble metal catalysts were prepared in concentrations of 0.5% (ie. 0.5%Re/SiO_2).

4.2.2 Activity Tests

Activity/performance tests were performed in a horizontal, stirred 55 mL stainless steel reactor at a reaction temperature of 350°C for 1 hour with 800 mg of glucose. Reduced catalysts were used in the reactor at a 1:5 catalyst to glucose mass ratio. 1MN (Sigma-Aldrich) was used as a solvent (20:1 solvent to glucose mass ratio) to promote heat and mass transfer. Thus, a horizontally stirred reactor was used to ensure contact between solid and gas phases. 350°C was selected as a reaction temperature as it is roughly the temperature at which cellulose undergoes rapid decomposition [8, 9, 28, 29] and is the temperature often associated with high temperature WGSR [34]. Prior to reactions, the reactor was vacuum purged with He and then filled with 37.6 kPaA of H_2. He was then

added until a total pressure of 310 kPaA was achieved in order to prevent the evaporation of the solvent during reaction.

Upon cooling to room temperature, gases within the reactor were tested using a RGA200 mass spectrometer. A HP-PLOT/U column (maintained at 30^{o}C) was used to separate the gases. Liquid and solid content from the reactor were separated and the solid contents were washed with acetone and dried in an oven at 80^{o}C overnight. Liquid outputs were analyzed using GC-MS (Shimadzu GCMS QP5000) and GC-FID (Varian GC450). The carbon and hydrogen contents of the solid residue was determined via CHNS analysis (Leco CHNS-932).

TGA analyses were performed using a TA Instruments TGA Q500 to determine the direct impact of the catalysts on the decomposition/weight loss of glucose. Catalysts along with glucose were loaded into the TGA at a ratio of 1:5. The TGA was heated from room temperature to 950^{o}C at a rate of 5^{o}C/min under flowing He (50 nmL/min).

4.2.3 Catalyst Characterization

Based on performance; selected catalysts underwent characterization. Surface area, pore volume, and pore size distribution were determined via BET/BJH physisorption techniques using an Autosorb 1-C. Temperature programmed reduction (TPR) analyses were performed using an Autosorb 1-C with a RGA200 mass spectrometer as the detector. A quartz u-cell was loaded with 150 mg of catalyst, which was then vacuum dried at 300^{o}C for 20 minutes under flowing helium (50 nmL/min). TPR analysis was then performed by

heating the catalyst from room temperature to 900°C at a rate of 10°C/min under flowing gas (50 nmL/min He with 1% H_2).

X-ray diffraction was performed at the UNB Geochemical and Spectrographic Facility using a Bruker AXS D8 XRD. XRD spectrums were gathered within the 2Theta range of 20-80° at a rate of 0.02°/second. HRTEM and STEM analyses were performed at the UNB Microscopy and Microanalysis Facility with a JEOL JEM-2010 (S)TEM. HRTEM Images were collected with a Gatan Ultrascan camera using Digital Micrograph. Verification of the metallic sites was determined by collecting EDS spectra with an EDAX Genesis 4000 Energy Dispersive X-ray (EDS) analyser. An accelerating voltage of 200 kV was used for the imaging and analysis. Images were processed using an open source image processing platform, Fiji, to determine the size distribution of metallic sites (Ni, Co) on the supporting material [193].

4.3 Results and Discussion

4.3.1 Solid Products

The output of solid organic material from glucose decomposition, although inevitable, is the least favorable output from the system. The resulting organic solids from the reaction represent an obstacle in the process – if any catalytic material is to be reused, the organic solids must be removed which may eventually require oxidative measures. As seen in Figure 4-1, most catalysts saw improvements in the conversion of organic solids into liquid and gas products over the base case with just glucose, particularly the Ni based catalysts which exhibited the highest reduction in organic solids. This was followed by Cu and Pd

catalysts while other catalysts did not appear to have significant impacts on the reduction of organic solids. The results from CHNS analysis, as seen in Figure 4-2, show that the addition of some catalysts such as 4%Ni/SiO_2 and 4%Co/SiO_2 increased the ratio of elemental hydrogen to carbon in the solid residue in comparison to the base case. Where the H:C ratios are 2 for glucose and 0 for pure carbon (char); an increase in H:C ratio upon catalyst addition infers that less char may have been formed. In general, most of the catalysts provided a slight increase in the H:C ratio with ratios exceeding a 10% increase; however, only the aforementioned catalysts approached an H:C value of 1 (an increase of approximately 42% for 4%Ni/SiO_2).

There are two ways to reduce solid residue – conversion of glucose and the prevention of formation of solids via char formation or the formation of polymerization products such as humins from tar compounds. Supported metals, Ni in particular, have been studied for their ability to promote tar cracking (which consists of aldehydes and other products from the decomposition of cellulose/glucose) and the subsequent reforming of small, volatile compounds during the pyrolysis of lignocellulosic material [24-27, 31-33]. Widyaningrum and co-workers [25] reported that supported Ni based catalysts prompted C-C and C-H bond breakages leading to the direct cracking of tar compounds. Therefore, it is likely that catalysts such as 0.5%Ni/SiO_2 and 0.5%Cu/SiO_2 promoted tar cracking better than 4%Ni/SiO_2 and 4%Cu/SiO_2 respectively.

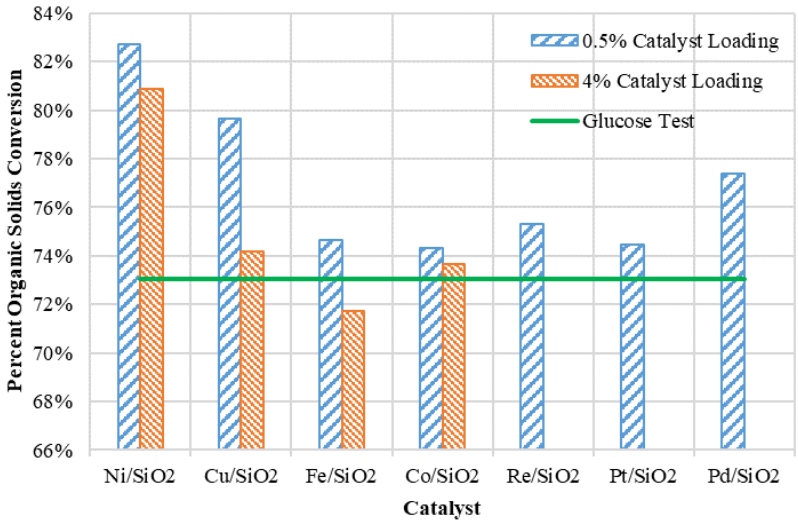

Figure 4-1: Percent Dry Organic Solids Conversion vs. Catalyst Type

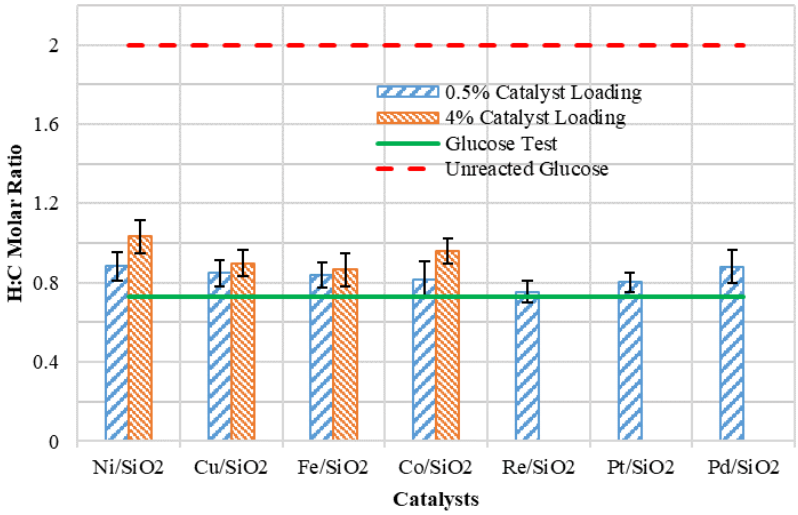

Figure 4-2: H:C Molar Ratio in Solid Residue

Comparing the catalysts to each other shows that Ni reduced the amount of organic solid residue the most with an additional 9% conversion of solids into liquid and gas phase products over the base case. Supported Ni catalysts have achieved higher tar-cracking activity when promoted with Pd, which catalyzed the reduction of the Ni^{2+} that was formed

during reactions back to Ni^0 [24]. This would more readily occur at a temperature ~60°C below that of unpromoted Ni. Therefore, a catalyst that is more readily reduced at decomposition temperatures may be more stable and thus more active in the long term.

4.3.1.1 Temperature Programmed Reduction (TPR) Analyses

Figure 4-3 shows the TPR profiles for various 4% monometallic catalysts along with corresponding metal oxide powders. Due to their low metal concentrations, 0.5% catalysts such as 0.5%Ni/SiO_2 and 0.5%Re/SiO_2 had very faint and indistinguishable profiles (this occurred even when the catalyst loading was doubled). For the Ni, Fe, and Co catalysts, it was obvious that the supporting material has an impact on the reducibility of the metals as these metals all experienced a shift to the right in their TPR profiles. 4%Ni/SiO_2 had a moderate peak centered at ~425°C and spanning from about 400-500°C. Compared to 4%Fe/SiO_2, which had a weaker TPR profile with two peaks at 450°C and 590°C that were attributed to different oxidative states of iron matching those shown in literature [139, 146]. It is undeniable that Ni's reducibility was an advantage over the Fe catalyst. The iron catalyst is obviously not readily reduced and although its oxophilic nature makes it appealing for removal of oxygen, thus it would need to be paired with another metal to make it more reducible.

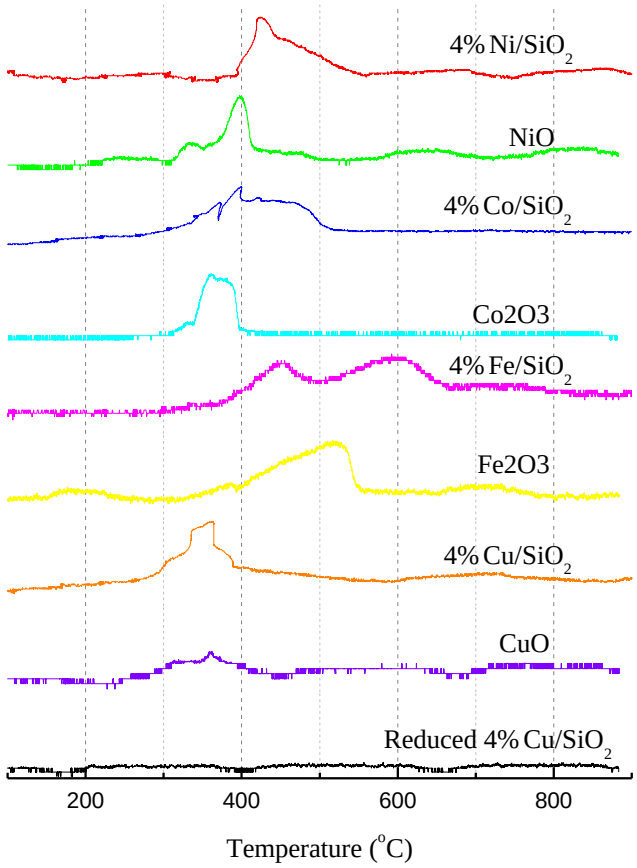

Figure 4-3: Hydrogen consumption profiles for various monometallic catalysts. 150 mg of catalyst/10 mg of associated metal oxide powders (NiO, Co_2O_3, Fe_2O_3, CuO) in gas flow of 50 nmL/min at 1% H_2 in He. Temperature ramp 10°C/min

Compared to Cu and Co, there are no obvious advantages with the Ni catalyst in terms of reducibility alone. Cu, for example, was much more reducible with a peak temperature of ~365°C. This may explain why 0.5%Cu/SiO_2 was competitive in lowering of solids output. Due to the various oxidative states of Co, two separate peaks were anticipated for the cobalt catalysts. This was demonstrated by Ning et al., [194] who reported two distinct peaks within the 300-400°C range for the reduction of a Co/SiO_2 catalyst with a similar heating rate of 10°C/min. The TPR profile for 4%Co/SiO_2 consisted of two distinct peaks, likely

attributed to its oxidative states Co^{3+} and Co^{2+}, with a broad shoulder. The reduction of the Co catalyst was centered around 400-450^{o}C which from the 550^{o}C used by Mortensen et al., [139]. However the broad, split peak profile and temperature range corresponds to that reported by Huynh et al., [132] and is likely attributed to low dispersion/large metallic sites and/or interactions with the support. Although Co does begin to reduce at a lower temperature, this would not make it advantageous over Ni for tar-cracking and preventing solid output as the temperature range in which Co^{0} is formed is similar to that of Ni.

4.3.1.2 TGA Tests

Given the lack of studies that have been performed on the decomposition of glucose or even cellulose in the presence of heterogeneous catalysts; TGA experiments were conducted to provide an additional understanding of how each catalyst may impact the decomposition of glucose. As demonstrated in Figure 4-4, the addition of catalysts such as 4%Ni/SiO_2 and 4%Co/SiO_2 had a significant impact on the rate in which glucose decomposed. Overall, the decomposition of glucose begins with a small weight loss of ~20-32% followed by a much larger weight loss of ~45-70% (depending on catalyst addition), as shown in Table 4-1. The addition of particular catalysts - such as Ni, Co, Fe, and Re catalysts - appears to reduce the temperatures in which the maximum rate of weight loss occurs for both periods of major weight loss. Pt, Pd, and Cu catalysts on the other hand had little to no effect on glucose decomposition temperature/rate.

As shown in greater detail in Table 4-1, for Ni, Co, Fe, and Re, not only were the temperatures of maximum decomposition rate decreased but the actual rate of

decomposition was changed as well, increasing the decomposition rate in the first peak and lowering the decomposition rate in the second. For example, the maximum rate of weight loss in the first period of decomposition went from 0.49 %/K at 215°C to 0.64 %/K at 199°C upon addition of 4%Co/SiO_2. In the second period of decomposition, the maximum rate of weight loss went from 0.92 %/K at 293°C to 0.50 %/K at 250°C. The significant change in the first period of decomposition demonstrates that the catalysts influence the glucose by promoting deoxygenation via dehydration (likely due the presence of Lewis acid sites) which is described as one of the first major reaction steps during glucose decomposition [8, 9, 18, 23, 48, 195].

Given that the decomposition model for glucose, as demonstrated by Vinu & Broadbelt [9], relies heavily on dehydration in its early steps, it was determined that the Ni, Co, Fe, and Re catalysts promote either dehydration of glucose itself or the ring-opening of glucose allowing for higher rates of dehydration. Although 0.5%Re/SiO_2 reduced the decomposition temperature of the first stage most significantly, the total weight loss in the first stage paled in comparison to the other catalysts. 4%Fe/SiO_2 and 4%Co/SiO_2 are regarded as having the highest impact on glucose decomposition as they both significantly lowered the decomposition temperatures all while achieving the highest weight loss in the first stage of decomposition.

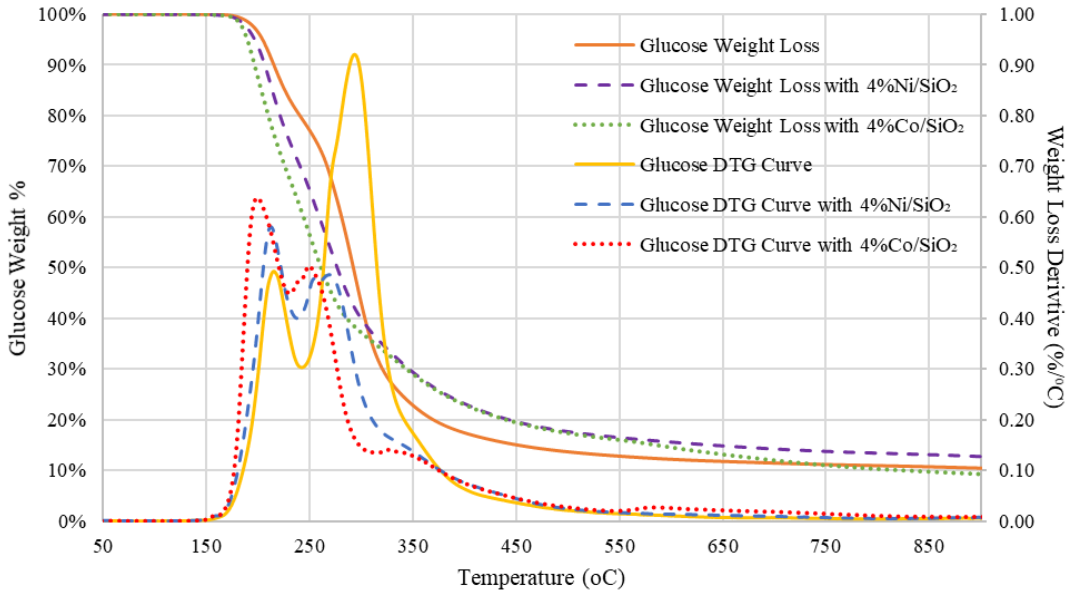

Figure 4-4: TGA Results of Glucose with and without 4%Ni/SiO_2 and 4%Co/SiO_2 catalyst. Catalysts added at 1:5 ratio with glucose.

Table 4-1: TGA results summary for glucose with catalyst additives. Temperature (T) program: 25°C to 900°C at 5 °C/min. Y = percent of solid remaining (does not include catalyst weight).

Catalyst	Initial Major Weight Loss					Valley			Second Major Weight Loss				
	T^a (°C)	Y^a (wt%)	T^b (°C)	Y^b (wt%)	$(-dY/dT)^b$ (%/K)	T^c (°C)	Y^c (wt%)	$(-dY/dT)^c$ (%/K)	T^d (°C)	Y^d (wt%)	$(-dY/dT)^d$ (%/K)	T^e (°C)	Y^e (wt%)
No Catalyst	178	99.6%	215	90.0%	0.49	242	79.4%	0.30	293	49.1%	0.92	417	16.4%
0.5%Ni/SiO_2	173	99.5%	215	87.4%	0.46	238	76.2%	0.35	281	41.4%	0.57	438	17.0%
4%Ni/SiO_2	174	99.5%	211	86.6%	0.58	238	71.5%	0.40	261	58.8%	0.48	440	20.2%
0.5%Co/SiO_2	175	99.5%	211	84.9%	0.61	235	70.8%	0.44	255	60.0%	0.49	438	21.7%
4%Co/SiO_2	173	99.5%	199	88.0%	0.64	231	67.5%	0.45	250	56.6%	0.50	440	20.0%
0.5%Fe/SiO_2	176	99.5%	207	88.3%	0.56	235	73.0%	0.39	269	55.8%	0.47	438	21.9%
4%Fe/SiO_2	171	99.5%	197	88.4%	0.64	229	69.2%	0.39	248	59.3%	0.43	430	25.5%
0.5%Cu/SiO_2	181	99.3%	221	87.4%	0.48	247	74.7%	0.36	289	51.1%	0.59	425	19.8%
4%Cu/SiO_2	181	99.3%	215	90.9%	0.36	239	81.5%	0.29	292	47.6%	0.85	407	10.6%
0.5%Re/SIO_2	154	99.8%	167	96.9%	0.26	224	86.3%	0.08	274	67.8%	0.59	446	22.4%
0.5%Pt/SIO_2	175	99.1%	221	89.0%	0.33	244	80.8%	0.27	295	47.6%	0.90	397	13.0%
0.5%Pd/SiO_2	178	99.1%	222	88.3%	0.36	246	79.3%	0.29	295	45.2%	0.92	397	10.3%

[a] – Point at which mass loss rate begins to exceed 0.05 %/K
[b] – First peak point on DTG curve
[c] – Valley point on DTG curve between first and second peak
[d] – Second peak point on DTG curve
[e] – Point at which mass loss rate declines below 0.05 %/K

Varying the metal concentrations from 0.5% to 4% increased the impact on glucose decomposition. In each case of Ni, Co, and Fe, going from 0.5% to 4% metal concentration shifted decomposition to lower temperatures with increases in weight loss rate in the first period and decreases in weight loss rate in the second period of decomposition. For Co, this effect was less dramatic than for Ni and Fe. The Cu catalysts on the other hand provided unusual results where both the 0.5% and 4% catalysts had little effect on the temperatures at which maximum weight loss occurred. The height of the peaks decreased; however, in the case of the 4% catalyst, the second peak became broader which allowed for a higher total weight loss at ~400^{o}C. This relates back to the influence the catalysts have on dehydration. As increasing metal concentration is expected to increase deoxygenation capabilities [186]; thus, in this study, increasing metal concentration increased activity towards dehydration reactions with the exception of the Cu catalyst.

Above all, it is important to note how the results from the TGA do not correlate with those of the activity tests. In the activity tests, 0.5% catalysts were shown to produce less solid residue (see Figure 4-1). TGA results, suggest that 4% catalysts would have the greatest impact on the decomposition of glucose. However, the activity tests were performed at 350^{o}C for 1 hour after heating from room temperature at an average heating rate of ~8^{o}C/min. It is expected that after such a period of time, the catalysts have consumed most of the glucose allowing for intermediates to undergo secondary reactions. These secondary reactions, which include tar cracking, could prevent solids from being produced and/or char formation/polymerization from occurring – owing to higher H:C ratios observed in Figure 4-2. In TGA since all volatilized matter is immediately removed, there is little

chance for secondary reactions of light compounds. This helps confirm the earlier suggestion that the superior reduction of solid content witnessed by 0.5%Ni/SiO_2 was not an increase in glucose conversion but rather an increase in tar cracking/reforming.

4.3.1.3 Electron Microscopy Analysis

The question arises, why does 0.5%Ni/SiO_2 offer a greater activity in the reduction of solid residue than 4%Ni/SiO_2 as seen in Figure 4-1? Although many characterization techniques such as TPR and XRD failed to analyze the 0.5% catalysts due to their low concentrations; HRTEM analyses paired with EDS was used to distinguish metallic sites were still capable of demonstrating obvious differences. Images from HRTEM clearly showed that the metallic sites of 0.5%Ni/SiO_2 were sparser than that of 4%Ni/SiO_2 – as would be expected. Further analysis of the catalyst particles on the SiO_2 support showed that the size distribution was similar between the two concentrations of Ni with most catalyst sites being within the range of 5-10 nm in size (approximate diameters). Sites smaller than 3 nm were not easily distinguishable with TEM. Ni sites were easily distinguishable in TEM images of 4%Ni/SiO_2 as clusters of vivid dark spots whereas for 0.5%Ni/SiO_2 some sites were clearly visible, however, there was greater need for additional verification via EDS to identify Ni site locations (see Figures 4-5a and 4-5b). Ruppert et al., [32] suggested that smaller Ni crystallites on ZrO_2 provided a higher activity in tar cracking resulting in higher yields of H_2. Therefore, a catalyst with small, well dispersed metal sites may be most ideal for treating tar during cellulose/glucose decomposition. In general, the size distribution of metallic Ni sites was comparable between the two catalysts (see Figure 4-6), however, the Ni sites of the 4%Ni catalyst appeared in large clusters while those of the 0.5%Ni catalyst

appeared to be more dispersed making them more difficult to identify. The 0.5%Ni catalyst likely benefited from its higher degree of dispersion providing a higher Ni surface area:volume ratio than the 4% catalyst which suffered from a clustering effect that may have hindered the usability of all the material. It is suspected that the clusters that were observed could potentially sinter or agglomerate and undergo crystal growth at elevated temperatures during prolonged use resulting in further deactivation.

For comparison, analyses were also performed on the Co catalysts which had an even more obvious difference between the 0.5% and 4% catalysts. Like 0.5%Ni/SiO_2; the 0.5%Co/SiO_2 catalyst was more dispersed than the 4% catalyst which appeared to suffer from agglomeration as the metallic sites were of larger size in general even when compared to the 4%Ni/SiO_2 catalyst. The metallic sites of the 4%Co catalyst material appear to be so heavily agglomerated that there are indications of possible lattice fringing in TEM images. Although the 0.5%Co/SiO_2 catalyst did not severely outperform the 4%Co/SiO_2, the 4% catalyst did not benefit from having extra material which may be attributed to the lack of dispersion.

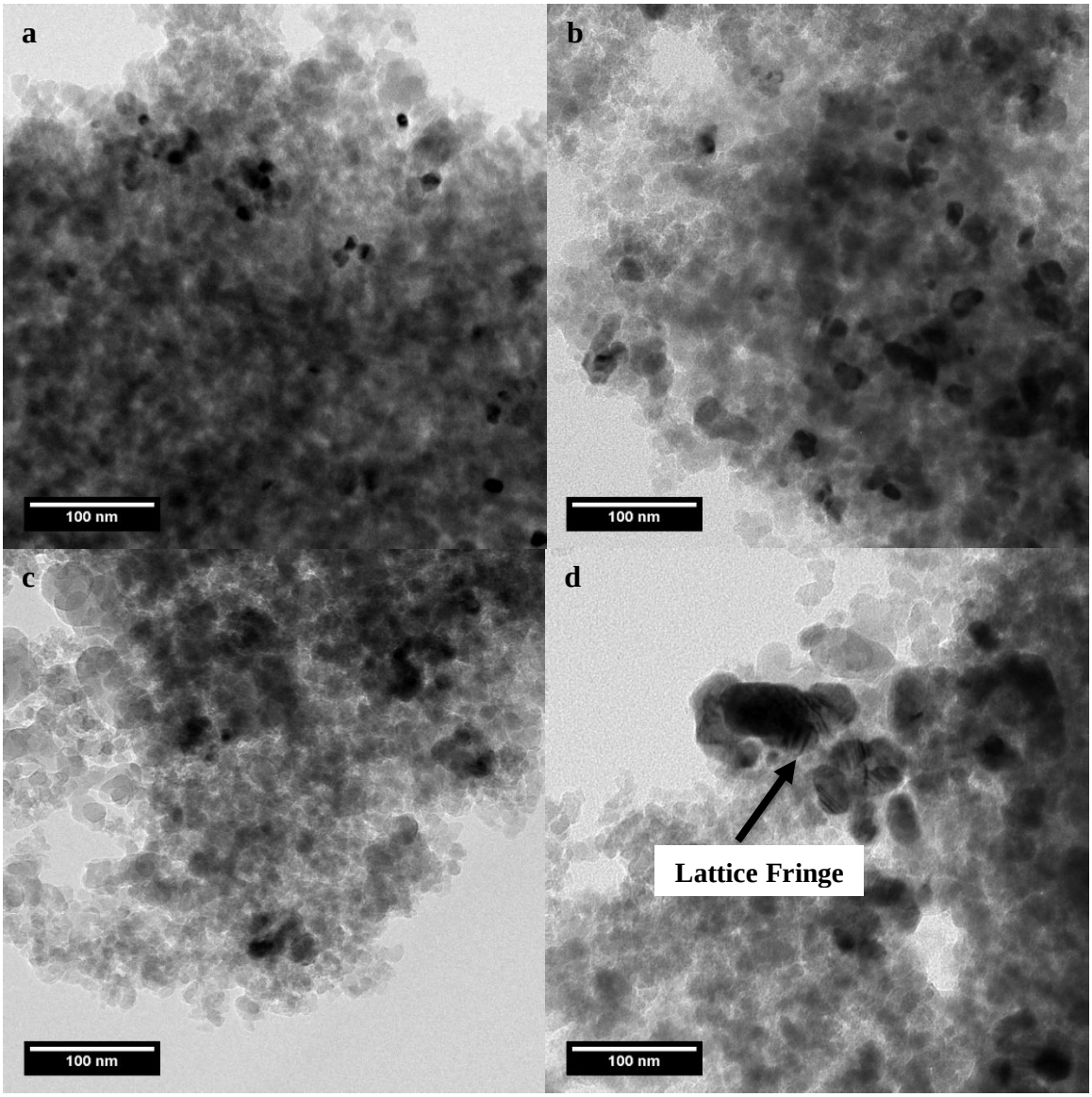

Figure 4-5: TEM Images of a. 0.5%Ni/SiO_2, b. 4%Ni/SiO_2, c. 0.5%Co/SiO_2, and d. 4%Co/SiO_2

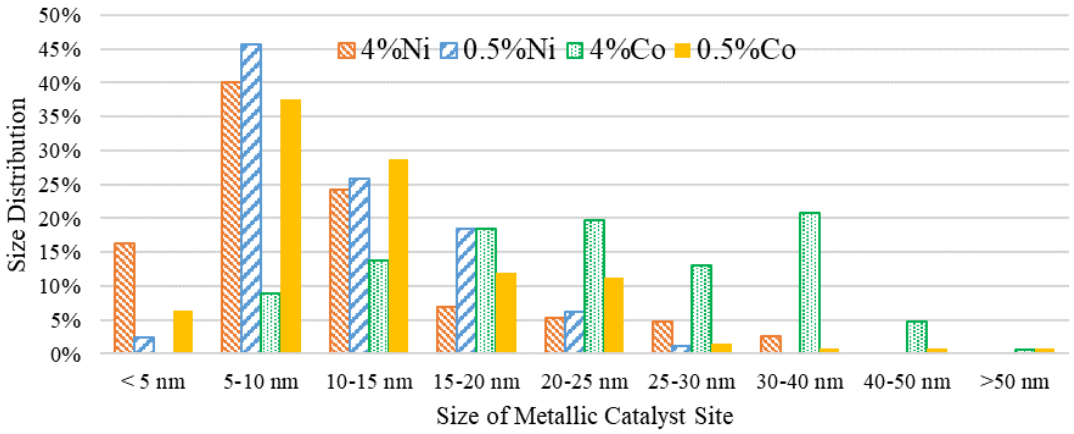

Figure 4-6: Size distribution of Ni and Co metallic catalyst sites from TEM analyses

4.3.1.4 Physisorption Analysis

Widyaningrum and co-workers [25] reported that pore size was a major concern during the pyrolysis of cellulose – too small of pores reduce accessibility as was noted as a key issue for SBA-15, instead a silica-MCF support with average pore sizes of 15-50 nm was more beneficial. Physisorption analyses that were performed on the 0.5% and 4% Ni/Co catalysts demonstrated that the catalyst materials did not significantly impact the surface area and pore volume of the supporting SiO_2 material and that the pore diameters of the catalysts are within the suggested range (see Table 4-2). There are concerns that some of the catalyst crystals may not fit within the pores – especially those of 4%Co – because at least ~7% of the catalyst crystals exceed the average pore diameter.

In conclusion, it is most likely that the 0.5% catalysts - Ni in particular - outperformed their 4% catalyst counterparts because of their dispersion. The higher concentration catalysts

may suffer from agglomeration of clustering of catalyst sites perhaps hindering mass transfer.

Table 4-2: Physisoprtion results for Ni and Co catalysts

Catalyst	BET surface area (m^2/g)	Pore volume (cm^3/g)	Average pore diameter (nm)
0.5%Ni/SiO_2	204	0.63	12.3
4%Ni/SiO_2	184	0.66	17.5
0.5%Co/SiO_2	176	0.63	17.5
4%Co/SiO_2	203	0.69	17.4

4.3.2 Gaseous Products

Aside from the inert gas that was initially used to charge the reactor, the output gas phase for each catalyst run mainly consisted of non-condensable gases H_2, CO_2, and CO, which are typical products from the decomposition of cellulose/glucose. With glucose as the precursor, H_2 is likely consumed by hydrogenation and deoxygenation reactions and produced by char formation, water-gas-shift, and reforming reactions [9]. Hypothetically, CO_2 is not likely to be consumed by any reaction but is produced via char formation and water-gas-shift reactions [9]. CO on the other hand, may be consumed by water-gas-shift and produced by reforming and decarbonylation reactions. According to the glucose thermal decomposition mechanism developed by Vinu & Broadbelt [9], there are no other known reaction routes in which H_2, CO_2, or CO is produced during glucose decomposition. However, it is noteworthy that cracking may occur producing various products including H_2, CO_2, and CO. In addition, any formic acid that is produced may rapidly decompose to either H_2O and CO or H_2 and CO_2.

As seen in Figures 4-7 to 4-9, the output of H_2 exceeded the amount that was initially charged into the reactor by as much as a ~71% (based on the percent difference from the initial loading of H_2) increase with exceptions for 4%Fe/SiO_2 and 0.5%Pd/SiO_2, which demonstrated an overall consumption of H_2. The performance of the catalysts is compelling compared to the base case (testing with just glucose) in terms of H_2 and CO output. Non-noble metal catalysts did not have remarkably high outputs of H_2, and CO compared to the base case. Based on the observed WGSR, tar cracking, and reforming activities of supported Ni and Co catalysts in the literature, it was expected that H_2 production would exceed the base case [25-27, 32-34, 196, 197]. Likewise, the other metals tested here have been investigated for WGSR activity [34, 42, 198-201]. One possible explanation is that these catalysts promote the *in-situ* production of H_2 via WGSR, however it is readily consumed for hydrogenation/ deoxygenation – reactions which the catalysts are also expected to be active towards (see Chapter 2, Section 2.2.4.3). This would also explain general increases in CO_2 output.

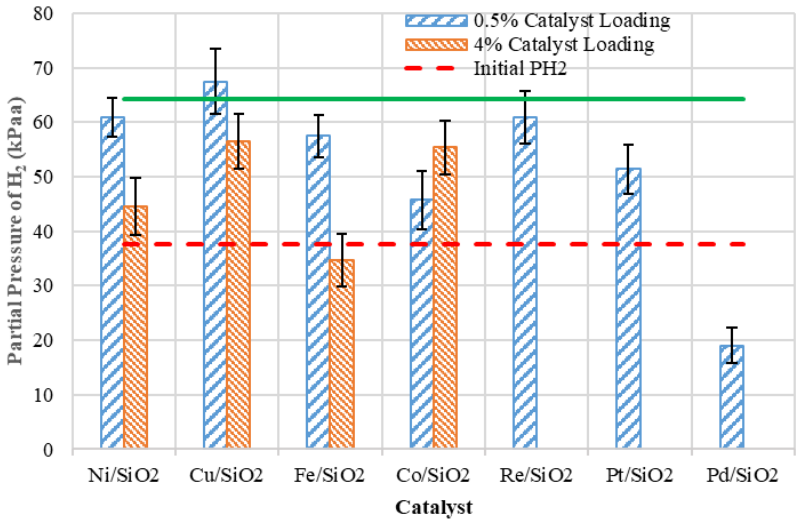

Figure 4-7: PH_2 Changes with Catalyst Type

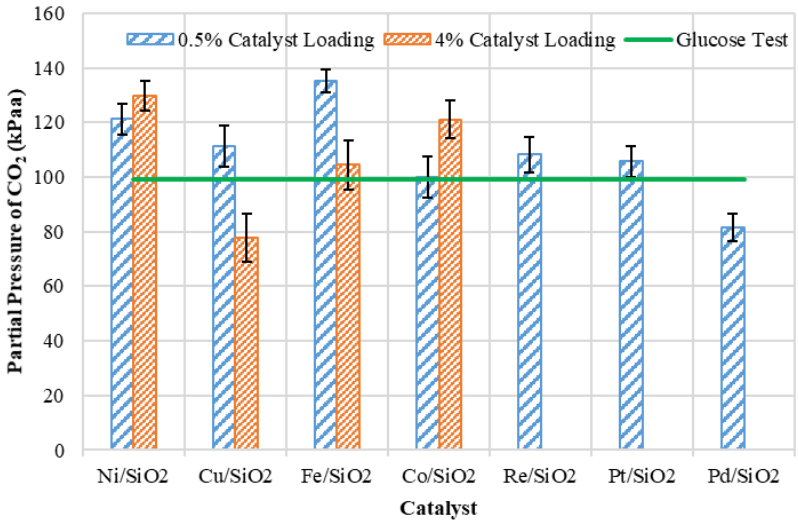

Figure 4-8: PCO_2 Changes with Catalyst Type

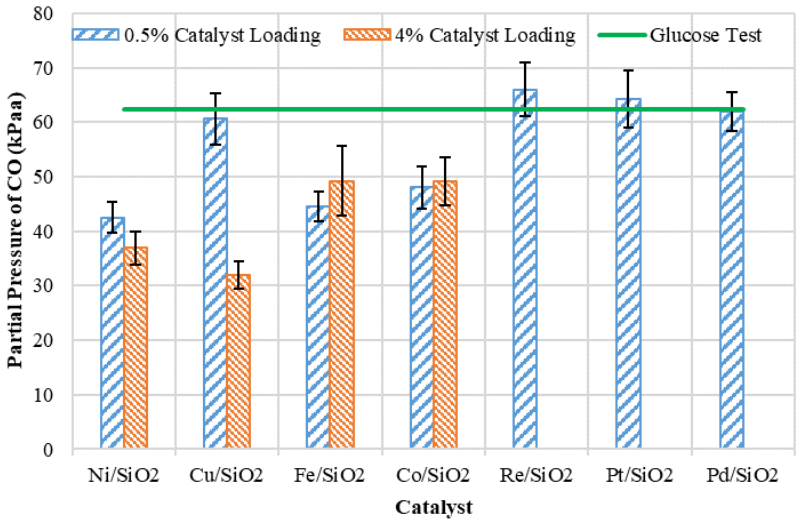

Figure 4-9: PCO Changes with Catalyst Type

In correspondence to the solid output results, the output of H_2 for 0.5%Ni/SiO_2, 0.5%Cu/SiO_2, and 0.5%Fe/SiO_2 exceeded that of their higher concentration counterparts. This could be either due to the 0.5% catalysts' ability to promote tar cracking - attributed to higher degrees of dispersion – or even a reduced rate in consumption due to lesser

hydrogenation/deoxygenation activity. Regardless, this trend is not complementary to the results of CO_2 and CO meaning the differences cannot be attributed to WGSR activity alone. For Ni, it seems reasonable that 0.5%Ni/SiO_2 would produce more H_2 and CO than 4%Ni/SiO_2 because 0.5%Ni/SiO_2 was more active towards tar cracking and reforming.

A reduction in CO_2 production upon addition of the 0.5%Pd/SiO_2 catalyst corresponded to a significant reduction in H_2. However, as seen in Figure 4-9, the output of CO is maintained on par with the base case. It is not surprising to see a consumption of H_2 by 0.5%Pd/SiO_2 because it is widely regarded as a reductive catalyst. The lower CO_2 production on the other hand suggests either a hindrance towards WGSR or char formation. As the CO output remained almost untouched, it is not entirely reasonable to assume that the 0.5%Pd/SiO_2 negatively impact WGSR activity as the base case has no catalytic activity. It is more reasonable to suggest that the reduction in H_2 and CO_2 is the result of H_2 being rapidly consumed via hydrogenation/deoxygenation to potentially stabilize the tar, or 0.5%Pd/SiO_2 hindered char formation. In Figure 4-2, it was shown that 0.5%Pd/SiO_2 had one of the highest H:C ratios in the solid residue. Although the increase in H:C ratio was not spectacular, it does further suggest that hindrance towards char formation was an impacting factor for the gas output.

Two catalysts that stand out are 0.5%Cu/SiO_2 and 0.5%Re/SiO_2. 0.5%Cu/SiO_2 was a competitive catalyst in terms of solid and gas output. As shown earlier 0.5%Cu/SiO_2 had the third least amount of organic solid residue with a corresponding high output of H_2. The 0.5%Cu/SiO_2 catalyst's competitiveness is likely attributed to both more dispersion and its

lower reduction temperature. Copper based catalysts have been used for low temperature WGSR processes due to its lower reduction temperature [34]. This would explain the higher amounts of H_2, and CO_2 produced by these catalysts however, again, this does not correspond to a decrease in CO.

The 0.5%Re/SiO_2 catalyst, on the other hand did not have a remarkably high reduction in solid residue but it had a competitively high output of H_2 – higher than the other two noble metals that were tested. Given the high CO output 0.5%Re/SiO_2 does not appear to be as active towards WGSR as other catalysts with CO outputs comparable to the base case. Given that the rhenium catalyst also had a low H:C ratio, it is suspected that 0.5%Re/SiO_2 did not hinder char formation like the other catalysts and most of the output H_2 witnessed here is the result of char formation.

Despite being more disperse and having smaller catalyst site sizes; the 0.5%Co/SiO_2 produced less H_2 and CO_2 than the 4%Co/SiO_2 catalyst which simply benefitted from having more catalytic material. The two catalysts however had similar amounts of organic solid residue, but the 4%Co had a higher H:C ratio. This suggests that the higher H_2 and CO_2 outputs were more likely the result of higher WGSR activity. Although having a higher Co concentration offers no advantage in reduction of solid residue; simply having more material does appear to have a small advantage in H_2, which is to insignificant to justify using the 4%Co/SiO_2 over the 0.5%Co/SiO_2

4.3.3 Liquid Products

Although typically in low concentrations, furanic compounds produced during the decomposition of cellulose/glucose were selected for monitoring *in-situ* deoxygenation reactions because they have a clear definition of a beginning and an end. HMF and furfural are typical furanic products that are described as products of cellulose decomposition. Performing deoxygenation of these two compounds yields 2-methylfuran (2MF) and 2,5-dimethylfuran (DMF). The deoxygenation pathways for producing 2MF and DMF have been well described in literature and are demonstrated in Chapter 2, Figure 2-13. DMF is produced from HMF via a sequence of hydrogenation and hydrogenolysis reactions to remove oxygen as water requiring a H_2:HMF molar ratio of 3:1. 2MF may be produced via the hydrogenation and hydrogenolysis of furfural or via a pathway from HMF involving DCO. It is important to note that, as described by Vinu & Broadbelt [9], both furfural and HMF may be produced via glucose decomposition. Therefore, the presence of 2MF in the products does not necessarily demonstrate a favoritism towards the DCO pathway.

The distribution of total furanic products for each test is represented in Figure 4-10. Aside from 2MF, DMF, furfural, and 5-methylfurfural, other furanic compounds that were detected were furfuryl alcohol, trimethylfuran, and 2-acetylfuran. Most interestingly, glucose on its own produced 2MF and DMF either via thermal reactions or catalyzed by the reactor wall; however, furfural still constituted a large portion of the furanic products.

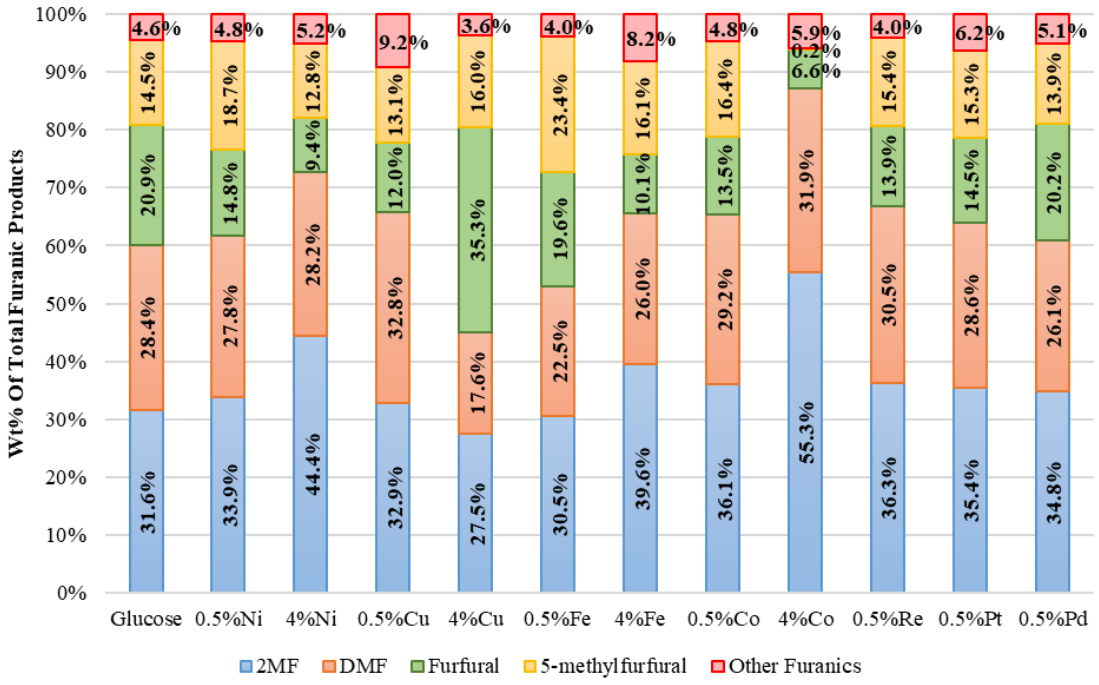

Figure 4-10: Total Furanic product distribution

When 0.5%Ni/SiO_2 was added, the distribution shifted slightly more towards 5-methylfurfural at the expense of furfural concentration. This demonstrates that the 0.5%Ni/SiO_2 catalyst was not necessarily active towards deoxygenation but instead altered the decomposition pathway. In contrast, 4%Ni/SiO_2 provided a noticeable difference in the fraction of 2MF at what appears to be an almost direct expense of furfural. In the literature, Ni catalysts have been shown to promote the deoxygenation of furanic compounds via various reaction pathways. Ni reportedly interacts with the aromatic ring thereby making it active towards the DCO of carbonyl groups on furan [142, 146]. Despite this, furan was not detected in the liquid products. Cu on the other hand, was inactive towards DCO [142]. Although the lesser metal concentration of the 0.5% Ni catalyst provides a beneficial degree of metal dispersion and crystal sizes for the reduction of solid

residue and H_2 production, the higher metal loading is required for *in-situ* deoxygenation. Apparently, the deoxygenation depends mostly on the number of active sites and less so on the dispersion compared to tar cracking, which apparently is more limited based on accessibility of the sites. Ideally, to promote both tar cracking and *in-situ* deoxygenation it would be most beneficial to have a very disperse catalyst with a higher concentration (>0.5%) of active metal, which may be achievable on a more suitable supporting material with a greater surface area and pore volume.

Here, the results of 4%Cu/SiO_2 show that the majority of the furanic products were furfural demonstrating that the catalyst is largely ineffective at reducing furfural. Alarmingly, the 4%Cu/SiO_2 was outperformed by the 0.5%Cu/SiO_2 catalyst. The first concern was that the 4%Cu/SiO_2 was not completely reduced however XRD analysis of the 4% catalysts demonstrated that all these catalysts were completely reduced with no sign of metal oxides (see Figure 4-11). Due to detection limits, XRD analyses failed to detect the crystal structures of the 0.5% catalysts. The fraction of furfural for the 4%Cu/SiO_2 catalyst exceeds that of the base case. One possible explanation for this could be that the 4%Cu/SiO_2 catalyst directed the decomposition of glucose to produce furfural via Grob fragmentation and dehydration reaction and/or the DCO and subsequent dehydrogenation of HMF. In consequence, the Cu catalyst was not active enough towards *in-situ* deoxygenation to handle extra furfural. Another possibility to consider would be deactivation due to the sintering of Cu sites.

Surprisingly, even Fe catalysts had a noticeable impact as they reduced the furfural fraction and increased the 2MF fraction. Fe's competitiveness may be related to its oxophilicity that may induce the adsorption of furanic compounds onto the catalyst surface, preferentially via oxygen containing functional groups [106, 130, 146]. However, Fe on its own is often regarded as having low activity for deoxygenation [105, 106, 139]. Of the noble metals, Re, Pd, and Pt; 0.5%Re/SiO_2 had the most remarkable performance with slightly higher fractions of 2MF and DMF and less furfural. Furthermore, compared to 0.5%Ni/SiO_2, the 0.5%Re/SiO_2 has more than 3 times less atoms of active metal species but remained competitive with slightly higher selectivity to 2MF and DMF. With a similar molar loading to the 0.5%Ni/SiO_2 catalyst, it is expected that the Re catalyst (as well as Pt and Pd) would be much more competitive and surpass the performance of 0.5%Ni/SiO_2 but with significant monetary costs.

Re is seldom used as a monometallic deoxygenation catalyst and is most often applied as a promoter material [157, 191]. Leiva et al., [192] reported that ReO_x/SiO_2 was more active towards the deoxygenation of guaiacol than reduced and sulfide Re catalysts. Unfortunately, due to the low concentration of the Re, it was not possible to determine if the catalyst was in a completely reduced state via XRD.

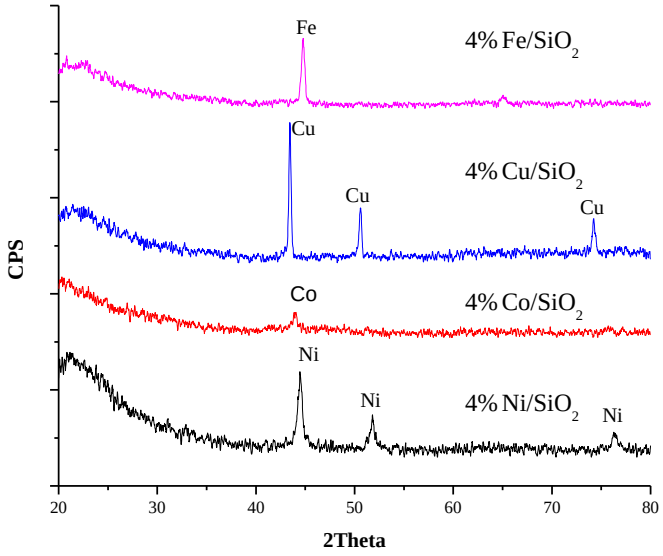

Figure 4-11: XRD analysis of 4% Ni, Co, Cu, and Fe catalysts

The most impressive catalysts that was used was 4%Co/SiO_2 – which almost eliminated the 5-methylfurfural fraction – lowered furfural fraction, and significantly increased the fractions of 2MF and DMF. Co has been shown to favour the direct deoxygenation of guaiacol and anisole to deoxygenated aromatic compounds more than other catalysts such as Ni and Pd [65, 184, 188]. Compared to Ni, which favoured C-C bond hydrogenation/hydrogenolysis, Co was shown to favour the hydrogenolysis of C-O bonds in guaiacol [65]. Favouritism towards the direct deoxygenation route for phenolic compounds demonstrates that the catalyst has weaker interactions with the aromatic ring structure and adsorption likely occurs via the oxygen containing functional group. This kind of activity is needed for the production of 2MF/DMF and is most common for bimetallic catalysts consisting of an active metal (such as Ni) and an oxophilic metal (such as Fe) [105, 106, 130, 131, 142, 146, 156, 159, 161]. Here, monometallic Co apparently behaved in a similar fashion. Having similar oxide structures as Fe, it may be possible that

Co readily adsorbed furanic compounds via their oxygen containing functional groups. Unlike Fe; Co is more readily reduced at lower temperatures (as shown in in the TPR results in Figure 4-3) meaning the absorbed oxygen can be easily removed as water. In comparison, monometallic Ni will absorb furanic compounds via the ring structures and can promote DCO and/or hydrogenation of the ring [146]. Absorption of the ring structure is not ideal in an environment with a very limited supply of H_2 as it may be consumed for the unfavourable ring-saturation reactions. Therefore, of all the monometallic catalysts tested here, Co is the most suitable option because of its selectivity towards absorption of oxygenated functional groups.

In general, the total concentration of furanic compounds does not exceed 4% of the liquid productions (1-methylnaphthalene free basis) with the catalysts offering little to no impact on the overall output of furanic compounds. Due to the low concentration of furanic products, it is not possible to relate these outcomes directly to the gaseous product results. For example, the changes in 2MF/DMF concentrations may have impacted the output of hydrogen by as little as 1-2%. However, the elevated presence of 2MF and DMF confirms that the catalysts do perform *in-situ* deoxygenation. Since furanic compounds are regarded as difficult to deoxygenate, it is reasonable to think that the catalysts would have also performed deoxygenation on other glucose decomposition products/intermediates, which would alter of accelerate specific reaction routes [17, 55, 56].

4.3.4 Magnetite Tests

Additional tests were performed without the addition of an initial source of hydrogen but instead an addition of Fe_3O_4. The intended purpose for Fe_3O_4 was to significantly promote the production of H_2 via WGSR which would then be used by the catalyst. However, as seen in Table 4-3, in comparison to previously presented results, the removal of hydrogen and introduction of magnetite provided some very adverse results. Firstly, it is seen that glucose on its own had a very low output of H_2. Earlier, when an initial source of H_2 was provided, the output of H_2 was almost ~70.7% greater than the initial input of H_2 equating to an additional 26.7 kPaA of H_2. Without an initial input of H_2, glucose was only able to produce 3.8 kPaA of H_2. Apparently, there is a sort of propagation effect with H_2 production whereby H_2 is used in reaction pathways that inevitably leads to the production of even more H_2. One possibility would be that H_2 is used to help remove water by stabilizing dehydration products via carbon-double-bond saturation. Stabilizing the structure would allow for further dehydration. All the water that is produced may be used by reforming or WGS reactions producing more H_2. Another interesting observation is that slightly less solid residue was obtained when there was no initial input of H_2.

Table 4-3: Results of magnetite addition – no initial source of hydrogen

	Glucose	**Glucose + Fe_3O_4**	**Glucose+ Fe_3O_4 + 0.5%Ni/SiO_2**	**Glucose + Fe_3O_4 + 0.5%Re/SiO_2**
Gaseous Products (Partial Pressures at 22.5°C) (kPaA):				
H_2	3.8	9.1	9.0	8.8
CO_2	96.5	181.7	183.8	155.1
CO	52.0	47.5	51.2	44.6
Solid Residue:				
%OSC	75.8%	82.0%	81.8%	85.9%
H:C	0.76	0.96	0.92	0.92
Fraction of Total Furanic Products:				

2MF	28.4%	45.8%	46.9%	43.8%
DMF	25.9%	37.8%	38.3%	37.3%
Furfural	24.9%	0.9%	1.4%	1.8%
5-methylfurfural	14.2%	2.8%	2.9%	5.6%
Other Furanics	6.6%	12.7%	10.5%	11.5%

The addition of magnetite did improve the output of H_2 slightly; however, more significant changes are seen elsewhere. The output of CO_2 for example was almost double that of just glucose which could be a sign of significant WGSR. In addition, the elimination of solids was increased and the fractions of 2MF and DMF in the furanic products was greatly improved demonstrating significant deoxygenation activity. This may the result of the Lewis acidity of Fe_3O_4 and WGSR activity. Many oxygen vacancies allow for the easy absorption of oxygenated compounds. On the other hand, the function of Fe_3O_4 during WGSR is to undergo oxidation by water producing Fe_2O_3 and surface hydrogen atoms that associate and become H_2. Fe_2O_3 is then reduced back to Fe_3O_4 by CO [34]. It is likely that H_2 did not even need to leave the surface - the hydrogen atoms may have been readily consumed for reactions, such as hydrogenolysis, on nearby sites thereby producing products such as DMF. This would explain why the output of H_2 did not increase very significantly.

The addition of the catalysts, 0.5%Ni/SiO_2 and 0.5%Re/SiO_2 with Fe_3O_4 offered little impact on the products over just the addition of Fe_3O_4. It is obvious that Fe_3O_4 controlled the reaction pathways. The 0.5%Re/SiO_2 catalyst offered a slight boost in solid residue elimination at the cost of a slight reduction in CO_2 and 2MF fraction. Overall the additional catalysts do not offer a significant change in performance to warrant their added use with

Fe_3O_4. One reason for their lack in performance is the extreme lack of H_2 in the gas phase as most "H_2" that is produced likely remains on the surface of Fe_3O_4/Fe_2O_3 and is readily consumed there.

To perform additional deoxygenation, Ni and Re would need hydrogen on their surface. For example, to produce 2MF from furfuryl alcohol, hydrogen is needed on the surface to perform hydrogenolysis and remove oxygen from the catalyst surface by releasing water. Without hydrogen, the catalyst surface may rapidly oxidize and become mostly inactive. In the presented system, for the Ni and Re catalysts to find use of hydrogen that is produced *in-situ*, it would need to associate, desorb from the iron oxide surface, transfer to the surface of the Ni/Re catalyst, absorb, and disassociate. In theory then, there is a possibility that Ni/Re may provide additional performance if they are supported on the iron oxide. It is worth noting that the fractions of furfural and 5-methylfurfural are significantly lowered upon magnetite addition offering little room for improvement. However, that does not necessarily mean that there is a limit for improvement among other oxygenated products or the possibility of achieving similar results at reduced reaction temperatures/times.

4.4 Conclusions

Of all the catalysts that were tested for *in-situ* deoxygenation during the decomposition of glucose, Ni and Co catalysts appeared to be the most interesting. The 4%Co/SiO_2 catalyst was regarded as having superior selective deoxygenation activity. Ni catalysts which were somewhat competitive for *in-situ* deoxygenation benefitted the system in another way by reducing the organic solid residue the most. Cu catalysts on the other hand appeared to be

poor at promoting *in-situ* deoxygenation; however, they may be helpful in producing internal H_2. In comparison, noble metal catalysts, Re, Pt, and Pd, provided underwhelming results.

For solid reduction and gas production, dispersion of catalyst sites on the support is a key issue. Catalysts with 0.5% of active material achieved better reduction in solids likely due to a higher degree of dispersion and smaller catalysts sites. However, 4%Co and 4%Ni catalysts achieved better deoxygenation results than that of 0.5% catalysts.

Overall, hydrogen appears to have a propagation effect as having an initial input of hydrogen can lead to the production of more hydrogen than what would normally be produced. Hydrogen likely becomes involved in the decomposition of glucose intermediates thereby stabilizing them and allowing for the removal of more water.

Chapter 5: Decomposition of Glucose with *in-situ* Deoxygenation in a Low H_2 Pressure Environment – Pt. II: Bimetallic Catalysts

5.1 Introduction

Traditional technologies for producing petroleum-compatible biofuels from lignocelluosic materials are heavily reliant on the use of hydrogen. Thermochemical processes like pyrolysis produce oxygen-rich bio-oil, which must be upgraded via hydroprocessing [4, 17, 19, 55, 115, 182]. Although these processes claim to be renewable/sustainable they remain reliant on fossil fuels as >95% of the world's H_2 is produced via fossil fuel resources [183].

The presence of CO_2, CO, H_2, H_2O, and light hydrocarbons in the outlets of lignocellulosic decomposition processes represents a missed opportunity [4]. CO and H_2O for example can potentially undergo water-gas-shift reaction (WGSR) and produce H_2 which can then be used for *in-situ* deoxygenation. The concept of producing H_2 internally and using it to produce renewable fuels in not entirely new. For example, Dumesic's research group from the University of Wisconsin demonstrated the aqueous phase reforming of sugars such as glucose to produce hydrogen which was followed by upgrading with Pt catalyst [202-204]. Aside from requiring a potentially expensive catalyst; such a system would require initial processing of lignocellulosic material to first separate lignin and then produce water-soluble sugars from cellulose and hemicellulose. On the other hand, a thermochemical process involving *in-situ* deoxygenation may utilize raw lignocellulosic material without the need of significant processing of the feedstock.

In the previous experimental phase, the decomposition of glucose and simultaneous deoxygenation in the presence of monometallic catalysts was evaluated. The reduction of furfural into selectively deoxygenated products such as 2-methylfuran (2MF) an 2,5-dimethylfuran (DMF) was demonstrated using a 4%Co/SiO_2. Although Ni catalysts were not as selective towards 2MF and DMF, they were beneficial for reducing the production of solid residue.

Bimetallic catalysts have received much attention for their activities in the selective deoxygenation of phenolic and furanic compounds derived from bio-oils. Dr. Resasco's research group at the University of Oklahoma studied the use of supported Ni-Fe bimetallic catalysts for the selective deoxygenation of m-cresol and furfural and determined that the oxophilic nature of Fe facilitated selective absorption via oxygen-containing functional groups, while Ni facilitated H_2 activation together permitting hydrogenolysis [105, 146]. Pd-Fe bimetallic catalysts have also received much attention, however, Pd was reportedly responsible for stabilizing Fe and preventing permanent oxidation [106, 130, 131, 205]. Other bimetallic catalysts have included supported PtZn [161], supported NiCu [134, 206], and PtCo nanocrystal [154] catalysts.

In this chapter, the decomposition of glucose (a model compound for cellulose) with *in-situ* deoxygenation in a low H_2 pressure environment is demonstrated further using supported bimetallic catalysts: NiFe, CoFe, PdFe, and PtCo. Since Ni/SiO_2 and Co/SiO_2 were shown to yield the most ideal results in Part 1 (Chapter 4); within this study, NiFe

and CoFe catalyst received much attention. The effect of impregnation method (co-impregnation versus sequential/stepwise impregnation) on catalyst activity was also studied. Unlike NiFe bimetallic catalysts, CoFe catalysts have previously not received much or any attention within the literature as deoxygenation catalysts. Cobalt-promoted iron catalysts have received some attention for their potential use for WGSR, which may also be useful in the present system [207-209]. Although some of the aforementioned catalysts have been used in WGSR studies; the *in-situ* production of H_2 is not yet the primary focus for the catalysts. As such, a small source of H_2 is provided (37.6 kPaA) in order to maintain activity of deoxygenation catalysts. Future research may further investigate *in-situ* hydrogen production. Furanic compounds in the products, which have distinct structures and deoxygenation pathways, were used to establish an understanding of deoxygenation activity.

5.2 Experimental

5.2.1 Catalyst Preparation

Various bimetallic catalysts were prepared using incipient wetness impregnation onto a SiO_2 supporting material (Aerosil 200). Both co-impregnation and stepwise impregnation methods were used. The catalysts that were prepared consisted of NiFe, CoFe, PtCo, and PdFe catalysts. Catalysts were prepared with one metal at 0.5wt% and the other at 4wt%. Catalysts were prepared using the following salts acquired from Sigma Aldrich: nickel (II) nitrate hexahydrate, cobalt (II) nitrate hexahydrate, iron (III) nitrate nonahydrate, tetraamineplatinum (II) nitrate, and palladium (II) nitrate dihydrate. Before impregnation, the silica support was dried at 120°C for 6 hours and calcined at 550°C for 4 hours. After

impregnation, catalysts were dried at 120°C for 6 hours and calcined in air at 550°C for 6 hours with heating rates of 5°C/min.

Stepwise impregnation was performed by impregnating the first metal onto the support then performing calcination. Upon cooling of the material; the second impregnation was performed followed by another calcination process. Catalysts that were prepared via step wise impregnation were denoted as "SWM" where M represents the metal that was impregnated first (ie. 4%Ni0.5%Fe/SiO_2-SWFe – Fe was impregnated onto the support first followed by the 4%Ni).

For performance testing, catalysts were pelletized and crush to a size range of 40-60 mesh. Catalyst were reduced in flowing H_2 at 50 nmL/min at desired reduction temperatures with a heating rate of 10°C/min. Temperatures used for reduction were 450°C for NiFe/SiO_2, 550°C for CoFe/SiO_2, 450°C for PdFe/SiO_2, and 450°C for PtCo/SiO_2 [105, 106, 146, 156].

5.2.2 Activity Tests

Activity tests were performed in accordance with the previous experimental phase. Activity/performance tests were performed in a horizontal, stirred 55 mL stainless steel reactor for 1 hour at 350°C with 800 mg of glucose. Reduced catalyst catalysts were used in the reactor at a 1:5 catalyst to glucose mass ratio. 1-methylnaphthalene (1MN) (Sigma-Aldrich) was used as a solvent (20:1 solvent to glucose mass ratio) to promote heat and mass transfer. 1MN was once again selected as the solvent due to its high boiling point temperature and its stability at reaction conditions even within the presence of a catalyst

showing no discernable changes in H_2 content and 1MN related by-products within the liquid phase. A reaction temperature of 350°C was selected because it represents a suitable temperature for both cellulose decomposition and WGSR [8, 9, 28, 29, 34]. Prior to reactions, the reactor was vacuum purged with He then filled with 37.6 kPaA of H_2. The reactor was subsequently filled with He to a total pressure of 320 kPaA to prevent the solvent from evaporating.

Gases within the reactor were tested using a RGA200 mass spectrometer at room temperature after undergoing separation via a HP-PLOT/U column held at 30°C. Upon separation from the liquid phase from the reactor, the solid contents were washed with acetone and dried in an oven at 80°C overnight. Liquid outputs were analyzed using GC-MS (Shimadzu GCMS QP5000) and GC-FID (Varian GC450). The hydrogen to carbon ratio of the solid residue was determined via CHNS analysis (Leco CHNS-932).

TGA analyses were performed using a TA Instruments TGA Q500 to determine the direct impact of selected catalysts on the decomposition/weight loss of glucose. The catalysts and glucose were loaded into the TGA at a ratio of 1:5. The TGA was heated from room temperature to 950°C at a rate of 5°C/min under flowing He (50 nmL/min).

5.2.3 Catalyst Characterization

Catalysts selected for characterization underwent TPR, XRD, and (S)TEM analyses with the objective of investigating the bimetallic catalyst structures and how the catalysts differ based on preparation method. Temperature programmed reduction (TPR) analyses were

performed using an Autosorb 1-C with a RGA200 mass spectrometer as the detector. A quartz cell was loaded with 150 mg of catalyst and vacuum dried at 300°C for 20 minutes under flowing helium (50 nmL/min). TPR analyses were performed using 1% H_2 in He gas mixture at a flow rate of 50 nmL/min. The Quartz cell was heated from room temperature to 900°C at a rate of 10°C/min. X-ray diffraction (XRD) of reduced catalysts was performed at the UNB Geochemical and Spectrographic Facility using a Bruker AXS D8 XRD. XRD spectrums were gathered within the 2Theta range of 10-90° at a rate of 0.02°/second.

(S)TEM analyses were performed at the UNB Microscopy and Microanalysis Facility using a JEOL JEM-2010 (S)TEM. Images were collected with a Gatan Ultrascan camera using Digital Micrograph. Metallic sites were identified on the supporting material (SiO_2) using both HRTEM (High Resolution TEM) and high angle annular darkfield STEM (HAADF-STEM) mode. With both techniques, a high contrast was observed between catalyst sites and the supporting SiO_2 material. Verification of the metallic sites was determined by collecting EDS spectra using an EDAX Genesis 4000 Energy Dispersive X-ray (EDS) analyzer. In addition, mapping of the metallic sites was performed using the EDS detector whilst in STEM mode to further determine the existence and distribution of both metals across an area of the material. An accelerating voltage of 200 kV was used for the imaging and analysis. Images were processed using an open source image processing platform, Fiji [193].

5.3 Results and Discussion

5.3.1 Solid Products

A high level of reduction of the solid content is desired to attain a liquid product and provide easy separation from the catalyst. Reduction of the solid content results from the conversion of glucose itself and the prevention of the formation of solid products such as char, heavy compounds, and polymers attributed as tars. Catalysts may prevent this by supporting tar cracking/reforming reactions to eliminate heavy compounds in favour of liquid and gaseous products [24-27, 31-33]. In Figure 5-1, most bimetallic catalysts were shown to aid in the reduction of solid residue over tests with just glucose. This is also demonstrated in Figure 5-2, where the H:C ratios of the solid residue were higher upon addition of the catalysts representing the possibility of less char formation.

As evidenced in Figure 5-2, NiFe catalysts were the most capable at reducing output solid residue. Based on what was previously observed for monometallic catalysts in Chapter 4, it is likely that the presence of Ni had a significant role. 0.5%Ni4%Fe-SWFe for example provided a similar reduction in solid residue to 0.5%Ni/SiO_2 as well as a very similar H:C ratio. Meanwhile, the co-impregnated and the SWNi variants of the 0.5%Ni4%Fe catalyst had comparatively lower levels of reduction in solid residue. For these two catalysts, the Ni phase may not have been directly exposed like the SWFe catalyst and thus may have suffered from an interference with Fe. However, the second highest reduction in solid residue occurred on the 4%Ni0.5%Fe-SWNi catalyst which may not have had Ni-phase that was exposed as the 4%Ni0.5%Fe-SWFe variant which had slightly more solid residue.

Meanwhile, the co-impregnated 4%Ni0.5%Fe catalyst suffered a loss in solid reduction compared to the 4%Ni/SiO_2 catalyst in Chapter 4. Co-impregnation may produce a more uniform NiFe alloy phase rather than a strictly separate Ni-phase, which is more active towards either the initial decomposition of glucose or tar cracking (see catalyst characterization in Section 5.3.4). When 0.5%Fe is layered on top of the 4%Ni, it may be possible that both Ni and Fe phases are exposed. The Fe phase may not completely cover the Ni phase possibly enabling a synergistic effect between the two metals in which each metal favours a different role in the reaction. This would explain why the SWNi performed slightly better than the SWFe layout which would have had a more completely exposed Ni phase.

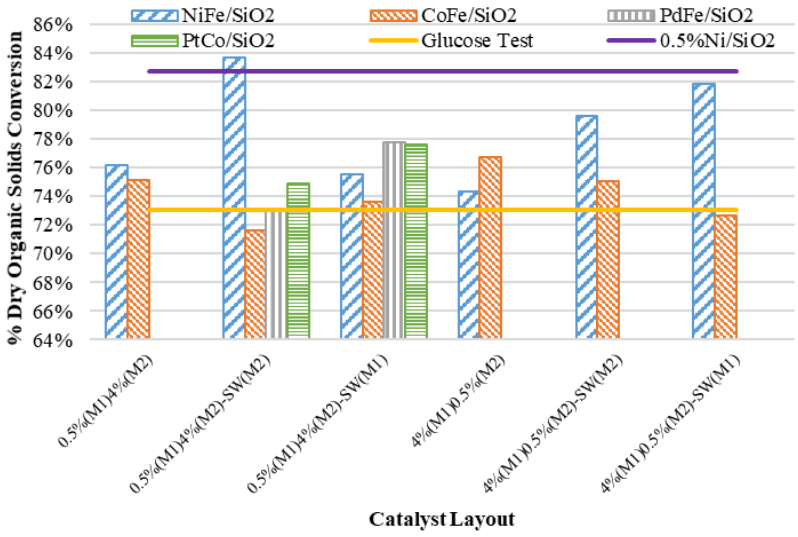

Figure 5-1: Percent removal of dry organic solids with bimetallic catalysts with data for 0.5%Ni/SiO_2 from Chapter 4

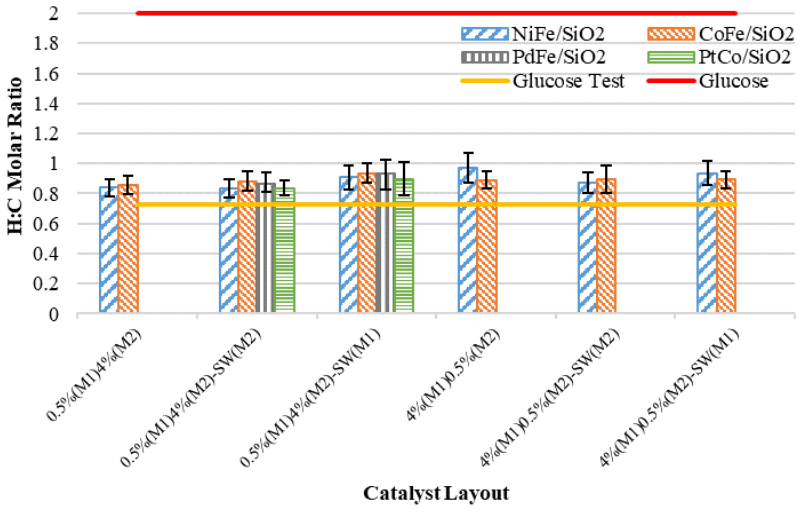

Figure 5-2: H:C Molar ratio in solid products

CoFe catalysts appear to behave in the opposite way and favour co-impregnation over the stepwise impregnation methods. Co-impregnated 4%Co0.5%Fe reduced the organic solid content by ~77% - slightly higher than the 4%Co/SiO_2 catalyst from Chapter 4 with 74%. Even more subtle differences were observed for the two sequentially impregnated 4%Co0.5%Fe catalysts. It is noteworthy that as monometallic catalysts, 0.5%Fe/SiO_2 and 4%Co/SiO_2 resulted in similar reductions in organic solid residue. Combining the two into a bimetallic catalyst apparently offered no significant improvement. Similar behavior was observed for the 0.5%Co4%Fe catalysts.

For the PdFe and PtCo catalysts, a slight reduction in solid residue reduction was observed when the noble (Pd and Pt) metals were added on top of the base metals (Fe and Co). In general, using bimetallic configurations of NiFe, CoFe, PdFe, and PtCo provides little advantage over their monometallic counterparts in terms of solid residue reduction.

Especially in the cases of PdFe and PtCo catalysts, the additional costs of these catalysts outweigh the benefits.

To further understand the impact that the catalysts have on the decomposition of glucose, TGA was performed using 0.5%Ni4%Fe and 0.5%Co4%Fe catalysts. As demonstrated in Figure 5-3, the catalysts had a significant effect on the decomposition of glucose by reducing the temperatures at which substantial decomposition begins. Without a catalyst additive, the decomposition of glucose has two main periods of decomposition one at 215°C and 293°C where glucose undergoes a faster rate of decomposition. In the presence of catalyst additives, the first stage of decomposition had the higher rate of decomposition. As seen in Table 5-1, the results for the two chosen catalysts and their three variants did not have appreciable differences. Iron played an important role in influencing the decomposition of glucose as the results are mostly comparable to those of 4%Fe/SiO_2 from Chapter 4. In some cases, there are discernable differences such as for co-impregnated 0.5%Ni4%Fe and 0.5%Co4%Fe catalysts (as shown in Figure 5-3), where the catalyst containing nickel achieved an overall lower residue content.

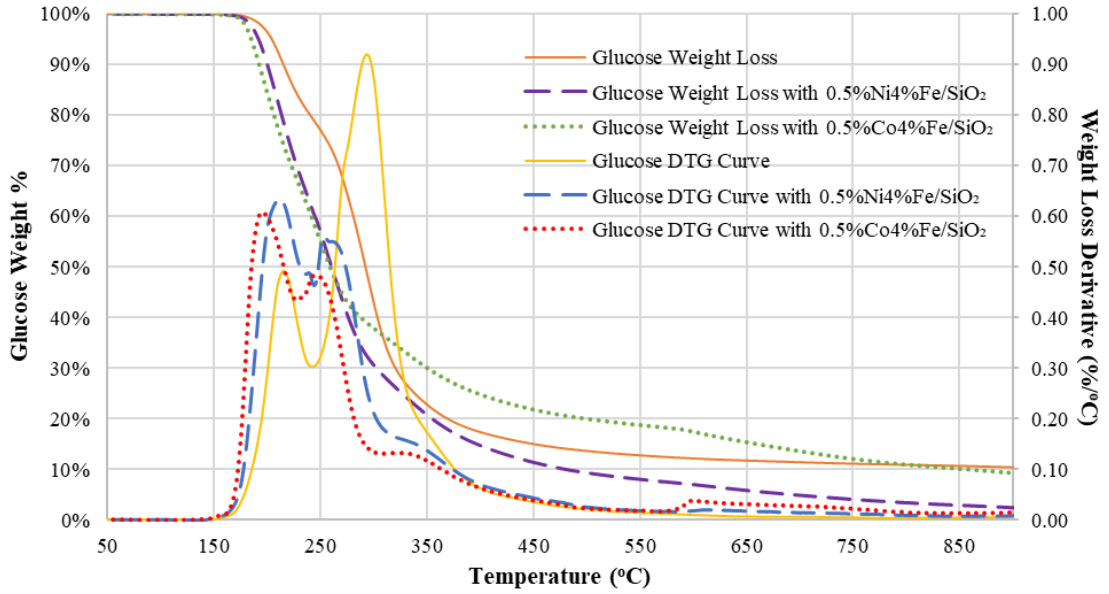

Figure 5-3: TGA results of glucose decomposition with and without 0.5%Ni4%Fe/SiO_2 and 0.5%Co4%Fe/SiO_2 catalyst. Catalysts added at 1:5 ratio with glucose.

Table 5-1: TGA results summary for glucose decomposition with catalyst additives. Temperature (T) program: 25°C to 900°C at 5 °C/min. Y = percent of solid remaining (does not include catalyst weight)

Catalyst	Initial Major Weight Loss					Valley			Second Major Weight Loss				
	T^a (°C)	Y^a (wt%)	T^b (°C)	Y^b (wt%)	$(-dY/dT)^b$ (%/K)	T^c (°C)	Y^c (wt%)	$(-dY/dT)^c$ (%/K)	T^d (°C)	Y^d (wt%)	$(-dY/dT)^d$ (%/K)	T^e (°C)	Y^e (wt%)
No Catalyst	178	99.6%	215	90.0%	0.49	242	79.4%	0.30	293	49.1%	0.92	417	16.4%
0.5%Ni4%Fe/SiO_2	173	99.5%	211	81.6%	0.63	244	60.3%	0.46	253	54.6%	0.56	435	12.2%
0.5%Ni4%Fe/SiO_2 SWFe	170	99.6%	194	89.5%	0.67	230	66.7%	0.40	242	60.8%	0.44	431	24.9%
0.5%Ni4%Fe/SiO_2 SWNi	171	99.8%	200	87.2%	0.61	234	66.8%	0.42	246	60.5%	0.49	433	21.2%
0.5%Co4%Fe/SiO_2	169	99.6%	195	87.9%	0.61	227	67.5%	0.43	245	57.9%	0.48	423	23.3%
0.5%Co4%Fe/SiO_2 SWFe	172	99.6%	200	87.0%	0.64	236	64.4%	0.44	248	58.0%	0.51	434	18.8%
0.5%Co4%Fe/SiO_2 SWCo	171	99.7%	199	86.6%	0.68	234	64.2%	0.43	245	58.2%	0.47	435	20.7%

[a] – Point at which mass loss rate begins to exceed 0.05 %/K
[b] – First peak point on DTG curve
[c] – Valley point on DTG curve between first and second peak
[d] – Second peak point on DTG curve
[e] – Point at which mass loss rate declines below 0.05 %/K

Given that 4%Fe likely played an important role in glucose decomposition, it is yet to be explained why the 0.5%Ni4%Fe-SWFe catalyst offered the highest reduction in solid

residue during the activity tests. It is most likely that the catalyst reduced the formation of solids from heavy hydrocarbons or char. In Chapter 4, 0.5%Ni/SiO_2 was shown to reduce solid residue due to its tar cracking abilities and its overall catalyst site dispersion. Having been impregnated separately from the Fe phase; the 0.5%Ni phase on the 0.5%Ni4%Fe-SWFe may have been separated and uninfluenced by the 4%Fe phase allowing the 0.5%Ni phase to act on its own in tar cracking.

5.3.2 Gaseous Products

One major purpose for the use of bimetallics in the proposed system is for the *in-situ* production of hydrogen. Bimetallic catalysts such as supported NiFe and PdFe catalysts have been studied for their activity in WGSR reactions [34, 37, 41, 42]. Chapter 4 demonstrated that monometallic catalysts can increase H_2 output during glucose decomposition. It was therefore anticipated that the synergy between two metals together would further improve the H_2 production over the monometallic catalysts.

Of all catalysts that were tested, 0.5%Co4%Fe catalysts had the highest output of H_2, doubling the amount of H_2 that was originally fed to the reactor (see Table 5-2). This is most noticeable for the co-impregnated 0.5%Co4%Fe catalyst, which produced the most H_2. Interestingly, in Chapter 4, 0.5%Co and 4%Fe catalysts produced relatively low amounts of H_2. Combining the two appears to have synergistic effect, which is more apparent when the two metals are added to the support via co-impregnation. A similar trend is also noted for CO_2 production highlighting the likelihood that WGSR occurred. The fact that the co-impregnation method provided the most H_2 suggests that there is a stronger

relationship between the two metals when they are formed together perhaps as an alloy. It is suggested that this is due to the similar oxide structures of the two metals producing cobalt iron oxides $Co_{3-x}Fe_xO_4$.

Table 5-2: Product gas composition - partial pressures at 22.5°C (kPaA)

		0.5%(M1) 4%(M2)	**0.5%(M1) 4%(M2) -SW(M2)**	**0.5%(M1) 4%(M2) -SW(M1)**	**4%(M1) 0.5%(M2)**	**4%(M1) 0.5%(M2) -SW(M2)**	**4%(M1) 0.5%(M2) -SW(M1)**
H_2	*Initial Input*			38			
	No Catalyst			64			
	NiFe/SiO₂	48	35	51	21	20	22
	CoFe/SiO₂	78	70	64	66	58	61
	PdFe/SiO₂		14	14			
	PtCo/SiO₂		28	30			
CO_2	*No Catalyst*			99			
	NiFe/SiO₂	163	138	118	100	122	136
	CoFe/SiO₂	153	129	114	145	121	130
	PdFe/SiO₂		103	122			
	PtCo/SiO₂		109	108			
CO	*No Catalyst*			62			
	NiFe/SiO₂	52	67	44	44	55	57
	CoFe/SiO₂	53	47	44	56	52	44
	PdFe/SiO₂		37	42			
	PtCo/SiO₂		44	39			

Having the noble metal in lower concentration than the oxophilic, Fe, also appeared to benefit the NiFe catalysts in terms of H_2 output. The 0.5%Ni4%Fe configurations of NiFe had a higher output of H_2 than the 4%Ni0.5%Fe catalysts. Although 0.5%Ni produced more H_2 as a monometal than 4%Fe in Part 1, co-impregnation or impregnation of the Fe last is more beneficial for H_2 demonstrating the importance of Fe exposure. Like CoFe, a similar trend is also noted for CO_2 production over the NiFe catalysts suggesting WGSR. According to Watanabe, et al., [41] NiFe catalysts behave synergistically for WGSR where

water oxidizes the Fe and H_2 is produced meanwhile, Ni facilitates better CO absorption which leads to the oxygenation of CO to CO_2 via the oxidized Fe site. It is possible that the CoFe catalyst behaves in a similar fashion, in which Co replaces the role of Ni.

For 4%Ni0.5%Fe it is noted that stepwise impregnation beginning with 4%Ni is most beneficial to produce CO_2 with no discernable differences in H_2 production among all three impregnation methods used for 4%Ni0.5%Fe. It is possible that internal H_2 is produced along with CO_2 via WGSR on the 4%Ni0.5%Fe catalysts; however, H_2 may be rapidly consumed by other reactions. Therefore, it is possible that the SWNi variant of the 4%Ni0.5%Fe catalyst produced more internal H_2 than the other two variants as signified by the higher CO_2 output.

The output of CO does not correlate with the output of CO_2 as expected. For a system purely based on WGSR, it is expected that the production of CO would decrease as the production of CO_2 increases. However, for some catalysts such as 4%Ni0.5%Fe, this trend was not observed. A possible explanation is that the production and subsequent consumption of internal hydrogen leads to the production of more CO and H_2O. Therefore, a higher output of CO alone does not represent low WGSR activity, as WGSR could have already occurred producing H_2, which enabled the production of additional CO.

Similarly, for 0.5%Pd4%Fe, impregnating 4%Fe after 0.5%Pd appears to produce more CO_2 than the alternative stepwise impregnation method as well as monometallic 4%Fe. Under the assumption that the 4%Fe covers the 0.5%Pd; this suggests that there is some

synergistic relationship. Pd causes electron delocalization, stabilizing the Fe surface and preventing permanent oxidation [205]. Alternatively, if Pd is directly exposed, it made become contaminated or easily coked. Similar to monometallic Pd, both configurations of 0.5%Pd4%Fe had an overall reduction of H_2 from initial input to output.

Combining Pt and Co together as a bimetallic catalyst negatively impacted the output of H_2 as there is a net consumption in H_2. As monometallic catalysts, Pt and Co catalysts had higher outputs of H_2 than the original H_2 input (see Chapter 4). Both stepwise configurations of 0.5%Pt4%Co catalysts produced the same amount of CO_2, however, combining Co with Pt appears to offer no advantage over Fe. Therefore, the oxophilic nature of Fe serves an important role in the CoFe catalysts as suggested earlier, by facilitating the oxygenation of CO to CO_2.

5.3.3 Liquid Products

As one may elude from the results reported for solid and gaseous products, the catalysts affect the yield of liquid products. As seen in Figure 5-4, the relative trend between the catalysts, for the most parts follows that of the organic solid conversion from Figure 5-1 with a few exceptions such as 4%Ni0.5%Fe/SiO_2 versus 4%Co0.5%Fe/SiO_2. As expected, the 0.5%Ni4%Fe/SiO_2-SWFe catalyst had the highest yield of liquid products among all bimetallic catalysts, as this catalyst was active towards tar cracking. However, the liquid yield was lower than that of 0.5%Ni/SiO_2 (from Chapter 4) due to its higher yields of CO and CO_2. Co-impregnated 0.5%Co4%Fe/SiO_2 yielded far less products in the liquid phase as it favoured the production of H_2 and CO_2. Along with the drop in CO production, it is

suggested that the reduction in liquid phase products is due to a reduction in water content as water would have been consumed for water-gas-shift.

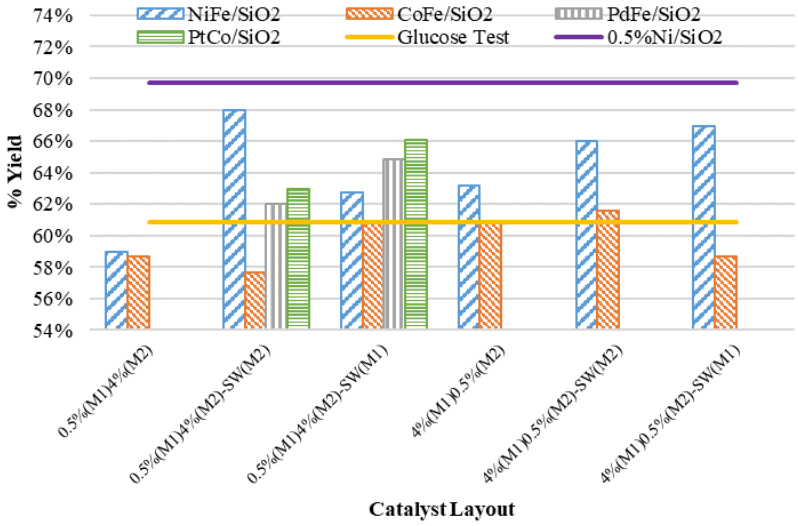

Figure 5-4: Percent yield of liquid products determine via mass balance where % Yield = (total mass of liquid products)/(mass of glucose feed)

In Chapter 4, it was determined that the Co catalysts were the most effective at performing *in-situ* deoxygenation with the highest selectivities to 2MF and DMF over furanic intermediates such as furfural. For 4%Co/SiO_2 in particular; ~87.2% of the furanic compounds were 2MF and DMF. As seen in Figure 5-5, none of the bimetallic catalysts quite achieved the same selectivity, however various 4%Fe-containing catalysts yielded competitive results as high as ~82%. For comparison, in Chapter 4, the fraction of 2MF and DMF totaled 65.6% for 4%Fe/SiO_2.

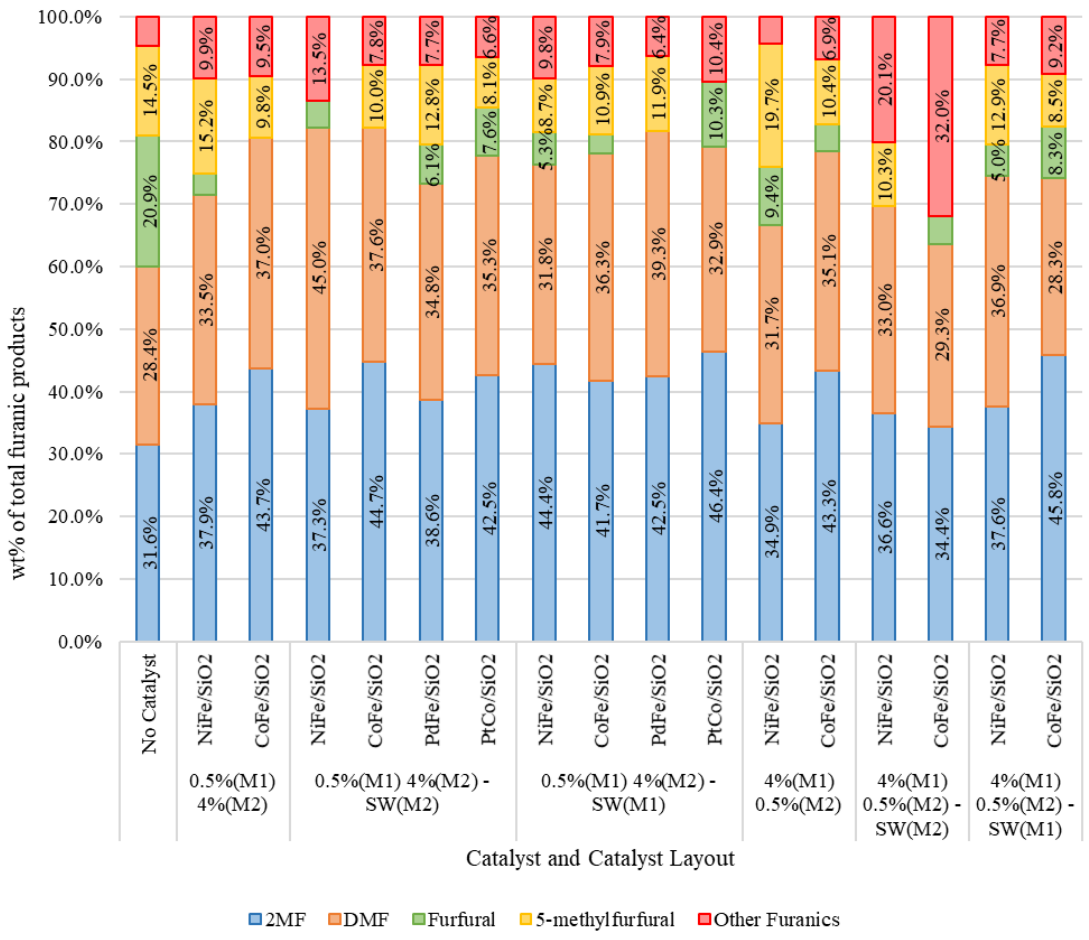

Figure 5-5: Distribution of total furanic products

Combining 4%Fe and 0.5%Ni made a more competitive catalyst than either of the metals on their own. Overall, 0.5%Ni4%Fe catalysts outperformed the 4%Ni0.5%Fe catalysts, which appeared to offer little improvement over monometallic 4%Ni in terms of 2MF and DMF selectivity. This is likely related to higher production of internal H_2 with the 0.5%Ni4%Fe catalysts, which had higher outputs of both H_2 and CO_2 suggesting higher degree of WGSR. This catalyst benefits from the stepwise impregnation procedure. When the 4%Fe phase was impregnated first, the result was a total elimination of the 5-methylfurfural intermediate and a higher selectivity towards DMF than the co-impregnated

catalyst. Of the three variants, the 0.5%Ni4%Fe-SWFe catalyst had the lowest output of H_2, which could be due to the elevated rate of consumption via deoxygenation.

The selective deoxygenation function of NiFe catalysts have received much attention. Both metals have been suggested to serve important roles. Fe facilitates adsorption preferentially via the oxygen containing functional groups, while Ni activates hydrogen for hydrogenolysis [105, 146, 156]. Therefore, both metals would have to be exposed. Impregnating 4%Fe after 0.5%Ni may have had a negative impact on Ni's ability to activate hydrogen; thus, the selectivities of 2MF and DMF are lower on the SWNi catalyst than the SWFe. Co-impregnation provides stronger interactions between the two metal rendering a NiFe alloy phase, which may inhibit the two metals from performing separate roles.

Similar to the NiFe catalysts; the 0.5%Co4%Fe catalysts appeared to outperform the 4%Co0.5%Fe catalysts. The co-impregnated and SWFe variants of 0.5%Co4%Fe eliminated the output of furfural. Unlike the NiFe catalysts, the co-impregnation method was very suitable for CoFe, competitively boosting 2MF and DMF selectivities for both the 0.5%Co4%Fe and 4%Co0.5%Fe catalysts. This provides additional evidence that the CoFe catalysts benefit from a strong interaction between the two metals perhaps as an alloy. The 4%Co0.5%Fe-SWFe catalyst produced interesting results, in which the furanic compounds consisted of a large portion (28.2%) of 2-acetylfuran - an unusual furanic compound that would signify either a major change in glucose decomposition or possibly a side reaction involving furfural. Trimethylfuran was present in low amounts (< 5% of

total furanics) in the products likely due to trans-alkylation reactions. Interestingly, although the fraction of 2MF achieved here was not as significant as 4%Co/SiO_2 in Chapter 4, 0.5%Co4%Fe/SiO_2 had no detectable amounts of furfural.

As a monometallic catalyst; 0.5%Pd was not very effective at reducing the amount of furfural among all furanic compounds. However, pairing 0.5%Pd and 4%Fe together as a bimetallic catalyst significantly reduced the content of furfural, which was eliminated when the 0.5%Pd phase was impregnated onto the support first. Like NiFe catalysts, PdFe catalysts have received a lot of attention for the selective deoxygenation of furanic and phenolic compounds. Previous research shows that Pd alone is more active towards ring interaction; however, when it is modified with Fe, the catalyst favours selective deoxygenation of constituents attached to the aromatic ring [106, 130, 131, 205]. Hensley et al., [205] described the roles of the two metals as Fe facilitating oxygenate absorption, while Pd imposes an electron delocalization effect that stabilizes Fe. As it outperformed the SWFe variant; it is suspected that the SWPd variant of 0.5%Pd4%Fe provided a stronger interaction between the two metals and/or was able to prevent Pd's interaction with the aromatic ring more effectively. Like the PtCo catalysts, which also had competitive results among all the catalysts, the PdFe catalysts appear to offer no significant advantages over the NiFe and CoFe catalysts that can justify the additional costs associated with using noble metal catalysts Pd and Pt.

5.3.4 Catalyst Characterization

The 0.5%Ni4%Fe and 0.5%Co4%Fe catalysts were selected for further tests and characterizations. Despite having lower concentrations of the expensive, active materials (Ni and Co), these catalysts provided competitive results in terms of both gas and liquid products along with the potential of reducing solid residue.

Due to the low concentrations of Ni and Co, TPR profiles (as shown in Figure 5-6) were faint as iron itself generally has a faint profile. Interestingly, the broad peaks which generally form at 450°C and 600°C for Fe were shifted and stretched when a second metal was used. For example – the 0.5%Ni4%Fe/SiO_2-SWFe catalyst had and an initial peak ~425°C followed by a very broad peak ~700°C. Clearly, there was an interaction between the two metals. The CoFe catalysts had very undiscernible peaks especially when prepared via the stepwise impregnation method.

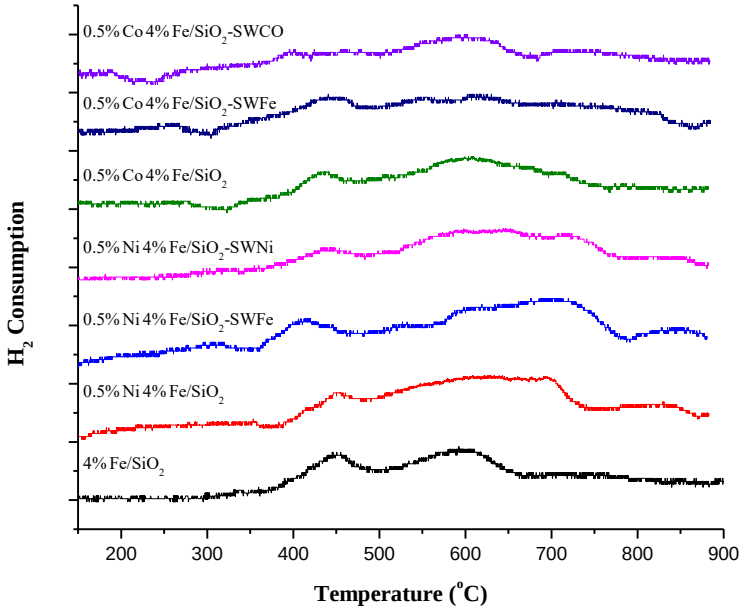

Figure 5-6: TPR profiles for 0.5%Ni4%Fe/SiO_2 and 0.5%Co4%Fe/SiO_2 catalysts

XRD analyses of the 0.5%Co4%Fe and 0.5%Ni4%Fe catalysts (see Figure 5-7) revealed that there was not an oxide phase present. Due to their low concentration; Ni and Co phases were not detectable on their own. XRD spectra for CoFe and NiFe alloys coincide with the spectrum for Fe, therefore making it difficult to distinguish if the peaks at ~45° correspond only to Fe or if they indicate the presence of an alloy phase. For the two co-impregnated catalysts, the peak appears to be a double peak which, could be described by the presence of both Fe and an alloy phase, however, the scale and resolution of these peaks are not strong enough to allow for verification.

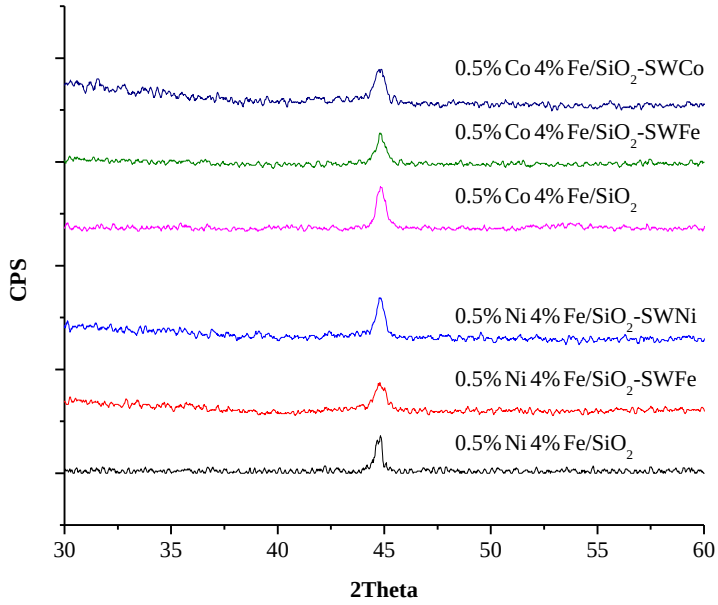

Figure 5-7: XRD Spectra for 0.5%Ni4%Fe/SiO_2 and 0.5%Co4%Fe/SiO_2 catalysts

HRTEM and STEM-HAADF analyses were performed with EDS to determine the presence of Co/Ni and Fe in the catalysts and to establish if there were separated or together as alloy phases. HRTEM images – as shown in Figure 5-8 - show no distinguishable difference between catalyst particles of different metals or the combination thereof. EDS proved to be the only method capable of determining the presence of either metal or possibly both metals at one location. Dispersion of the metals appeared to be most significant on the SWFe catalysts, as the catalyst sites tended to be small and separated. The other two preparation methods (especially the SWNi/SWCo variants) yielded catalyst sites that were quite clustered perhaps. This effect was mostly independent on the selection of the most active metal (Ni vs. Co). For the co-impregnated samples, it was a regular occurrence to find sites that were composed of both metals. Meanwhile, for the stepwise

impregnated samples, metallic sites consisted of both monometallic and bimetallic phases. Even the metals of lower concentrations (Co and Ni) were found separated.

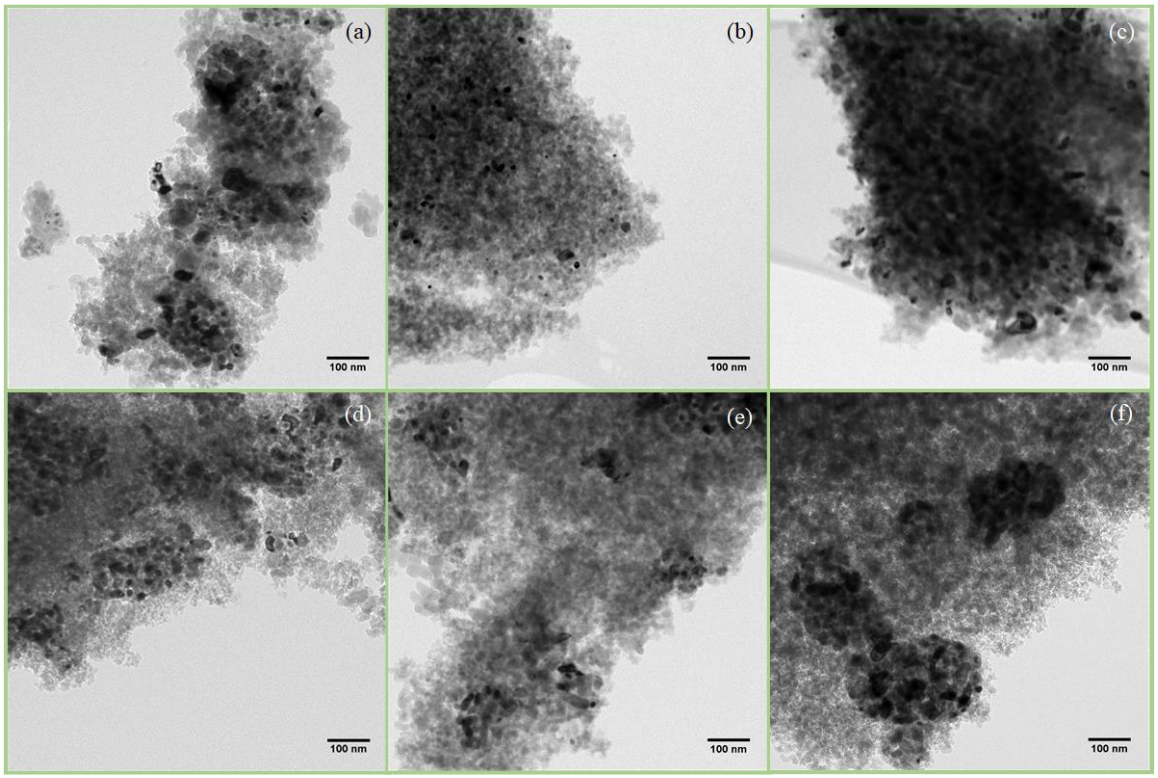

Figure 5-8: HRTEM Images of: (a) 0.5%Ni4%Fe/SiO_2 (b) 0.5%Ni4%Fe/SiO_2-SWFe (c) 0.5%Ni4%Fe/SiO_2-SWNi (d) 0.5%Co4%Fe/SiO_2 (d) 0.5%Co4%Fe/SiO_2-SWFe and (e) 0.5%Co4%Fe/SiO_2-SWCo

STEM-HAADF images and EDS mappings were performed to further investigate the metallic site compositions. STEM-HAADF images (Figures 5-9 a-c) clearly show the dispersion of the catalyst sites and their relative densities compared to the SiO_2 support. Corresponding EDS mappings (Figures 5-9 d-f) demonstrated distinct differences between co-impregnated and stepwise impregnated 0.5%Ni4%Fe. Figure 5-9d shows that the Ni sites easily coincide with the Fe sites without separation, strongly suggesting that the two metals formed an alloy. Figures 5-9e and 5-9f, on the other hand, show a clear separation

of the Ni and Fe sites for the 0.5%Ni4%Fe catalysts prepared via stepwise impregnation. This matches earlier suggestions that the co-impregnated catalysts experienced alloying while the stepwise impregnated catalysts consisted of separate phases. EDS mapping of the CoFe catalysts was not possible as the spectra for Fe can interfere with that of Co.

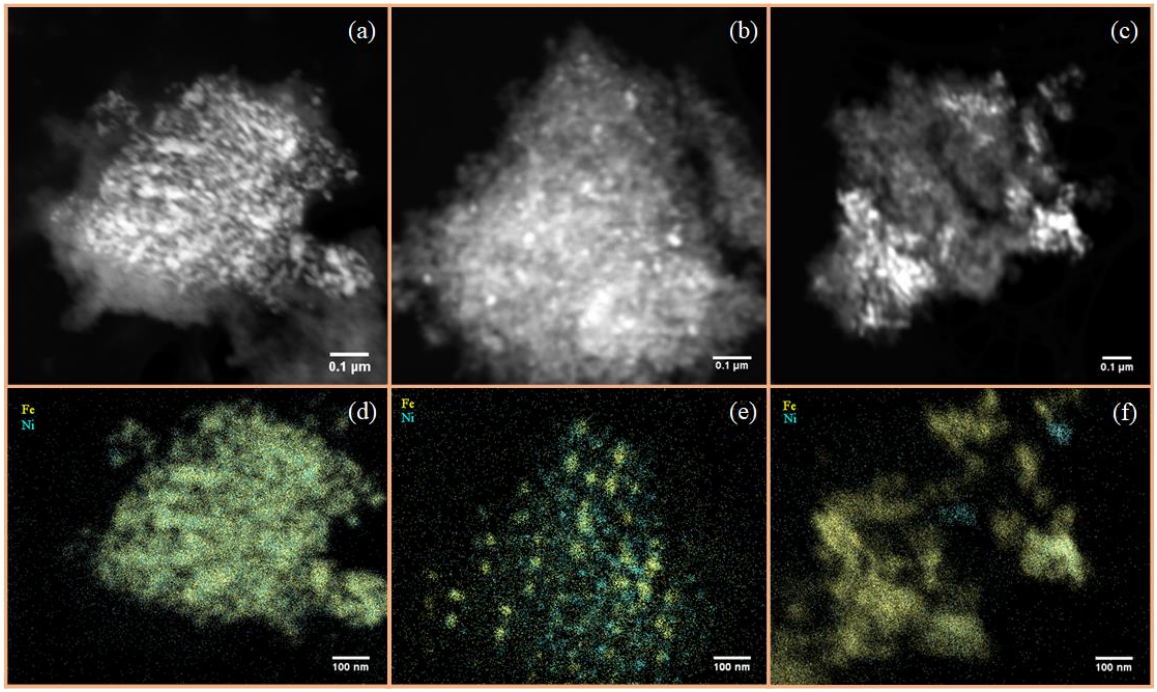

Figure 5-9: STEM-HAADF images and EDS mappings of 0.5%Ni4%Fe/SiO_2 catalysts. (a)-(c): STEM-HAADF images of NiFe, NiFe-SWFe, and NiFe-SWNi respectively. (d)-(f): EDS mappings of NiFe, NiFe-SWFe, and NiFe-SWNi respectively.

Given the earlier observations, it can be concluded that 0.5%Co4%Fe/SiO_2 benefits most from alloying. This co-impregnated catalyst boosted competitive levels of deoxygenation and the highest output of H_2. Based on findings of other bimetallic catalysts, it is hypothesized that incorporating Co into Fe effectively helps stabilize Fe which facilitates absorption via oxygen containing functional group [205]. For 0.5%Ni4%Fe/SiO_2 alloying Ni and Fe via co-impregnation, although competitive, was not as favourable as stepwise

impregnation. Stepwise impregnation (SWFe) kept some of the 0.5%Ni phase separate from the Fe allowing for greater reduction in solid residue and higher deoxygenation activity. However, the SWFe catalyst had lower output of H_2 perhaps due to the higher consumption of H_2 related to its deoxygenation activity. Ni and Fe may need to be kept separated for them to perform separate roles for both solids decomposition and deoxygenation.

5.3.5 Magnetite Tests

Of all the bimetallic catalysts that were tested, the two catalysts that proved to be the most interesting were the 0.5%Ni4%Fe/SiO_2-SWFe and 0.5%Co4%Fe/SiO_2 catalysts. The former provided the best reduction in organic solid residue at 83.7% reduction, while the latter provided the highest output of H_2 at 78.2 kPaA. Both catalysts were competitive towards the production of deoxygenated furanic compounds 2MF and DMF. Like in previous tests with 0.5%Ni/SiO_2 and 0.5%Re/SiO_2 in Chapter 4; these two catalysts were tested again without an initial charge of H_2 but instead with Fe_3O_4 fed at the same ratio as the catalysts. The intended purpose for the Fe_3O_4 was to produce internal H_2 (via WGSR), which the catalysts would be dependent upon.

The addition of the deoxygenation catalysts appeared to have only a small effect on the outcome of the process as seen in Table 5-3. Adding the catalysts slightly reduced the amount of organic solids from a 82.0% reduction (%OSC) to 85.2% for the NiFe catalyst and 86.3% for the CoFe catalyst. The NiFe catalyst seemingly increased the output of gases, especially CO_2, which can be attributed to additional WGSR and reforming activity.

However, where the CoFe catalyst maintained the selectivity of furanic compounds, the NiFe catalyst seemed to reduce the selectivity of 2MF and DMF in favour of other furanic compounds such as 2-acetylfuran.

Table 5-3: Summary of results for tests with magnetite. NiFe catalyst = 0.5%Ni4%Fe/SiO_2-SWFe. CoFe catalyst = 0.5%Co4%Fe/SiO_2

	Glucose	Glucose + Fe_3O_4	Glucose + Fe_3O_4 + NiFe Catalyst	Glucose + Fe_3O_4 + CoFe Catalyst
Gaseous Products (Partial Pressures at 22.5°C) (kPaA):				
H_2	3.8	9.1	10.0	10.5
CO_2	96.5	181.7	200.3	170.6
CO	52.0	47.5	53.4	51.3
Solid Residue:				
%OSC	75.8%	82.0%	85.2%	86.3%
H:C	0.76	0.96	0.97	0.90
Fraction of Total Furanic Products:				
2MF	28.4%	45.8%	41.9%	45.5%
DMF	25.9%	37.8%	32.5%	39.4%
Furfural	24.9%	0.9%	3.3%	2.0%
5-methylfurfural	14.2%	2.8%	4.0%	0.0%
Other Furanics	6.6%	12.7%	18.2%	13.2%

Overall, the catalysts do not appear to add any significant bonus on top of the Fe_3O_4. One issue that has been considered is that the hydrogen produced on the magnetite is not readily available to the added catalysts. Ideally, WGSR and deoxygenation reactions should occur on the same catalyst, on nearby sites, so that hydrogen can be produced on the surface and readily consumed for deoxygenation, thus eliminating many mass transfer barriers.

Combining WGSR and deoxygenation on a single catalyst surface would mitigate the need for H_2 (from WGSR) or even water (from dehydration) to be desorbed from the catalyst surface – only CO_2. The mechanism would ideally proceed similarly to the WGSR

mechanism suggested for NiFe/ CeO_2-ZrO_2 by Watanabe et al., [41]. In contrast, instead of the active material (NiFe) being oxidized by water, it is oxidized by the oxygenates undergoing hydrogenolysis. Catalysts would require an initial amount of hydrogen to provide activation to start hydrogenolysis. The oxygen on the surface may then be transferred to an appropriate supporting material containing oxygen vacancies thereby temporarily stabilizing the active metal. CO is required to reduce the catalyst producing CO_2. Surface CO may be derived either via the actual absorption of carbon monoxide or possibly via decarbonylation. In summary, water which is typically produced during hydrogenolysis is not immediately associated and desorbed from the surface, and essentially oxygen is instead removed as CO_2. A summary of this theoretical process is demonstrated in Figure 5-10 based on the mechanisms described by Watanabe et al., [41] for WGSR and Sitthisa et al., [146] for deoxygenation.

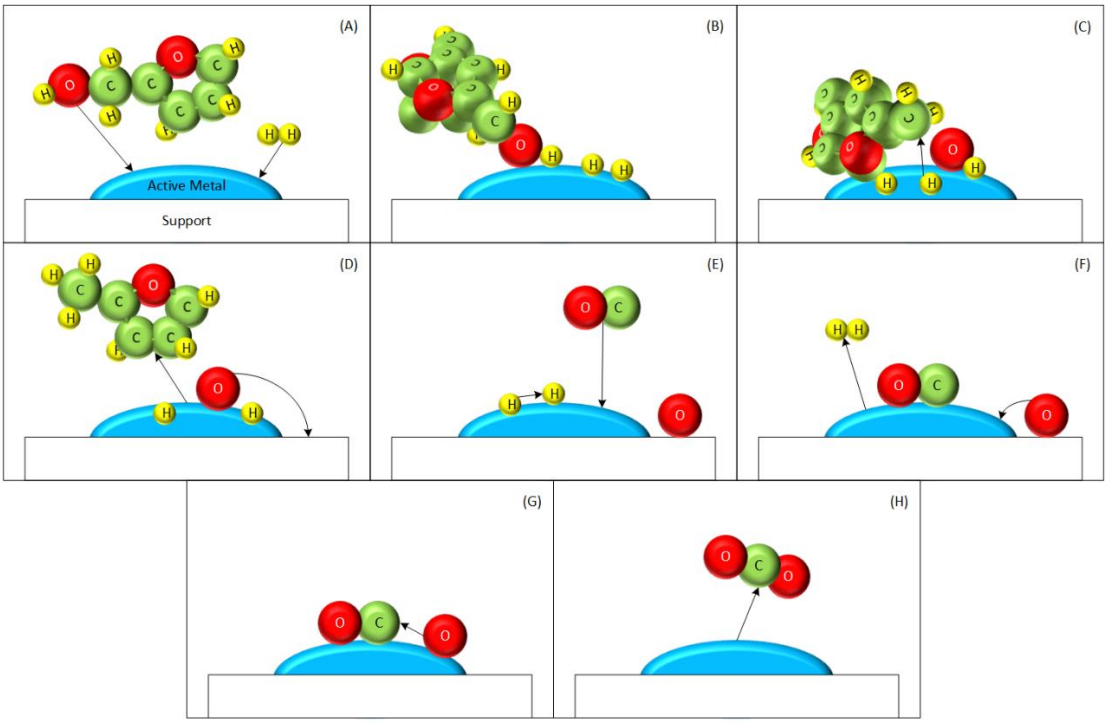

(A) Adsorption of furfuryl alcohol; adsorption and dissociation of H_2. **(B)** Furfuryl alcohol is adsorbed via the oxygen of the hydroxymethyl group (likely on Fe of NiFe catalyst). **(C)** Hydrogenolysis of furfuryl alcohol. **(D)** 2MF desorbed from the surface; oxygen is transferred to the active support's oxygen vacancy (such as CeO_2-ZrO_2). **(E)** CO is adsorbed onto catalyst surface (likely via Ni of NiFe); hydrogen atoms at any time may associate. **(F)** Oxygen back-transfer from support to active metal (Fe of NiFe); desorption of H_2. **(G)** Oxidation of CO to produce CO_2. **(H)** Final desorption of CO_2.

Figure 5-10: Proposed combination of WGSR and Deoxygenation (furfuryl alcohol shown as example) on the surface of an active metal with an active support with oxygen vacancies.

5.4 Conclusions

Of all the catalysts that were studied, the superior catalysts were selected as 0.5%Co4%Fe/SiO_2 and 0.5%Ni4%Fe/SiO_2-SWFe. Due to strong dispersion of the two metals among each other, potentially forming an alloy phase, 0.5%Co4%Fe/SiO_2 offered competitive deoxygenation properties, eliminating furfural content, while boosting *in-situ* H_2 production. As an alloy, Co stabilizes Fe, preventing permanent oxide formation. On the other hand, sequential impregnation of 0.5%Ni4%Fe/SiO_2 catalyst was favourable as it provided a distinct separation of the Ni and Fe phases allowing them to perform their

individual roles. As a result, the 0.5%Ni4%Fe/SiO_2-SWFe catalyst provided competitive deoxygenation properties with elevated DMF fractions and higher reduction of solid residue content. Aside from their ability to help reduce solid residue, catalysts with 4wt% Co/Ni 0.5% provided underwhelming results. 0.5%Pd4%Fe/SiO_2-SWPd also eliminated furfural content, however, H_2 consumption was a concern.

Going forward, it was concluded that proceeding studies should focus on improving catalyst site dispersion on supporting materials and the selection of appropriate materials that promote *in-situ* hydrogen production. A bifunctional catalyst that promotes both deoxygenation and WGSR instead of two separate catalysts would likely eliminate barriers associated with the mass transfer of H_2.

Chapter 6: Guaiacol Deoxygenation using Ceria-Zirconia Based Catalysts with Hydrogen Produced Internally via Water-Gas-Shift Reaction

6.1 Introduction

The production of biofuels via thermal processing of biomass material requires hydrogen gas to upgrade the crude bio-oil to achieve acceptable oxygen content. However, therein lies a problem – cost and sustainability issues regarding hydrogen consumption. In any case, it is beneficial to reduce hydrogen requirements. One idea that has been discussed for is to use a catalyst that couples selective deoxygenation activity with water-gas-shift reaction (WGSR) activity. Given that deoxygenation systems produce H_2O and CO in cases where decarbonylation or reforming reactions occur, performing WGSR to regenerate H_2 and remove oxygen as CO_2 would be ideal for reducing overall hydrogen requirements.

Some of the hardest - yet highly abundant - compounds in typical crude bio-oil to undergo deoxygenation are phenolic compounds which could consist of guaiacol. Guaiacol is often used as a model compound because it is difficult to deoxygenate its two oxygenated constituent groups. Since guaiacol is an aromatic compound, it requires hydrogen to undergo deoxygenation, ideally via hydrogenolysis and trans-alkylation reaction pathways. Selectively deoxygenating guaiacol rather than saturating the ring-structure can potentially reduce hydrogen requirements. Studies have shown that guaiacol and other phenolic compounds can undergo selective deoxygenation on bimetallic catalysts containing an

active (sometimes noble) metal such as Ni or Pd and an oxophilic metal such as Fe [105, 106, 130, 131, 147, 205, 210-212].

Hong et al., [131] reported that Pd helps stabilize Fe which facilitates adsorption of phenolic compounds via their oxygenated constituents, limiting interactions with the aromatic-rings, and thus proceeding with direct deoxygenation of the hydroxyl group from the aromatic structure. It was later demonstrated by Hensley et al., [205] that the synergistic effect between Pd and Fe is likely due to a partial electron donation from Pd to Fe. Nie et al., [105] on the other hand reported the selective deoxygenation of *m*-cresol to toluene over a potentially cheaper catalyst. Fe reportedly prevents Ni from interacting with the ring structure. This was further demonstrated theoretically by Liu et al., [212] who compared NiFe to PtFe and determined that NiFe catalysts have significantly less activity towards saturating the ring-structure of guaiacol. NiFe catalysts have also been shown to perform selective deoxygenation of furanic compounds as the addition of Fe provided preferential adsorption of reactants via their oxygenated constituents rather than the ring-structure [146, 155, 156].

In Chapter 5; the deoxygenation of furanic compounds during the decomposition of glucose was found to be favourable on a 0.5%Ni4%Fe/SiO_2 catalyst that was prepared via sequential addition as Fe facilitated adsorption and Ni facilitated hydrogen activation. Meanwhile, in the same study, a 0.5%Co4%Fe/SiO_2 catalyst that was prepared via co-impregnation behaved similarly as the aforementioned PdFe catalysts – Co helped stabilize

the Fe phase, making it more reducible. This CoFe catalyst was also shown to favour internal H_2 generation highlighting the possibility of coupling deoxygenation with WGSR.

Ceria based catalysts including metals supported on ceria-containing materials such as Ni or NiFe have also been shown to be active towards water-gas-shift reaction [39, 41, 198, 213] Watanabe et al., [41] reported the capabilities of NiFe/CeO_2-ZrO_2 for the water-gas-shift reaction and described CeO_2-ZrO_2 as a supplier for oxygen storage/transport from the active Ni and Fe phases. Using a Ce/Zr molar ratio of 67/33 as determined from a study by Goscianska, et al., [214]; the addition of Zr into the framework as a mixed oxide provides the support with structural stabilization. For high WGSR activity, Boaro et al., [38] recommended that active metals and supports should display a strong interaction at the metal-support interface in which oxygen storage plays a secondary role. This could be achieved by the appropriate selection of bimetals as Tepamatr et al., [42] demonstrated with the addition of Re to Cu on a Gd-doped CeO_2 support. The stronger metal-support interaction that was achieved through the addition of Re effectively led to an increase in CeO_2 reducibility.

In addition to the WGSR activity; ceria and ceria-zirconia catalysts have also been studied for their usefulness in deoxygenation (due to their inherent Lewis acidity)[69, 215, 216], and steam reforming of light compounds [217-219] and even phenolic compounds at high temperatures [220]. For the coupling of deoxygenation with WGSR, a ceria-zirconia catalyst such as NiFe/CeO_2-ZrO_2, which has been proven for WGSR activity may be ideal as the NiFe phase alone is likely to be active towards deoxygenation. The oxygen storage

capabilities of the support could also be beneficial for helping prevent severe oxidation of Fe. In addition, the oxygen vacancy sites on $CeO\text{-}ZrO_2$ may increase the catalyst's overall ability to adsorb oxygenated compounds.

Watanabe et al., [41] highlighted that the activity of a ceria-zirconia catalyst is dependent on its physical properties (surface area). The physical properties can of course be altered by using different preparation techniques such as co-precipitation and nano-casting (also known as templating) methods. Of these methods, nano-casting is considered highly favourable as it can produce a well ordered mixed-oxide (ceria-zirconia) support with higher surface areas [41, 221-224]. For example, the ceria-zirconia support prepared via nano-casting on KIT-6 by Watanabe et al., [41] had a BET surface area of 101 m^2/g compared to their co-precipitated support with 13 m^2/g BET surface area. The nano-casted catalyst ultimately achieved a higher CO conversion rate with less activity towards methanation.

Herein, a study was performed on the potential of using ceria-zirconia supported catalysts to perform the selective deoxygenation of guaiacol as a model compound for bio-oil using only hydrogen that is produced internally primarily via WGSR. This is done so by feeding water and carbon monoxide into the reactor rather than hydrogen gas. Making use of the nano-casting preparation technique for ceria-zirconia; this study focuses on catalyst development/selection and to evaluate the role of hydrogen. Reactions were performed in a horizontally stirred batch reactor similar to that of Chapters 4 and 5.

6.2 Experimental

6.2.1 Catalyst Preparation

MCM-41 and SBA-15 silica supports/templates were purchased from ACS Materials. Ceria-zirconia was nano-casted from MCM-41 (800 m^2/g) and SBA-15 (550 m^2/g) via a slightly modified templating protocol as described by Deng et al., [223] using a Ce:Zr molar ratio of 67/33, which is similar to that used by Watanabe et al., [41] for the water-gas-shift reaction. For this, zirconia and ceria precursors were impregnated onto the silica templates with a two-step infiltration process each that was followed by calcination at 800°C for 6 hours. For each step, the precursor solution was prepared by dissolving appropriate amounts of zirconyl chloride octahydrate (0.2610/g MCM-41; 0.5077 g/g SBA-15) and cerium nitrate hexahydrate (0.7092 g/g MCM-41; 1.3805 g/g SBA-15) (Sigma-Aldrich) in ethanol (6 mL/g MCM-41; 12 mL/g SBA-15) and stirred for 1 hour to ensure complete dissolution. Upon completion of the second calcination process; the silica templates were then removed using 2M NaOH solutions followed by washing of the remaining CeO_2-ZrO_2 with deionized water using a centrifuge. Subsequently, the material was dried via a heating procedure like the calcination process to ensure that all water was removed with no lingering chloride/nitrate salts. The ceria-zirconia supports are denoted as CZ-41 (nano-casted from MCM-41) and CZ-15 (nano-casted from SBA-15). Commercial ceria-zirconia (prepared via co-precipitation) denoted as CZ-com was purchased from Sigma-Aldrich for the purpose of comparison. A detailed procedure for preparing CZ-41 and CZ-15 is described in Appendix B.

Supported catalysts, consisting of Ni, Fe, and Co, were prepared via incipient wetness impregnation with appropriate amounts of the corresponding nitrate-salts. NiFe catalysts such as 2%Ni4%Fe/CZ-41 (2 wt% Ni and 4 wt% Fe) were prepared via sequential addition of the two metals starting with Fe as per the results from Chapter 5. When Co is introduced, it is added via co-addition with Fe; therefore, a trimetallic 2%Ni0.5%Co4%Fe/CZ-41 catalyst was prepared first via co-addition of Co and Fe followed by the sequential addition of Ni.

6.2.2 Catalyst Characterization

BET surface areas of the as prepared ceria-zirconia materials (including CZ-com) were determined via N_2 physisorption using an Autosorb 1-C. X-ray diffraction (XRD) was performed at the UNB Geochemical and Spectrographic Facility using a Bruker AXS D8 XRD within the 2Theta range of 20-80° (0.02°/second). High-resolution transmission electron microscopy (HRTEM) analyses were performed at the UNB Microscopy and Microanalysis Facility with a JEOL JEM-2010 (S)TEM and a Gatan Ultrascan Camera using Digital Micrograph.

6.2.3 Catalytic Activity Tests

Guaiacol was treated in a horizontally stirred 55 mL reactor at 350°C. The reactor was loaded with approximately 0.4 g of guaiacol (Sigma-Aldrich) at a 1:10 mass ratio with a solvent 1-methylnaphthalene (1MN) (Sigma-Aldrich). Catalyst was added at a 2:5 mass ratio with the guaiacol (0.16 g of catalyst). The reactor was loaded with 515 kPaA of CO at room temperature and 88 µL (0.0874 g) of water to produce steam at 350°C. Upon 100% conversion via WGSR; this amount of CO and H_2O could produce near-stoichiometric

amounts of H_2 for the complete conversion of guaiacol to benzene (without accounting for the water produced from guaiacol deoxygenation). Initial catalyst screening tests to determine the most suitable supporting material (and active metal NiFe vs CoFe) were performed using a reaction time of 6 hours. The selected catalyst then underwent further testing to determine the impact of hydrogen availability using a reaction time of 1 hour.

The reaction products were analyzed after cooling the reactor to 22.5°C. Firstly, the product gases were tested using a RGA200 mass spectrometer with the primary products being H_2, CO_2, CO, and CH_4. A HP-PLOT/U column, which was maintained at 30°C was paired with the RGA200 in order to provide adequate separation of the gases. Liquid products that were attained from the reactor were tested via GC-MS (Shimadzu GCMS QP5000) for qualitative analysis and GC-FID (Varian GC450) for quantitative analysis. Once repeatability was confirmed, some experiments were not repeated because of a high volume of experiments with limited catalyst resources. Errors are estimated at ± 2.5% deviation for guaiacol conversion, ± 0.4% deviation for liquid product yields, and a percent error of 5% on gas partial pressures.

6.3 Results and Discussion

6.3.1 WGSR Pre-testing

Pre-tests were performed to ensure that the reaction system was capable of supporting WGSR. Typical WGSR reaction systems are packed bed reactors with only gas phase – no liquid phase should be present [34]. The reaction system used herein is a batch reactor containing both liquid and gas phases thus potentially limiting the contact between the solid

catalyst (which is being continuously stirred) and the gas phase reactants. The reactor is stirred horizontally (200 rpm) to promote contact between the two phases without the solid catalyst sinking to the bottom of the reactor.

The reactor was loaded with 0.16 g of 0.5%Co4%Fe/CZ-com catalyst, ~245 kPaA CO, and 88 µL of water and was tested with and without the addition of 16 g of 1MN as the solvent at a reaction temperature of 350°C for 1 hour (~ 44 mL headspace volume at 22.5 °C with 1MN). The output gas was tested as per the catalytic activity testing procedure. Without the solvent, 0.87 mmol of H_2 (H_2 partial pressure of 38 kPaA) was produced. With the addition of the solvent, the net production of H_2 was reduced to 0.48 mmol (29 kPaA) - a drop of 45%. Therefore, introducing the liquid phase to the reaction system does pose a barrier, however, this is reasonable because the headspace volume changes when adding the solvent reducing the initial CO loading from ~5.7 mmol to ~4.1 mmol. For comparison, using magnetite as the catalyst without solvent yielded 0.24 mmol of H_2. Overall these results demonstrated that the reaction system can support internal hydrogen production via WGSR.

6.3.2 Catalyst Characterization

Via N_2 physisorption, the BET surface areas of CZ-com, CZ-15, and CZ-41 were determined to be 43 m^2/g, 93 m^2/g, and 213 m^2/g respectively. MCM-41 likely produced a ceria-zirconia support with superior BET surface area because of its small pores (3.5-4 nm pore diameter for MCM-41 versus 6-11 nm for SBA-15). For comparison, Watanabe et al.,

[41] reported a ceria-zirconia support that was prepared via nano-casting on KIT-6 as having a surface area of 101 m^2/g.

Through HRTEM analysis an understanding can be gained as to why CZ-41 has superior physical properties than CZ-com and CZ-15. The HRTEM images in Figure 6-1 show vast differences among the three materials. In Figure 6-1(a) the CZ-com material, which was likely produced via a co-precipitation method, is very crystalline due to its easily identifiable geometry with a non-porous structure. Figure 6-1(b) shows that the CZ-15 material had a very ordered structure owing to pore structure of the SBA-15 template which has cross branching between the pores allowing for the resulting rod-like structures of CZ-15 to stay connected with one another [222]. The CZ-41 material in Figure 6-1(c) on the other hand, is not highly ordered like the CZ-15 material and instead appears to be more amorphous or even a culmination of ceria-zirconia nanoparticles, which explains its high surface area. This is more evident at higher magnifications – see Figure 6-2.

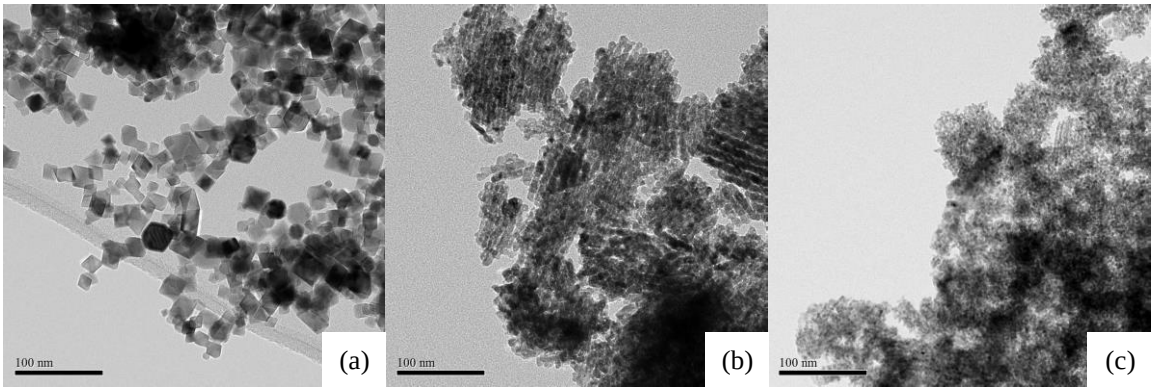

Figure 6-1: HRTEM Images of (a) CZ-com (b) CZ-15 and (c) CZ-41

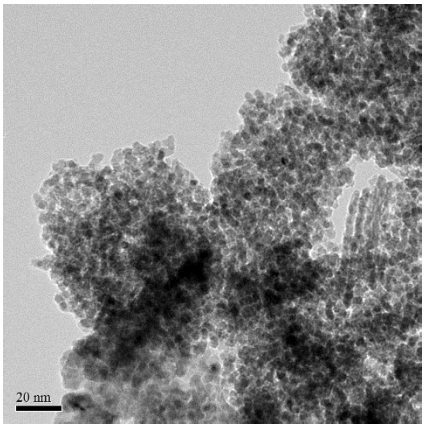

Figure 6-2: HRTEM image of CZ-41 (Figure 6-1(c) at higher magnification)

XRD results for the CZ-41 and CZ-15 materials (see Figure 6-3) were comparable to those of Watanabe et al., [41] for ceria-zirconia of a similar Ce/Zr ratio, which is close to that of $Ce_{0.75}Zr_{0.25}O_2$ and $Ce_{0.6}Zr_{0.4}O_2$. CZ-com closely resembles $Ce_{0.5}Zr_{0.5}O_2$ with a slight shift in the signal to the right. Of all three ceria-zirconia materials, CZ-com had the strongest signal with a maximum intensity of 440 cps compared to 56 cps for CZ-15 and a mere 25 cps for CZ-41. This comes to no surprise as it is clear from the HRTEM images that the CZ-com had a crystalline structure.

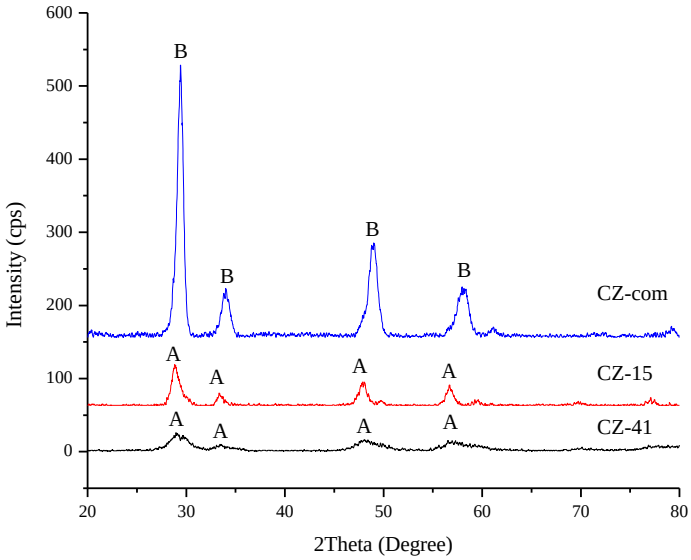

Figure 6-3: XRD spectra of CZ-com, CZ-15, and CZ-41 after final drying; (A) $Ce_{0.75}Zr_{0.25}O_2$/$Ce_{0.6}Zr_{0.4}O_2$ (B) $Ce_{0.5}Zr_{0.5}O_2$

6.3.3 6-Hour Activity Tests

Activity tests were performed for 6 hours to permit the distinguishability between the active metals (NiFe vs CoFe) and the supporting materials. Given that CZ-15 and CZ-41 were produced using the same methodology and ceria-to-zirconia ratios; a long reaction time was desired in order to compare the supports under the same experimental conditions with significantly different results.

6.3.3.1 Active metals: NiFe vs. CoFe

For initial screening, 2%Ni4%Fe/CZ-41 was compared with 2%Co4%Fe/CZ-41 in order to select the most appropriate active pair of metals. As seen in Figure 6-4, adding in the catalysts improved guaiacol conversion from 31.9% to 46.2% and 53.7% respectively. The conversion of guaiacol without the addition of a catalyst is likely through thermal reactions

such as cracking or catalytic behaviour of the reactor wall. Despite having a lower conversion of guaiacol, the CoFe catalyst achieved a higher yield of phenol than the NiFe catalyst at the expense of catechol. However, the NiFe catalyst achieved much higher H_2 and CO_2 partial pressures signifying its dominance over the CoFe catalyst with regards to WGSR activity (see Table 6-1).

Prepared via co-impregnation, CoFe is present on the supporting material as a single phase while the NiFe is present as separate Ni and Fe phases (see Chapter 5). Watanabe et al., [41] proposed that Ni and Fe of their ceria-zirconia supported NiFe catalyst perform separate roles. Fe facilitates adsorption of water via oxidation and production of H_2 during WGSR, Ni facilitates adsorption of CO, and the ceria-zirconia support allows for oxygen transfer/storage. Bi-functional oxidation of CO to CO_2 would then occur from neighbouring Fe-O and Ni-CO sites. Therefore, having a singular phase in which Co makes Fe more reducible may not behave as bifunctionally separate Ni and Fe phases – the oxophilic (Fe) and active (Ni/Co) metals must be able to perform their separate roles.

In the present study, catalyst development proceeded with the NiFe catalyst due to its higher conversion of guaiacol and valuable WGSR activity, which would be useful in conjunction with previous works reported in Chapters 4 and 5.

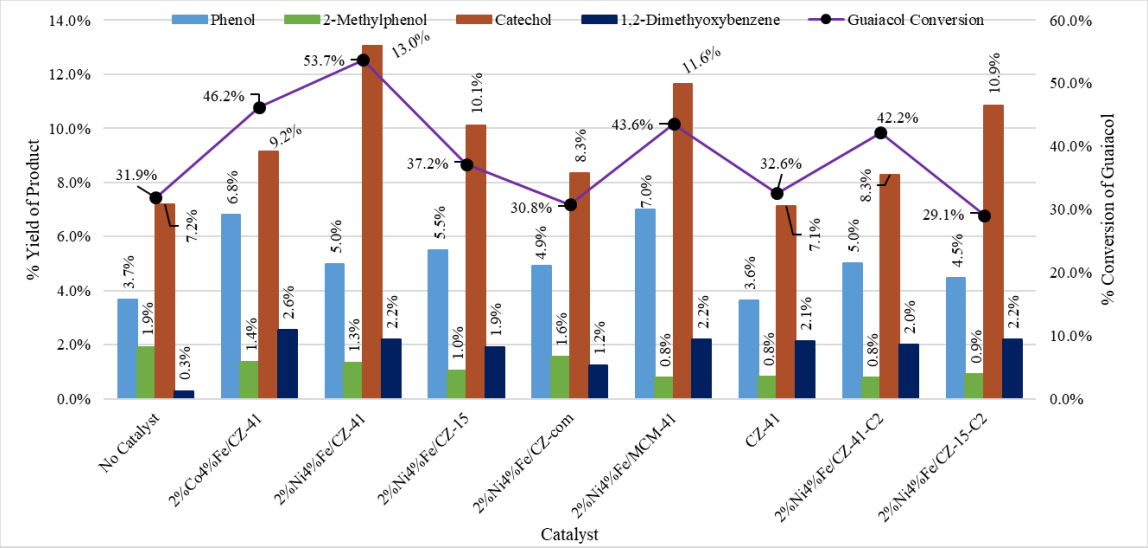

Figure 6-4: Guaiacol conversion and product yields from 6-hour screening tests

Table 6-1: Product gas partial pressures from 6-hour screening tests

Catalyst	Product Gas Partial Pressures (kPaA) @ 22.5°C			
	H_2	CO_2	CH_4	CO
No Catalyst	6	5	26	481
2%Co4%Fe/CZ-41	10	17	28	429
2%Ni4%Fe/CZ-41	58	107	48	358
2%Ni4%Fe/CZ-15	26	45	28	463
2%Ni4%Fe/CZ-com	28	35	29	442
2%Ni4%Fe/MCM-41	16	30	21	449
CZ-41	6	12	21	473
2%Ni4%Fe/CZ-41-C2	47	65	29	411
2%Ni4%Fe/CZ-15-C2	29	41	21	434

6.3.3.2 Support Selection

Upon selecting the active metal pair, screening was performed in order to determine a suitable supporting material. It is noteworthy that in all cases, the products yield did not match the guaiacol conversion suggesting that guaiacol undergoes other reactions producing unidentified products. Other possible reactions could include oligomerization to

heavy compounds, and/or reforming of guaiacol itself. Schimming et al., [215] reported oligomeric products during the hydrodeoxygenation of guaiacol over that ceria catalysts. Oligomerization may be more prevalent due to the extended reaction time and lack of hydrogen gas, which instead promote immediate deoxygenation. However, the presence of oligomers could not be verified in the present study.

Overall, the catalyst supported on CZ-41 achieved the best results in terms of guaiacol conversion (Figure 6-4), H_2 production (Table 6-1), and CO_2 production. The 2%Ni4%Fe/MCM-41 catalyst (which was tested for comparison purposes) provided a moderate conversion of guaiacol, a high yield of phenol, and small amounts of H_2 and CO_2. This demonstrated that NiFe on its own is active towards WGSR. However, NiFe benefits greatly from having an active support that can help transfer/store oxygen as a significant jump in H_2 and CO_2 content is seen when using a ceria-zirconia support such as CZ-41.

It is suspected that the CZ-41 support out-performed other CZ supports because of superior physical properties – a higher surface area resulting in greater dispersion of NiFe. MCM-41 offers high dispersion of the metals which may make up for the inactivity of the supporting material compared to ceria-zirconia. CZ-41 on the other hand appears to offer a decent surface area along with activity of the material. When CZ-41 was tested alone, it offered only slight changes (if any) to gas composition and guaiacol conversion compared to the case with no catalyst. However, an increase in 1,2-dimethoxybenzene yield was observed. Schimming et al., [215] reported that ceria-zirconia promotes trans-alkylation particularly that of the $-CH_3$ from the methoxy group on guaiacol. It was suggested that

this is due to Lewis acid/oxygen vacancy sites on the ceria-zirconia. This could explain the occurrence of both 1,2-dimethoxybenzene and 2-methylphenol in the liquid products. However, the MCM-41 supported catalyst also yielded similar amounts of these products; therefore, the trans-alkylation activity is likely attributed to the active metals, Ni and/or Fe.

The conversion of guaiacol appeared to be very sensitive to the preparation of the catalysts. In Figure 6-4 (and Table 6-1) it is seen that catalysts listed as C2 – representing catalysts prepared from a second batch of CZ-41 and CZ-15 - provided inferior results compared to the initial batch. The CZ supports for the C2 catalysts were separated from the NaOH leaching fluid and washed using vacuum filtration as opposed to a centrifuge which was used for initial batch. This is likely due to insufficient separation/washing when utilizing vacuum filtration.

Another possibility to explore is that SBA-15 has a large pore volume for templating – about twice as much as MCM-41 thus allowing for more ceria-zirconia. Deng et al., [223] suggested that the casted material (CZ) can take up to 15% of the pore volume of the template material. Large volumes of ethanol must be used for the infiltration process in order to add enough CZ in two steps because of the high molecular weights and poor solubility of the precursors. As suggested by Deng et al., [223], a large ethanol:template ratio may result in the non-uniform addition of CZ to the silica template. As a result, preparing CZ-15 through the two-step infiltration process may be risky as repeatability may be more difficult to achieve. To reconcile this, it would be worth exploring the preparation of CZ-15 via a 4-step infiltration process which would use a similar

ethanol:template ratio as the CZ-41 preparation process. Note that too small of a ethanol:template ratio will inhibit adequate mixing.

Compared to the case without a catalyst, 2%Ni4%Fe/CZ-com and 2%Ni4%Fe/CZ-15-C2 were very underwhelming in terms of guaiacol conversion. One possibility is that the catalysts promote the reverse of an unknown reaction, which consumes guaiacol when no catalysts are implemented. This cannot be verified however due to detection limitations such as the inability to analyze possible oligomeric compounds.

Above all, 2%Ni4%Fe/CZ-41 was selected as the main catalyst for following developments and tests. With a high surface area ceria-zirconia support, this catalyst provided the greatest conversion of guaiacol and production of H_2 *in-situ* making it the most promising catalyst.

6.3.4 1-Hour Hydrogen Tests

With hydrogen having such a crucial role in the deoxygenation of guaiacol, it was important to determine how varying hydrogen availability could impact the outcome. Although 2%Ni4%Fe/CZ-41 was able to achieve greater than 50% conversion of guaiacol along with a significant *in-situ* production of H_2, it required a reaction time of 6 hours. Reaction times as such can prove to be problematic as the solvent, 1MN, will ultimately degrade or even react with intermediates. Indeed, in the previous 6-hour screening tests, trans-alkylation products of 1MN (albeit small concentrations compared to guaiacol conversion products), such as dimethylnaphthalene, were witnessed in the products via

GCMS analyses. Therefore, it is worthwhile investigating how the catalyst will perform at a reduced reaction time (1-hour) and how it may be enhanced by the addition of H_2. Brief comparisons were also made to other catalysts such as 2%Co4%Fe/CZ-41 and a new trimetallic catalyst 2%Ni0.5%Co4%Fe/CZ-41.

6.3.4.1 Impact of Varying Hydrogen

At a reaction time of 1 hour, 2%Ni4%Fe/CZ-41 provides a guaiacol conversion of 24.0% compared to ~54% at a reaction time of 6 hours. Without a catalyst, the conversion is far less at 8.3%. An increase in conversion of guaiacol is observed in Figure 5 as a shift is made from utilizing entirely internally produced hydrogen to H_2 provided from external sources without any addition of water or CO. It is obvious that the conversion of guaiacol is dependent on increasing the presence of hydrogen.

At 515 kPaA of hydrogen, the reaction has stoichiometrically enough hydrogen for the complete conversion of guaiacol. This is the amount of hydrogen that would be produced if WGSR reached 100% conversion of the CO provided in the tests without additional hydrogen. 310 kPaA of hydrogen represents the stoichiometric amount of hydrogen that would be required to convert guaiacol to toluene, utilizing a trans-alkylation reaction route for the methyoxy group. With the NiFe/CZ-41 catalyst, increasing hydrogen pressure to 515 kPaA (and removing CO and water from the initial conditions) manages to raise conversion to 28.9% (see Figure 6-5). With the catalyst, at 38 kPaA H_2 a small dip in guaiacol conversion is observed. At 108 kPaA and 310 kPaA, H_2 provides no benefits for guaiacol conversion. Without a catalyst, adding hydrogen appears to help with conversion

as guaiacol either reacts with the reactor walls or undergoes thermal conversion. With the catalyst, even at 515 kPaA hydrogen, conversion of guaiacol slightly increases from 24.0% to 28.9%, demonstrating that a significant amount of hydrogen – beyond stoichiometric amounts – would be required for complete conversion.

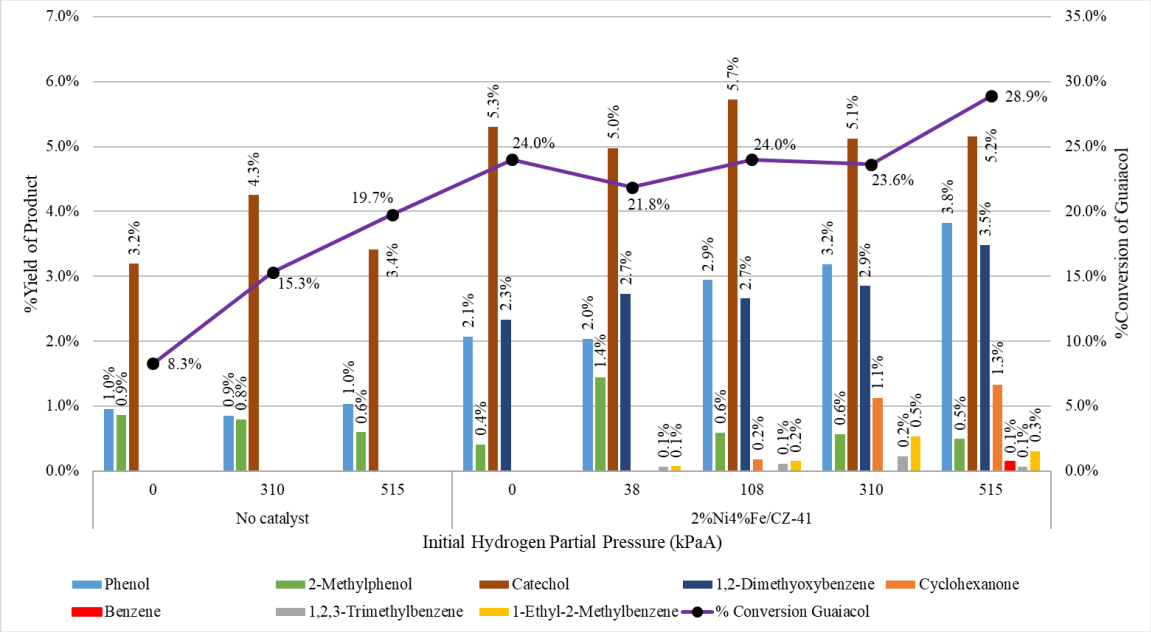

Figure 6-5: Conversion of guaiacol and yields of liquid products with changes in initial hydrogen supply

Switching to the hydrogen atmosphere aided the conversion of intermediates. As seen in Figure 6-5, switching to the pure hydrogen atmosphere increased the percent yield of phenol and introduced new products, such as cyclohexanone, which are very dependent on elevated hydrogen supplies [16, 100-102, 139]. Acidity of the catalyst support may have caused phenol to undergo the HYD reaction route, producing cyclohexanone (via partial hydrogenation-tautomerization route or hydrogenation-dehydrogenation) – a potential precursor in removing the final oxygen group – rather than benzene via a straightforward

hydrogenolysis reaction [139]. Although consideration should be taken for the conversion of guaiacol without a catalyst – up to 19.7% upon switching to a hydrogen atmosphere.

Catechol is an intermediate that is directly impacted by guaiacol conversion and it is consumed to produce other intermediates – such as phenol. Again, a strange occurrence of 1,2-dimethoxybenzene was observed – especially when the catalyst was used due to its trans-alkylation activity. Again, the amount of detectable product material does not correlate with the conversion of guaiacol with up to half of the reacted guaiacol unaccounted for. It is likely that some of the undetectable products of guaiacol conversion are either in low concentration or elute at the same time as the solvent 1MN (such as methylcatechol). An increase in CO partial pressure (see Table 6-2) could indicate the occurrence of steam reforming; however, the amount of CO that is produced is miniscule in comparison to the amount of reacted guaiacol corresponding to that of missing products.

CO production may relate to the reforming of CH_4 instead. With the catalyst employed, hydrogen production continues until the addition of CO and H_2O is eliminated. In the purely H_2 environment, the lack of CO makes it difficult to regenerate H_2 once it has been consumed. The fact that reactions such as those producing cyclohexanone occur also makes this difficult. The only possibility for extending H_2 availability in this case would be to develop the catalyst with a higher focus on reforming CH_4. The presence of CO and CO_2 in the outlet gas when using the catalyst with an initial condition of 515 kPaA H_2 suggests that CH_4 reforming (or reforming in general) is indeed a strong possibility.

Table 6-2: Product gas composition as a result of changing initial hydrogen supply

Catalyst	Water Added?	Initial P_{H2} (kPaA)	Product Gas Partial Pressures (kPaA) @ 22.5			
			H_2	CO_2	CH_4	CO
No catalyst	Yes	0	5	3	14	485
	Yes	310	367	3	14	119
	No	515	439	0	11	0
2%Ni4%Fe/ CZ-41	Yes	0	18	23	14	482
	Yes	38	44	22	14	414
	Yes	108	111	15	18	340
	Yes	310	336	4	20	114
	No	515	442	3	19	10

6.3.4.2 Catalyst Comparisons

At zero addition of H_2, 2%Ni4%Fe/CZ-41 was compared to 2%Co4%Fe/CZ-41 and a trimetallic 2%Ni0.5%Co4%Fe/CZ-41 (see Figure 6-6 and Table 6-3). A catalyst with a similar Ni:Fe ratio as in Chapter 5 (using a silica support) (0.5%Ni4%Fe/CZ-41) was also tested to determine if the Ni content had a significant impact on WGSR and guaiacol conversion. It is evident in Figure 6-6 that reducing the Ni content from 2wt% to 0.5wt% reduces the overall effectiveness of the catalyst significantly as conversion of guaiacol dropped to 15.2% along with reduced yield of catechol and phenol. As seen in Table 6-3, the catalyst containing 0.5wt% Ni produced more H_2, however, it lacks some ability to re-utilize H_2 for deoxygenation of guaiacol.

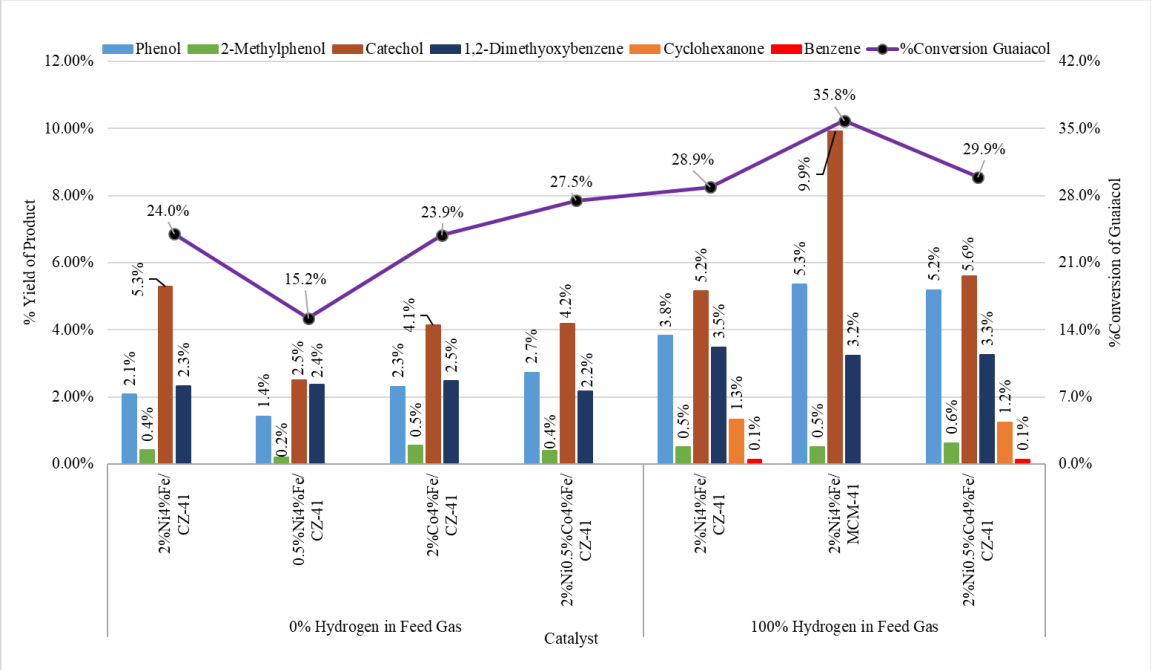

Figure 6-6: Catalyst comparisons via guaiacol conversion and product yield (with and without initial H_2 atmosphere)

Table 6-3: Product gas compositions with various catalysts (with and without initial H_2 atmosphere)

Initial P_{H2} (kPaA)	Catalyst	Product Gas Partial Pressures (kPaA) @ 22.5°C			
		H_2	CO_2	CH_4	CO
0	2%Ni4%Fe/CZ-41	18	23	14	482
	0.5%Ni4%Fe/CZ-41	25	21	9	464
	2%Co4%Fe/CZ-41	8	7	15	447
	2%Ni0.5%Co4%Fe/CZ-41	38	39	15	431
515	2%Ni4%Fe/CZ-41	442	3	19	10
	2%Ni4%Fe/MCM-41	427	3	17	10
	2%Ni0.5%Co4%Fe/CZ-41	441	0	19	11

Employing the 2%Co4%Fe/CZ-41 catalyst provided similar liquid product compositions and guaiacol conversions as the 2%Ni4%Fe/CZ-41 catalyst with a slightly higher yield of phenol. Its shortcoming however was its lower production of H_2 and CO_2 – the CoFe

catalyst is seemingly less active towards *in-situ* H_2 production than the NiFe catalyst. A sharper decrease in CO content for the CoFe catalyst suggests that the NiFe produces excess amounts of H_2 and CO via reforming reactions compared to the CoFe catalyst likely due to the exposed Ni phase.

The 2%Ni0.5%Co4%Fe/CZ-41 catalyst, which was tested both with and without H_2, was selected based on previous results (Chapter 5), which indicated that alloying Co with Fe stabilized Fe making the oxophilic phase of the bimetallic NiFe catalyst more reducible. The purpose here was to make the catalyst more readily perform the bi-functional oxidation of CO to CO_2 as discussed in Section 6.3.3.1, thus enabling the higher adsorption of water and hence, greater H_2 production. This proved to be successful as the trimetallic catalyst produced more H_2 and CO_2 (at the cost of CO) (see Table 6-3) than the bimetallic catalyst it was based on, 2%Ni4%Fe/CZ-41 (no external H_2 added). Compared to the NiFe catalyst, the NiCoFe catalyst had a slightly higher guaiacol conversion and produced more phenol at the expense of catechol.

Under a 100% hydrogen atmosphere, the 2%Ni4%Fe/CZ-41 and 2%Ni0.5%Co4%Fe/CZ-41 catalysts were compared to 2%Ni4%Fe/MCM-41. Compared to the CZ-41 based catalysts which were intended to produce their own hydrogen source, the MCM-41 based catalyst is intended as a net consumer of H_2 which would benefit from the presence of a hydrogen atmosphere. As seen in Figure 6-6, the 2%Ni4%Fe/MCM-41 catalyst provided superior conversion of guaiacol and yields of phenol and catechol than the CZ-41 based catalysts along with a greater consumption of H_2 (see Table 6-3). This is likely because

MCM-41 has a far greater surface area than CZ-41 allowing for higher dispersion of the active metals on its surface. In contrast, the CZ-41 based catalysts produced cyclohexanone whereas the MCM-41 catalyst did not likely due to Lewis acidity of CZ-41.

Under the 100% hydrogen atmosphere, the trimetallic NiCoFe catalyst excels over the bimetallic NiFe catalyst with slightly higher yields of phenol and catechol and very comparable gas phase results. This appears to be a clear example of how adding Co to the Fe phase is beneficial as it makes the Fe phase more reducible. For example, upon undergoing hydrogenolysis, an oxygen is left on the Fe surface. Being more reducible, the Co-Fe alloy more readily uptakes hydrogen from Ni than solo Fe allowing for faster production and release of water from the catalyst surface. The addition of Co could also potentially improve reducibility of the supporting material due to improved oxygen transfer between the CZ-41 and Fe – similar to the results obtained by Tepamatr et al., [42] when Re was added to Cu on a ceria catalyst.

After 1-hour of reaction, guaiacol conversions of 24-28% at a guaiacol:catalyst mass ratio of 5:2, can be regarded as low. In comparison, Dongil et al.,[225] achieved >80% guaiacol conversion after 1-hour of reaction in a batch reactor with a 15%Ni/CNT catalyst at 300°C and 5 MPa of H_2 along with a higher guaiacol:catalyst loading of ~11.5:1. Near 100% conversion was achieved after 2 hours of reaction. This demonstrates the need for elevated hydrogen pressures for complete guaiacol conversion. Therefore, the role of the multifunctional catalysts developed herein is not to replace current HDO technology but to modify it in order to reduce overall hydrogen requirements. There are two possible uses

for these multifunctional catalysts in industry. The first option is to make use of the multifunctional catalysts in a hydrogen-free environment during the initial stages of deoxygenation, thus providing initial conversion without the consumption of hydrogen gas. The second option that should be explored is the use of these multifunctional gases in a traditional HDO setting but with syngas rather than pure hydrogen gas. This would both make use of the catalyst's ability to perform WGSR and deoxygenation while eliminating the need for upstream WGSR processes.

6.4 Conclusions

Ceria-Zirconia support NiFe catalysts were shown to be effective at producing H_2 internally to allow the deoxygenation of guaiacol. For the active materials, a sequentially prepared 2%Ni4%Fe supported on ceria-zirconia catalyst was superior to a co-impregnated 2%Co4%Fe catalyst in terms of guaiacol conversion and H_2 production. This was because ceria-zirconia supported catalysts behave most bifunctionally and efficiently when the ceria-zirconia support can transfer oxygen to/from a Fe phase that is separate from the Ni (Co) phase, which can adsorb CO and help with the release of H_2. Of the three ceria-zirconia supports, CZ-41 – ceria-zirconia templated from MCM-41 – was found to be superior due to a much higher surface area.

Tests with hydrogen demonstrated that in order to improve guaiacol conversion over the ceria-zirconia catalysts, H_2 availability would need to exceed the stoichiometric amounts. The addition of Co to the Fe phase of the sequentially prepared NiFe catalyst improves H_2 production and slightly increases guaiacol conversion. Co makes the Fe more reducible

allowing the bi-functional oxidation of CO to CO_2 to occur more readily thus improving WGSR activity. Since the NiFe/CZ-41 and NiCoFe/CZ-41 catalysts strongly promoted internal WGSR; future work is recommended on their use as dedicated WGSR catalysts for hydrogen production in industry. These catalysts may also be incorporated into a modified HDO process that uses syngas as an alternative to pure hydrogen.

Chapter 7: Glucose Decomposition with Internal Hydrogen Production and Deoxygenation via Nano-Casted Ceria-Zirconia Catalysts

7.1 Introduction

The thermolysis of biomass material can lead to the production of useful gases/vapours such as H_2, H_2O, CO, and CH_4 [4, 9]. The bio-oil produced from biomass decomposition requires upgrading via hydrodeoxygenation processes which requires hydrogen. Therefore, it is advantageous to utilize the gases produced during the initial thermolysis stage to perform some preliminary deoxygenation thereby reducing the hydrogen requirements of downstream processes.

Chapters 4 and 5 demonstrated that *in-situ* deoxygenation during glucose decomposition (as a model for cellulose) is possible using monometallic and bimetallic catalysts supported on SiO_2. In addition, the catalysts demonstrated the potential of increasing the overall solid conversion to useful liquid products. However, such work was conducted using atmospheres containing externally sourced H_2. Herein, attention is given towards catalysts that promote the production of additional H_2 internally and use it for *in-situ* deoxygenation as the sole source for H_2. As with previous studies (Chapters 4 and 5), there is a high demand for the catalysts to promote selective deoxygenation – that is selectively using H_2 to remove oxygen rather than saturate carbon-double bonds.

Potential methods to consider for internal H_2 production include water-gas-shift reaction (WGSR), steam reforming, and tar cracking. Florin & Harris, [28] and Widyawati et al.,

[29] both demonstrated the possibility of using WGSR to produce H_2 during biomass pyrolysis using CaO to help capture CO_2, thermodynamically pushing the WGSR to produce more H_2. The same research group has studied the use of SiO_2 supported Ni and Co catalysts for H_2 production [24-27] during cellulose pyrolysis via tar cracking and steam reforming. Reportedly, this is enabled by a build-up of steam between 300-425°C resulting in elevated H_2 production via reforming (and WGSR) as temperatures approach 400°C [25, 27]. However, promoting cracking and reforming reactions too much may lead to the reduction in liquid product yield as H_2 may be produced at the cost of lighter components. Thus, a balance must be met with regards to producing internal H_2 and maintaining liquid product yields. This may be done by using the WGSR option at reduced temperatures to avoid significant reforming.

Ideally, the catalyst that is used for promoting WGSR should also be active towards *in-situ* deoxygenation. Ceria and Ceria-Zirconia catalysts, which use ZrO_2 to provide stability for CeO_2, have been shown to be active towards both deoxygenation [69, 215, 216] and WGSR [39, 41, 198, 213]. Watanabe et al., [41] for example, used a bimetallic NiFe phase catalyst supported on CeO_2-ZrO_2 (CZ) nano-cased from KIT-6 and reported that the oxygen storage/transport capabilities of CZ assisted in the bi-functional roles of Ni and Fe. CZ has been demonstrated to be effective at deoxygenating guaiacol due to its Lewis acid sites (oxygen vacancies). However, Schimming et al., [215] suggested that Lewis acidity may also have an influence on oligomerization. Vasconcelos, et al., [226] reported that CZ was useful for gas phase dehydration of glycerol within the temperature range of 150-350°C because of the acid-base cooperativity of moderately basic sites and Lewis acid sites on

their $Ce_{0.8}Zr_{0.2}O_2$. During glucose decomposition, dehydration reactions may be important for the initial deoxygenation of intermediates [23, 48].

Ni-based catalysts are valuable due to their ability to promote dehydration in the early stages of glucose decomposition and reduce organic solid residue by promoting mild tar cracking (Chapters 4 and 5). Therefore, the catalyst's impact on biomass decomposition must be greatly considered. Chloride salts acting as Lewis acids have been shown to significantly impact biomass decomposition [44, 46]. Carvalho et al., [44] for example, demonstrated that the addition of $ZnCl_2$ to biomass reduced the temperatures at which high decomposition rates are observed. As a Lewis acid, $ZnCl_2$ promoted early C-C and C-O bond breakage which resulted in heavy dehydration and char formation.

Although scarce, some work has been conducted using heterogenous catalysts to improve biomass decomposition/pyrolysis. A $NiCu/\gamma\text{-}Al_2O_3$ catalyst was shown to have an impact on the pyrolysis of coffee grounds by Kan et al., [51]. Introducing the catalyst resulted in an increase in CO and CO_2 production and a change in decomposition rates within the range of 360-513°C. Ding et al., [227] reported that CeO_2 was capable of removing oxygen from the vapours produced during the pyrolysis of corn stover and attributed it to the catalyst's ketonization ability. In their study, the original biomass material was separated from the catalyst by quartz wool and therefore did not have any immediate interactions between the biomass and the catalyst. Jeon et al., [50] similarly performed catalytic pyrolysis using mesoporous catalysts separated from the biomass using quartz and reported

that the acidic sites of AlSBA-15 promoted dehydration and cracking of the pyrolysis vapours.

In the present study, ceria-zirconia catalysts nano-casted from MCM-41 (denoted as CZ-41) were used in a horizontally stirred reactor for the decomposition of glucose, internal production of H_2 (via WGSR), and *in-situ* deoxygenation. Catalysts 2%Ni4%Fe/CZ-41 and 2%Ni0.5%Co4%Fe/CZ-41 were selected based on previous results (Chapter 6) that proved these two catalysts can perform deoxygenation using H_2 produced internally via WGSR. Herein, the catalysts were tested for their ability to perform internal deoxygenation and hydrogen production during the decomposition of glucose. As opposed to adding H_2 to the system, the catalysts had to utilize gases formed from the decomposition reactions to produce internal H_2. This study also focused on the impact that the catalysts have on glucose decomposition. As with Chapters 4 and 5, furanic products such as 2-methylfuran, 2,5-dimethylfuran, and furfural were used as indicators for *in-situ* deoxygenation activity due to their ease of identification and difficulty to undergo deoxygenation. The selected catalyst and reaction conditions were also used for cellulose decomposition to glean the impact the catalyst has on real biomass decomposition.

7.2 Experimental

7.2.1 Catalyst Preparation

Catalysts were selected and prepared based on the work presented in Chapter 6. For a support, CZ-41 – ceria-zirconia nano-casted from MCM-41 based on a modified templating protocol described by Deng et al., [223] – was used because it has superior

physical properties (203 m^2/g BET surface area) in Chapter 6. Catalysts, 2%Ni4%Fe/CZ-41 and 2%Ni0.5%Co4%Fe/CZ-41, were prepared via sequential addition using the incipient wetness impregnation method. For these catalysts, the precursors for Fe or CoFe (iron nitrate and cobalt nitrate) were added to the support first and then calcined (600°C for 6 hours), followed by Ni addition (nickel nitrate) and calcination. See Appendix B for a detailed procedure for preparing CZ-41.

7.2.2 Catalyst Characterization

X-ray diffraction (XRD) was performed using a Bruker AXS D8 XRD within the 2Theta range of 20-80° (0.02°/second) at the University of New Brunswick Geochemical and Spectrographic Facility. Temperature programmed reduction (TPR) analyses of the catalysts were performed using an Autosorb 1-C paired with a RGA200 mass spectrometer. 150 mg of catalyst was first vacuum dried *in-situ* at 300°C for 20 minutes with flowing helium at 50 nmL/min in a quartz u-cell. TPR analysis was then performed by flowing a mixture of He an H_2 through the u-cell (50 nmL/min He with 1% H_2) and heating from room temperature to 900°C at 10°C/min.

7.2.3 Catalytic Activity Tests

Activity tests for glucose decomposition with *in-situ* deoxygenation using internally produced H_2 were conducted using a horizontally stirred (200 rpm) 55 mL reactor with 800 mg of glucose. Catalyst was added at a 1:5 catalyst-to-glucose mass ratio while a solvent, 1-methylnaphthalene (1MN) was added at 10:1 solvent-to-glucose mass ratio. The reactor was flushed with He to remove oxygen then filled with He to a pressure of 310 kPaA. The reactor was then heated to a desired temperature (300°C, 325°C, 350°C) and held for the

desired reaction time (0.5 hr, 1 hr, 1.5 hr). Cellulose decomposition was tested in a similar manner using the same reactor, feed ratios, and conditions.

Testing of the product gas was performed using a RGA200 mass spectrometer once the reactor was cooled to 22.5°C. A HP-PLOT/U column held at 30°C was used to ensure separation of gases such as CO and CO_2. Solids were separated from the liquid product using a centrifuge, washed with acetone, dried overnight at 80°C, then finally weighed. The H:C molar ratio of the solid residue was determined using a Perkin Elmer 2400 CHNS/O Series II elemental analyzer at the Limerick Pulp and Paper Center at the University of New Brunswick. Liquid products underwent qualification and quantification analyses via GC-MS (Shimadzu GCMS QP5000) and GC-FID (Varian GC450) respectively.

Supplementary analyses of the impact that catalysts have on glucose decomposition were conducted via thermogravimetric analyses (TGA) which were performed using a TA Instruments TGA Q500. For these analyses, glucose and catalysts were loaded onto platinum TGA pans at a 1:5 catalyst-to-glucose mass ratio. The TGA was heated from room temperature to 950°C at a rate of 5°C/min under flowing He (50 nmL/min). The use of alumina pans is not recommended with the CZ-41 catalysts as inherent small particle sizes of CZ-41 (CZ-41 structure resembles a culmination of nanoparticles) may permanently damage the alumina pans.

At the end of the activity tests, solid residue was found to be bound to the walls of the reactor. As a result, the solid residue was extremely difficult to remove – especially when no catalysts were added. Rigorous cleaning had to be used to successfully remove all solid content from the reactor. This involved loading the reactor with water, sodium bicarbonate, and hydrogen peroxide then heating the reactor at 95-100°C for 2 hours. Upon completion, solid content could be easily removed. To account for the solids that were not collected previously with the liquid sample, the reactor was dried at 80°C and weighed.

7.3 Results

7.3.1 Catalyst Characterization

XRD analyses of CZ-41, 2%Ni4%Fe/CZ-41, and 2%Ni0.5%Co4%Fe/CZ-41 (see Figure 7-1) showed no significant changes to the spectra of CZ-41 upon addition of Ni, Fe, and Co. No peaks were detected indicating the presence of either metal or alloy suggesting that the metals were highly dispersed on the surface.

TPR of the catalysts showed significant differences among the three tested materials. As seen in Figure 7-2, CZ-41 is reducible, generating oxygen vacancies as low as ~380°C and reaching significant hydrogen consumption by ~630°C. Two peaks were observed for CZ-41 reduction. The first reduction peak (~630°C) was likely due to surface reduction and the second attributed to bulk reduction (~850°C) [215]. The addition of Ni, Fe, and Co lowered the overall catalyst reduction temperature and appeared to increase the overall hydrogen consumption. The NiFe catalyst started to consume hydrogen earlier and the overall peaks became broader as nickel oxide began to reduce at lower temperatures than the CZ-41.

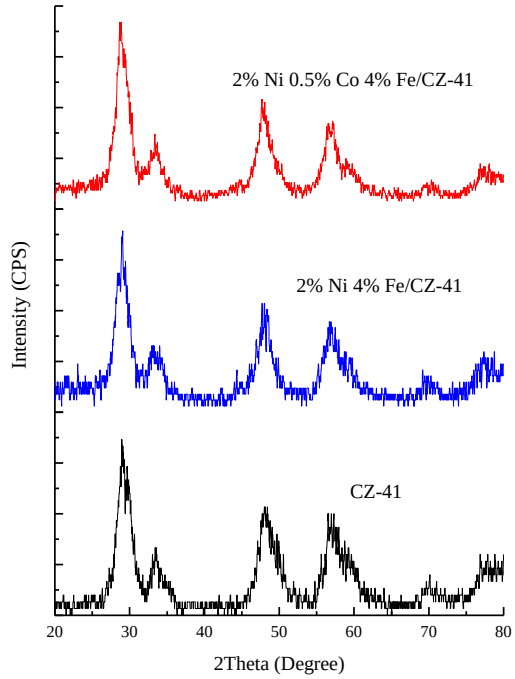

Figure 7-1: XRD Spectra of CZ-41 supported catalysts after reduction

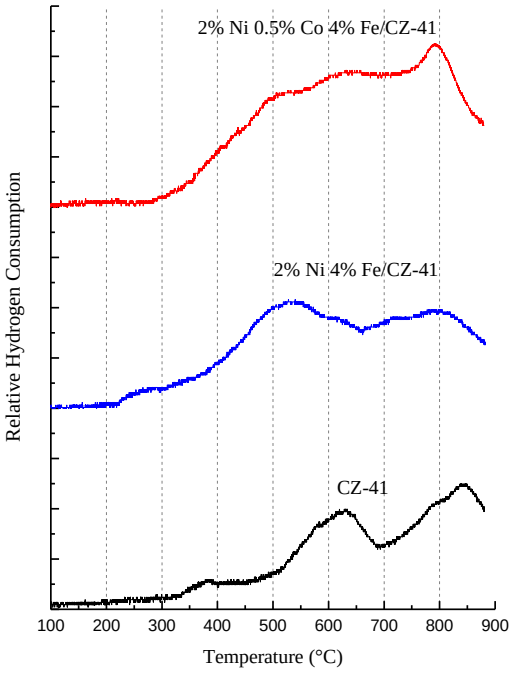

Figure 7-2: TPR – hydrogen consumption profiles for CZ-41 supported catalysts. 150 mg of catalyst in gas flow of 50 nm L/min at 1% H_2 in He. Temperature ramp 10°C/min

A significant change was observed with the NiCoFe with a large, very broad hydrogen consumption profile with a small peak on top at ~890°C. This demonstrates that the addition of the 0.5wt% Co to the Fe significantly altered the reducibiliy of the catalyst as intended. With such a high impact on the overall reducibility it is suspected that the active metal phases, Ni and CoFe, have a strong interaction with the support. These results are similar to those of Tepamatr et al., [42] who reported that the addition of Re to a Cu catalyst supported on Gd-doped ceria helped Cu reduce ceria and produce oxygen vacancies. For the NiCoFe catalyst presented herein, the proposed reduction mechanism involves the following: Ni in general facilitates the activation of hydrogen via dissociation and donates it to the CoFe phase where it is used to remove oxygen as water. The ceria-zirconia support, in addition to undergoing hydrogen dissociation and oxygen removal itself, readily transfers oxygen to the CoFe phase where it is again removed as water with the help of Ni allowing for a rapid, deep reduction of the entire catalyst. A thorough theoretical investigation using computational methods is recommended in order to verify and gain a greater understanding of the proposed reduction mechanism.

7.3.2 Catalyst Activity Tests

7.3.2.1 Catalyst Selection

For the process of selecting between 2%Ni4%Fe/CZ-41 and 2%Ni0.5%Co4%Fe/CZ-41, activity tests were performed with and without adding the catalysts for 1 hr at 350°C. These reactions conditions were selected to correspond with Chapters 4 and 5. These catalysts demonstrated their ability to reduce organic solid material. As seen in Figure 7-3, the

NiCoFe catalyst was superior for both solids conversion and liquid product yield. The NiFe catalyst had similar liquid yield to the base case without catalyst because of higher gas yields. The NiCoFe, which had similar gas yields (see Table 7-1) as the NiFe catalyst achieved a higher liquid yield because of the higher overall conversion of organic solids. In addition to reducing solid content, the catalysts increased the H:C molar ratio of the organic solids (see Figure 7-3), which altogether explains why solid material was easier to remove from the reactor when catalysts were involved. This could demonstrate the addition of internally produced hydrogen to tar leading to a reduction in char formation.

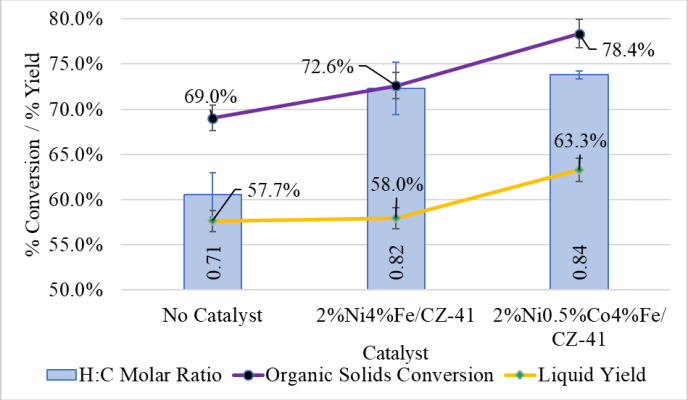

Figure 7-3: Organic solid conversion, liquid yield, and H:C molar ratio (solid residue) results from tests using CZ-41 supported catalysts; Reaction temperature: 350°C, reaction time: 1 hr

Table 7-1: Product gas composition results from tests using CZ-41 supported catalysts; Reaction temperature: 350°C, reaction time: 1 hr

Catalyst	Product Gas Partial Pressure (kPaA) @ 22.5°C			
	H_2	CO_2	CO	CH_4
No Catalyst	6	78	37	5
2%Ni4%Fe/CZ-41	8	112	30	6
2%Ni0.5%Co4%Fe/CZ-41	9	116	30	6

The improved reduction in solid residue with the NiCoFe catalyst is likely due to improved catalyst stability rather than improved tar cracking activity. Tar cracking activity has largely been attributed to monometallic Ni phases [24-26, 32]. When studying the impact that both monometallic and bimetallic catalysts (Chapters 4 and 5), Co and CoFe catalysts did not display significant activity towards tar cracking. Therefore, the improved reduction in solid residue is due to the strong interaction between the NiCoFe and the CZ-41 support. As seen in the TPR results, the NiCoFe catalyst is more reducible than the NiFe catalyst due to an improved oxygen transfer mechanism between the CZ support and CoFe phases. Being able to transfer/store oxygen on the support makes CoFe less prone o deactivation via oxidation.

As seen in Table 7-1, the catalysts did not have a huge impact on the overall output of H_2. H_2 could have been produced and readily consumed. Along with a very slight increase in H_2, a slight decrease in CO and an increase in CO_2 was observed upon catalyst addition suggesting WGSR activity. Ultimately it was difficult to confirm that significant WGSR activity occurred because H_2 may be rapidly consumed.

Adding the catalysts significantly reduced the relative selectivities towards furanic intermediates furfural and 5-methylfurfural instead favouring the net production of the desired 2-methylfuran (2MF) product – see Figure 7-4. This demonstrated that both catalysts were capable of producing hydrogen and performing *in-situ* deoxygenation. The addition of the catalysts also netted small portions of furfuryl alcohol (FA) – a product of furfural hydrogenation, which is considered an intermediate step in the deoxygenation

process to produce 2MF [17, 55, 56]. Compared to the NiFe catalyst, the NiCoFe catalyst had a slightly higher selectivity towards 2,3,5-trimethylfuran and 2-acetylfuran, which indicates side reactions such as trans-alkylation or production of maltol/isomaltol followed by deoxygenation [228, 229]. Neither maltol nor isomaltol were identified within the liquid products.

Furan was a suspected product; however, it was not possible to discern from other potential products such as acetone. Both compounds are noted as having similar retention indices. The GC-MS spectra showed what looked like a culmination of acetone and furan mass spectra.

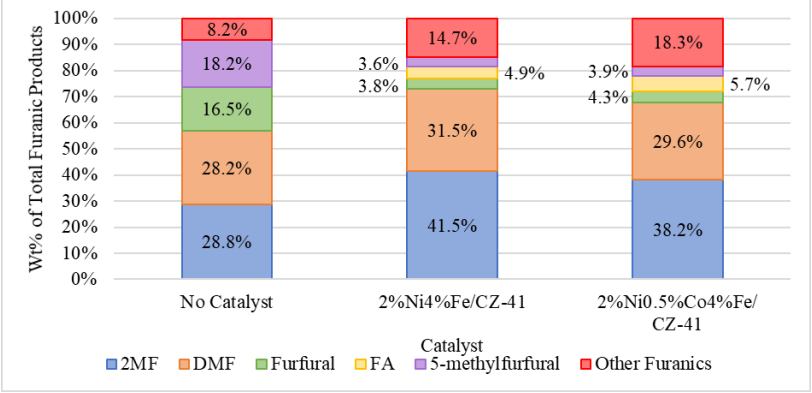

Figure 7-4: Distribution and relative selectivities of detectable furanic compounds results from using CZ-41 supported catalysts; Reaction temperature: 350°C, reaction time: 1 hr

7.3.2.2 Thermogravimetric Analysis

Thermogravimetric analyses were performed to provide a better understanding of the impact that the CZ-41 catalysts have on glucose decomposition. As seen in Figure 7-5, the addition of the CZ-41 catalysts, including CZ-41 had a very noticeable impact on glucose decomposition. With the catalysts, weight loss occurs ~50°C sooner and much more rapid

at ~200°C. Although the catalysts were added at a 1:5 mass ratio with the glucose; at temperatures greater than 650°C the remaining weight dips below 16.7% demonstrating that there is a weight loss also associated with the catalyst – potentially the release of oxygen from the catalyst surface as CO_2 at high temperatures. Pairing the TGA with a RGA200 mass spectrometer to monitor outlet gases reveals the release of H_2O and CO_2 during the early stages of weight loss and H_2, CO, and CO_2 at high temperatures (>650°C).

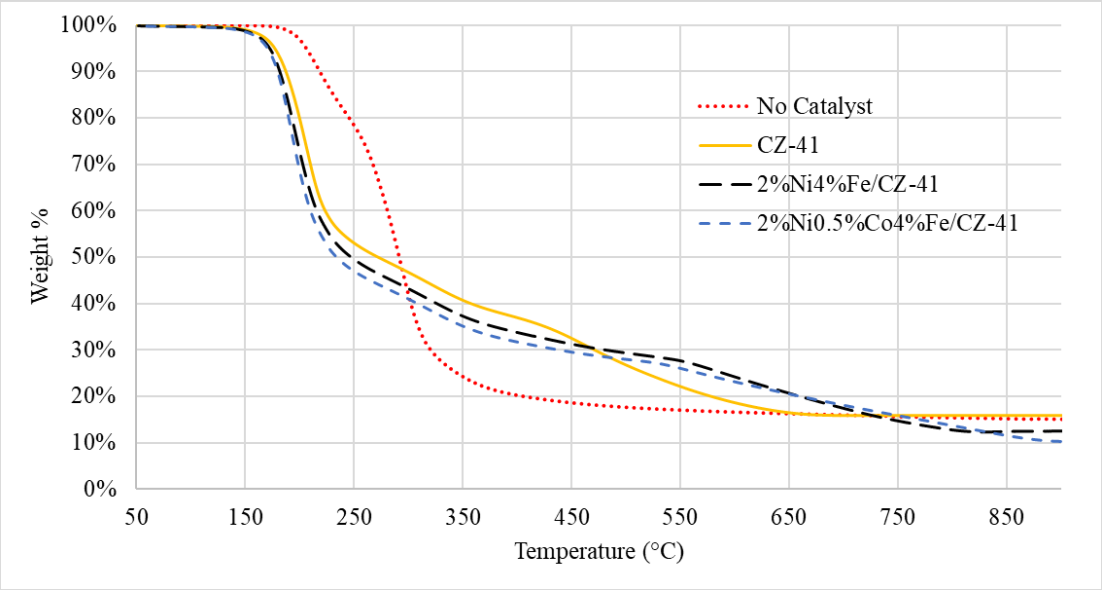

Figure 7-5: TGA results of glucose with the addition of CZ-41 catalysts at a 5:1 glucose-to-catalyst ratio

Differential thermal analyses (DTA – negative weight loss derivative) of the glucose with the catalysts further reveals that the CZ-41 catalysts significantly altered the reaction pathway for glucose decomposition – see Figure 7-6. Glucose on its own decomposes in two periods, the first being for its initial dehydration. Adding the catalysts caused a more rapid weight loss during the early dehydration stages. Given that such a massive shift also occurs with unpromoted CZ-41, CZ-41 clearly contributes the most. This is likely due to

the Lewis acidity of the CZ-41 material as Lewis acids have been shown to promote significant dehydration of sugars [44, 46].

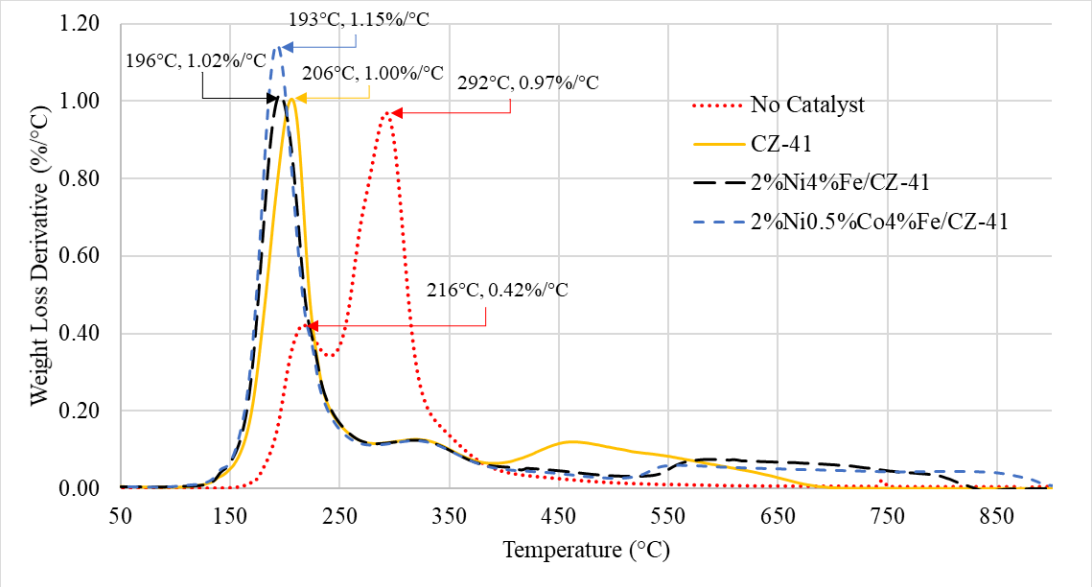

Figure 7-6: DTA (weight loss derivative from TGA) results of glucose with the addition of CZ-41 catalysts at a 5:1 glucose-to-catalyst ratio

Again, the 2%Ni0.5%Co4%Fe/CZ-41 catalyst had a greater impact than the 2%Ni4%Fe/CZ-41 catalyst. This could be because of CoFe having greater interaction with CZ-41 or because of CoFe's own reaction with glucose as it was previously demonstrated that 0.5%Co4%Fe/SiO_2 also has an impact on glucose decomposition, favouring earlier dehydration (Chapter 5).

7.3.2.3 Impact of Temperature

A selected catalyst was tested at various temperatures in order to further optimize the system for liquid product yield and *in-situ* deoxygenation. The impact of temperature is extremely important as Co and Ni catalysts are known to favour tar cracking and reforming reactions at temperatures >350°C due to a build-up of steam [25, 27]. Steam build-up is a

strong possibility in the batch reactor used in this system especially since the catalysts promote the dehydration of glucose. Although reforming would significantly improve internal H_2 production it will inadvertently lower liquid product yields. As such, substantial reforming activity is to be avoided here. The catalyst that was selected was the 2%Ni0.5%Co4%Fe/CZ-41 as this catalyst had the greatest liquid product yields with comparable gas and liquid product composition as the 2%Ni4%Fe/CZ-41 catalyst.

Increasing temperature 300-325-350°C, as seen in Figure 7-7, increased solids conversion and liquid product yield. This is to no surprise as it is expected that increasing temperature would help with the decomposition of glucose and also improve tar cracking activity. Conversely, the H:C molar ratio decrease slightly with temperature. In conjunction with the gas results from Table 7-2; increasing temperature helps retain hydrogen in the liquid product. Evidently, increasing temperature helps liberate some hydrogen content from the solids possibly through tar cracking.

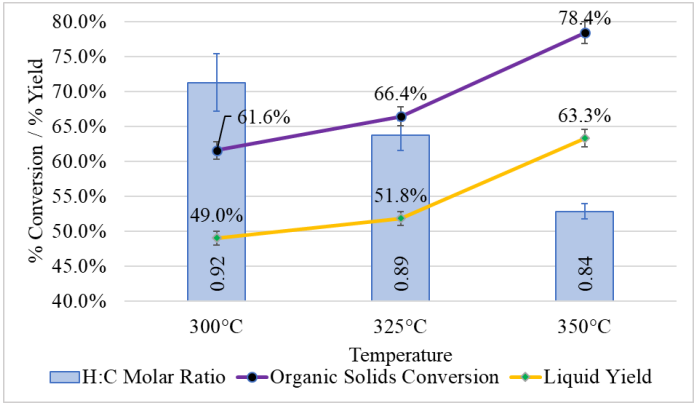

Figure 7-7: Impact of temperature on organic solid conversion, liquid product yield, and H:C molar ratio of solid residue; Catalyst: 2%Ni0.5%Co4%Fe/CZ-41, Reaction time: 1 hr

Table 7-2: Impact of temperature on product gas composition; Catalyst: 2%Ni0.5%Co4%Fe/CZ-41, Reaction time: 1 hr

Temperature (°C)	Product Gas Partial Pressure (kPaA) @ 22.5°C			
	H_2	CO_2	CO	CH_4
300	9	99	22	5
325	8	112	24	5
350	9	116	30	6

Although the output of H_2 and CH_4 appear to remain unchanged with increasing temperatures; CO and CO_2 output increase. The increase in CO_2 and retention of hydrogen in the liquid products suggests WGSR activity, however, H_2 was rapidly consumed. It is possible that during WGSR, H_2 was not released from the catalyst surface, instead it remained disassociated on the surface where it can be readily consumed for deoxygenation. This would be beneficial as it would eliminate mass transfer steps of H_2 to/from the catalyst surface – as was the intent of developing a bi-functional catalyst.

The lack of difference between 325°C and 350°C for CO_2 output suggests that there may not be a significant increase in WGSR activity. Indeed, WGSR being an exothermic reaction can have reduced conversion at elevated temperatures due to equilibrium. Typical iron-based catalysts for industrial WGSR tend to have these issues at temperatures exceeding 350°C [34].

As seen if Figure 7-8, increasing temperature decreased the fractions of furfural and 2-methylfurfural in the furanic products while slightly increasing selectivity towards DMF demonstrating that the temperature gains may be beneficial for *in-situ* deoxygenation.

However, it is noted that 2-acetylfuran selectivity also increased, which currently has an unknown origin. 350°C was selected as the most suitable temperature due to higher liquid product yields and decent 2MF and DMF fractions.

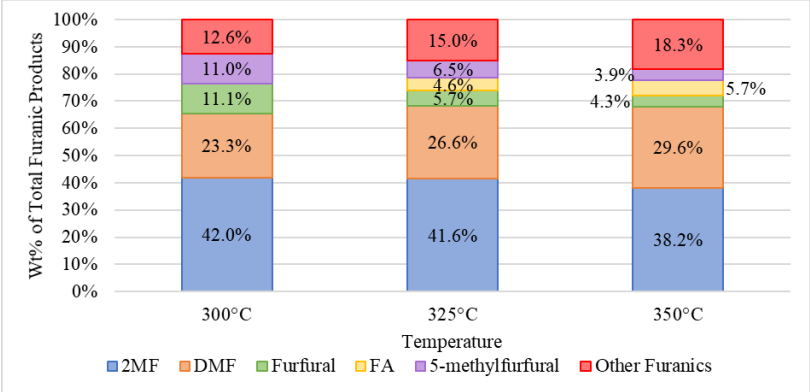

Figure 7-8: Impact of temperature on total furanic product distribution/relative selectivities; Catalyst: 2%Ni0.5%Co4%Fe/CZ-41, Reaction time: 1 hr

7.3.2.4 Impact of Reaction Time

To further optimize the reaction system, time trails were performed at 350°C with the 2%Ni0.5%Co4%Fe/CZ-41 catalyst with additional trials at 0.5 hr and 1.5 hr reaction times (these reaction time do not include the time required to heat up/cool down). As seen in Figure 7-9, reducing the reaction time from 1 hr to 0.5 hr results in a lower organic solid conversion and less liquid product. Increasing reaction time to 1.5 hr caused a slight decrease of organic solids conversion and liquid yield. Over the three time trials, the H:C molar ratio changed insignificantly. Over extended reaction times it is suspected that side reactions such as oligomerization or reforming may occur leading to the production of heavy compounds (solids/tar) and H_2 respectively.

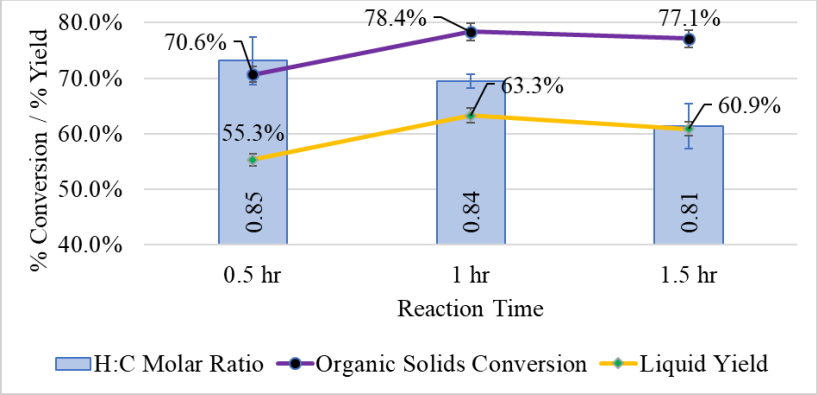

Figure 7-9: Impact of reaction time on organic solid conversion, liquid product yield, and H:C molar ratio of solid residue; Catalyst: 2%Ni0.5%Co4%Fe/CZ-41, Reaction temperature: 350°C

Reaction time did not have a significant impact on gas composition aside from CO_2 output which changed slightly (see Table 7-3). Significant reforming is not suspected to have occurred as there was neither a change in H_2 content or CH_4. As seen in Figure 7-10, the relative selectivies of the furanic compounds did not change much with reaction time – 2MF/DMF selectivies change slightly. This independence on reaction time indicates that *in-situ* deoxygenation occurs quickly. Therefore, improving *in-situ* deoxygenation would be dependent on improving internal hydrogen production (whether it is gaseous or surface bound). Above all, for the reaction system used herein, a reaction time of 1 hr is most suitable because of higher liquid product yields.

Table 7-3: Impact of reaction time on product gas composition; Catalyst: 2%Ni0.5%Co4%Fe/CZ-41, Reaction temperature: 350°C

Reaction Time (hr) @ 350°C	Product Gas Partial Pressure (kPaA) @ 22.5°C			
	H_2	CO_2	CO	CH_4
0.5	8	120	27	6
1	9	116	30	6
1.5	8	128	28	6

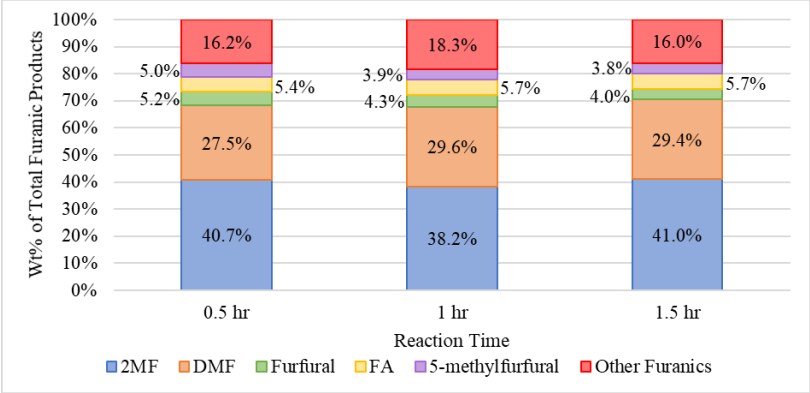

Figure 7-10: Impact of reaction time on total furanic product distribution/relative selectivities; Catalyst: 2%Ni0.5%Co4%Fe/CZ-41, Reaction temperature: 350°C

7.3.3 Cellulose Decomposition

In the previous activity tests; glucose was used as a model compound for cellulose as its reaction pathways are more well defined thereby limiting potential products/intermediates. This allowed the catalysts' impact on dehydration reactions to be studied more readily. As such, the next stage of this study was to demonstrate the impact that the catalyst may have on real biomass decomposition with internal hydrogen production and deoxygenation by decomposing cellulose with 2%Ni0.5%Co4%Fe/CZ-41.

For these tests (including TGA), cellulose replaced glucose in the activity tests and was decomposed at the ideal conditions of 350°C for 1 hour with the solvent 1MN. Without any catalyst, the organic solid content was reduced by 69% with a liquid product yield of 54%. Using 2%Ni0.5%Co4%Fe/CZ-41 increased the conversion of solids to 78% with a liquid product yield of 57%. As seen in Table 7-4, the addition of the catalyst led to a massive change in gas production. The overall H_2 production almost doubled while CO output decreased. Meanwhile, adding the catalyst led to a large increase in CO_2 from 87

kPaA to 141 kPaA in the product gas. This demonstrated the catalyst's ability to produce internal hydrogen via WGSR that could then be used for deoxygenation. However, the low drop in CO is irrespective to the high increase in CO_2. It suggests that either CO_2 was produced from an alternative route or additional CO was produced via steam reforming of light components, while H_2 was consumed via treatment of condensable products.

Table 7-4: Product gas composition from cellulose decomposition with and without 2%Ni0.5%Co4%Fe/CZ-41

Catalyst	Product Gas Partial Pressure (kPaA) @ 22.5°C			
	H_2	CO_2	CO	CH_4
No Catalyst	6	87	70	7
2%Ni0.5%Co4%Fe/CZ-41	11	141	64	7

Surprisingly, on its own, cellulose decomposition produced competitive amounts of 2MF and DMF likely due to extended reaction times and catalytic impact of the reactor wall (see Figure 7-11). However, oxygenated compounds, furfural, and 5-methylfurfural were also prevalent. Upon addition of the catalyst, its selectivity was shifted towards 2MF at the DMF, possibly due to decarbonylation activity. However, as with glucose, the 2%Ni0.5%Co4%Fe/CZ-41 demonstrated its activity towards trans-alkylation as trimethylfuran was a noteworthy product. Undoubtedly, the catalysts impacted the decomposition of cellulose intermediates. For example, adding the catalyst led to an increase in 2-acetylfuran, which could be generated via trans-alkylation or an alteration of the decomposition pathways. In addition, when the catalyst was employed, non-aromatic-ring products such as cyclopentenone were much more apparent than without the catalyst.

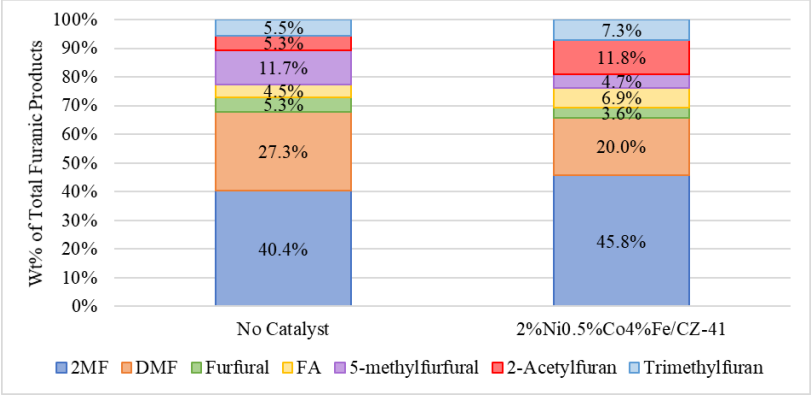

Figure 7-11: Total furanic product distribution of cellulose decomposition

Thermogravimetric analyses (and DTA), similar to those of glucose, were performed to further study the impact that 2%Ni0.5%Co4%Fe/CZ-41 has on cellulose decomposition. As seen in Figures 7-12 and 7-13, the catalyst did not have a significant role in the decomposition of cellulose as it did with glucose. In Figure 7-12, an offset in final weight after major decomposition was noticed due to the additional weight of the catalyst. As with the glucose experiments, the final weight drops below 16.7% representing a loss of weight from the catalyst itself. As seen in Figure 7-13, although the temperature did not decrease, the catalyst addition slightly decreased the rate of weight loss suggesting that it contributed to the production of slightly fewer volatile compounds. In earlier tests with glucose, it was noted that the catalyst had a significant activity towards the dehydration of glucose which is considered a product of cellulose decomposition [7-9, 23]. Given that the decomposition of cellulose occurs at 340°C – nearly 50°C higher than glucose – it is suspected that with or without the catalyst, once glucose is produced it will readily undergo dehydration. It is not surprising that the catalysts do not have a significant impact on the initial breakdown of cellulose because it has a large polymeric structure, which prevents it from adsorbing onto the heterogenous catalyst surface.

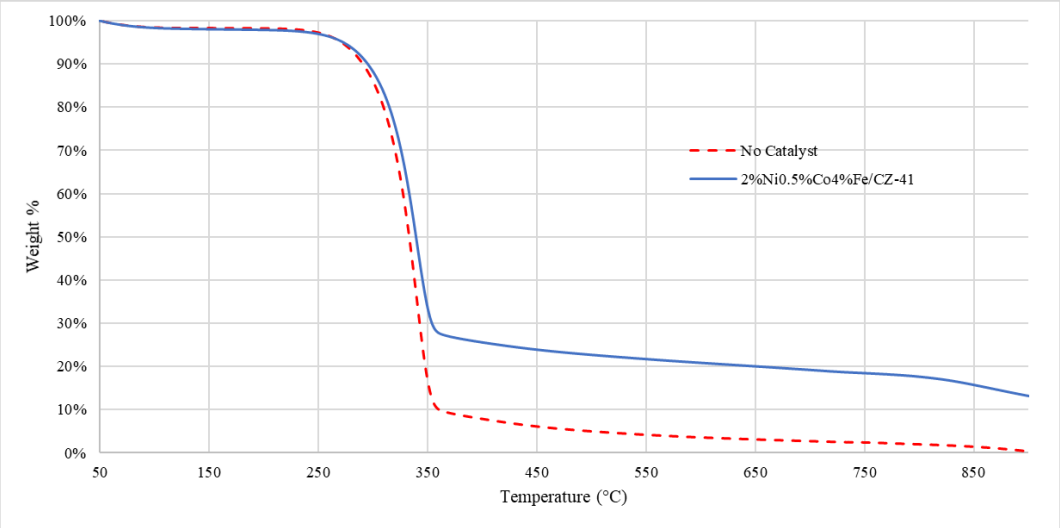

Figure 7-12: TGA results of cellulose with the addition of 2%Ni0.5%Co4%Fe/CZ-41 catalysts at a 5:1 cellulose-to-catalyst ratio

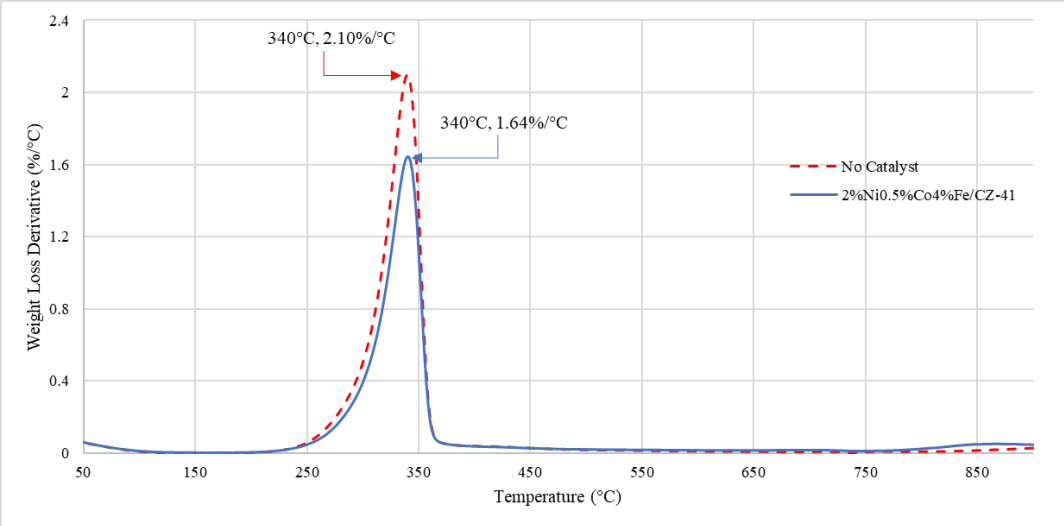

Figure 7-13: DTA (weight loss derivative from TGA) results of cellulose with the addition of 2%Ni0.5%Co4%Fe/CZ-41 catalysts at a 5:1 cellulose-to-catalyst ratio

7.4 Discussion

Upon considering the process of *in-situ* deoxygenation using internally produced hydrogen; reactor design requires attention. Activity tests were performed in batch

operation, over long periods of time. During these tests with glucose it was found that 350°C was a suitable reaction temperature. At this condition, the highest liquid product yield was achieved with a modest deoxygenation of furanic compounds. Reforming was not significant even when extending the reaction time. This selection of temperature was further substantiated by TGA tests using cellulose which, decomposed most rapidly at 340°C. Overall, *in-situ* deoxygenation is very dependent on the internal hydrogen production which needs to be improved. Potential solutions include using a more appropriate reactor design and/or eliminating the use of the solvent.

The solvent, 1MN was added primarily for heat transfer purposes. The intent is for the solvent to prevent biomass material from immediately sintering to the wall of the reactor. Using 1MN as a solvent is a hindrance towards WGSR as it presents a mass transfer barrier. In previous work with guaiacol, it was demonstrated that WGSR can still occur when using the solvent, however, a decrease in H_2 production is expected. With or without a solvent, ensuring adequate contact between gaseous products and the heterogeneous catalysts needs to be a priority.

Therefore, an ideal reactor type that could be used is a flow reactor where both biomass and the catalyst are fluidized. Such a reactor could be more appropriate for controlling the temperature. For example, the reactor could start with a cold initial section for primary decomposition stage and transition to a hotter section for internal hydrogen production and deoxygenation. This may also allow for better gas/vapour contact with the catalyst and prevent tar formation/oligomerization by reducing exposure time for intermediates.

Without a solvent, high temperature tests can also be performed without concern of solvent reactions and the reactor does not need to be pressurized with an inert gas to prevent solvent evaporation. Testing high temperatures may be crucial as real biomass consists of hemicellulose and lignin, with the latter tending to have a higher decomposition temperature than cellulose [4]. In summary, the proposed reaction system for future work resembles a low temperature pyrolysis unit where biomass and a bifunctional catalyst are fluidized for internal hydrogen production and deoxygenation.

7.5 Conclusions

Glucose was decomposed in the presence of CZ-41, ceria-zirconia catalysts for the purpose of internal hydrogen production and deoxygenation. Of the two supported catalysts that were used, the trimetallic catalyst, 2%Ni0.5%Co4%Fe/CZ-41 was found to be superior as it yielded more liquid product and comparable furanic product distribution as 2%Ni4%Fe/CZ-41. The addition of 0.5wt% Co to the Fe phase makes the Fe more reducible due to stronger interactions with the support, potentially leading to better oxygen transfer/storage capabilities. Of the conditions that were tested, a reaction temperature of 350°C and reaction time of 1 hr were most suitable for producing a high yield of liquid product.

Chapter 8: Conclusions and Recommendations

The production of bio-oils/biofuels from thermal processes such as pyrolysis is not without problems. Crude bio-oil which has a high oxygen content must undergo upgrading process – deoxygenation which is problematic as this requires hydrogen gas. In this project, different methods for reducing overall hydrogen requirements were evaluated. In an extensive literature review, it was highlighted that selective deoxygenation can be performed with bimetallic catalysts thus reducing the amount of hydrogen required to remove hydrogen.

The major focus of this project was to develop catalysts and establish a process by which deoxygenation occurs during biomass decomposition using internally produced hydrogen, thereby reducing oxygen content before the bio-oil reaches the major upgrading stage. Glucose – a model compound for cellulose/biomass – was decomposed with and without catalysts initially in the presence of very low hydrogen atmosphere. Here monometallic and bimetallic catalysts (supported on silica) were tested for their ability to perform *in-situ* deoxygenation. The catalysts were also studied for their impact on glucose decomposition. Furanic compounds were used as indicators of *in-situ* deoxygenation activity.

Of the monometallic catalysts, 4%Co/SiO_2 was found to be the most selective towards the *in-situ* deoxygenation of furanic compounds. Ni catalysts were beneficial for reducing solid residue as they promote tar cracking more than other catalysts. Interestingly though, 0.5%Ni/SiO_2 outperformed 4%Ni/SiO_2 because of a higher Ni particle dispersion. For bimetallic catalysts, the superior catalysts were surprisingly found to be 0.5%Ni4%Fe/SiO_2

and 0.5%Co4%Fe/SiO_2. The preferential preparation method for the NiFe catalyst was sequential addition of the two metals with Fe first as the two metals need to perform separate roles. This catalyst was competitive towards selectively deoxygenating furanic compounds *in-situ* and due to the exposed Ni phase, it was also beneficial for reducing solid residue. For the CoFe catalyst, co-addition is beneficial as alloying the two metals together where the Co can help stabilize Fe by making it more reducible. This catalyst was also competitive towards *in-situ* deoxygenation and helped produce additional H_2.

To develop and demonstrate catalysts that can perform both WGSR and deoxygenation, guaiacol was deoxygenated using NiFe/CeO_2-ZrO_2 catalysts in an atmosphere consisting of CO and H_2O. The catalysts produced their own hydrogen internally via WGSR and used it to convert guaiacol into products such as phenol. Ceria-zirconia prepared via the nano-casting on MCM-41 was beneficial as the resulting ceria-zirconia support, CZ-41 had a high surface area which allowed for the highest activity. Adding 0.5wt% Co to the Fe phase of 2%Ni4%Fe/CZ-41 catalyst proved to be beneficial for guaiacol conversion and internal hydrogen production. Achieving bifunctionality with these catalysts eliminates mass transfer and adsorption/desorption steps that would otherwise be present if using separate WGSR and deoxygenation catalysts.

It was highly recommended that future work focuses on using the 2%Ni4%Fe/CZ-41 and 2%Ni0.5%Co4%Fe/CZ-41 catalysts as dedicated WGSR catalysts, potentially replacing traditional iron-oxide catalysts. In addition, avenue for research is available for the HDO process. Typical HDO processes require the production of pure H_2 gas through either a

steam reforming or gasification process followed by WGSR and separation processes. With a bifunctional catalyst such as 2%Ni0.5%Co4%Fe/CZ-41, the product gas from the steam reforming/gasification process could be sent directly to the HDO process, bypassing the WGSR and separation.

The 2%Ni4%Fe/CZ-41 and 2%Ni0.5%Co4%Fe/CZ-41 catalysts were then used for glucose decomposition with internal hydrogen production and deoxygenation within an inert atmosphere. Although both catalysts had comparable results in term of *in-situ* deoxygenation selectivity and internal hydrogen production, the NiCoFe/CZ-41 catalyst was most favourable as it achieved higher liquid product yields and less solid residue. Overall, the trimetallic catalyst had the largest impact on glucose decomposition. The addition of Co to the Fe phase made the overall catalyst more reducible due to its enhanced ability to transfer oxygen to and from the support. The most appropriate temperature for the reaction was determined as 350°C for 1-hour.

All reactions performed in this study used 1-methylnaphthlane as a solvent to aid heat transfer and to prevent the sintering of glucose to the reactor walls. It is recognized that the reactor used in this study along with the solvent may not be ideal. A flow reactor, mixing biomass solids and catalysts is appropriate because it would be most beneficial for a continuous process all while enabling better control of temperature gas-solid contact. For this, fluidized bed reactor (FBR) technologies such as an ebullated/slug-flow reactor and a fluidized catalytic cracking (FCC) reactor should receive attention.

In this study, it was determined that the most appropriate catalyst for performing *in-situ* deoxygenation and internal hydrogen production is NiCoFe/CZ-41. With the development of a new reaction process such as the previously suggested fluidized reactor, catalyst development will need to continue. In an ebullated reactor, since both organic solid residue and solid catalyst will be present; catalysts should be developed in such a way that they are either separated from the organic material. Options for doing this include using catalysts with significantly different particle sizes and densities to the biomass material and/or developing catalysts that have magnetic properties. In an FCC-like reactor design, catalyst separation and coking may become a significant problem requiring an oxidation process to remove all solid residue and coke. For this process, a catalyst such as NiCoFe/CZ-41 would be inappropriate. Therefore, the development of mixed-oxide or zeolite catalysts would be required.

Upon development of an appropriate reaction system, future work should also study the use of higher temperatures (>350°C) which was hindered by the solvent which begins to react/degrade at elevated temperatures. Based on work by the Harris group, [24-27, 31], it is likely that reforming reactions will become prevalent at higher reaction temperatures leading to increased H_2 generation. It is suspected that this may reduce the yield of liquid products which is the desired product fraction. However, there may be an optimal temperature at which reforming of very light compounds may occur without having a significant impact on desired liquid products. This opens the door for additional catalyst development and optimization. In general, improving internal hydrogen production is very important as hydrogen availability is the limiting factor for *in-situ* deoxygenation.

Future work involving catalysts and reactor design, should focus on the use of real biomass materials such as wood. Due to the large sizes of the polymers in lignocellulosic biomass material, multifunctional heterogeneous catalysts are not expected to have a large impact on initial depolymerization reactions but will have a large impact on the intermediate products due to dehydration reactions. Char/tar/coke formation will be a larger concern for reactor design. For example, a slurry reactor could be used with appropriate dispersion of solid phase (high fluid-to-solid ratio, small solid particle size) and uniform heat distribution to prevent material from sintering to reactor walls.

Bibliography

[1] G. Anitescu, T.J. Bruno, Liquid biofuels: Fluid properties to optimize feedstock selection, processing, refining/blending, storage/transportation, and combustion, Energy and Fuels, 26 (2012) 324-348.

[2] M. Balat, H. Balat, A critical review of bio-diesel as a vehicular fuel, Energy Conversion and Management, 49 (2008) 2727-2741.

[3] R.W. Gosselink, S.A.W. Hollak, S.W. Chang, J. Van Haveren, K.P. De Jong, J.H. Bitter, D.S. Van Es, Reaction pathways for the deoxygenation of vegetable oils and related model compounds, ChemSusChem, 6 (2013) 1576-1594.

[4] F.X. Collard, J. Blin, A review on pyrolysis of biomass constituents: Mechanisms and composition of the products obtained from the conversion of cellulose, hemicelluloses and lignin, Renewable and Sustainable Energy Reviews, 38 (2014) 594-608.

[5] M.N. Uddin, W.M.A.W. Daud, H.F. Abbas, Effects of pyrolysis parameters on hydrogen formations from biomass: A review, RSC Advances, 4 (2014) 10467-10490.

[6] M.S. Mettler, S.H. Mushrif, A.D. Paulsen, A.D. Javadekar, D.G. Vlachos, P.J. Dauenhauer, Revealing pyrolysis chemistry for biofuels production: Conversion of cellulose to furans and small oxygenates, Energy and Environmental Science, 5 (2012) 5414-5424.

[7] P.R. Patwardhan, D.L. Dalluge, B.H. Shanks, R.C. Brown, Distinguishing primary and secondary reactions of cellulose pyrolysis, Bioresource Technology, 102 (2011) 5265-5269.

[8] D.K. Shen, S. Gu, The mechanism for thermal decomposition of cellulose and its main products, Bioresource Technology, 100 (2009) 6496-6504.

[9] R. Vinu, L.J. Broadbelt, A mechanistic model of fast pyrolysis of glucose-based carbohydrates to predict bio-oil composition, Energy and Environmental Science, 5 (2012) 9808-9826.

[10] S. Czernik, A.V. Bridgwater, Overview of applications of biomass fast pyrolysis oil, Energy and Fuels, 18 (2004) 590-598.

[11] D.C. Elliott, Historical developments in hydroprocessing bio-oils, Energy and Fuels, 21 (2007) 1792-1815.

[12] S. Lestari, P. Mäki-Arvela, J. Beltramini, G.M. Lu, D.Y. Murzin, Transforming triglycerides and fatty acids into biofuels, ChemSusChem, 2 (2009) 1109-1119.

[13] J. Fu, X. Lu, P.E. Savage, Hydrothermal decarboxylation and hydrogenation of fatty acids over Pt/C, ChemSusChem, 4 (2011) 481-486.

[14] E. Santillan-Jimenez, M. Crocker, Catalytic deoxygenation of fatty acids and their derivatives to hydrocarbon fuels via decarboxylation/decarbonylation, Journal of Chemical Technology and Biotechnology, 87 (2012) 1041-1050.

[15] S.K. Tanneru, P.H. Steele, Production of liquid hydrocarbons from pretreated bio-oil via catalytic deoxygenation with syngas, Renewable Energy, 80 (2015) 251-258.

[16] Q. Bu, H. Lei, A.H. Zacher, L. Wang, S. Ren, J. Liang, Y. Wei, Y. Liu, J. Tang, Q. Zhang, R. Ruan, A review of catalytic hydrodeoxygenation of lignin-derived phenols from biomass pyrolysis, Bioresource Technology, 124 (2012) 470-477.
[17] S. De, B. Saha, R. Luque, Hydrodeoxygenation processes: Advances on catalytic transformations of biomass-derived platform chemicals into hydrocarbon fuels, Bioresource Technology, 178 (2015) 108-118.
[18] V. Seshadri, P.R. Westmoreland, Concerted reactions and mechanism of glucose pyrolysis and implications for cellulose kinetics, Journal of Physical Chemistry A, 116 (2012) 11997-12013.
[19] A. Sanna, Advanced Biofuels from Thermochemical Processing of Sustainable Biomass in Europe, Bioenergy Research, 7 (2014) 36-47.
[20] S. Wang, B. Ru, H. Lin, Z. Luo, Degradation mechanism of monosaccharides and xylan under pyrolytic conditions with theoretic modeling on the energy profiles, Bioresource Technology, 143 (2013) 378-383.
[21] R.J. Evans, T.A. Milne, Molecular characterization of the pyrolysis of biomass. 1. Fundamentals, Energy & Fuels, 1 (1987) 123-137.
[22] C.E. Brewer, K. Schmidt-Rohr, J.A. Satrio, R.C. Brown, Characterization of biochar from fast pyrolysis and gasification systems, Environmental Progress & Sustainable Energy, 28 (2009) 386-396.
[23] H.B. Mayes, M.W. Nolte, G.T. Beckham, B.H. Shanks, L.J. Broadbelt, The alpha-bet(a) of glucose pyrolysis: Computational and experimental investigations of 5-hydroxymethylfurfural and levoglucosan formation reveal implications for cellulose pyrolysis, ACS Sustainable Chemistry and Engineering, 2 (2014) 1461-1473.
[24] R.N. Widyaningrum, T.L. Church, A.T. Harris, Promoting effect of Pd on H_2 production from cellulose pyrolysis over mesocellular-foam-supported Ni catalysts, Catalysis Communications, 35 (2013) 45-50.
[25] R.N. Widyaningrum, T.L. Church, M. Zhao, A.T. Harris, Mesocellular-foam-silica-supported Ni catalyst: Effect of pore size on H_2 production from cellulose pyrolysis, International Journal of Hydrogen Energy, 37 (2012) 9590-9601.
[26] M. Zhao, N.H. Florin, A.T. Harris, The influence of supported Ni catalysts on the product gas distribution and H2 yield during cellulose pyrolysis, Applied Catalysis B: Environmental, 92 (2009) 185-193.
[27] M. Zhao, N.H. Florin, A.T. Harris, Mesoporous supported cobalt catalysts for enhanced hydrogen production during cellulose decomposition, Applied Catalysis B: Environmental, 97 (2010) 142-150.
[28] N.H. Florin, A.T. Harris, Hydrogen production from biomass coupled with carbon dioxide capture: The implications of thermodynamic equilibrium, International Journal of Hydrogen Energy, 32 (2007) 4119-4134.
[29] M. Widyawati, T.L. Church, N.H. Florin, A.T. Harris, Hydrogen synthesis from biomass pyrolysis with in situ carbon dioxide capture using calcium oxide, International Journal of Hydrogen Energy, 36 (2011) 4800-4813.
[30] N.J. Amos, M. Widyawati, S. Kureti, D. Trimis, A.I. Minett, A.T. Harris, T.L. Church, Design and synthesis of stable supported-CaO sorbents for CO2 capture, Journal of Materials Chemistry A, 2 (2014) 4332-4339.

[31] M. Zhao, T.L. Church, A.T. Harris, SBA-15 supported Ni-Co bimetallic catalysts for enhanced hydrogen production during cellulose decomposition, Applied Catalysis B: Environmental, 101 (2011) 522-530.
[32] A.M. Ruppert, M. Niewiadomski, J. Grams, W. Kwapiński, Optimization of Ni/ZrO2 catalytic performance in thermochemical cellulose conversion for enhanced hydrogen production, Applied Catalysis B: Environmental, 145 (2014) 85-90.
[33] J. Grams, N. Potrzebowska, J. Goscianska, B. Michalkiewicz, A.M. Ruppert, Mesoporous silicas as supports for Ni catalyst used in cellulose conversion to hydrogen rich gas, International Journal of Hydrogen Energy, 41 (2016) 8656-8667.
[34] C. Ratnasamy, J.P. Wagner, Water gas shift catalysis, Catalysis Reviews, 51 (2009) 325-440.
[35] C.V. Ovesen, B.S. Clausen, B.S. Hammershøi, G. Steffensen, T. Askgaard, I. Chorkendorff, J.K. Nørskov, P.B. Rasmussen, P. Stoltze, P. Taylor, A Microkinetic Analysis of the Water–Gas Shift Reaction under Industrial Conditions, Journal of Catalysis, 158 (1996) 170-180.
[36] C.V. Ovesen, P. Stoltze, J.K. Nørskov, C.T. Campbell, A kinetic model of the water gas shift reaction, Journal of Catalysis, 134 (1992) 445-468.
[37] X. Wang, R.J. Gorte, The effect of Fe and other promoters on the activity of Pd/ceria for the water-gas shift reaction, Applied Catalysis A: General, 247 (2003) 157-162.
[38] M. Boaro, M. Vicario, J. Llorca, C. de Leitenburg, G. Dolcetti, A. Trovarelli, A comparative study of water gas shift reaction over gold and platinum supported on ZrO2 and CeO2-ZrO2, Applied Catalysis B: Environmental, 88 (2009) 272-282.
[39] B. Chamnankid, K. Föttinger, G. Rupprechter, P. Kongkachuichay, Cu/Ni-loaded CeO2-ZrO2 Catalyst for the water-gas shift reaction: Effects of loaded metals and CeO2 addition, Chemical Engineering and Technology, 37 (2014) 2129-2134.
[40] T. Wang, M.D. Porosoff, J.G. Chen, Effects of oxide supports on the water-gas shift reaction over PtNi bimetallic catalysts: Activity and methanation inhibition, Catalysis Today, 233 (2014) 61-69.
[41] K. Watanabe, T. Miyao, K. Higashiyama, H. Yamashita, M. Watanabe, Preparation of a mesoporous ceria-zirconia supported Ni-Fe catalyst for the high temperature water-gas shift reaction, Catalysis Communications, 12 (2011) 976-979.
[42] P. Tepamatr, N. Laosiripojana, S. Charojrochkul, Water gas shift reaction over monometallic and bimetallic catalysts supported by mixed oxide materials, Applied Catalysis A: General, 523 (2016) 255-262.
[43] P.R. Patwardhan, J.A. Satrio, R.C. Brown, B.H. Shanks, Influence of inorganic salts on the primary pyrolysis products of cellulose, Bioresource Technology, 101 (2010) 4646-4655.
[44] W.S. Carvalho, I.F. Cunha, M.S. Pereira, C.H. Ataíde, Thermal decomposition profile and product selectivity of analytical pyrolysis of sweet sorghum bagasse: Effect of addition of inorganic salts, Industrial Crops and Products, 74 (2015) 372-380.
[45] F.X. Collard, J. Blin, A. Bensakhria, J. Valette, Influence of impregnated metal on the pyrolysis conversion of biomass constituents, Journal of Analytical and Applied Pyrolysis, 95 (2012) 213-226.

[46] D. Liu, Y. Yu, J.I. Hayashi, B. Moghtaderi, H. Wu, Contribution of dehydration and depolymerization reactions during the fast pyrolysis of various salt-loaded celluloses at low temperatures, Fuel, 136 (2014) 62-68.
[47] Q. Lu, Z. Wang, C.Q. Dong, Z.F. Zhang, Y. Zhang, Y.P. Yang, X.F. Zhu, Selective fast pyrolysis of biomass impregnated with ZnCl2: Furfural production together with acetic acid and activated carbon as by-products, Journal of Analytical and Applied Pyrolysis, 91 (2011) 273-279.
[48] H.B. Mayes, M.W. Nolte, G.T. Beckham, B.H. Shanks, L.J. Broadbelt, The Alpha-Bet(a) of Salty Glucose Pyrolysis: Computational Investigations Reveal Carbohydrate Pyrolysis Catalytic Action by Sodium Ions, ACS Catalysis, 5 (2015) 192-202.
[49] M. Zabeti, T.S. Nguyen, L. Lefferts, H.J. Heeres, K. Seshan, In situ catalytic pyrolysis of lignocellulose using alkali-modified amorphous silica alumina, Bioresource Technology, 118 (2012) 374-381.
[50] M.J. Jeon, J.K. Jeon, D.J. Suh, S.H. Park, Y.J. Sa, S.H. Joo, Y.K. Park, Catalytic pyrolysis of biomass components over mesoporous catalysts using Py-GC/MS, Catalysis Today, 204 (2013) 170-178.
[51] T. Kan, V. Strezov, T. Evans, Catalytic pyrolysis of coffee grounds using NiCu-impregnated catalysts, Energy and Fuels, 28 (2014) 228-235.
[52] S. Sorrell, J. Speirs, R. Bentley, A. Brandt, R. Miller, Global oil depletion: A review of the evidence, Energy Policy, 38 (2010) 5290-5295.
[53] A. Demirbas, Biorefineries: Current activities and future developments, Energy Conversion and Management, 50 (2009) 2782-2801.
[54] R.J. French, J. Stunkel, S. Black, M. Myers, M.M. Yung, K. Iisa, Evaluate impact of catalyst type on oil yield and hydrogen consumption from mild hydrotreating, Energy and Fuels, 28 (2014) 3086-3095.
[55] P.M. Mortensen, J.D. Grunwaldt, P.A. Jensen, K.G. Knudsen, A.D. Jensen, A review of catalytic upgrading of bio-oil to engine fuels, Applied Catalysis A: General, 407 (2011) 1-19.
[56] Y. Nakagawa, M. Tamura, K. Tomishige, Catalytic reduction of biomass-derived furanic compounds with hydrogen, ACS Catalysis, 3 (2013) 2655-2668.
[57] M. Snåre, I. Kubičková, P. Mäki-Arvela, K. Eränen, D.Y. Murzin, Heterogeneous catalytic deoxygenation of stearic acid for production of biodiesel, Industrial and Engineering Chemistry Research, 45 (2006) 5708-5715.
[58] M.A. Alotaibi, E.F. Kozhevnikova, I.V. Kozhevnikov, Deoxygenation of propionic acid on heteropoly acid and bifunctional metal-loaded heteropoly acid catalysts: Reaction pathways and turnover rates, Applied Catalysis A: General, 447-448 (2012) 32-40.
[59] H. Bernas, K. Eränen, I. Simakova, A.R. Leino, K. Kordás, J. Myllyoja, P. Mäki-Arvela, T. Salmi, D.Y. Murzin, Deoxygenation of dodecanoic acid under inert atmosphere, Fuel, 89 (2010) 2033-2039.
[60] K. Hengst, M. Arend, R. Pfützenreuter, W.F. Hoelderich, Deoxygenation and cracking of free fatty acids over acidic catalysts by single step conversion for the production of diesel fuel and fuel blends, Applied Catalysis B: Environmental, 174-175 (2015) 383-394.

[61] K.C. Kwon, H. Mayfield, T. Marolla, B. Nichols, M. Mashburn, Catalytic deoxygenation of liquid biomass for hydrocarbon fuels, Renewable Energy, 36 (2011) 907-915.
[62] J. Lu, S. Behtash, M. Faheem, A. Heyden, Microkinetic modeling of the decarboxylation and decarbonylation of propanoic acid over Pd(1 1 1) model surfaces based on parameters obtained from first principles, Journal of Catalysis, 305 (2013) 56-66.
[63] A.T. Madsen, E.H. Ahmed, C.H. Christensen, R. Fehrmann, A. Riisager, Hydrodeoxygenation of waste fat for diesel production: Study on model feed with Pt/alumina catalyst, Fuel, 90 (2011) 3433-3438.
[64] E. Meller, U. Green, Z. Aizenshtat, Y. Sasson, Catalytic deoxygenation of castor oil over Pd/C for the production of cost effective biofuel, Fuel, 133 (2014) 89-95.
[65] C. Ochoa-Hernández, Y. Yang, P. Pizarro, V.A. De La Peña O'Shea, J.M. Coronado, D.P. Serrano, Hydrocarbons production through hydrotreating of methyl esters over Ni and Co supported on SBA-15 and Al-SBA-15, Catalysis Today, 210 (2013) 81-88.
[66] B. Peng, C. Zhao, S. Kasakov, S. Foraita, J.A. Lercher, Manipulating catalytic pathways: Deoxygenation of palmitic acid on multifunctional catalysts, Chemistry - A European Journal, 19 (2013) 4732-4741.
[67] B. Rozmyslowicz, P. Mäki-Arvela, A. Tokarev, A.R. Leino, K. Eränen, D.Y. Murzin, Influence of hydrogen in catalytic deoxygenation of fatty acids and their derivatives over Pd/C, Industrial and Engineering Chemistry Research, 51 (2012) 8922-8927.
[68] M. Ruinart De Brimont, C. Dupont, A. Daudin, C. Geantet, P. Raybaud, Deoxygenation mechanisms on Ni-promoted MoS 2 bulk catalysts: A combined experimental and theoretical study, Journal of Catalysis, 286 (2012) 153-164.
[69] J.O. Shim, D.W. Jeong, W.J. Jang, K.W. Jeon, B.H. Jeon, S.Y. Cho, H.S. Roh, J.G. Na, C.H. Ko, Y.K. Oh, S.S. Han, Deoxygenation of oleic acid over Ce(1-x)Zr(x)O2 catalysts in hydrogen environment, Renewable Energy, 65 (2014) 36-40.
[70] E. Vonghia, D.G.B. Boocock, S.K. Konar, A. Leung, Pathways for the deoxygenation of triglycerides to aliphatic hydrocarbons over activated alumina, Energy and Fuels, 9 (1995) 1090-1096.
[71] C. Zhang, P.P. Sun, W.D. Zhang, Y.B. Chen, F. Yin, L. Xu, X.L. Zhao, J. Liu, S.Q. Liu, Effect of hydrogen partial pressure on hydrocarbon production from deoxygenation of stearic acid, Advanced Materials Research, 2013, pp. 165-169.
[72] H. Zhang, H. Lin, W. Wang, Y. Zheng, P. Hu, Hydroprocessing of waste cooking oil over a dispersed nano catalyst: Kinetics study and temperature effect, Applied Catalysis B: Environmental, 150-151 (2014) 238-248.
[73] H. Zhang, H. Lin, Y. Zheng, The role of cobalt and nickel in deoxygenation of vegetable oils, Applied Catalysis B: Environmental, 160-161 (2014) 415-422.
[74] A.S. Berenblyum, T.A. Podoplelova, R.S. Shamsiev, E.A. Katsman, V.Y. Danyushevsky, On the mechanism of catalytic conversion of fatty acids into hydrocarbons in the presence of palladium catalysts on alumina, Petroleum Chemistry, 51 (2011) 336-341.
[75] D. Kubička, L. Kaluža, Deoxygenation of vegetable oils over sulfided Ni, Mo and NiMo catalysts, Applied Catalysis A: General, 372 (2010) 199-208.

[76] D. Kubička, P. Šimáček, N. Žilkova, Transformation of vegetable oils into hydrocarbons over mesoporous-alumina-supported CoMo catalysts, Topics in Catalysis, 52 (2009) 161-168.
[77] T. Morgan, D. Grubb, E. Santillan-Jimenez, M. Crocker, Conversion of triglycerides to hydrocarbons over supported metal catalysts, Topics in Catalysis, 53 (2010) 820-829.
[78] A.S. Berenblyum, V.Y. Danyushevsky, E.A. Katsman, T.A. Podoplelova, V.R. Flid, Production of engine fuels from inedible vegetable oils and fats, Petroleum Chemistry, 50 (2010) 305-311.
[79] L. Boda, G. Onyestyák, H. Solt, F. Lónyi, J. Valyon, A. Thernesz, Catalytic hydroconversion of tricaprylin and caprylic acid as model reaction for biofuel production from triglycerides, Applied Catalysis A: General, 374 (2010) 158-169.
[80] S.W. Hu, X.Y. Wang, T.W. Chu, X.Q. Liu, Influence of H2 on the gas-phase decomposition of formic acid: A theoretical study, Journal of Physical Chemistry A, 109 (2005) 9129-9140.
[81] R. Sotelo-Boyás, Y. Liu, T. Minowa, Renewable diesel production from the hydrotreating of rapeseed oil with Pt/zeolite and NiMo/Al2O3 catalysts, Industrial and Engineering Chemistry Research, 50 (2011) 2791-2799.
[82] Z.D. Yigezu, K. Muthukumar, Catalytic cracking of vegetable oil with metal oxides for biofuel production, Energy Conversion and Management, 84 (2014) 326-333.
[83] J. Asomaning, P. Mussone, D.C. Bressler, Thermal cracking of free fatty acids in inert and light hydrocarbon gas atmospheres, Fuel, 126 (2014) 250-255.
[84] G. Ramya, R. Sudhakar, J.A.I. Joice, R. Ramakrishnan, T. Sivakumar, Liquid hydrocarbon fuels from jatropha oil through catalytic cracking technology using AlMCM-41/ZSM-5 composite catalysts, Applied Catalysis A: General, 433-434 (2012) 170-178.
[85] N. Taufiqurrahmi, S. Bhatia, Catalytic cracking of edible and non-edible oils for the production of biofuels, Energy and Environmental Science, 4 (2011) 1087-1112.
[86] J. Fu, X. Lu, P.E. Savage, Catalytic hydrothermal deoxygenation of palmitic acid, Energy and Environmental Science, 3 (2010) 311-317.
[87] S.A.W. Hollak, M.A. Ariëns, K.P. De Jong, D.S. Van Es, Hydrothermal deoxygenation of triglycerides over Pd/C aided by in situ hydrogen production from glycerol reforming, ChemSusChem, 7 (2014) 1057-1062.
[88] O.I. Şenol, T.R. Viljava, A.O.I. Krause, Hydrodeoxygenation of methyl esters on sulphided NiMo/γ-Al 2O3 and CoMo/γ-Al2O3 catalysts, Catalysis Today, 100 (2005) 331-335.
[89] P. Šimáček, D. Kubička, G. Šebor, M. Pospíšil, Hydroprocessed rapeseed oil as a source of hydrocarbon-based biodiesel, Fuel, 88 (2009) 456-460.
[90] S. Kovács, T. Kasza, A. Thernesz, I.W. Horváth, J. Hancsók, Fuel production by hydrotreating of triglycerides on NiMo/Al2O3/F catalyst, Chemical Engineering Journal, 176-177 (2011) 237-243.
[91] S. Lestari, M.A. Päivi, H. Bernas, O. Simakova, R. Sjöholm, J. Beltramini, G.Q. Max Lu, J. Myllyoja, I. Simakova, D.Y. Murzin, Catalytic deoxygenation of stearic acid in a continuous reactor over a mesoporous carbon-supported pd catalyst, Energy and Fuels, 23 (2009) 3842-3845.

[92] Y. Liu, R. Sotelo-Boyás, K. Murata, T. Minowa, K. Sakanishi, Hydrotreatment of vegetable oils to produce bio-hydrogenated diesel and liquefied petroleum gas fuel over catalysts containing sulfided Ni-Mo and solid acids, Energy and Fuels, 25 (2011) 4675-4685.
[93] D. Kubička, J. Horáček, Deactivation of HDS catalysts in deoxygenation of vegetable oils, Applied Catalysis A: General, 394 (2011) 9-17.
[94] S. Gong, A. Shinozaki, M. Shi, E.W. Qian, Hydrotreating of jatropha oil over alumina based catalysts, Energy and Fuels, 26 (2012) 2394-2399.
[95] P. Mäki-Arvela, I. Kubickova, M. Snåre, K. Eränen, D.Y. Murzin, Catalytic deoxygenation of fatty acids and their derivatives, Energy and Fuels, 21 (2007) 30-41.
[96] M. Snåre, I. Kubičková, P. Mäki-Arvela, K. Eränen, J. Wärnå, D.Y. Murzin, Production of diesel fuel from renewable feeds: Kinetics of ethyl stearate decarboxylation, Chemical Engineering Journal, 134 (2007) 29-34.
[97] B. Peng, Y. Yao, C. Zhao, J.A. Lercher, Towards quantitative conversion of microalgae oil to diesel-range alkanes with bifunctional catalysts, Angewandte Chemie - International Edition, 51 (2012) 2072-2075.
[98] B. Peng, X. Yuan, C. Zhao, J.A. Lercher, Stabilizing catalytic pathways via redundancy: Selective reduction of microalgae oil to alkanes, Journal of the American Chemical Society, 134 (2012) 9400-9405.
[99] Q. Zhang, J. Chang, T. Wang, Y. Xu, Review of biomass pyrolysis oil properties and upgrading research, Energy Conversion and Management, 48 (2007) 87-92.
[100] T. Prasomsri, T. Nimmanwudipong, Y. Román-Leshkov, Effective hydrodeoxygenation of biomass-derived oxygenates into unsaturated hydrocarbons by MoO3 using low H2 pressures, Energy and Environmental Science, 6 (2013) 1732-1738.
[101] V.N. Bui, D. Laurenti, P. Afanasiev, C. Geantet, Hydrodeoxygenation of guaiacol with CoMo catalysts. Part I: Promoting effect of cobalt on HDO selectivity and activity, Applied Catalysis B: Environmental, 101 (2011) 239-245.
[102] V.N. Bui, D. Laurenti, P. Delichère, C. Geantet, Hydrodeoxygenation of guaiacol. Part II: Support effect for CoMoS catalysts on HDO activity and selectivity, Applied Catalysis B: Environmental, 101 (2011) 246-255.
[103] C. Sepúlveda, K. Leiva, R. García, L.R. Radovic, I.T. Ghampson, W.J. Desisto, J.L.G. Fierro, N. Escalona, Hydrodeoxygenation of 2-methoxyphenol over Mo2N catalysts supported on activated carbons, Catalysis Today, 172 (2011) 232-239.
[104] H.Y. Zhao, D. Li, P. Bui, S.T. Oyama, Hydrodeoxygenation of guaiacol as model compound for pyrolysis oil on transition metal phosphide hydroprocessing catalysts, Applied Catalysis A: General, 391 (2011) 305-310.
[105] L. Nie, P.M. De Souza, F.B. Noronha, W. An, T. Sooknoi, D.E. Resasco, Selective conversion of m-cresol to toluene over bimetallic Ni-Fe catalysts, Journal of Molecular Catalysis A: Chemical, 388-389 (2014) 47-55.
[106] J. Sun, A.M. Karim, H. Zhang, L. Kovarik, X.S. Li, A.J. Hensley, J.S. McEwen, Y. Wang, Carbon-supported bimetallic Pd-Fe catalysts for vapor-phase hydrodeoxygenation of guaiacol, Journal of Catalysis, 306 (2013) 47-57.

[107] J. Wildschut, F.H. Mahfud, R.H. Venderbosch, H.J. Heeres, Hydrotreatment of fast pyrolysis oil using heterogeneous noble-metal catalysts, Industrial and Engineering Chemistry Research, 48 (2009) 10324-10334.
[108] E. Furimsky, Catalytic hydrodeoxygenation, Applied Catalysis A: General, 199 (2000) 147-190.
[109] W. Li, C. Pan, Q. Zhang, Z. Liu, J. Peng, P. Chen, H. Lou, X. Zheng, Upgrading of low-boiling fraction of bio-oil in supercritical methanol and reaction network, Bioresource Technology, 102 (2011) 4884-4889.
[110] R.C. Runnebaum, T. Nimmanwudipong, D.E. Block, B.C. Gates, Catalytic conversion of compounds representative of lignin-derived bio-oils: A reaction network for guaiacol, anisole, 4-methylanisole, and cyclohexanone conversion catalysed by Pt/γ-Al 2O 3, Catalysis Science and Technology, 2 (2012) 113-118.
[111] E.O. Odebunmi, D.F. Ollis, Catalytic hydrodeoxygenation. II. Interactions between catalytic hydrodeoxygenation of m-cresol and hydrodesulfurization of benzothiophene and dibenzothiophene, Journal of Catalysis, 80 (1983) 65-75.
[112] Y.C. Lin, C.L. Li, H.P. Wan, H.T. Lee, C.F. Liu, Catalytic hydrodeoxygenation of guaiacol on Rh-based and sulfided CoMo and NiMo catalysts, Energy and Fuels, 25 (2011) 890-896.
[113] T.R. Viljava, R.S. Komulainen, A.O.I. Krause, Effect of H2S on the stability of CoMo/Al2O3 catalysts during hydrodeoxygenation, Catalysis Today, 60 (2000) 83-92.
[114] Y. Wang, H. Lin, Y. Zheng, Hydrotreatment of lignocellulosic biomass derived oil using a sulfided NiMo/γ-Al2O3 catalyst, Catalysis Science and Technology, 4 (2014) 109-119.
[115] H. Wang, J. Male, Y. Wang, Recent advances in hydrotreating of pyrolysis bio-oil and its oxygen-containing model compounds, ACS Catalysis, 3 (2013) 1047-1070.
[116] M. Badawi, J.F. Paul, S. Cristol, E. Payen, Y. Romero, F. Richard, S. Brunet, D. Lambert, X. Portier, A. Popov, E. Kondratieva, J.M. Goupil, J. El Fallah, J.P. Gilson, L. Mariey, A. Travert, F. Maugé, Effect of water on the stability of Mo and CoMo hydrodeoxygenation catalysts: A combined experimental and DFT study, Journal of Catalysis, 282 (2011) 155-164.
[117] E. Laurent, B. Delmon, Influence of water in the deactivation of a sulfided NiMo γ-Al2O3 catalyst during hydrodeoxygenation, Journal of Catalysis, 146 (1994) 281-285,288-291.
[118] D.R. Moberg, T.J. Thibodeau, F.G. Amar, B.G. Frederick, Mechanism of hydrodeoxygenation of acrolein on a cluster model of MoO 3, Journal of Physical Chemistry C, 114 (2010) 13782-13795.
[119] V.M.L. Whiffen, K.J. Smith, Hydrodeoxygenation of 4-methylphenol over unsupported MoP, MoS2, and MoOx catalysts, Energy and Fuels, 24 (2010) 4728-4737.
[120] J.A. Cecilia, A. Infantes-Molina, E. Rodríguez-Castellón, A. Jiménez-López, S.T. Oyama, Oxygen-removal of dibenzofuran as a model compound in biomass derived bio-oil on nickel phosphide catalysts: Role of phosphorus, Applied Catalysis B: Environmental, 136-137 (2013) 140-149.

[121] E. Santillan-Jimenez, M. Perdu, R. Pace, T. Morgan, M. Crocker, Activated carbon, carbon nanofiber and carbon nanotube supported molybdenum carbide catalysts for the hydrodeoxygenation of guaiacol, Catalysts, 5 (2015) 424-441.
[122] A.L. Jongerius, R.W. Gosselink, J. Dijkstra, J.H. Bitter, P.C.A. Bruijnincx, B.M. Weckhuysen, Carbon nanofiber supported transition-metal carbide catalysts for the hydrodeoxygenation of guaiacol, ChemCatChem, 5 (2013) 2964-2972.
[123] S. Boullosa-Eiras, R. Lødeng, H. Bergem, M. Stöcker, L. Hannevold, E.A. Blekkan, Catalytic hydrodeoxygenation (HDO) of phenol over supported molybdenum carbide, nitride, phosphide and oxide catalysts, Catalysis Today, 223 (2014) 44-53.
[124] R. Ma, K. Cui, L. Yang, X. Ma, Y. Li, Selective catalytic conversion of guaiacol to phenols over a molybdenum carbide catalyst, Chemical Communications, 51 (2015) 10299-10301.
[125] L. Nie, D.E. Resasco, Kinetics and mechanism of m-cresol hydrodeoxygenation on a Pt/SiO 2 catalyst, Journal of Catalysis, 317 (2014) 22-29.
[126] T.M. Sankaranarayanan, A. Berenguer, C. Ochoa-Hernández, I. Moreno, P. Jana, J.M. Coronado, D.P. Serrano, P. Pizarro, Hydrodeoxygenation of anisole as bio-oil model compound over supported Ni and Co catalysts: Effect of metal and support properties, Catalysis Today, 243 (2015) 163-172.
[127] D.M. Alonso, S.G. Wettstein, J.A. Dumesic, Bimetallic catalysts for upgrading of biomass to fuels and chemicals, Chemical Society Reviews, 41 (2012) 8075-8098.
[128] P.T.M. Do, A.J. Foster, J. Chen, R.F. Lobo, Bimetallic effects in the hydrodeoxygenation of meta-cresol on γ-Al2O3 supported Pt-Ni and Pt-Co catalysts, Green Chemistry, 14 (2012) 1388-1397.
[129] M.A. González-Borja, D.E. Resasco, Anisole and guaiacol hydrodeoxygenation over monolithic Pt-Sn catalysts, Energy and Fuels, 25 (2011) 4155-4162.
[130] A.J.R. Hensley, Y. Wang, J.S. McEwen, Phenol deoxygenation mechanisms on Fe(110) and Pd(111), ACS Catalysis, 5 (2015) 523-536.
[131] Y. Hong, H. Zhang, J. Sun, K.M. Ayman, A.J.R. Hensley, M. Gu, M.H. Engelhard, J.S. McEwen, Y. Wang, Synergistic catalysis between Pd and Fe in gas phase hydrodeoxygenation of m -cresol, ACS Catalysis, 4 (2014) 3335-3345.
[132] T.M. Huynh, U. Armbruster, M.M. Pohl, M. Schneider, J. Radnik, D.L. Hoang, B.M.Q. Phan, D.A. Nguyen, A. Martin, Hydrodeoxygenation of phenol as a model compound for bio-oil on non-noble bimetallic nickel-based catalysts, ChemCatChem, 6 (2014) 1940-1951.
[133] S.A. Khromova, A.A. Smirnov, O.A. Bulavchenko, A.A. Saraev, V.V. Kaichev, S.I. Reshetnikov, V.A. Yakovlev, Anisole hydrodeoxygenation over Ni-Cu bimetallic catalysts: The effect of Ni/Cu ratio on selectivity, Applied Catalysis A: General, 470 (2014) 261-270.
[134] X. Zhang, T. Wang, L. Ma, Q. Zhang, Y. Yu, Q. Liu, Characterization and catalytic properties of Ni and NiCu catalysts supported on ZrO2-SiO2 for guaiacol hydrodeoxygenation, Catalysis Communications, 33 (2013) 15-19.
[135] H. Ohta, B. Feng, H. Kobayashi, K. Hara, A. Fukuoka, Selective hydrodeoxygenation of lignin-related 4-propylphenol into n-propylbenzene in water by Pt-Re/ZrO2 catalysts, Catalysis Today, 234 (2014) 139-144.

[136] S. Crossley, J. Faria, M. Shen, D.E. Resasco, Solid nanoparticles that catalyze biofuel upgrade reactions at the water/oil interface, Science, 327 (2010) 68-72.
[137] M. Saidi, F. Samimi, D. Karimipourfard, T. Nimmanwudipong, B.C. Gates, M.R. Rahimpour, Upgrading of lignin-derived bio-oils by catalytic hydrodeoxygenation, Energy and Environmental Science, 7 (2014) 103-129.
[138] P.M. De Souza, L. Nie, L.E.P. Borges, F.B. Noronha, D.E. Resasco, Role of oxophilic supports in the selective hydrodeoxygenation of m-cresol on Pd catalysts, Catalysis Letters, 144 (2014) 2005-2011.
[139] P.M. Mortensen, J.D. Grunwaldt, P.A. Jensen, A.D. Jensen, Screening of catalysts for hydrodeoxygenation of phenol as a model compound for bio-oil, ACS Catalysis, 3 (2013) 1774-1785.
[140] X. Chen, W. Sun, N. Xiao, Y. Yan, S. Liu, Experimental study for liquid phase selective hydrogenation of furfuryl alcohol to tetrahydrofurfuryl alcohol on supported Ni catalysts, Chemical Engineering Journal, 126 (2007) 5-11.
[141] Y. Román-Leshkov, C.J. Barrett, Z.Y. Liu, J.A. Dumesic, Production of dimethylfuran for liquid fuels from biomass-derived carbohydrates, Nature, 447 (2007) 982-985.
[142] S. Sitthisa, D.E. Resasco, Hydrodeoxygenation of furfural over supported metal catalysts: A comparative study of Cu, Pd and Ni, Catalysis Letters, 141 (2011) 784-791.
[143] C. Wang, H. Xu, R. Daniel, A. Ghafourian, J.M. Herreros, S. Shuai, X. Ma, Combustion characteristics and emissions of 2-methylfuran compared to 2,5-dimethylfuran, gasoline and ethanol in a DISI engine, Fuel, 103 (2013) 200-211.
[144] S.H. Pang, J.W. Medlin, Adsorption and reaction of furfural and furfuryl alcohol on Pd(111): Unique reaction pathways for multifunctional reagents, ACS Catalysis, 1 (2011) 1272-1283.
[145] D. Scholz, C. Aellig, I. Hermans, Catalytic transfer hydrogenation/hydrogenolysis for reductive upgrading of furfural and 5-(hydroxymethyl)furfural, ChemSusChem, 7 (2014) 268-275.
[146] S. Sitthisa, W. An, D.E. Resasco, Selective conversion of furfural to methylfuran over silica-supported NiFe bimetallic catalysts, Journal of Catalysis, 284 (2011) 90-101.
[147] W. Yu, J.G. Chen, Reaction pathways of model compounds of biomass-derived oxygenates on Fe/Ni bimetallic surfaces, Surface Science, (2015).
[148] H.Y. Zheng, Y.L. Zhu, B.T. Teng, Z.Q. Bai, C.H. Zhang, H.W. Xiang, Y.W. Li, Towards understanding the reaction pathway in vapour phase hydrogenation of furfural to 2-methylfuran, Journal of Molecular Catalysis A: Chemical, 246 (2006) 18-23.
[149] F. Delbecq, P. Sautet, A density functional study of adsorption structures of unsaturated aldehydes on Pt(111): A key factor for hydrogenation selectivity, Journal of Catalysis, 211 (2002) 398-406.
[150] A.S. Gowda, S. Parkin, F.T. Ladipo, Hydrogenation and hydrogenolysis of furfural and furfuryl alcohol catalyzed by ruthenium(II) bis(diimine) complexes, Applied Organometallic Chemistry, 26 (2012) 86-93.

[151] G.R. Jenness, D.G. Vlachos, DFT study of the conversion of furfuryl alcohol to 2-methylfuran on RuO2 (110), Journal of Physical Chemistry C, 119 (2015) 5938-5945.
[152] Y. Nakagawa, H. Nakazawa, H. Watanabe, K. Tomishige, Total Hydrogenation of Furfural over a Silica-Supported Nickel Catalyst Prepared by the Reduction of a Nickel Nitrate Precursor, ChemCatChem, 4 (2012) 1791-1797.
[153] V. Vorotnikov, G. Mpourmpakis, D.G. Vlachos, DFT study of furfural conversion to furan, furfuryl alcohol, and 2-methylfuran on Pd(111), ACS Catalysis, 2 (2012) 2496-2504.
[154] G.H. Wang, J. Hilgert, F.H. Richter, F. Wang, H.J. Bongard, B. Spliethoff, C. Weidenthaler, F. Schüth, Platinum-cobalt bimetallic nanoparticles in hollow carbon nanospheres for hydrogenolysis of 5-hydroxymethylfurfural, Nature Materials, 13 (2014) 293-300.
[155] L. Yu, L. He, J. Chen, J. Zheng, L. Ye, H. Lin, Y. Yuan, Robust and Recyclable Nonprecious Bimetallic Nanoparticles on Carbon Nanotubes for the Hydrogenation and Hydrogenolysis of 5-Hydroxymethylfurfural, ChemCatChem, (2015).
[156] W. Yu, K. Xiong, N. Ji, M.D. Porosoff, J.G. Chen, Theoretical and experimental studies of the adsorption geometry and reaction pathways of furfural over FeNi bimetallic model surfaces and supported catalysts, Journal of Catalysis, 317 (2014) 253-262.
[157] B. Chen, F. Li, Z. Huang, G. Yuan, Tuning catalytic selectivity of liquid-phase hydrogenation of furfural via synergistic effects of supported bimetallic catalysts, Applied Catalysis A: General, 500 (2015) 23-29.
[158] M. Lesiak, M. Binczarski, S. Karski, W. Maniukiewicz, J. Rogowski, E. Szubiakiewicz, J. Berlowska, P. Dziugan, I. Witońska, Hydrogenation of furfural over Pd-Cu/Al2O3 catalysts. The role of interaction between palladium and copper on determining catalytic properties, Journal of Molecular Catalysis A: Chemical, 395 (2014) 337-348.
[159] A.B. Merlo, V. Vetere, J.F. Ruggera, M.L. Casella, Bimetallic PtSn catalyst for the selective hydrogenation of furfural to furfuryl alcohol in liquid-phase, Catalysis Communications, 10 (2009) 1665-1669.
[160] S.C. Tsang, N. Cailuo, W. Oduro, A.T.S. Kong, L. Clifton, K.M.K. Yu, B. Thiebaut, J. Cookson, P. Bishop, Engineering preformed cobalt-doped platinum nanocatalysts for ultraselective hydrogenation, ACS Nano, 2 (2008) 2547-2553.
[161] D. Shi, J.M. Vohs, Deoxygenation of Biomass-Derived Oxygenates: Reaction of Furfural on Zn-Modified Pt(111), ACS Catalysis, 5 (2015) 2177-2183.
[162] M. Tamura, K. Tokonami, Y. Nakagawa, K. Tomishige, Rapid synthesis of unsaturated alcohols under mild conditions by highly selective hydrogenation, Chemical Communications, 49 (2013) 7034-7036.
[163] M. Chia, Y.J. Pagán-Torres, D. Hibbitts, Q. Tan, H.N. Pham, A.K. Datye, M. Neurock, R.J. Davis, J.A. Dumesic, Selective hydrogenolysis of polyols and cyclic ethers over bifunctional surface sites on rhodium-rhenium catalysts, Journal of the American Chemical Society, 133 (2011) 12675-12689.

[164] S. Koso, I. Furikado, A. Shimao, T. Miyazawa, K. Kunimori, K. Tomishige, Chemoselective hydrogenolysis of tetrahydrofurfuryl alcohol to 1,5-pentanediol, Chemical Communications, (2009) 2035-2037.
[165] M. Choura, N.M. Belgacem, A. Gandini, Acid-catalyzed polycondensation of furfuryl alcohol: Mechanisms of chromophore formation and cross-linking, Macromolecules, 29 (1996) 3839-3850.
[166] A. Chuntanapum, Y. Matsumura, Formation of tarry material from 5-HMF in subcritical and supercritical water, Industrial and Engineering Chemistry Research, 48 (2009) 9837-9846.
[167] L.R. Baker, G. Kennedy, M. Van Spronsen, A. Hervier, X. Cai, S. Chen, L.W. Wang, G.A. Somorjai, Furfuraldehyde hydrogenation on titanium oxide-supported platinum nanoparticles studied by sum frequency generation vibrational spectroscopy: Acid-base catalysis explains the molecular origin of strong metal-support interactions, Journal of the American Chemical Society, 134 (2012) 14208-14216.
[168] D. Kusdiana, S. Saka, Two-step preparation for catalyst-free biodiesel fuel production: Hydrolysis and methyl esterification, Applied Biochemistry and Biotechnology - Part A Enzyme Engineering and Biotechnology, 115 (2004) 781-791.
[169] S. Matsubara, Y. Yokota, K. Oshima, Palladium-catalyzed decarboxylation and decarbonylation under hydrothermal conditions: Decarboxylative deuteration, Organic Letters, 6 (2004) 2071-2073.
[170] Y. Yang, C. Ochoa-Hernández, P. Pizarro, V.A. De la Peña O'Shea, J.M. Coronado, D.P. Serrano, Synthesis of nickel phosphide nanorods as catalyst for the hydrotreating of methyl oleate, Topics in Catalysis, 55 (2012) 991-998.
[171] B.H. Gross, R.C. Mebane, D.L. Armstrong, Transfer hydrogenolysis of aromatic alcohols using Raney catalysts and 2-propanol, Applied Catalysis A: General, 219 (2001) 281-289.
[172] J. Jae, W. Zheng, R.F. Lobo, D.G. Vlachos, Production of dimethylfuran from hydroxymethylfurfural through catalytic transfer hydrogenation with ruthenium supported on carbon, ChemSusChem, 6 (2013) 1158-1162.
[173] N. Thakar, N.F. Polder, K. Djanashvili, H. van Bekkum, F. Kapteijn, J.A. Moulijn, Deuteration study to elucidate hydrogenolysis of benzylic alcohols over supported palladium catalysts, Journal of Catalysis, 246 (2007) 344-350.
[174] T. Thananatthanachon, T.B. Rauchfuss, Efficient production of the liquid fuel 2,5-dimethylfuran from fructose using formic acid as a reagent, Angewandte Chemie - International Edition, 49 (2010) 6616-6618.
[175] H.P. Reddy Kannapu, C.A. Mullen, Y. Elkasabi, A.A. Boateng, Catalytic transfer hydrogenation for stabilization of bio-oil oxygenates: Reduction of p-cresol and furfural over bimetallic Ni-Cu catalysts using isopropanol, Fuel Processing Technology, 137 (2015) 220-228.
[176] Y. Lei, N.W. Cant, D.L. Trimm, Activity patterns for the "water gas shift reaction over supported precious metal catalysts", Catalysis Letters, 103 (2005) 133-136.

[177] Y. Lei, N.W. Cant, D.L. Trimm, Kinetics of the water-gas shift reaction over a rhodium-promoted iron-chromium oxide catalyst, Chemical Engineering Journal, 114 (2005) 81-85.
[178] D.L. Trimm, Minimisation of carbon monoxide in a hydrogen stream for fuel cell application, Applied Catalysis A: General, 296 (2005) 1-11.
[179] M.V. Domínguez-Barroso, C. Herrera, M.A. Larrubia, L.J. Alemany, Diesel oil-like hydrocarbon production from vegetable oil in a single process over Pt-Ni/Al2O3 and Pd/C combined catalysts, Fuel Processing Technology, 148 (2016) 110-116.
[180] A.D. Sutton, J.K. Kim, R. Wu, C.B. Hoyt, D.B. Kimball, L.A. Silks, J.C. Gordon, The Conversion of Starch and Sugars into Branched C_{10} and C_{11} Hydrocarbons, ChemSusChem, 9 (2016) 2298-2300.
[181] D.R. Vardon, B.K. Sharma, H. Jaramillo, D. Kim, J.K. Choe, P.N. Ciesielski, T.J. Strathmann, Hydrothermal catalytic processing of saturated and unsaturated fatty acids to hydrocarbons with glycerol for in situ hydrogen production, Green Chemistry, 16 (2014) 1507-1520.
[182] M. Asadieraghi, W.M. Ashri Wan Daud, H.F. Abbas, Heterogeneous catalysts for advanced bio-fuel production through catalytic biomass pyrolysis vapor upgrading: A review, RSC Advances, 5 (2015) 22234-22255.
[183] B.C.R. Ewan, R.W.K. Allen, A figure of merit assessment of the routes to hydrogen, International Journal of Hydrogen Energy, 30 (2005) 809-819.
[184] T. Mochizuki, S.Y. Chen, M. Toba, Y. Yoshimura, Deoxygenation of guaiacol and woody tar over reduced catalysts, Applied Catalysis B: Environmental, 146 (2014) 237-243.
[185] H. Jahromi, F.A. Agblevor, Upgrading of pinyon-juniper catalytic pyrolysis oil via hydrodeoxygenation, Energy, 141 (2017) 2186-2195.
[186] H. Jahromi, F.A. Agblevor, Hydrodeoxygenation of pinyon-juniper catalytic pyrolysis oil using red mud-supported nickel catalysts, Applied Catalysis B: Environmental, 236 (2018) 1-12.
[187] H. Jahromi, F.A. Agblevor, Hydrotreating of guaiacol: A comparative study of Red mud-supported nickel and commercial Ni/SiO2-Al2O3 catalysts, Applied Catalysis A: General, 558 (2018) 109-121.
[188] Y. Yang, G. Lv, L. Deng, B. Lu, J. Li, J. Zhang, J. Shi, S. Du, Renewable aromatic production through hydrodeoxygenation of model bio-oil over mesoporous Ni/SBA-15 and Co/SBA-15, Microporous and Mesoporous Materials, 250 (2017) 47-54.
[189] F.A. Agblevor, H. Jahromi, Aqueous-Phase Synthesis of Hydrocarbons from Furfural Reactions with Low-Molecular-Weight Biomass Oxygenates, Energy & Fuels, 32 (2018) 8552-8562.
[190] N.T.T. Tran, Y. Uemura, S. Chowdhury, A. Ramli, Vapor-phase hydrodeoxygenation of guaiacol on Al-MCM-41 supported Ni and Co catalysts, Applied Catalysis A: General, 512 (2016) 93-100.
[191] I.T. Ghampson, C. Sepúlveda, A.B. Dongil, G. Pecchi, R. García, J.L.G. Fierro, N. Escalona, Phenol hydrodeoxygenation: Effect of support and Re promoter on the reactivity of Co catalysts, Catalysis Science and Technology, 6 (2016) 7289-7306.

[192] K. Leiva, N. Martinez, C. Sepulveda, R. García, C.A. Jiménez, D. Laurenti, M. Vrinat, C. Geantet, J.L.G. Fierro, I.T. Ghampson, N. Escalona, Hydrodeoxygenation of 2-methoxyphenol over different Re active phases supported on SiO2 catalysts, Applied Catalysis A: General, 490 (2015) 71-79.
[193] J. Schindelin, I. Arganda-Carreras, E. Frise, V. Kaynig, M. Longair, T. Pietzsch, S. Preibisch, C. Rueden, S. Saalfeld, B. Schmid, J.-Y. Tinevez, D.J. White, V. Hartenstein, K. Eliceiri, P. Tomancak, A. Cardona, Fiji: an open-source platform for biological-image analysis, Nature Methods, 9 (2012) 676.
[194] W. Ning, H. Shen, Y. Jin, X. Yang, Effects of Weak Surface Modification on Co/SiO2 Catalyst for Fischer-Tropsch Reaction, PLOS ONE, 10 (2015) e0124228.
[195] N.A.S. Ramli, N.A.S. Amin, Thermo-kinetic assessment of glucose decomposition to 5-hydroxymethyl furfural and levulinic acid over acidic functionalized ionic liquid, Chemical Engineering Journal, 335 (2018) 221-230.
[196] C. Courson, L. Udron, D. Świerczyński, C. Petit, A. Kiennemann, Hydrogen production from biomass gasification on nickel catalysts: Tests for dry reforming of methane, Catalysis Today, 76 (2002) 75-86.
[197] D. Sutton, B. Kelleher, J.R.H. Ross, Review of literature on catalysts for biomass gasification, Fuel Processing Technology, 73 (2001) 155-173.
[198] P.A. Deshpande, G. Madras, Support-dependent activity of noble metal substituted oxide catalysts for the water gas shift reaction, AIChE Journal, 56 (2010) 2662-2676.
[199] C.M. Kalamaras, P. Panagiotopoulou, D.I. Kondarides, A.M. Efstathiou, Kinetic and mechanistic studies of the water-gas shift reaction on Pt/TiO2 catalyst, Journal of Catalysis, 264 (2009) 117-129.
[200] F. Mariño, C. Descorme, D. Duprez, Noble metal catalysts for the preferential oxidation of carbon monoxide in the presence of hydrogen (PROX), Applied Catalysis B: Environmental, 54 (2004) 59-66.
[201] P. Zhang, M. Chi, S. Sharma, E. McFarland, Silica encapsulated heterostructure catalyst of Pt nanoclusters on hematite nanocubes: Synthesis and reactivity, Journal of Materials Chemistry, 20 (2010) 2013-2017.
[202] G.W. Huber, R.D. Cortright, J.A. Dumesic, Renewable Alkanes by Aqueous-Phase Reforming of Biomass-Derived Oxygenates, Angewandte Chemie International Edition, 43 (2004) 1549-1551.
[203] R.D. Cortright, R.R. Davda, J.A. Dumesic, Hydrogen from catalytic reforming of biomass-derived hydrocarbons in liquid water, Nature, 418 (2002) 964-967.
[204] G.W. Huber, J.A. Dumesic, An overview of aqueous-phase catalytic processes for production of hydrogen and alkanes in a biorefinery, Catalysis Today, 111 (2006) 119-132.
[205] A.J.R. Hensley, Y. Hong, R. Zhang, H. Zhang, J. Sun, Y. Wang, J.S. McEwen, Enhanced Fe2O3 reducibility via surface modification with Pd: Characterizing the synergy within Pd/Fe catalysts for hydrodeoxygenation reactions, ACS Catalysis, 4 (2014) 3381-3392.
[206] Q. Guo, M. Wu, K. Wang, L. Zhang, X. Xu, Catalytic hydrodeoxygenation of algae bio-oil over bimetallic Ni-Cu/ZrO2 catalysts, Industrial and Engineering Chemistry Research, 54 (2015) 890-899.

[207] R. Watanabe, S. Watanabe, N. Hirata, C. Fukuhara, Effect of Promoter Addition on Water Gas Shift Property over Structured-Type Iron Oxide Catalyst, Catalysis Letters, 146 (2016) 2478-2484.
[208] F. Meshkani, M. Rezaei, High temperature water gas shift reaction over promoted iron based catalysts prepared by pyrolysis method, International Journal of Hydrogen Energy, 39 (2014) 16318-16328.
[209] Sonal, K. Kondamudi, K.K. Pant, S. Upadhyayula, Synergistic Effect of Fe-Co Bimetallic Catalyst on FTS and WGS Activity in the Fischer-Tropsch Process: A Kinetic Study, Industrial and Engineering Chemistry Research, 56 (2017) 4659-4671.
[210] P.J. Hsu, J.W. Jiang, Y.C. Lin, Does a Strong Oxophilic Promoter Enhance Direct Deoxygenation? A Study of NiFe, NiMo, and NiW Catalysts in p-Cresol Conversion, ACS Sustainable Chemistry and Engineering, 6 (2018) 660-667.
[211] L. Pan, Y. He, M. Niu, Y. Dan, W. Li, Selective hydrodeoxygenation of: P -cresol as a model for coal tar distillate on Ni-M/SiO_2 (M = Ce, Co, Sn, Fe) bimetallic catalysts, RSC Advances, 9 (2019) 21175-21185.
[212] X. Liu, W. An, Y. Wang, C.H. Turner, D.E. Resasco, Hydrodeoxygenation of guaiacol over bimetallic Fe-alloyed (Ni, Pt) surfaces: reaction mechanism, transition-state scaling relations and descriptor for predicting C–O bond scission reactivity, Catalysis Science & Technology, 8 (2018) 2146-2158.
[213] S. Hilaire, X. Wang, T. Luo, R.J. Gorte, J. Wagner, A comparative study of water-gas-shift reaction over ceria-supported metallic catalysts, Applied Catalysis A: General, 258 (2004) 271-276.
[214] J. Goscianska, M. Ziolek, E. Gibson, M. Daturi, Novel mesoporous zirconia-based catalysts for WGS reaction, Applied Catalysis B: Environmental, 97 (2010) 49-56.
[215] S.M. Schimming, O.D. Lamont, M. König, A.K. Rogers, A.D. D'Amico, M.M. Yung, C. Sievers, Hydrodeoxygenation of Guaiacol over Ceria-Zirconia Catalysts, ChemSusChem, 8 (2015) 2073-2083.
[216] C.A. Teles, P.M. de Souza, A.H. Braga, R.C. Rabelo-Neto, A. Teran, G. Jacobs, D.E. Resasco, F.B. Noronha, The role of defect sites and oxophilicity of the support on the phenol hydrodeoxygenation reaction, Applied Catalysis B: Environmental, 249 (2019) 292-305.
[217] L. Pastor-Pérez, A. Sepúlveda-Escribano, Multicomponent NiSnCeO_2/C catalysts for the low-temperature glycerol steam reforming, Applied Catalysis A: General, 529 (2017) 118-126.
[218] X. Luo, Y. Hong, H. Zhang, K. Shi, G. Yang, T. Wu, Highly efficient steam reforming of ethanol (SRE) over CeO_x grown on the nano Ni_xMg_yO matrix: H_2 production under a high GHSV condition, International Journal of Energy Research, 43 (2019) 3823-3836.
[219] C. Ruocco, V. Palma, A. Ricca, Kinetics of Oxidative Steam Reforming of Ethanol Over Bimetallic Catalysts Supported on CeO_2–SiO_2: A Comparative Study, Topics in Catalysis, 62 (2019) 467-478.
[220] T.M.C. Hoang, N.K. Rao, L. Lefferts, K. Seshan, Investigation of Ce-Zr oxide-supported Ni catalysts in the steam reforming of meta-cresol as a model component for bio-derived tar, ChemCatChem, 7 (2015) 468-478.

[221] S. Jampa, A. Luengnaruemitchai, T. Chaisuwan, S. Wongkasemjit, High potential of mesoporous ceria/ceria-zirconia synthesized via nanocasting pathway for catalytic applications, Advanced Materials - TechConnect Briefs 2017, 2017, pp. 25-28.
[222] A.H. Lu, F. Schüth, Nanocasting: A Versatile Strategy for Creating Nanostructured Porous Materials, Advanced Materials, 18 (2006) 1793-1805.
[223] X. Deng, K. Chen, H. Tüysüz, Protocol for the Nanocasting Method: Preparation of Ordered Mesoporous Metal Oxides, Chemistry of Materials, 29 (2017) 40-52.
[224] D. Devaiah, L.H. Reddy, S.E. Park, B.M. Reddy, Ceria–zirconia mixed oxides: Synthetic methods and applications, Catalysis Reviews - Science and Engineering, 60 (2018) 177-277.
[225] A.B. Dongil, I.T. Ghampson, R. García, J.L.G. Fierro, N. Escalona, Hydrodeoxygenation of guaiacol over Ni/carbon catalysts: effect of the support and Ni loading, RSC Advances, 6 (2016) 2611-2623.
[226] S.J.S. Vasconcelos, C.L. Lima, J.M. Filho, A.C. Oliveira, E.B. Barros, F.F. de Sousa, M.G.C. Rocha, P. Bargiela, A.C. Oliveira, Activity of nanocasted oxides for gas-phase dehydration of glycerol, Chemical Engineering Journal, 168 (2011) 656-664.
[227] K. Ding, A. He, D. Zhong, L. Fan, S. Liu, Y. Wang, Y. Liu, P. Chen, H. Lei, R. Ruan, Improving hydrocarbon yield via catalytic fast co-pyrolysis of biomass and plastic over ceria and HZSM-5: An analytical pyrolyzer analysis, Bioresource Technology, 268 (2018) 1-8.
[228] Q. Lu, Z.F. Zhang, C.Q. Dong, X.F. Zhu, Catalytic upgrading of biomass fast pyrolysis vapors with nano metal oxides: An analytical Py-GC/MS study, Energies, 3 (2010) 1805-1820.
[229] S. Wang, X. Guo, T. Liang, Y. Zhou, Z. Luo, Mechanism research on cellulose pyrolysis by Py-GC/MS and subsequent density functional theory studies, Bioresource Technology, 104 (2012) 722-728.

Appendix A - Reactor Assembly

The horizontally stirred, 55 mL stainless steel reactor was constructed using parts from Swagelok and Zook as well as some custom fabricated pieces for the purpose of stirring. The reactor, as per design of the rupture disk, is rated for 700 psi (4.8 MPa) at 350°C. All custom fabricated parts are designed in such a way that no new pressure boundaries are created – see Figure A-1. As such, the stir rod assembly can be friction fitted inside the reactor during preparation for a reaction and removed after reaction for cleaning. A threaded hex-ring slips over the 1" end cap allowing for the stir adapter to be threaded on. This then allows for a threaded rod – which can be rotated by a motor – to screw in and drive the reactor. Securely fitting the threaded rod prevents the reactor from wobbling.

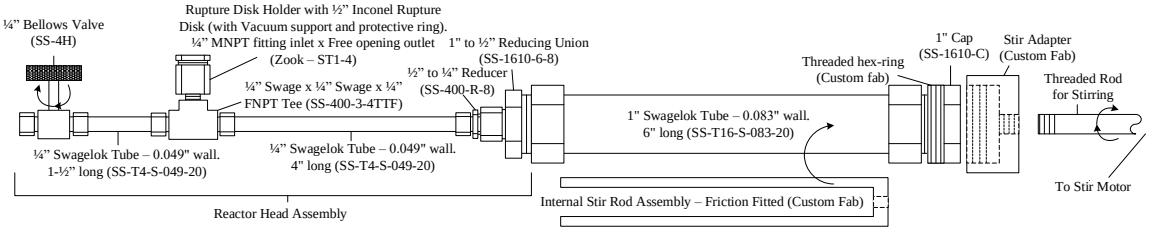

Figure A-1: Reactor assembly and parts list

To load the reactor, first the stir rod is placed within the main body of the reactor. The end-cap, fitted with the hex-ring, is then assembled to the "bottom" of the reactor. The reactor is then loaded with the desired contents (liquid and solid) and sealed by attaching the "reactor head assembly". Gas can then be filled into the reactor via the bellows valve. Before loading the reactor with the desired gas, the reactor should be leak tested. When placed inside the furnace, the valve and rupture disk assemblies are kept outside of the furnace to ensure that they are not damaged (See Figure A-2). When performing a reaction,

it is advisable that a ball-valve be attached in series with the bellows valve to prevent accidental leakage.

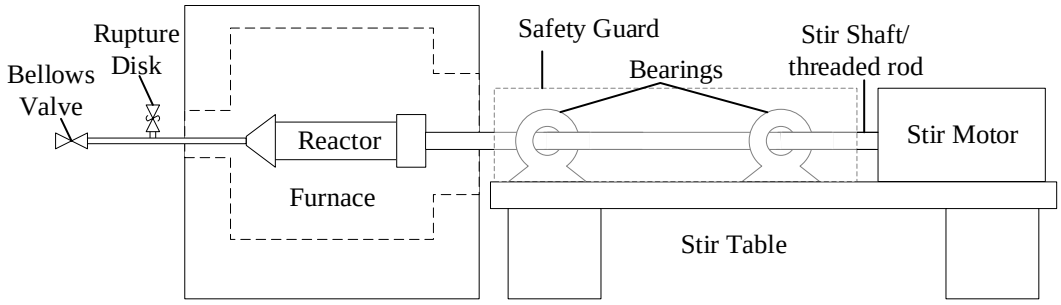

Figure A-2: Reactor setup with Furnace

Appendix B - Procedure for Nano-Casting Ceria-Zirconia Catalysts

Ceria-zirconia supports were prepared via nano-casting on ordered silica supports. The procedure for nano-casting consists of first an infiltration process to add ceria and zirconia precursors to the silica support followed by calcination. Silica was then removed via leaching followed by washing and drying to produce the end product. This procedure was adopted and modified from Deng et al., [223]. Ratios of ceria to zirconia (67/33) adopted from Watanabe et al., [41]

CZ-41 – Ceria-Zirconia nano-casted from MCM-41

CZ-15 – Ceria-Zirconia nano-casted from SBA-15

Procedure:

1. Add 1 g of silica material (SBA-15/MCM-41) into a glass vessel (ie. glass beaker - 20 mL) with a magnetic stir bar. Cover the vessel (ie. with parafilm).
2. Prepare infiltrate solution (1 dose) (see steps 2a and 2b for recipes). These recipes were used to prepare a 0.4 M solution that produces an oxide that occupied 15% of the pore volume of the silica material. Deng et al., [223] recommends preparing an 0.8 M solution however it was determined for this process, that will lead to issues as the volume of solution used will be too small and stirring of the slurry will not be possible (especially when using MCM-41 as the template). Stir the solution to ensure all precursors have been adequately dissolved.
    a. CZ-41: 6 mL ethanol solution containing 0.2610 g of zirconyl chloride octahydrate and 0.7092 g of cerium nitrate hexahydrate.

b. CZ-15: 12 mL ethanol solution with 0.5077 g of zirconyl chloride octahydrate and 1.3805 g of cerium nitrate hexahydrate. Cover with parafilm to prevent evaporation.

3. With the silica-containing vessel from step 1 on a stir plate, slowly inject the infiltrate solution (ie. With a pipette) and reseal the vessel and continue with stirring for 1 hour.
4. Uncover the vessel and remove the stir bar. Place the vessel on a heating plate and heat at temperature of 55°C for 3-4 hours until sample looks dry.
5. Once most of the ethanol is gone, move contents to a crucible for drying and calcination over night. The drying/calcination process is as follows: 3°C/min room temperature to 60°C – hold for 6 hours (slowly remove ethanol still in pores); 3°C/min to 120°C – hold for 2 hours (remove any adsorbed water); 3°C/min to 800°C – hold for 6 hours (calcination of precursors). Let cool to room temperature.
6. Move and contents from crucible to glass vessel as in step 1 and seal it. Grinding/crushing of the calcination product to a powder may be necessary. Repeat steps 2-5.
7. Prepare 2 M NaOH solution by dissolving 8 g of NaOH into 100 mL of deionized water (maintain this ratio).
8. Remove the contents of the crucible into a PPCO centrifuge bottle and leach with 20 mL of NaOH solution prepared in step 7. Shake and mix contents well and place in the over at 70°C for 5 hours/overnight. Shake periodically.
9. Decant the solution. Add 20 mL of fresh NaOH solution and leach at 90°C for 24 hours. Shake periodically.

10. Repeat step 9 once for a total of 3 leaching stages.
11. Decant the NaOH solution and refill with deionized water for washing. Shake/mix well then centrifuge: 6000 rpm (20 min) -> 8000 rpm (20 min) -> 9000 rpm (30 min) -> 10000 rpm (30 min). perform this washing procedure 3 times.
12. Decant the deionized water and dry overnight at 50°C in the oven.
13. Removed ceria-zirconia from centrifuge bottle and place into crucibles. Dry/calcine the material again to ensure appropriate removal of all water and calcination of nitrate/chloride salts. The drying/calcination procedure is as follows: room temperature to 120°C at 3°C/min, hold for 2 hours, heat to 800°C at 3°C/min, and hold for 2 hours. Grinding/crushing the ceria-zirconia before this drying/calcination procedure may be necessary.

Curriculum Vitae

Candidate's full name: Kyle A. Rogers

Universities attended: BScE in Chemical Engineering, University of New Brunswick, 2009-2014

Publications:

[1] K.A. Rogers, Y. Zheng, Selective Deoxygenation of Biomass-Derived Bio-oils within Hydrogen-Modest Environments: A Review and New Insights, ChemSusChem, 9 (2016) 1750-1772.
[2] K.A. Rogers, Y. Zheng, Decomposition of glucose with *in situ* deoxygenation in a low H_2 pressure environment – Part I: Monometallic catalysts, Applied Catalysis A: General, (2019) 75-85.
[3] K.A. Rogers, Y. Zheng, Decomposition of glucose with *in situ* deoxygenation in a low H_2 pressure environment – Pt. II: Bimetallic catalysts, Applied Catalysis A: General, 578 (2019) 10-19.
[4] K.A. Rogers, Y. Zheng, Guaiacol Deoxygenation using Ceria-Zirconia Based Catalysts with Hydrogen Produced Internally via Water-Gas-Shift Reaction, To Be Submitted
[5] K.A. Rogers, Y. Zheng, Glucose Decomposition with Internal Hydrogen Production and Deoxygenation via Nano-Casted Ceria-Zirconia Catalysts, To Be Submitted

Conference Presentations:

[1] K.A. Rogers, Y. Zheng, Decomposition of Glucose with *in Situ* Deoxygenation Via Monometallic and Bimetallic Ni, Co, and Fe Catalysts, 26th North American Catalysis Society Meeting, June 23-28, 2019. Chicago, Illinois, USA

Awards:

- 2019 – Kokes Award for 26th North American Catalysis Society Meeting in Chicago, Illinois, USA
- 2014 – New Brunswick Innovation Foundation (NBIF) Scholarship